Thermoplastic Elastomers with Crystalline Aliphatic Hard Segments Derived from Plant Oils

Dissertation

zur Erlangung des akademischen Grades eines
Doktors der Naturwissenschaften (Dr. rer. nat.)

vorgelegt von

Brigitta Franziska Schemmer

an der

Universität Konstanz

Mathematisch-Naturwissenschaftliche Sektion
Fachbereich Chemie

Konstanz, 2023

Dissertation der Universität Konstanz
Tag der mündlichen Prüfung 14.09.2023

1. Referent: Prof. Dr. Stefan Mecking
2. Referentin: Prof. Dr. Christine Peter
Prüfungsvorsitz: Prof. Dr. Karin Hauser

Audaces fortuna adiuvat!

Die vorliegende Dissertation entstand in der Zeit von März 2014 bis April 2018 unter der Leitung von Herrn Prof. Dr. Stefan Mecking im Fachbereich Chemie der Universität Konstanz.

Danksagung - Acknowledgement

Allen voran danke ich Prof. Dr. Stefan Mecking für die Betreuung dieser Arbeit, seine Unterstützung und stetiges Interesse an meiner Forschungsarbeit.
Daneben danke ich Prof. Dr. Christine Peter für die Übernahme der Zweitbetreuung und Prof. Dr. Karin Hauser für die Übernahme des Prüfungsvorsitzes.
Mein Dank gilt außerdem der Landesstiftung Baden-Württemberg für die Finanzierung dieser Arbeit durch ein Stipendium im Rahmen des Landesgraduiertenförderungsgesetzes.
Darüber hinaus danke ich Florian Stempfle für die geleistete Vorarbeit und Hilfe auf dem Gebiet der langkettigen aliphatischen Polyester, sowie meinen Leidensgenossen Justus Walther und Judith Schwaderer für die enge Zusammenarbeit im Bereich der Diamin- und Polyamidsynthese.
Bei Anna-Lena Öchsle und Cathrin Kronenbitter möchte ich mich für ihr Engagement während ihrer jeweiligen Forschungspraktika und/oder Bachelorarbeiten bedanken, die einen essenziellen Beitrag zu dieser Arbeit geleistet haben.
Des Weiteren danke ich Melissa Birkle für die WAXD-Messungen und Lars Bolk für die Durchführung und Auswertung zahlreicher DSC und GPC Messungen, sowie für die kompetente Unterstützung bei der Lösung von diversen Software Problemen. Robin Kirsten und Patrick Ortmann danke ich für die enge Zusammenarbeit bei der Betreuung des Erstsemesterpraktikums.
Mein besonderer Dank gilt außerdem den Mitarbeitern der wissenschaftlichen Werkstätten der Universität Konstanz für die Konstruktion von diversen Glasapparaturen und maßgeschneiderten Sonderanfertigungen, die die Untersuchung der Materialeigenschaften vieler meiner hergestellten Polymere erst ermöglicht haben.
Für die gute Arbeitsatmosphäre und die schöne Zeit im Labor und außerhalb auch nach Feierabend danke ich außerdem ganz herzlich der gesamten AG Mecking.

Publications

Parts of this work have been published:

Stempfle, F.; Schemmer, B.; Oechsle, A.-L.; Mecking, S. Thermoplastic polyester elastomers based on long-chain crystallizable aliphatic hard segments. *Polym. Chem.* **2015**, *6*, 7133-7137

Schemmer, B.; Kronenbitter, C.; Mecking, S. Thermoplastic polyurethane elastomers with aliphatic hard segments based on plant-oil-derived long-chain diisocyanates. *Macromol. Mater. Eng.* **2018**, *303*, 1700416

Oral and Poster Presentations:

Schemmer, B.; Hess, S. K.; Witt, T.; Ewe, D.; Kroth, P.; Mecking, S. Linear long-chain polycondensates from sustainable plant- and algae-derived fatty acids. Oral and poster presentation at the **Macromolecular Colloquium** in Freiburg, February 2016.

Schemmer, B.; Stempfle, F. Thermoplastic polyester elastomers based on plant-oil derived long-chain crystallizable aliphatic hard segments; poster presentation at the **8th Workshop on Fats and Oils as Renewable Feedstock for the Chemical Industry** in Karlsruhe, March 2015.

Zusammenfassung - Abstract

Kunststoffe sind aus unserem Alltag heute nicht mehr wegzudenken. Ob als Verpackungsmaterial für Lebensmittel, als Textilien in der Bekleidungsindustrie, als Bauteile in der Medizintechnik oder in der Form von Hochleistungsverbundmaterialien in der Luft- und Raumfahrttechnik, kaum ein Werkstoff hat die moderne Gesellschaft in den letzten Jahrzehnten so sehr geprägt wie synthetische Polymere. Dazu gehören auch thermoplastische Elastomere, eine Gruppe von Kunststoffen, die die Elastizität und Duktilität von klassischen Elastomeren mit der thermoplastischen Verarbeitbarkeit von Thermoplasten vereinen. Diese einzigartige Kombination von Materialeigenschaften kann unter anderem durch Copolymerisation von kristallisierbaren, „harten" Monomeren mit amorphen, „weichen" Monomeren erreicht werden, wobei segmentierte Copolymere entstehen, in denen sich kristallisierbare harte und amorphe weiche Blöcke unterschiedlicher Länge abwechseln. Durch die Selbstorganisation und das Auskristallisieren der typischerweise auf kurzen, teils aromatischen, Polyester-, Polyurethan- oder Polyamidblöcke basierenden Hartsegmente kommt es zur Mikrophasenseparation und es entstehen kleine, in der amorphen Matrix dispergierte Kristallite, die als physikalische Vernetzungspunkte fungieren und für das elastische Verhalten des thermoplastischen Elastomers verantwortlich sind. Im Gegensatz zur kovalenten Vernetzung in klassischen Elastomeren ist diese physikalische Vernetzung thermisch reversibel, weshalb thermoplastische Elastomere nicht nachträglich vernetzt werden müssen und Schmelzpunkte aufweisen, oberhalb derer sie thermoplastisch verarbeitbar sind. Dadurch sind sie zusätzlich recycelbar und finden dementsprechend vielfältige Anwendungen. Allerdings basiert die Herstellung eines Großteils der heute verwendeten thermoplastischen Elastomere - wie die Herstellung von Kunststoffen allgemein - nach wie vor auf der Nutzung von fossilen Rohstoffen, was in Zeiten des Klimawandels und steigender politischer Instabilität immer stärker in die Kritik gerät. Dementsprechend wenden sich Forschung und Industrie zunehmend nachwachsenden Rohstoffen wie Kohlenhydraten aus Getreide oder ungesättigten Fettsäuren aus Pflanzenölen als alternative Ausgangsstoffe für die Synthese von sowohl „harten" als auch „weichen" Monomeren zu. Amorphe Makrodiole auf Polyetherbasis wie Polytetramethylenglykol (PTMG) und Polytrimethylenglykol (PPDO) werden dabei bereits heute ausgehend von nachhaltiger Glukose in industriellem Maßstab produziert. Bezüglich der Synthese neuartiger „harter" Monomere sind dank der Entwicklung von neuen katalytischen Verfahren wie der isomerisierenden Alkoxycarbonylierung unter anderem ungesättigte Fettsäuren aus Pflanzenölen und ihre Derivate von besonderem Interesse, da sie

aufgrund ihrer langen, linearen Methylensequenzen in Kombination mit dem Vorhandensein von internen olefinischen Doppelbindungen ideale Ausgangsstoffe für die Synthese diverser langkettiger, α,ω-bifunktioneller Monomere darstellen. Letztere bilden die Basis für die Entwicklung neuartiger, teilkristalliner, rein aliphatischer Polykondensate, die aufgrund ihrer stark reduzierten Dichte an funktionellen Gruppen einzigartige Materialeigenschaften aufweisen. So besitzen aliphatische Polyester basierend auf langkettigen α,ω-Dicarbonsäuren und α,ω-Diolen dieselbe Kristallstruktur wie Polyethylen und erreichen ungewöhnlich hohe Schmelzpunkte von über 100 °C.

Im Rahmen dieser Arbeit wurden daher ausgehend von Pflanzenölen neue lineare, aliphatische, α,ω-funktionalisierte Monomere synthetisiert und deren Eignung als Bausteine für teilkristalline, aliphatischen Hartsegmenten in komplett erneuerbaren thermoplastischen Elastomeren untersucht.

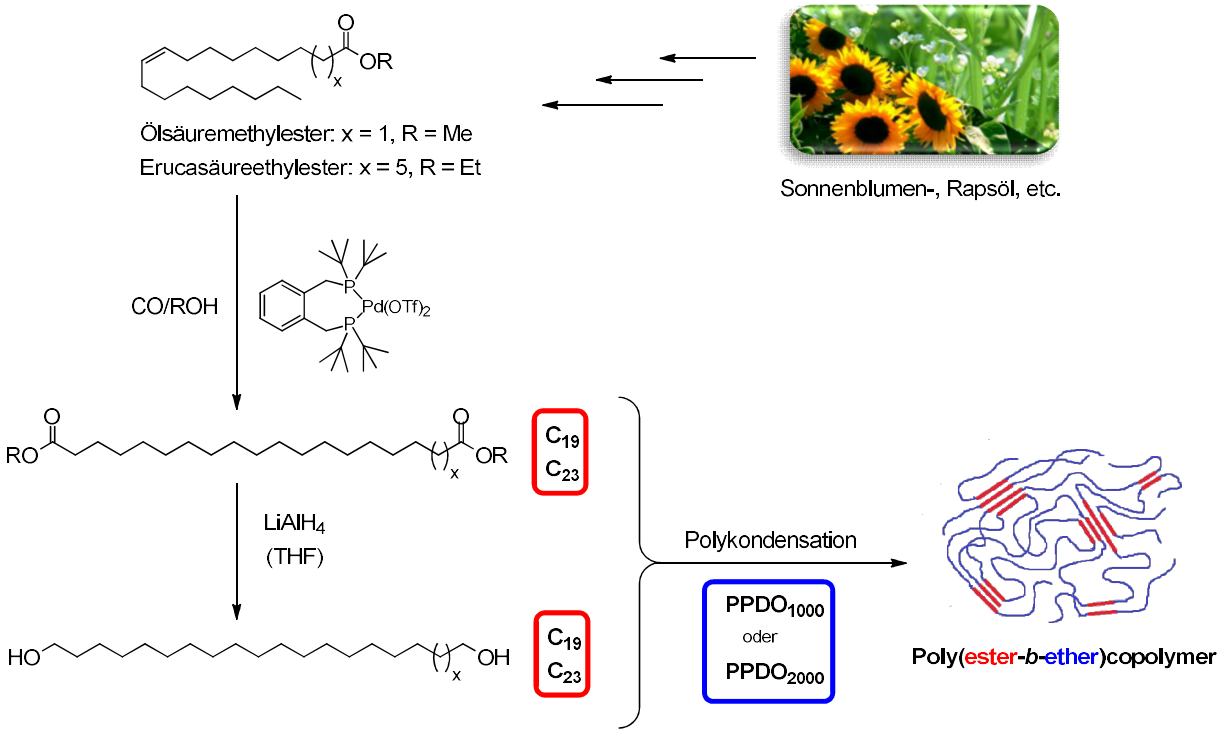

Abbildung 1: Synthese von segmentierten thermoplastischen Copolyesterelastomeren mit langkettigen, aliphatischen Polyesterhartsegmenten auf Pflanzenölbasis.[1]

Ausgehend von Öl- und Erucasäure wurde dabei beginnend mit der isomerisierenden Alkoxycarbonylierung der entsprechenden Methyl- oder Ethylester erfolgreich eine Reihe von linearen, α,ω-bifunktionellen C_{19}- und C_{23}-Polykondensationsmonomeren hergestellt. Die bereits bekannte Synthese der entsprechenden α,ω-Diester Dimethyl-1,19-nonadecandioat und Diethyl-1,23-

tricosandioat wurde vereinfacht, wobei gezeigt werden konnte, dass Spuren von Wasser keinen negativen Einfluss auf das Reaktionsergebnis haben und ein Hochskalieren der Reaktion auf einen Maßstab von annähernd 200 g möglich ist. Polykondensation mit den entsprechenden durch Reduktion erhaltenen langkettigen C_{19}- bzw. C_{23}-Diolen zusammen mit einem zuckerbasierten, dihydroxyterminierten Poly(1,3-propandiol) Polyetherweichsegment ($PPDO_{1000}$ oder $PPDO_{2000}$) ergab eine Reihe von segmentierten Poly(ester-*b*-ether)blockcopolymeren (**Abbildung 1**) mit zahlenmittleren Molekulargewichten von bis zu 5,2 x 10^4 g mol^{-1} und Schmelzpunkten, die abhängig von der Polymerzusammensetzung und dem Molekulargewicht des Polyetherweichsegments zwischen 14 °C und 95 °C lagen. Der Einsatz eines langkettigen C_{19}- bzw. C_{23}-Diols als Kettenverlängerer erwies sich dabei als nötig, um die Schmelz- und/oder Kristallisationspunkte auf Werte über 25 °C anzuheben und die thermoplastische Verarbeitbarkeit mittels Standardtechniken wie Spritzgießen zu gewährleisten. Röntgenkristallstrukturuntersuchungen bestätigten das Vorhandensein von Kristalliten mit einer polyethylenähnlichen, orthorhombischen Kristallstruktur, die als physikalische Vernetzungspunkte fungieren. Die mechanischen Eigenschaften und das elastische Verhalten der hergestellten Polymere wurden außerdem mittels Zug-Dehn-Versuchen und zyklischen Hysteresemessungen an spritzgegossenen Prüfkörpern untersucht, wobei für die Bruchdehnung teilweise Werte von über 1100 % erreicht wurden und die Prüfkörper im Extremfall nach 10 Zyklen wiederkehrender Dehnung um 100 % eine verbleibende Restdehnung von nur 15 % aufwiesen. Eine besonders vorteilhafte Kombination von exzellentem elastischen Verhalten, guter Duktilität und einem hohen Schmelzpunkt von 86 °C konnte für TPC-$C_{23}PPDO_{2000}$-65wt% festgestellt werden, einem segmentiertem Poly(ester-*b*-ether)copolymer mit Polyesterhartsegmenten basierend auf C_{23}-Monomeren und einem Mol-Verhältnis von hartem zu weichem Diol von 1:1: Im Vergleich dazu wies TPC-$C_{12}PPDO_{2000}$-62wt%, ein äquivalentes segmentiertes Poly(ester-*b*-ether)copolymer mit Polyesterhartsegmenten basierend auf kommerziell erhältlichen C_{12}-Monomeren und ähnlicher Blocklängenverteilung, einen stark reduzierten Schmelzpunkt von nur 66 °C und eine stark verringerte Duktilität auf, während das elastische Verhalten vergleichbar war.

Zusätzlich zu Materialien auf Polyesterbasis wurde ausgehend von Methyloleat und Ethylerucat außerdem eine Reihe von neuartigen thermoplastischen Elastomeren mit langkettigen, aliphatischen Polyurethanhartsegmenten auf Pflanzenölbasis hergestellt. Dazu wurde ausgehend von Dimethyl-1,19-nonadecandioat und Diethyl-1,23-tricosandioat eine mehrstufige Syntheseroute für die Herstellung pflanzenölbasierter C_{19}- und C_{23}-Polyurethanpräkursor in der Form von 1,19-Diisocyanatononadecan und 1,23-Diisocyanatotricosan entwickelt (**Abbildung 2**). Entscheidender

letzter Schritt dabei war das Ersetzen der Bromidsubstituenten in 1,19-Dibromononadecan und 1,23-Dibromotricosan durch Isocyanatgruppen in einer nukleophilen Substitution mit Kaliumcyanat. Besonderes Augenmerk galt dabei der Optimierung der Reaktionsbedingungen, um unerwünschte Nebenreaktionen wie die Bildung von Isocyanuraten durch Trimerisierung von Isocyanatverbindungen zu unterdrücken. Als wichtigste Faktoren wurden dabei die Wahl des richtigen Lösungsmittels, der optimalen Reaktionstemperatur, sowie der korrekten Reaktionszeit identifiziert. So konnten nach Destillation an einem speziell designten Kühlfinger sowohl 1,19-Diisocyanatononadecan als auch 1,23-Diisocyanatotricosan mit einer Reinheit von über 99 % und in Ausbeuten von bis zu 35 bzw. 40 % isoliert werden.

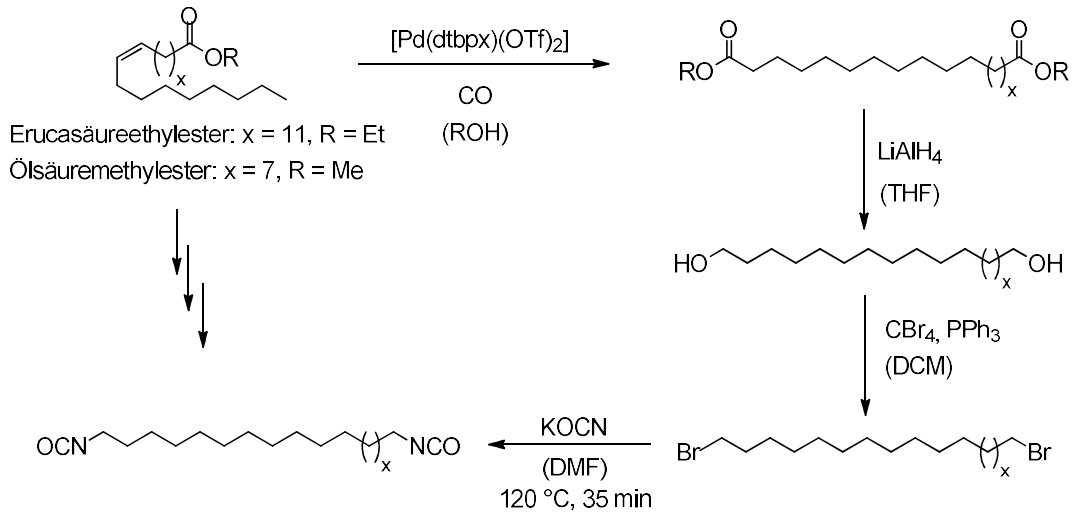

Abbildung 2: Mehrstufige Syntheseroute für die Herstellung von 1,19-Diisocyanatononadecan und 1,23-Diisocyanatotricosan ausgehend von ungesättigten Fettsäureestern.

Copolymerisation von 1,19-Diisocyanatononadecan und 1,23-Diisocyanatotricosan mit den entsprechenden langkettigen C_{19}- und C_{23}-Diolen und dem amorphem Makrodiol $PPDO_{2000}$ in einer Polyadditionsreaktion in Lösung ergab eine Reihe von segmentierten Poly(urethan-*b*-ether)blockcopolymeren (**Abbildung 3**) mit zahlenmittleren Molekulargewichten von bis zu 5,0 x 10^4 g mol^{-1}.

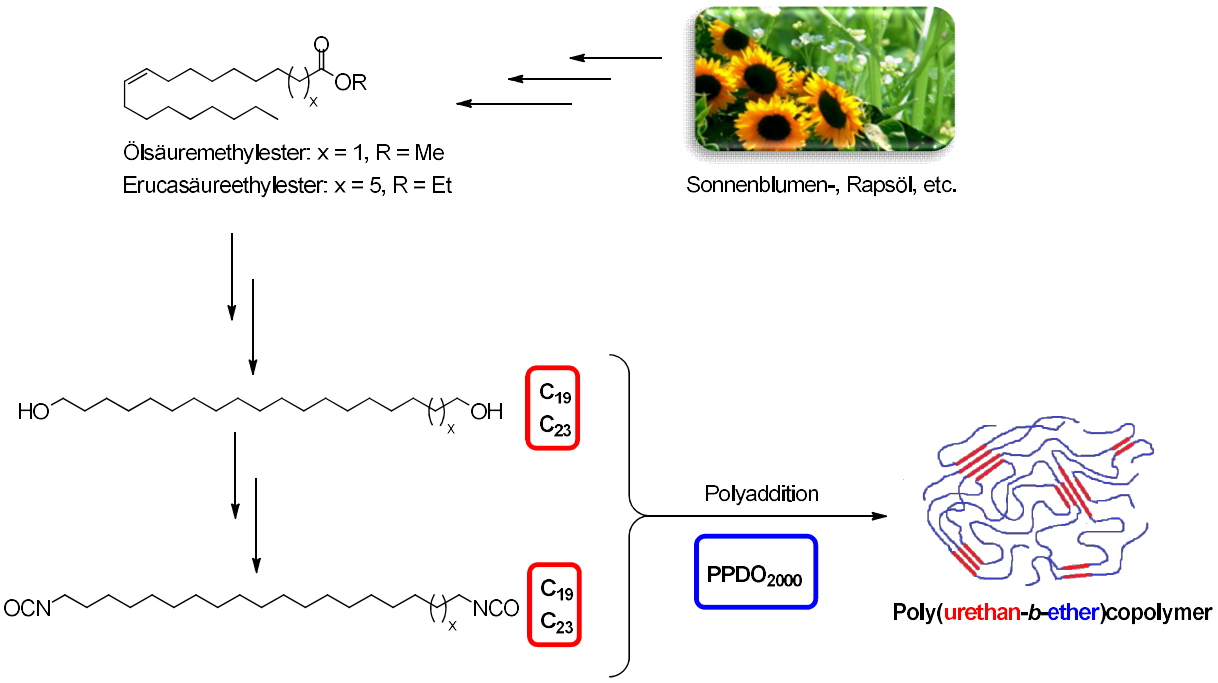

Abbildung 3: Synthese von segmentierten thermoplastischen Polyurethanelastomeren mit langkettigen aliphatischen Hartsegmenten auf Pflanzenölbasis.[1]

Röntgenkristallstrukturuntersuchungen bestätigten, dass trotz der langen Methylensequenzen der zugrunde liegenden C_{19}- und C_{23}-Monomere und der daraus resultierenden reduzierten Urethangruppendichte in den aliphatischen Polyurethanhartsegmenten das Kristallisationsverhalten der harten Blöcke nach wie vor von der Bildung von Wasserstoffbrückenbindungen bestimmt wird. Dementsprechend lagen die Schmelzpunkte der hergestellten Poly(urethan-*b*-ether)blockcopolymeren deutlich über den Schmelzpunkten vergleichbarer polyesterbasierter thermoplastischer Elastomere und rangierten abhängig von der durchschnittlichen Länge der PU-19.19 bzw. PU-23.23 Hartsegmente zwischen 62 °C und 116 °C. Im Vergleich dazu lag der Schmelzpunkt eines zu TPU-C_{23}PPDO$_{2000}$-63wt% mit einem Molverhältnis von hartem zu weichem Diol von 1:1 äquivalenten thermoplastischen Polyurethanelastomers basierend auf PU-12.12 Polyurethanhartsegmenten mit ähnlicher Blocklängenverteilung, TPU-C_{12}PPDO$_{2000}$-59wt%, aufgrund seiner höheren Wasserstoffbrückenbindungsdichte mehr als 10 °C höher. Gleichzeitig enthüllten Untersuchungen der Phasenstruktur mittels Infrarotspektroskopie, dass thermoplastische Polyurethanelastomere mit Hartsegmenten basierend auf C_{19}- bzw. C_{23}-Monomeren im Vergleich zu TPU-C_{12}PPDO$_{2000}$-59wt% einen deutlich verbesserten Phasenseparationsgrad von über 85 %

aufwiesen. Alle hergestellten Materialien wiesen außerdem eine akzeptable bis gute Duktilität und gutes elastisches Verhalten auf, wobei beides mit zunehmender Polyurethanblocklänge abnahm und die besten Ergebnisse für Copolymere erzielt wurden, deren Hartsegmente kein hartes Diol als Kettenverlängerer enthielten und nur aus isolierten Diisocyanateinheiten bestanden. Des Weiteren enthüllte ein direkter Vergleich der mechanischen Eigenschaften von TPU-C_{23}PPDO$_{2000}$-63wt% mit TPU-C_{12}PPDO$_{2000}$-59wt%, dass die reduzierte Wasserstoffbrückenbindungsdichte in den aliphatischen Polyurethanhartdomänen einen negativen Einfluss auf das elastische Verhalten und die Duktilität hat.

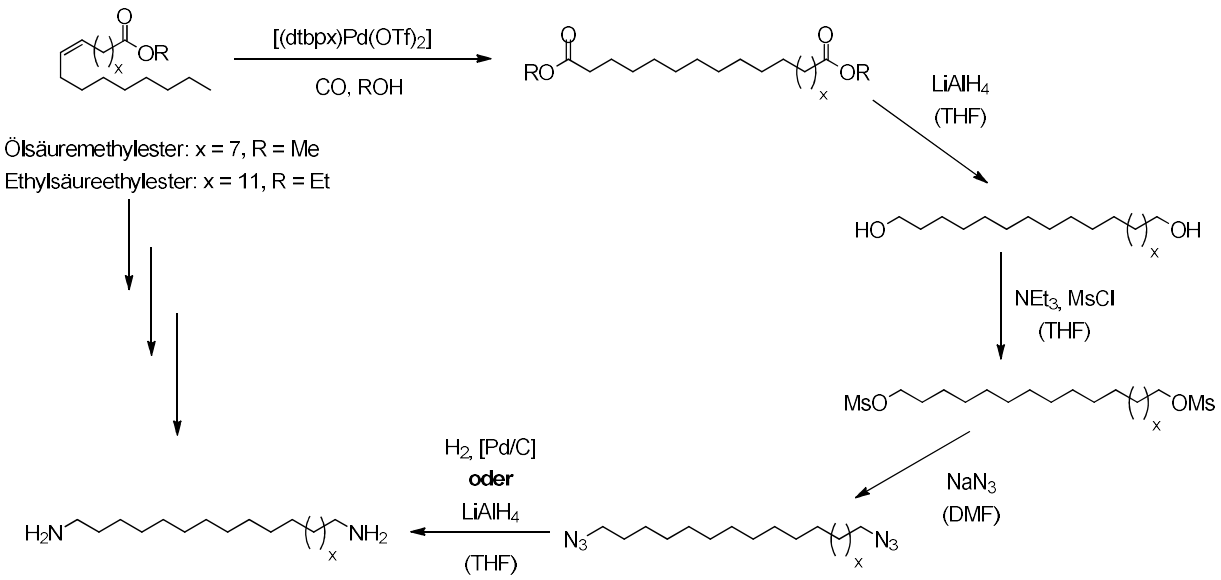

Abbildung 4: Mehrstufige Synthese von Nonadecan-1,19-diamin und Tricosan-1,23-diamin ausgehend von ungesättigten Fettsäureestern.

Des Weiteren wurden ausgehend von Methyloleat und Ethylerucat in einer mehrstufigen Synthese Nonadecan-1,19-diamin und Tricosan-1,23-diamin als Polyamidpräkursor für die Synthese von segmentierten thermoplastischen Polyamidelastomeren hergestellt (**Abbildung 4**). Entscheidender Schritt dabei war die Generierung von terminalen Aminogruppen aus den entsprechenden Aziden entweder durch Reduktion mit $LiAlH_4$ oder katalytische Hydrierung mit Hilfe von Pd/C. Letztere erwies sich als anfällig für Nebenreaktionen, was zur Verunreinigung des Produkts mit nicht entfernbaren Nitrilverbindungen und sekundären Aminen führte. Als entscheidende Faktoren für die Unterdrückung der Bildung von unerwünschten Nebenprodukten wurden die Katalysator- und

Substratkonzentration identifiziert. Vor allem letztere durfte einen Wert von 0,2 M nicht überschreiten, um eine finale Reinheit des gewünschten Produkts von über 98 % auch im 10 g Maßstab sicherzustellen, wobei Ausbeuten von bis zu 86 % erzielt werden konnten.

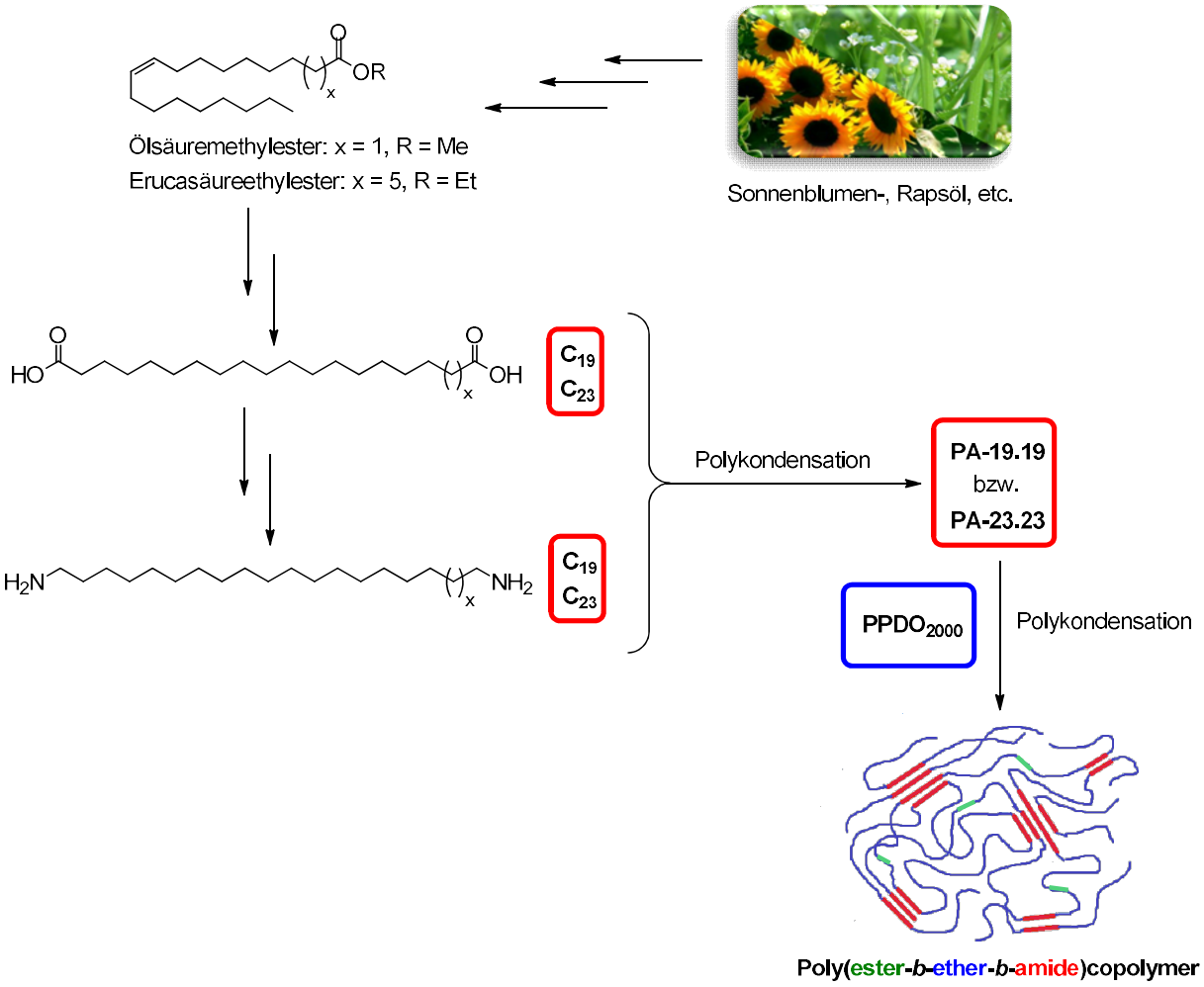

Abbildung 5: Synthese von segmentierten thermoplastischen Polyamidelastomeren mit langkettigen aliphatischen Polyamidhartsegmenten auf Pflanzenölbasis.[1]

Anders als bei vergleichbaren Materialien mit Hartsegmenten auf Polyester- oder Polyurethanbasis war für die Herstellung von pflanzenölbasierten thermoplastischen Polyamidelastomeren eine zweistufige Polymerisationsprozedur notwendig, was zu einer leicht veränderten Blocklängenverteilung in den Hartsegmenten führte. Polykondensation der im ersten Schritt erzeugten dicarboxyterminierten PA-19.19 und PA-23.23 Oligoamide mit einem Poly(1,3-propandiol) Polyetherweichsegment ($PPDO_{2000}$) resultierte in der Bildung von segmentierten

Poly(ester-*b*-ether-*b*-amid)copolymeren (PEEAs) (**Abbildung 5**) mit Molekulargewichten von bis zu 16,4 x 10^4 g mol^{-1}. Eine Untersuchung der Phasenstruktur der so hergestellten Multiblockcopolymere mittels FTIR-Spektroskopie bestätigte die physische Vernetzung über selektive Bildung von Wasserstoffbrückenbindungen zwischen Amidgruppen der Polyamidsegmente, was zu einem sehr hohen Mikrophasenseparationsgrad der Polyamidphase von der Polyether- und Esterphase von etwa 95 % führte. Eine Analyse der Kristallstruktur der harten Domänen mittels Röntgendiffraktometrie bestätigte außerdem, dass das Kristallisationsverhalten ausschließlich von der Ausbildung der Wasserstoffbrückenbindungen geprägt wird, während isolierte aliphatische C_{19} bzw. C_{23}-Diesterblöcke in der weichen Polyethermatrix gelöst blieben. Dementsprechend wiesen die hergestellten PEEAs abhängig von der durchschnittlichen Blocklänge der Polyamidhartsegmente im Vergleich zu strukturell ähnlichen thermoplastischen Elastomeren auf Polyester- oder Polyurethanelastomeren erhöhte obere Schmelzpunkte im Bereich von 128 °C bis 152 °C auf, wobei bei niedrigeren Temperaturen aufgrund der komplizierten polymorphen Kristallstruktur der Hartsegmente zusätzliche thermische Übergänge beobachtet werden konnten. Aufgrund der reduzierten Wasserstoffbrückenbindungsdichte in den kristallinen Polyamiddomänen, entsprach dies dennoch einer drastischen Reduktion des Schmelzpunkts von ca. 30 °C relativ zu ansonsten vergleichbaren thermoplastischen Polyamidelastomeren auf Basis kurzkettiger aliphatischer Polyamide, wie ein Vergleich zwischen pflanzenölbasiertem, langkettigem TPA-C_{23}PPDO$_{2000}$-65wt% und PA-12.12-basiertem TPA-C_{12}PPDO$_{2000}$-62wt% zeigte. Zusätzlich zur einfacheren thermoplastischen Verarbeitung wirkte sich die reduzierte Wasserstoffbrückenbindungsdichte positiv auf die Tendenz zur Feuchtigkeits- und Wasseraufnahme der hergestellten Materialien aus. Vor allem unter nassen Bedingungen absorbierte ein thermoplastisches Polyamidelastomer basierend auf PA-23.23 Hartsegmenten nur etwa 33 % der Menge an Wasser, die ein vergleichbares Polymer basierend auf PA-12.12 Blöcken unter gleichen Bedingungen aufnahm. Im Vergleich zu den anderen untersuchten segmentierten thermoplastischen Elastomeren auf Pflanzenölbasis waren die hergestellten Poly(ester-*b*-ether-*b*-amide) generell weniger duktil und ihr elastisches Verhalten und Rückstellvermögen erwies sich als stark abhängig von der exakten Zusammensetzung des untersuchten Materials. Während PEEAs mit einem Polyetherweichsegmentanteil von über 75 gew.% nach 10 Zyklen konsekutiver Dehnung um 100 % eine verbleibende Restdehnung von weniger als 10 % aufwiesen, stieg dieser Wert auf etwa 20% für Copolymere mit etwa 65 gew.% Polyetheranteil. Materialien mit einem noch geringeren Weichsegmentanteil zeigten kein elastisches Verhalten unter den gewählten Testbedingungen. Ein Ersetzen der langkettigen PA-23.23-basierten

Hartsegmente in TPA-C_{23}PPDO$_{2000}$-65wt% durch PA-12.12-basierte Hartsegmente mit ähnlicher Blocklängenverteilung aber höherer Wasserstoffbrückenbindungsdichte in TPA-C_{12}PPDO$_{2000}$-62wt% resultierte in einer höheren Duktilität aber reduziertem elastischen Verhalten.

[1] Photograph of *crambe abyssinica* by Kurt Stüber by distributed under a CC-BY 2.0 license and of *Helianthus annuus* by Frank Vincentz under a GNU license for free documentation.

Table of Contents

List of Abbreviations

Equipment and Methods

DSC	Differential scanning calorimetry
FTIR	Fourier transformation infrared spectroscopy
GPC	Gel permeation chromatography
NMR	Nuclear magnetic resonance
WAXD	Wide-angle X-ray diffraction

NMR-Spectroscopy

br	Broad
s	Singlet
d	Doublet
t	Triplet
q	Quartet
quint.	Quintet
m	Multiplet
$^{n}J_{xy}$	Coupling constant of atom X and Y over n bounds
ppm	Parts per million
δ	Chemical shift in ppm

Tensile Testing

E_t	Young's modulus
ε_b	Elongation at break

Compounds

DBTDL	Dibutyltin dilaurate
dtbpx	1,2-Bis[(di-*tert*-butylphosphino)methyl]benzene
PA-X.Y	Polyamide derived from linear aliphatic C_x-diamine and C_y-diacid
PEBA	Poly(ether-*b*-amide)
PEEA	Poly(ester-*b*-ether-*b*-amide)

PE-X.Y	Polyester derived from linear aliphatic C_x-diol and C_y-diacid
$PPDO_n$	Poly(1,3-propanediol) with an average molecular weight of *n* g mol^{-1}
$PTMG_n$	Poly(tetramethylene ether) glycol with an average molecular weight of *n* g mol^{-1}
PU-X.Y	Polyurethane derived from linear aliphatic C_x-diol and C_y-diisocyanate
TCE	1,1,2,2-Tetrachloroethane
TPA	Thermoplastic polyamide elastomer
TPC	Thermoplastic copolyester elastomer
TPE	Thermoplastic elastomer
TPU	Thermoplastic polyurethane elastomer

Other abbreviations

DP_n	Degree of polymerization = M_n/M_0 (M_0 molecular weight of the repeat unit)
mol%	Mol fraction
M_n	Number average molecular weight
M_w	Weight average molecular weight
M_w/M_n	Molecular weight distribution
T_c	Crystallization temperature
T_g	Glass transition temperature
T_m	Melting temperature
wt.%	Percentage by mass

1. General Introduction

Synthetic polymers are an integral part of our modern life, with applications ranging from everyday items like food packaging, clothes, and shoes to sophisticated composite materials vital for the construction of airplanes or modern medical technology devices. However, the vast majority of polymeric materials is derived from petrochemicals, and even though polymer manufacturing accounts for less than 10% of worldwide oil and gas production,[1] in a world where fossil fuel reserves are dwindling the idea of producing polymers from renewable biomass is gaining more and more traction. Thanks to intense research, today platform monomers like ethylene or ethylene glycol can be readily produced from agricultural feedstocks like corn, wheat, or sugar cane, and renewable polyethylene (Bio-PE) as well as partly bio-derived polyethylene terephthalate (Bio-PET) have become commercially available.[2] However, in addition to replacing standard petrochemicals in the production of already well-established polymers, the unique chemical compounds found in plants, fungi, and animal products also offer the opportunity to develop bio-based polymers with novel sets of material properties. For example, renewable polylactic acid has been used in biodegradable medical appliances and in food-related applications for decades.[3] Similarly, technologically relevant polyamide 11 is prepared from castor oil on a large industrial scale.[4] Still, the exploration of the full potential of biomass as a monomer source for the development of novel synthetic polymers is far from complete and research into materials derived from carbohydrates, triglycerides, proteins, and other bio-based compounds like *e.g.* terpenes is ongoing.[5] In this context, unsaturated fatty acids from plant oils have garnered much interest in recent years as their long hydrocarbon chains and internal olefinic double bonds make them interesting substrates for the preparation of a new type of linear aliphatic polycondensation monomers with a long aliphatic backbone. Thanks to recent advances in catalyst research, it is now possible to selectively convert unsaturated fatty acid substrates into linear long-chain α,ω-difunctionalized compounds[6],[7] that provide access to novel long-chain aliphatic polycondensates like polyesters,[7e-g],[8] polyamides,[7f, g],[8a] and polyacetals[9] with very low functional group densities and, in some cases, polyethylene-like crystallinity,[7f, g],[8b],[10] giving them the potential to bridge the gap between aliphatic polyolefins and traditional polycondensates. However, so far research regarding the utilization of bio-derived long-chain polycondensation monomers has mostly been limited to the synthesis of thermoplastics,[8a, b] while their application in more complex polymeric materials like thermoplastic elastomers has not yet been systematically studied.

1.1. Thermoplastic Elastomers

1.1.1. Definition and general structure

Thermoplastic elastomers (TPEs) are a relatively new class of polymeric materials that have only been introduced to the rubber/plastics market in the 1950's.[11] However, due to their unique set of material properties as well as their chemical versatility, they have experienced steady growth in market size ever since then. Today, their total production value amounts to an estimated USD 20 billion (2021)[12] and they find widespread application in such varied areas as *e.g.* electronics, clothing, automotive components, medical devices, adhesives, coatings, and tubing.[13]

As their name indicates, TPEs bridge the gap between thermoplastics and conventional elastomers by combining many of the advantageous properties of both types of polymeric materials. At service temperature TPEs exhibit the elastomeric behavior, ductility, and flexibility characteristic for vulcanized rubbers; however, unlike vulcanized rubbers that rely on the formation of irreversible covalent bonds between polymer chains for crosslinking to obtain their elastomeric properties and can therefore no longer be processed once the material is shaped and cured, TPEs instead possess thermoreversible crosslinks that dissolve at sufficiently high temperatures and reform upon cooling. As a result, TPEs can be melt processed as thermoplastics, which allows for the application of high throughput plastic processing techniques like extrusion and injection molding as well as the recycling of scrap material.[11a],[13] The nature of these thermoreversible crosslinks varies and can include thermally unstable covalent bonds,[14] but most TPEs rely on physical forces like ionic interactions,[11a],[15] interphase interactions, coalescence of glassy domains, or crystallite formation due to *e.g.* hydrogen bond formation for crosslinking.[11a],[13] They are generally phase-separated systems consisting of at least one type of thermoplastic hard phase in which the physical crosslinks are concentrated and an amorphous elastomeric soft phase that provides the material with flexibility and elasticity.[11a]

Polymeric materials with this type of multiphase morphology can be obtained by blending a thermoplastic with a (partly) vulcanized rubber, however most TPEs are block copolymers comprised of so-called 'hard' and 'soft' blocks that are thermodynamically incompatible at ambient temperatures and therefore microphase-separate in the final product, resulting in a multiphase morphology where high melting thermoplastic hard domains are embedded in a continuous elastomeric soft phase (**Figure 1.1**).[11a],[13],[16]

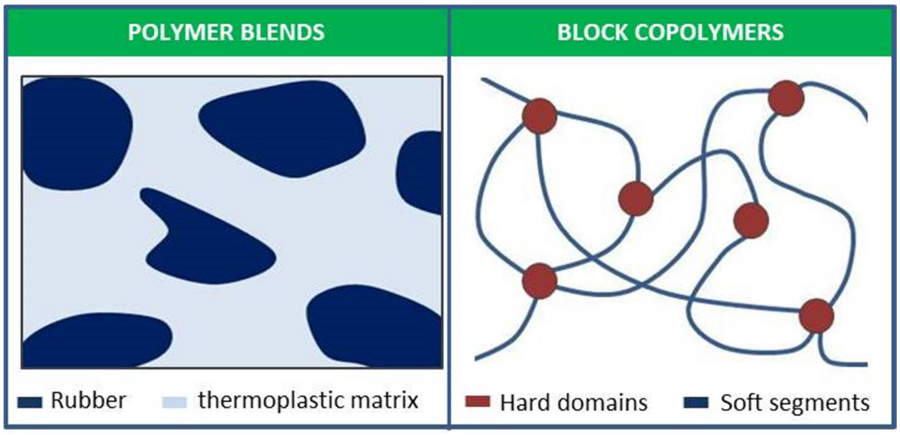

Figure 1.1: General morphological structure of TPE blends (left) and block copolymers (right).

Depending on their exact chemical structure, these copolymer TPEs can be further divided into two main groups [13] (though other less relevant types of copolymer TPEs like ionomers,[15] or star block polymers[17] also exist): The first group is comprised of styrenic ABA triblock copolymers like the widely used poly(styrene-b-butadiene-b-styrene) (SBS) rubber which are usually obtained via chain-growth polymerization reactions like multi-step anionic polymerization or transfer radical polymerization to produce polymers with a defined ABA-type structure. [16],[18] Physical crosslinking in these materials is provided by the formation of high melting, glassy polystyrene domains that are a result of the agglomeration of the styrene end blocks, while the comonomer blocks form the elastomeric soft phase.[16] The other major group of copolymer TPEs - which are of special interest for this thesis - are linear segmented multiblock copolymers based on crystallizable polyester,[19] polyurethane,[20] or polyamide[21] hard segments of varying block lengths that alternate repeatedly with amorphous, low-melting polyester or polyether soft segments like poly(tetramethylene ether) glycol (PTMG)[13] whose thermodynamic incompatibility with the hard blocks at ambient temperatures ensures microphase separation in the final product (**Figure 1.2**).[11a]

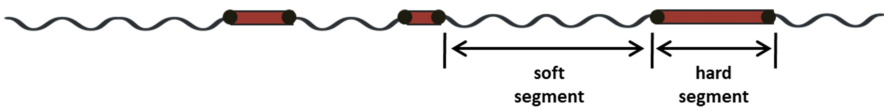

Figure 1.2: Schematic representation of linear segmented copolymer TPEs.[19a]

Synthesis approaches employed to obtain these materials vary depending on the chemical nature of the employed hard and soft blocks, but in general most segmented copolymer TPEs are prepared via classical step-growth polymerization reactions in which either a preprepared crystallizable oligomeric hard segment or the respective hard difunctionalized polycondensation monomers are copolymerized with a soft amorphous macrodiol to form a segmented block copolymer with a (-A-B-)$_n$-type multiblock structure (**Scheme 1.1**).[13],[22]

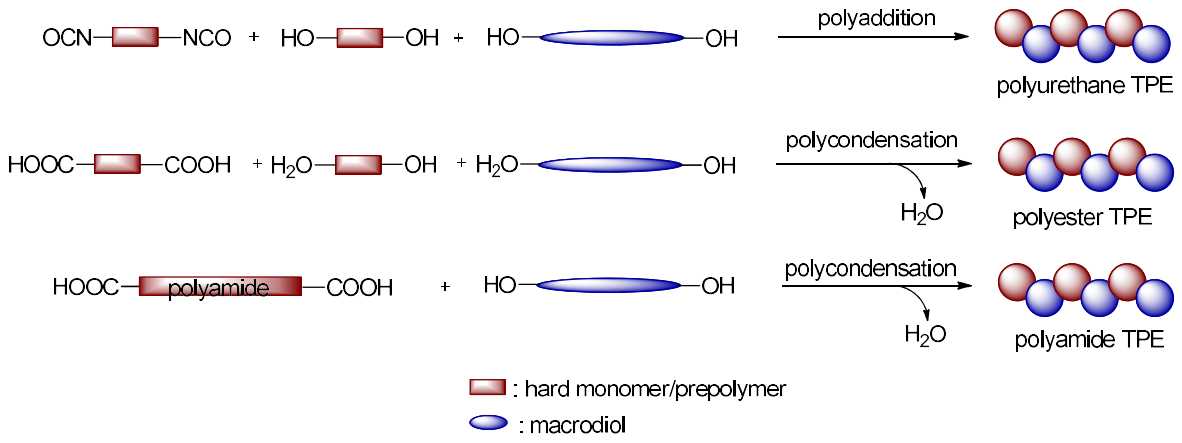

Scheme 1.1: Schematic representation of the most common synthesis routes for the preparation of common segmented copolymer thermoplastic elastomers.

Just like with the formation of glassy polystyrene domains in ABA triblock TPEs, the hard blocks in segmented copolymer TPEs agglomerate to form rigid, typically crystalline thermoplastic hard domains that are embedded in the continuous soft matrix generated by the amorphous soft blocks. Driving force for the agglomeration of the polyester,[11a],[19],[23] polyamide,[11a],[21] or polyurethane[11a],[20] hard blocks respectively are attractive intermolecular forces acting between polymer chains. In case of polyamide- and polyurethane-based materials, this happens via the formation of hydrogen bonds between their respective functional groups, while commercially available polyester-based TPEs typically rely on the incorporation of rigid, planar aromatic rings in the polymer backbone to improve crystallization conditions and maximize cohesive forces acting between polyester hard segments. Crystallization of the linear hard blocks happens in ordered arrays that eventually grow into small crystallites and form (semi)crystalline hard domains embedded within the continuous soft matrix (**Figure 1.3**). These crystalline hard domains provide the material with physical crosslinking and, on a macroscopic level, account for the TPE's mechanical stability and stiffness as well as

determining the polymer's upper service temperature, melting point, and thermoplastic behavior. The soft blocks, on the other hand, are responsible for the material's softness, flexibility, and elasticity as well as its low-heat performance and lower service temperature.[11a],[13],[22a]

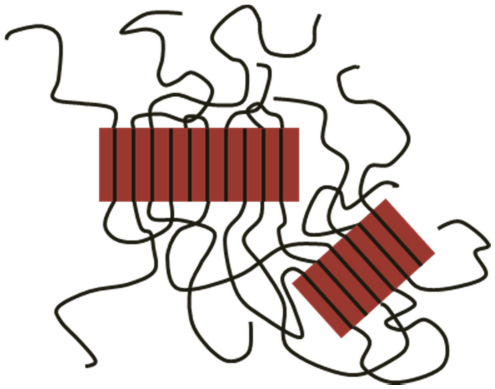

Figure 1.3: Schematic representation of the morphology of segmented block copolymer TPEs as proposed by Cella:[22a] (thick line) hard blocks, (~~) soft blocks.

1.1.2. Thermal properties of segmented copolymer thermoplastic elastomers

Segmented copolymer thermoplastic elastomers generally possess several distinct melt and/or glass transition points that roughly correspond to the respective thermal transitions observed for the different homopolymer blocks they are comprised of. If phase separation is complete, meaning if no hard blocks remain dissolved in the soft phase and no co-crystallization of soft segments within the hard domains occurs, the glass transition temperature and lower service temperature of the material are identical to the glass transition point observed for the pure oligomeric soft segment, while the upper service temperature and upper melting point of the TPE approach the melting point of the thermoplastic on which the hard segments are based.[11a],[13],[22a] However, in reality phase separation is often far from complete and the degree of phase separation found in a specific polymer sample can vary depending on the sample's thermal history as well as the exact polymer composition, especially the lengths of the different blocks and the ratio of hard to soft phase.[11a],[22a] For example, extensive DSC experiments conducted on a variety of segmented polyester TPEs based on terephthalic acid-derived hard blocks and poly(tetramethylene ether) glycol soft segments[22a] have shown that with increasing content of hard phase and hard block lengths the material's glass transition temperature eventually rises drastically, indicating that once a certain threshold is reached the hard blocks can no

longer be fully incorporated in the crystalline lattice due to chain entanglement and the increasing viscosity of the polymer melt inhibiting chain mobility. Consequently, a portion of the hard blocks remains dissolved in the soft phase, leading to higher glass transition temperatures. In case of the segmented polyester TPEs studied by Cella,[22a] the glass transition temperature of the PTMG soft phase (T_g = - 79 °C) saw little change for a hard phase content of up to about 30 wt.%. However, once the a hard phase content rose to 50 wt.% an increase in the T_g by about 10 °C was observed, and for polymers containing 75 wt.% of polyester hard phase the T_g increased by about 80 °C. In addition, a lower degree of phase separation generally leads to a broadening of the melting peaks observed during DSC experiments and in overall lower melting points being recorded for the hard phase because cocrystallization of soft segments in the hard domains disrupts crystallization of the hard blocks.[11a],[22a] On the other hand, as long as phase separation is not compromised, an increase in the average hard block length, which especially for segmented copolymer TPEs often goes hand in hand with an overall higher mole content of hard monomers, leads to more favorable crystallization conditions for the hard segments and therefore higher upper melting points whose values symptotically approach the melting points recorded for the thermoplastic homopolymers.[19c],[22a]

1.1.3. Mechanical properties of segmented copolymer thermoplastic elastomers

As for the tensile properties of copolymer TPEs, the exact values recorded for parameters like the Young's modulus, yield strain, or elongation at break vary widely depending on the composition of the material but also on outside factors like annealing conditions and test parameters applied during tensile testing. In case of segmented copolymer TPEs, determining structural parameters include the nature of physical crosslinking, the average block length of both the hard and soft segments, as well as the ratio of hard to soft phase. However, while the quantitative aspects of the recorded stress-strain curves differ, qualitatively the same general observations can be made for all segmented copolymer TPEs: When the material is elongated, the ordered arrays formed by the hard blocks inside the rigid thermoplastic domains stay initially intact while the continuous crystalline matrix undergoes pseudo-elastic deformation (**Figure 1.4**, **region I**). High Young's moduli (E_i) are recorded at this stage, and below elongations of about 10% the deformation is largely reversible and little to no hysteresis is observed in cyclic deformation tests.

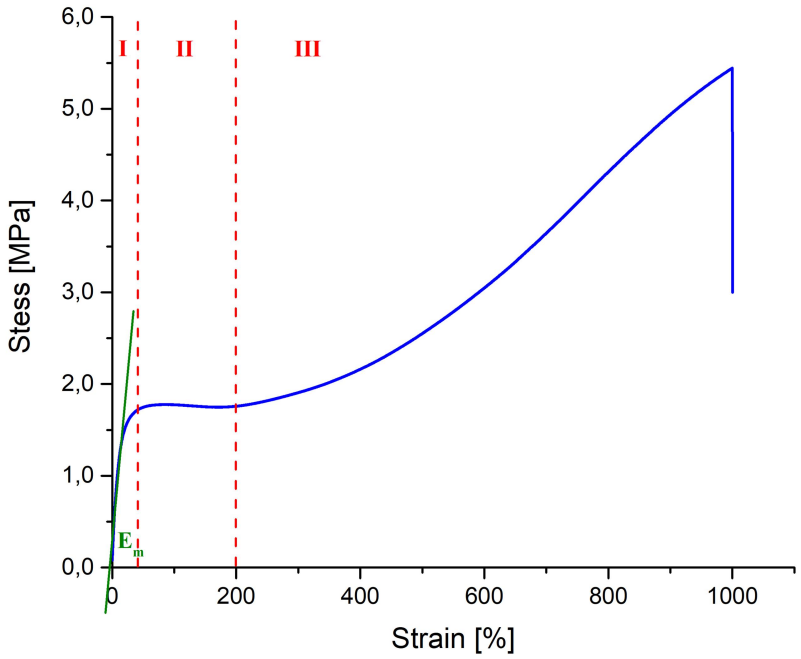

Figure 1.4: Exemplary stress-strain curve of a typical segmented thermoplastic elastomer showing three main regions of response.

If the material is stretched further it eventually reaches its yield point at which the deformation of the crystalline matrix reaches its limits. After this point, stress relief within the polymer is achieved by extensive crystallite reorientation, which results in a draw plateau being observed in the strain-stress curve (**Figure 1.4, region II**) However, this process involves an irreversible change in polymer morphology as the alignment of the hard blocks within the hard domains is disrupted and a dissipation of energy occurs. Consequently, the test specimen is no longer capable of completely recovering its original shape and dimensions, therefore exhibiting a pronounced hysteresis during cyclic deformation tests as well as increasing levels of permanent set after relaxation (**Figure 1.5**). Once realignment of the crystallites is complete, the draw plateau ends and further elongation slowly but steadily requires ever increasing amounts of force as the applied stress is now primarily transmitted by the continuous elastomeric soft phase, which results in the stress-strain curve of the TPE now resembling the more or less linear curve of a conventional elastomer (**Figure 1.4, region III**). Finally, when the soft phase eventually fails, the test specimen breaks.[11a],[22a]

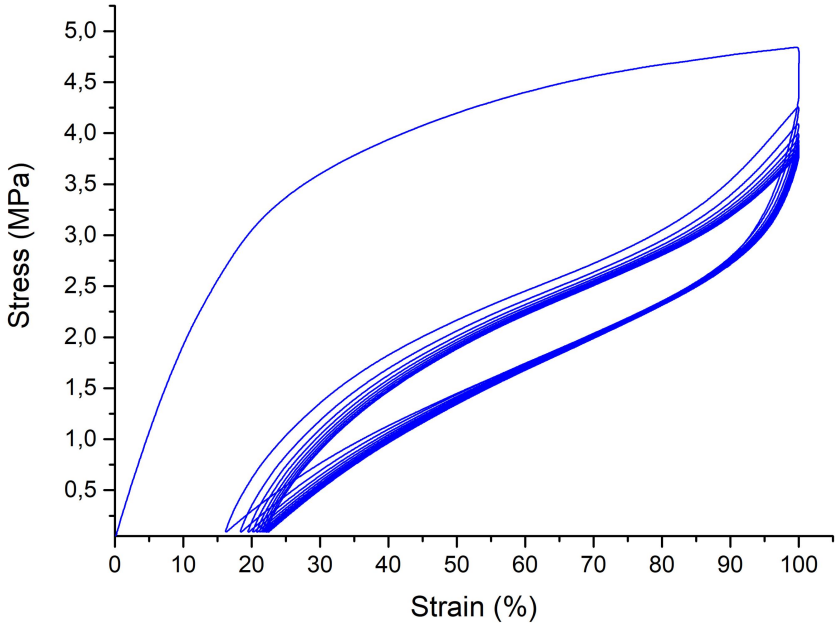

Figure 1.5: Exemplary stress-strain curve from the cyclic deformation test of a segmented thermoplastic elastomer with pronounced hysteresis (10 cycles displayed).

The value calculated for the Young's modulus of a TPE provides a measure of the force required to deform the polymer's crystalline matrix, while the recorded yield stress can be used to determine the force necessary to reorient the crystallites of the hard domains. Accordingly, the values for both parameters increase with increasing content of crystallizable hard segments as the overall degree of crystallinity rises and the crystallites become larger until the crystalline nature of the hard phase becomes dominant, at which point stress-strain curves increasingly resemble the curve of a typical glassy or crystalline thermoplastic. This usually includes erratic draw behavior, a pronounced yield point, and breaking at relatively low elongations. The stress-strain curves of TPEs with a very low hard phase content on the other hand typically more resemble the stress-strain curves recorded for classic elastomers, with values for Young's moduli being low and no pronounced yield being observed.[11a],[22a]

1.1.4. Renewable feedstocks as a potential monomer source

As with other types of polymers, thermoplastic elastomers are still predominantly produced from petrochemicals. However, research in the utilization of biomass as a monomer source is ongoing.[24] For example, various at least partly biomass-derived analogues to the widely used petroleum-derived poly(styrene-b-butadiene-*b*-styrene) (SBS) and poly(styrene-*b*-isoprene-b-styrene) (SIS) ABA-triblock copolymer TPEs have been developed in recent years.[24],[25] In context of segmented copolymer TPEs, the majority of sustainable monomers prepared from renewable feedstocks - especially on an industrial scale - are amorphous macrodiols for the generation of soft segments, as transforming oxygen-rich biomass like saccharides and triglycerides into low-molecular weight aliphatic diols or dicarboxylic acids that can subsequently be converted into amorphous polyester or polyether macrodiols is typically comparatively easy.[26] Consequently, a wide variety of linear and branched macrodiols have been synthesized from biomass and their utilization as soft segments in segmented copolymer TPEs have been explored extensively.[26],[27] In relation to plant oils, a notable example for a fatty acid-derived, branched polyester macrodiol is polyricinoleate diol (**Figure 1.6**) prepared via the polycondensation of castor oil-derived methyl ricinoleate and diethylene glycol, which, on a laboratory scale, has been successfully used as a soft segment in renewable thermoplastic polyurethane elastomers.[28] However, on an industrial scale, unsaturated fatty acids from plant oils and their triglycerides are rarely used to synthesize macrodiols, instead they are typically converted into polyols with at least three alcohol functionalities that find application in the preparation of covalently linked thermosets and elastomers, especially in polyurethane chemistry for the generation of polyurethane foams.[26],[27]

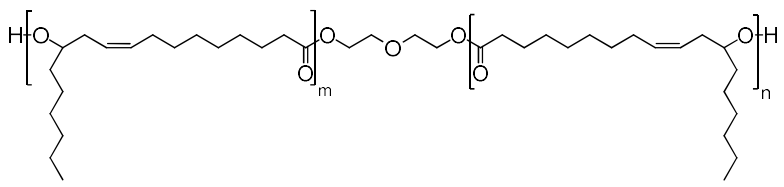

Figure 1.6: Schematic representation of a ricinoleic acid-derived macrodiol.[28]

Instead, the market for renewable amorphous macrodiols is dominated by linear polyesters and polyethers derived from saccharides like glucose or, in some cases, synthesized from plant oil-derived glycerol as these bio-based macrodiols are often identical to or mimic the properties of similar

already established petroleum-based polyether and polyester macrodiols.[26] For example, commonly employed poly(ε-caprolactone) can today be synthesized from corn-derived bio-ethanol,[29] and succinic acid obtained from the fermentation of corn-derived glucose[30] can be converted into polyester macrodiols that have the potential to replace similar petroleum-derived adipic acid-based macromonomers.[26],[31] Similarly, a variety of bio-derived amorphous polyethers that constitute green alternatives to their petroleum-derived analogues are produced on an industrial scale by an ever increasing number of companies and are therefore today commercially available.[26] In order to produce these "green" polyether macromonomers, five and six carbon sugars either extracted directly from crops like sugarcane or obtained through the hydrolysis of more complex carbohydrates like starch and cellulose or, in some cases, glycerol obtained from plant oils serve as a starting material to produce short-chain aliphatic diols like ethylene glycol,[32] 1,3-propanediol,[33] and 1,4-butanediol.[34] These aliphatic diols can then either be directly employed as chain extenders in the generation of partly renewable polyester and polyurethane hard segments[26] or are used as monomers for the production of bio-derived macrodiols like "green" polyethylene glycol (PEG),[26],[35] poly(1,3-propanediol) (PPDO),[34a],[36] and poly(tetramethylene ether) glycol (PTMG) (**Figure 1.7**).[26],[37]

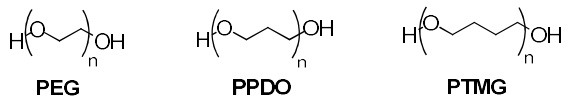

Figure 1.7: Structures of PEG (left), PPDO (center), and PTMG (right).

Of these, PEG and PTMG have been thoroughly investigated regarding their utilization as soft segments in the past because both polyethers are also readily available and cheap to produce from fossil fuels and petroleum-derived versions of both are therefore well-established macromonomers in the industrial production of TPEs. In contrast, PPDO constitutes a comparatively new addition to the polyether macromonomer family as it is not as readily available from fossil fuels and generally more costly to produce. Consequently, its utilization as a soft segment in TPEs has not yet been thoroughly investigated despite the fact that PPDO has the potential to fill the gap between hydrophobic, comparatively high-melting PTMG and water-soluble, low-melting, but relatively unstable PEG. However, comparatively cheap "green" PPDO produced from typically corn-derived glucose in a multistep process (**Scheme 1.2)** has recently become commercially available and is today sold under the trademark Cerenol® by DuPont.[36e],[38]

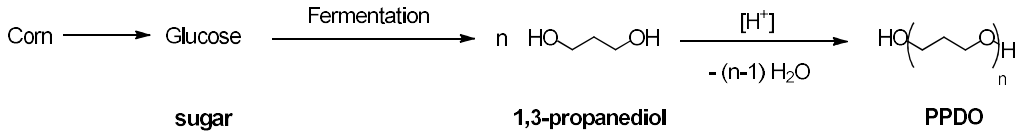

Scheme 1.2: Multistep synthesis of renewable poly(1,3-propanediol) (PPDO) from biomass.[36c]

In comparison, replacing petroleum-derived hard monomers suitable for the generation of (semi-)crystalline hard segments in segmented copolymer TPEs with bio-based building blocks is generally more challenging. This is especially true for TPEs based on polyester or polyurethane hard segments as the respective hard blocks in these materials typically rely on six ring aromatic dicarboxylic acids and diisocyanates respectively in combination with short-chain aliphatic diols to produce materials with adequate properties.[13] And while short-chain aliphatic diols are comparatively easy to prepare from biomass,[21] aromatic compounds like terephthalic acid and 4,4'-methylenediphenyl diisocyanate (MDI) are not, though processes to access terephthalic acid from renewable feedstocks have been developed in recent years.[2] As an alternative, terephthalic acid can be replaced with biomass-derived 2,5-furandicarboxylic acid as the chemical structure of this compound with its five carbon aromatic ring is similar (**Figure 1.8**)[39] and significant progress in the synthesis of furan dicarboxylic acid-based polyesters suitable for serving as hard segments in thermoplastic polyester elastomers (TPCs) has been made in recent years.[40]

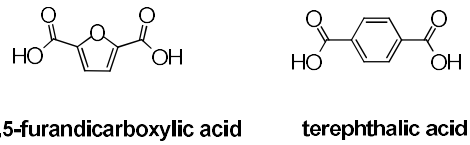

Figure 1.8: Structure of 1,5-furandicarboxylic acid and. terephthalic acid.

In contrast, bio-based difunctionalized monomers suitable for the generation of crystallizable aliphatic polyamide hard segments are relatively easy to access, especially from unsaturated fatty acids from plant oils. Pyrolysis and alkali fusion for the conversion of castor oil-derived ricinoleic acid into either 11-aminoundecanoic acid (C_{11})[41] or sebacic acid (C_{10})[41],[42] for the generation of PA-11 and *e.g.* PA-6.10 hard blocks respectively have been well established on an industrial scale for decades (**Scheme 1.3**),[11a],[41a],[43] and a series of renewable PA-11-based poly(ether-*b*-amide) TPEs have been commercialized by Arkema Company under the trademark PEBAX®.[11a],[43b]

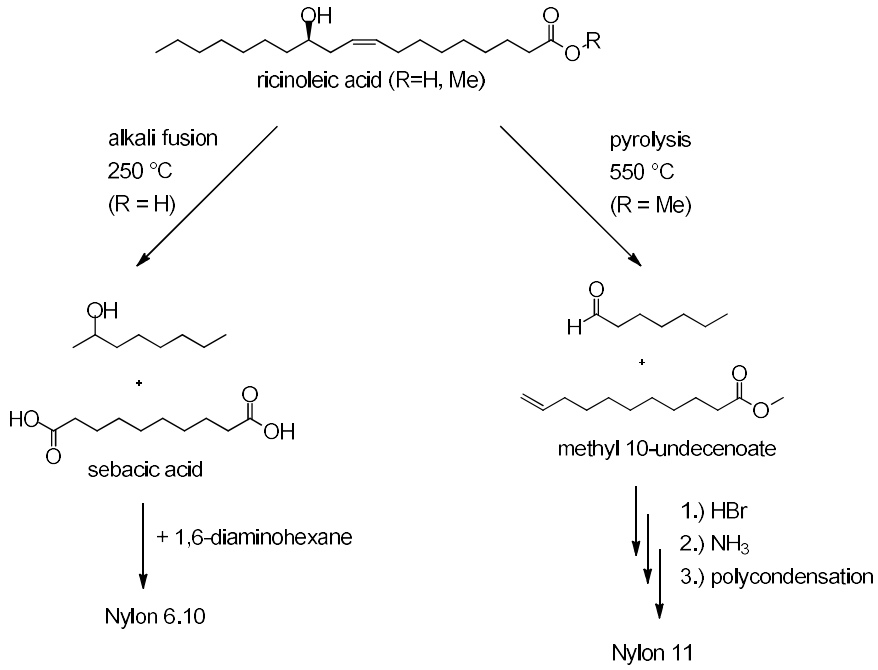

Scheme 1.3: Monomer and polymer generation from castor oil-derived ricinoleic acid derivatives via alkali fusion (left pathway) and pyrolysis (right pathway).

Other suitable short- to mid-chain aliphatic monomers like azelaic acid (C_9) and brassylic acid (C_{13}) are accessible from unsaturated fatty acids like oleic acid and erucic acid respectively via either ozonolysis[44] or oxidative cleavage of the olefinic double bond using an oxidizing agent like hydrogen peroxide.[45] However, in all of these processes the linear fatty acid hydrocarbon chain is cut roughly in half and only a part of it is incorporated into the final product, while the other half forms less valuable coupling products. As a result, the chain lengths of the thus obtained α,ω-difunctionalized aliphatic polycondensation monomers do not exceed thirteen carbon atoms, thereby wasting the potential of the long fatty acid hydrocarbon chain to possibly induce polyethylene-like crystallinity into especially polyester-based materials[7e],[8a],[10] and to allow for the design of novel all-aliphatic segmented copolymer TPEs with new sets of material properties. In order to maximize feedstock utilization and explore the full potential of unsaturated fatty acids as a monomer source, other synthesis approaches are required. But thanks to recent advances in catalyst research, it is now possible to selectively convert unsaturated fatty acid substrates from plant oils into various linear long-chain α,ω-difunctionalized polycondensation monomers that contain at least 18 carbon atoms[6],[7] and are potential monomers for the generation of a new type of renewable, aliphatic polyester,[7e-g],[8] polyamide,[7e, 8a] and polyurethane hard blocks in segmented copolymer TPEs.

1.2. Isomerizing Alkoxycarbonylation and Long-Chain Aliphatic Monomers

In theory, there are many different ways to synthesize linear α,ω-difunctionalized compounds with a long aliphatic hydrocarbon backbone, including classic organic synthesis.[8a] However, while step by step build up reactions starting from low molecular weight petroleum-derived building blocks can be used to prepare linear aliphatic polycondensation monomers containing up to 192 carbon atoms,[46] these multistep synthesis procedures are very laborious, inefficient, and the purification of the desired product becomes more and more complicated the more the chain length of the product increases, making classic organic synthesis only viable on a small laboratory scale.[8a] In contrast, synthesis approaches starting from plant oil-derived unsaturated fatty acids that strive to incorporate the characteristic long fatty acid hydrocarbon chain in its entirety into the final product have proven to be much more practical. These approaches include biocatalytic ω-oxidation,[6],[47] olefin metathesis,[48] and catalytic isomerizing ω-functionalization reactions like isomerizing hydroformylation,[6],[49] isomerizing hydroboration,[6],[50] and isomerizing silylation.[6],[51] However, the synthesis approach that has probably proven to be the most effective method for converting unsaturated fatty acid substrates from plant oils[52] and microbial oils[53] into linear long-chain α,ω-difunctionalized compounds suitable to serve as polycondensation monomers is isomerizing alkoxycarbonylation (**Scheme 1.4**).[7a-e]

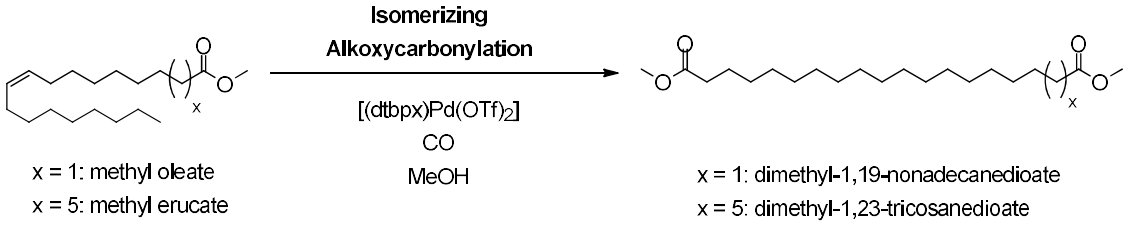

Scheme 1.4: Isomerizing alkoxycarbonylation of methyl oleate and methyl erucate with CO and methanol facilitated by a Pd(II)-based catalyst.[7e]

Alkoxycarbonylation reactions as a whole are a well-known and mechanistically well-understood way of converting olefinic double bonds into ester groups[6],[54] and are already used on an industrial scale *e.g.* as part of a new process for the commercial production of methyl methacrylate from ethylene.[55],[56] However, first reports about the capability of Pd(II)-based catalysts to isomerize

internal olefinic double bonds and selectively convert them into terminal ester groups were only published in 2001, when Pugh *et al.*[57] demonstrated that, under comparably mild conditions (115 °C, 30 bar CO), *in situ* Pd(II) catalyst systems containing bulky, electron-rich bisphophine ligands are capable of transforming the internal olefinic double bond of various linear C_{14}-olefins into a terminal ester group, thereby converting the different substrates into methyl 1-pentadecanoate regardless of the position of the double bond in the substrate hydrocarbon chain . Another major breakthrough was achieved when it was discovered that the selectivity for the terminal position could be increased from 70-80 %[57] to 94 %[7b] by employing 1,2-bis[(di-tert-butylphosphino)methyl]benzene (dtbpx) as a ligand, a discovery that was soon followed by Cole-Hamilton and coworkers[7a] proving that the same *in situ* catalyst system is also capable of converting methyl oleate into dimethyl 1,19-dodecanedioate with selectivity for the linear product exceeding 95 %, thereby proving that isomerizing alkoxycarbonylization can also be applied to functionalized alkenes in general and fatty acid esters in particular. This includes, polyunsaturated substrates like methyl linoleate and methyl linoleate, though selectivity for the corresponding unsaturated linear diesters is significantly reduced.[7a],[58],[59] Further optimization of the reaction conditions (90 °C, 20 bar CO)[7f, g] and application of $[(dtbpx)Pd(OTf)_2]$[7e] as a defined catalyst precursor instead of an *in situ* system resulted in an increase of catalyst productivity by 30-50 % for the conversion of monounsaturated fatty acid esters like methyl oleate and ethyl erucate[7e-g],[60] and also opened up the possibility of catalyst recycling.[61]

Extensive experimental and theoretical studies into the isomerizing alkoxycarbonylation of methyl oleate including DFT calculations as well as dedicated NMR experiments were conducted in order to investigate the mechanism of the reaction and explain its high selectivity for functionalization of the ω-position in fatty acid substrates.[6],[7d],[58],[60],[62],[63] It was found that during the reaction linear (**B1**) as well as branched (**B2**) alkyl-Pd species can be formed which can both undergo subsequent carbon monoxide insertion to generate the corresponding acyl complexes **C1** and **C2**. However, because of the significantly higher energy barrier, the branched acyl complex **C2** resists subsequent irreversible alcoholysis to form a branched diester product. Instead, the insertion and isomerization steps leading up to the formation of **C2** are reversed until eventually the linear pathway is followed, alcoholysis takes place, and the linear α,ω-diester is formed (**Scheme 1.5**).

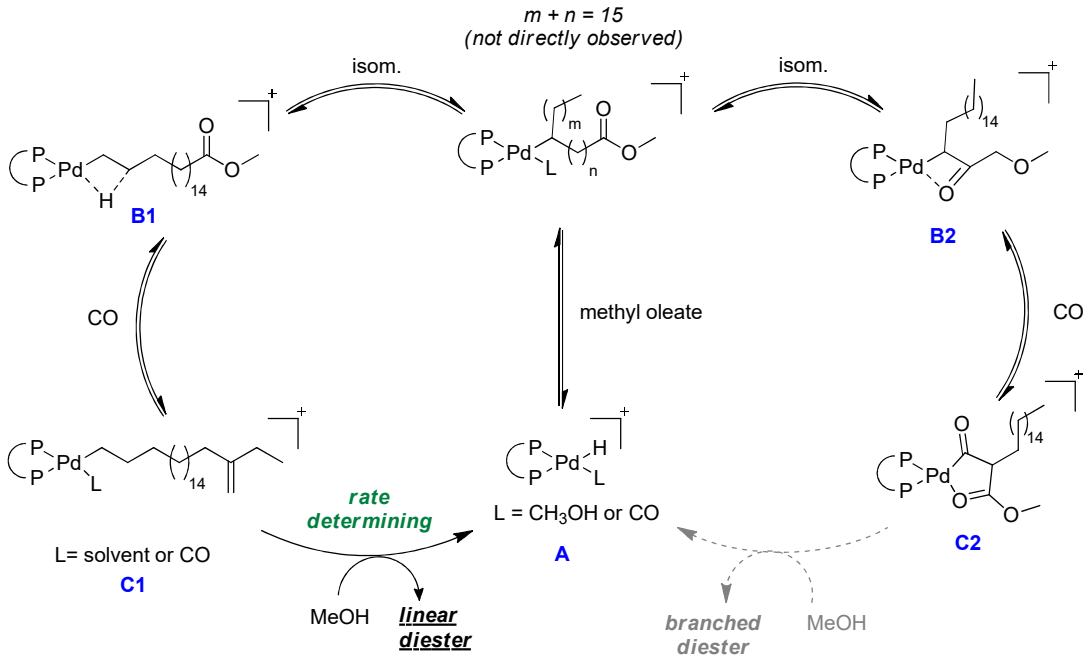

Scheme 1.5: Major pathways of the isomerizing alkoxycarbonylation of methyl oleate catalyzed by [(dtbpx)Pd(OTf)$_2$] as suggested by various mechanistic studies.[6],[7d]

Further experimental studies have also found that isomerizing alkoxycarbonylation generally is also very tolerant towards impurities and that selectivity for the linear long-chain product barely varies between pure methyl oleate (99 %), technical grade methyl oleate (92.5 %), high oleic sunflower oil,[52b] various commercial plant oils,[52a] and microbial oils,[53] with the composition of the obtained mixture of α,ω-diesters correlating with the fatty acid composition of the starting material. The exact overall yields vary depending on the degree of purity of the substrate, but dimethyl 1,19-nonadecanedioate (from technical grade methyl oleate) and diethyl 1,23-tricosanedioate (from technical grade diethyl erucate) are typically isolated in overall yields ranging from about 75 % to 85 %[7f, g] but final product yields can reach values of up to 97 % for dimethyl 1,19-nonadecanedioate if high oleic sunflower oil is employed.[52b] Isolation of the obtained linear long-chain α,ω-diesters in purities exceeding 99 % is readily achieved via simple crystallization from the solvent, thereby qualifying the obtained dimethyl 1,19-nonadecanedioate and diethyl 1,23-tricosanedioate for being used as monomers in polycondensation reactions.[7e-g],[8b]

In addition, subsequent reduction of the terminal ester groups either with stoichiometric amounts of $LiAlH_4$ or by catalytic hydrogenation with Saudan's ruthenium catalyst[64] allows for the preparation

of the corresponding α,ω-diols 1,19-nonadecanediol and 1,23-tricosanediol in yields exceeding 80 %[7e-g],[8b] which can then be further converted into the corresponding α,ω-diamines using a multistep organochemical synthesis procedure to obtain 1,19-nonadecanediamine and 1,23-tricosanediamine respectively in overall yields of 65–70 % in regards to the corresponding diol.[7e] Using these monomers, a variety of long-chain thermoplastics including semicrystalline polyesters like poly[1,19-nonadecadiyl-1,19-nonadecandioate] (PE-19.19) and poly[1,23-tricosadiyl-1,23-tricosandioate] (PE-23.23),[7e-g],[8] the corresponding hydrophobic long-chain polyamides PA-19.19 and PA-23.23[7e-g] as well as series of hydrolytically degradable long-chain polyacetals[9] have been successfully synthesized (**Scheme 1.6**).

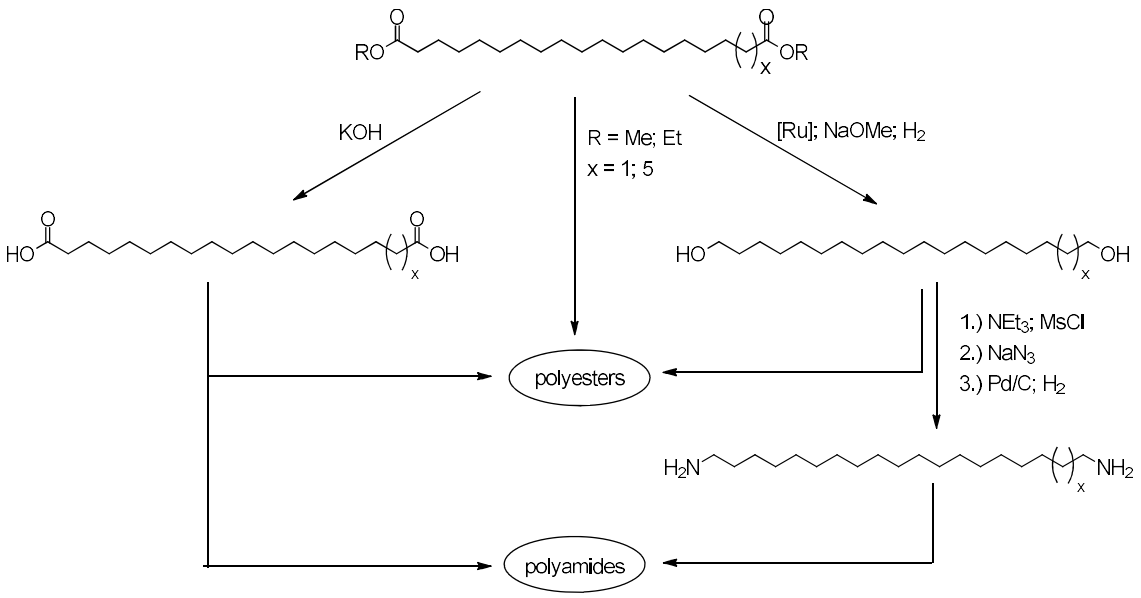

Scheme 1.6: Long-chain, α,ω -difunctionalized polycondensation monomers from unsaturated fatty acid ester-derived α,ω-diesters (x = 1, methyl oleate as starting material; x = 5, erucic acid ester).[7e]

In addition, it has been shown that rearrangement reactions like the Lossen and Curtius rearrangement can be used to convert fatty acid-derived linear long-chain α,ω-difunctionalized compounds into long-chain α,ω-dicarbamates.[65],[66], or α,ω-diisocyanates[67] to serve as monomers for the synthesis of novel renewable polyurethanes.[65],[67] Using this approach, ricinoleic acid-derived dimethyl 1,20-icosanedioate has been successfully transformed into dimethyl 1,18-octadecanedicarbamate via a multistep procedure that included a Lossen rearrangement reaction to ultimately generate the long-chain polyurethane PU-20.18 among others.[65] As an alternative, Curtius rearrangement reactions can be used to obtain more reactive renewable

long-chain α,ω-diisocyanates, as has been demonstrated by Hojabri *et al.*[67] who succeeded in preparing unsaturated 1,16-diisocyanatohexadec-8-ene from oleic acid-derived 1,18-octadec-9-enedioic acid (**Scheme 1.7**).

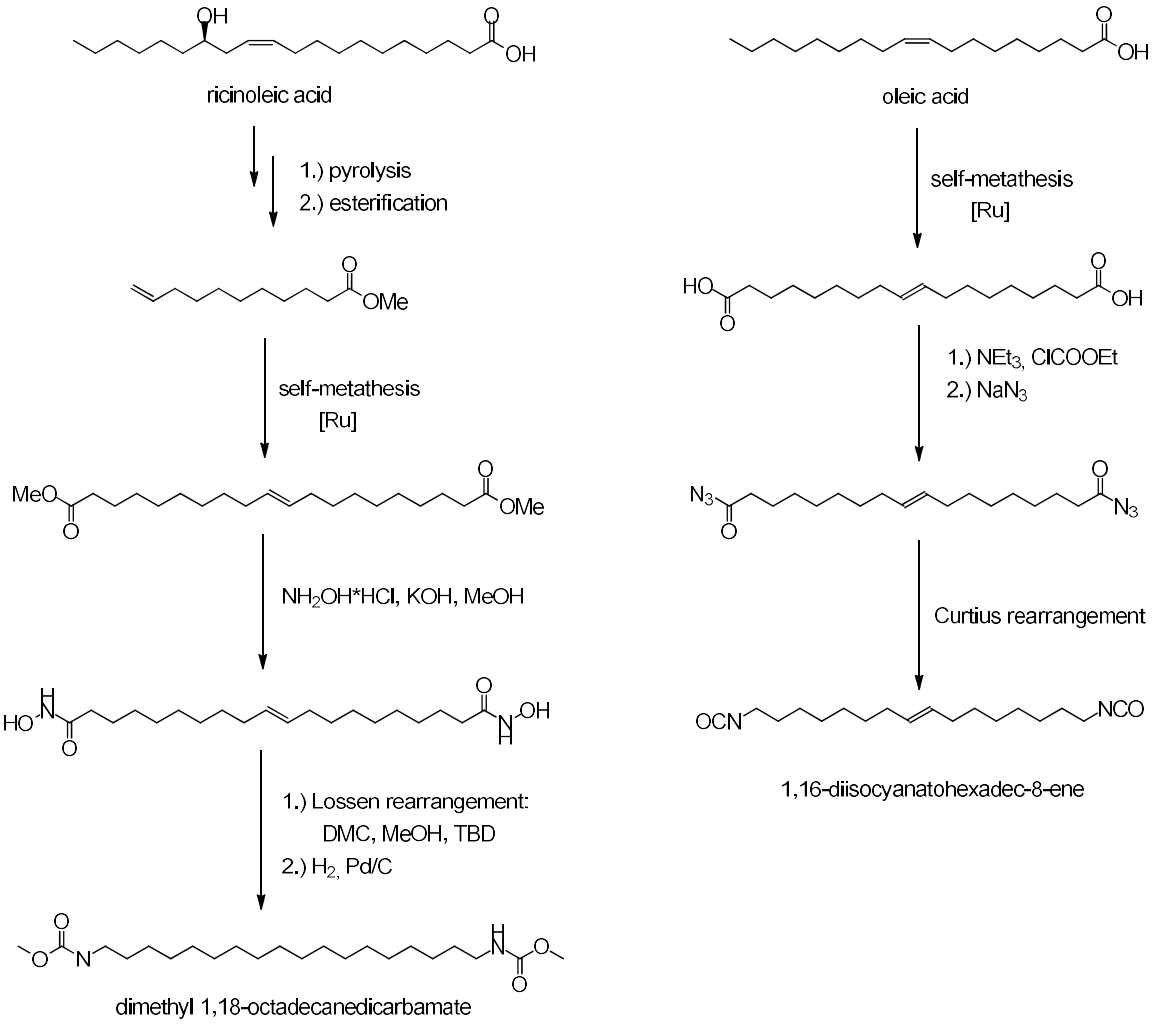

Scheme 1.7: Synthesis of linear long-chain α,ω-dicarbamates (left) and α,ω-diisocyanates (right) from unsaturated fatty acids via rearrangement reactions.[65],[67]

1.3. Long-Chain Aliphatic Polycondensates

1.3.1. Synthesis

Polyesters and polyamides

Polycondensates like polyesters (PEs), polyamides (PAs), and polyurethanes (PUs) are most commonly prepared via classic polycondensation or polyaddition reactions between bifunctional AA-type or AB-type monomers,[68] though synthesis approaches involving chain-growth polymerization reactions like ring opening polymerization (ROP) for the production of *e.g.* poly(ε-caprolactone)[69] as well as a variety of other short- and mid-chain aliphatic polyesters and polyamides are also commonly employed.[70] However, for the preparation of long-chain aliphatic polycondensates ROP is rarely feasible because the necessary large-ring lactones and lactams are not readily available and the reduction of ring strain, which drives polymerization especially for short-chain monomers, is negligible in macrocycles.[8a],[70b],[71] Consequently, research regarding the synthesis of aliphatic polyesters with elongated methylene sequences via ring opening polymerization has so far been mostly limited to mid-chain lactones and especially poly(pentadecalactone),[72] as the corresponding macrolactone monomer, ω-pentadecalactone (C_{15}), can be relatively easily produced from *Angelica archangelica* root oil,[73] though the synthesis and ring opening polymerization of larger ring lactones has also been explored in recent years (**Scheme 1.8**. **c**).[8a],[71a],[74] In contrast, the synthesis of linear aliphatic polyamides from macrocyclic lactams has so far been limited to ω-laurolactam (C_{12}).[8a],[75] Other, less traditional synthesis approaches like acyclic diene metathesis (ADMET) copolymerization of ester-, amide- or urethane-functionalized α,ω-diene monomers (**Scheme 1.8. d**)for the generation of linear long-chain aliphatic model polycondensates with a very low overall functional group density,[8a],[76-78] or the direct polyamidation of long-chain α,ω-diols and α,ω-diamines via catalytic dehydrogenation to produce long-chain polyamides have been explored but overall tend to yield comparatively poor results, with average molecular weights (M_n) of the obtained polymers barely exceeding 2.0 x 10^4 g mol^{-1}.[79]

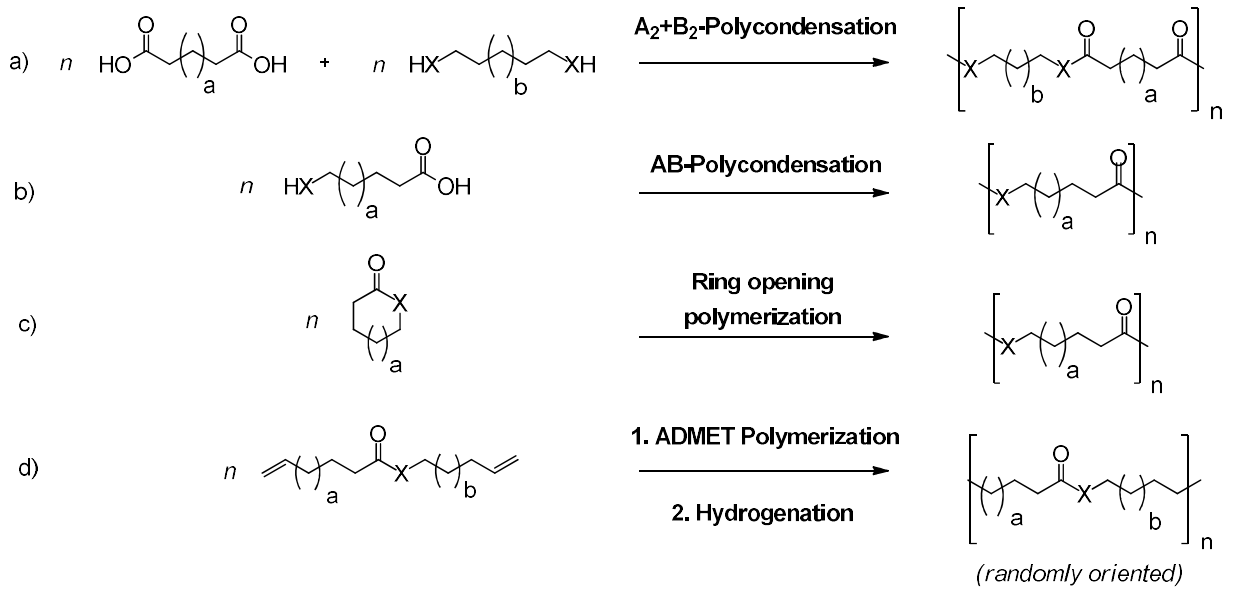

Scheme 1.8: Synthesis pathways for the generation of long-chain polyesters (X = O) and polyamides (X = NH): a) Polycondensation of AA-type monomers (R = H, Me). b) Polycondensation of AB-type monomers. c) ROP. d) ADMET of functionalized α,ω-dienes.

In comparison, classic polycondensation and polyaddition approaches (**Scheme 1.8 a)** and **b)**) have proven to be much more practical; though, as asymmetric AB-type long-chain polycondensation monomers are generally harder to access, most linear long-chain aliphatic polycondensates are A_2B_2-type copolymers prepared from the corresponding symmetric AA-type long-chain polycondensation monomers comparatively easily accessible *e.g.* by isomerizing alkoxycarbonylation of plant oils (cf. **Chapter 1.2**).[8a] However, as polycondensation and polyaddition reactions proceed in a step-growth polymerization manner, high degrees of polymerization (DP_n) and consequently high molecular weights in the range of several 10^4 g mol^{-1} can only be achieved if functional group conversion exceeds 99 % in accordance with the polycondensation principles established by Flory[80] and Carothers.[81] Consequently, the purity of monomers must exceed 99 % and, in case of A_2+B_2-copolymerizations, perfect stoichiometry of the employed AA-type monomers is required. However, for polycondensation and polyaddition systems based on linear long-chain α,ω-difunctionalized monomers both requirements present a challenge as purification of long-chain aliphatic α,ω-difunctionalized compounds can be difficult[82] and retrospective adjustment of the functional group ratio in the reaction mixture by removal of excess monomer via distillation as is common practice *e.g.* in the production of poly(ethylene terephthalate) (PET) from terephthalic acid and an excess of

ethylene glycol[83] is generally not possible for long-chain polymerization systems due to the comparatively high molecular weight and consequently high boiling points of the employed monomers. For example, to remove even a mid-chain diol like tetradecane-1,14-diol temperatures exceeding 200 °C at 9 Torr would be required.[84] In addition, the presence of even one long-chain monomer in a polymerization system can influence important system parameters like the melting point in case of melt polymerizations or solubility in commonly used solvents for solution polymerization systems. As a result, reaction procedures commonly employed in the preparation of short- or mid-chain aliphatic polycondensates and addition polymers can generally not simply be transferred to their long-chain analogs. Instead, existing polycondensation and polyaddition protocols need to be modified and reaction parameters like the used solvent, the reaction temperature, or the reaction time need to be adapted to fit the requirements of every new polycondensation or polyaddition system.[7e],[8a, b],[85] For long-chain polyesters like PE-19.19 and PE-23.23, this requirement for modifications manifests in synthesis protocols typically being based on the melt transesterification of linear long-chain α,ω-diesters and α,ω-diols[7e-g],[8a],[86] instead of the direct esterification approach typically employed in the production of standard polyesters,[87] though reaction protocols based on the direct esterification of long-chain α,ω-dicarboxylic acids and α,ω-diols also exist.[8c],[88] Similarly, long-chain polyamides are rarely prepared via the standard direct melt polycondensation approach in which a α,ω-diamine reacts with a α,ω-dicarboxylic acid.[89],[90] Instead, the employed long-chain α,ω-diamines and α,ω-dicarboxylic acid monomers are usually first converted into the corresponding carboxylate/ammonium salts to ensure perfect stoichiometry.[7e],[91]

Polyurethanes

Classical polyurethanes differ from comparable polyesters and polyamides insofar as they are commonly generated via the polyaddition of diisocyanate and diol monomers instead of polycondensation reactions, which has the advantage that no continuous removal of water or another low molecular weight byproduct is required to drive the reaction forward. In addition, due to the high reactivity of isocyanate functionalities, the reaction often proceeds at ambient temperatures and without the presence of a catalyst being necessary; though, *e.g.* organo tin catalysts can be employed to facilitate the reaction and improve molecular weights of the obtained polymer.[92] However, with increasing chain lengths of the employed aliphatic monomers the reactivity of the isocyanate group decreases. Consequently, the synthesis of linear long-chain aliphatic polyurethanes via polyaddition typically requires for the reaction to take place at elevated temperatures, either in the

form of a melt polymerization process[93] or in solution in polar solvents like dimethylsulfoxide (DMSO) or dimethylformamide (DMF).[67],[94] This way, molecular weights M_w of up to 80.000 g mol^{-1} can be achieved.[93] However, because the synthesis of the necessary toxic diisocyanate monomers commonly involves the treatment of the corresponding diamines with highly toxic phosgene or one of its derivatives[95] and because the research regarding fatty acid-derived polymers is heavily driven by the concept of sustainability, studies on the synthesis of long-chain polyurethanes have so far heavily focused on the exploration of polycondensation reactions not involving isocyanates,[8a],[65] even though alternative, more sustainable routes for the synthesis of diisocyanates exist.[96] Such polycondensation approaches typically involve linear long-chain α,ω-dicarbamates obtained from fatty acid-derived α,ω-dicarboxylic acids via rearrangement reactions (cf. **Chapter 1.2**) that react with a α,ω-diol to produce polyurethanes like PU-10.18 and PU-20.18 in combination with a low molecular weight alcohol as a byproduct (**Scheme 1.9**).[65],[66]

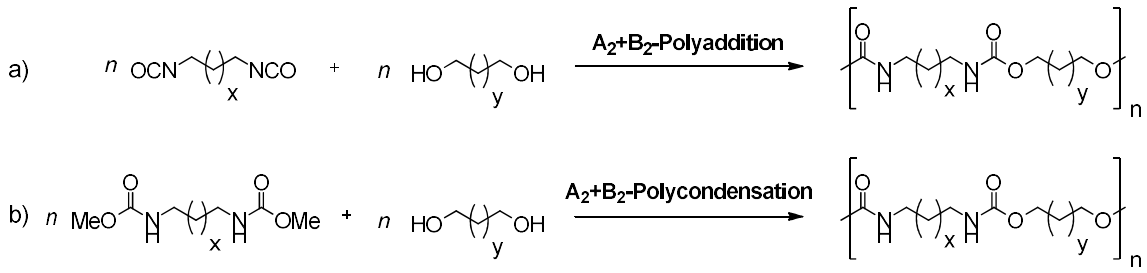

Scheme 1.9: Synthetic approaches to long-chain A_2B_2-type polyurethanes. a) polyaddition of diols and diisocyanates. b) polycondensation of dicarbamates and diols.

1.3.2. Material properties

In terms of material properties, polycondensates based on linear long-chain aliphatic monomers can differ greatly from their short- and mid-chain monomer-derived analogs because the physical properties of aliphatic polycondensates are largely determined by their functional groups and the intermolecular forces acting between them. For example, the large number of strong hydrogen bonds formed between the amide groups in polyamide-6,6 (PA-6.6) gives rise to the material's advantageously high heat deflection temperature, melting point and modulus,[97] while a high content of hydrolytically degradable ester groups in classic short-chain aliphatic polyesters like polylactic acid allows for the design of biodegradable materials.[98] Consequently, a reduced functional group density due to the incorporation of long-chain monomers in the aliphatic polymer backbone can have a

massive impact on various material properties including thermal properties, mechanical properties, water absorption, and hydrolytical degradability as the extensive amount of data summarized by Stempfle *et al.*[8a] poignantly illustrates.

Polyesters

Because classic aliphatic polyesters based on short- and mid-chain bifunctional monomers lack strong intermolecular interactions between their functional groups, they do not reach high degrees of crystallinity and tend to suffer from very low melt and crystallization points.[99] For example, poly(ε-caprolactone) and poly(butylene adipate) melt at 60 °C and 55 °C respectively.[100] As a consequence, thermoplastic processing of these materials is more complicated and they are very susceptible to premature softening at elevated temperatures which limits their practical applications. In commercial polyester products this problem is typically solved by incorporating aromatic repeat units into the aliphatic polymer backbone.[87] Alternatively, the thermal properties and hydrolytic stability of aliphatic polyesters can be improved by elongating the aliphatic segments between ester groups. By incorporating additional crystallizable methylene units into the aliphatic segments of the polymer backbone, the conditions for crystallization via Van-der-Waals forces acting between the aliphatic chain segments improve while the ester groups that act as structural defects in the crystal lattice progressively lose influence. Therefore, with increasing length of the methylene sequences and consequently lower ester group density, aliphatic polyesters begin to favor crystallizing in an orthorhombic, polyethylene-like structure. Simultaneously, the degree of crystallinity rises to levels up to 80 % compared to linear polyethylene reference material, the hydrolytic stability improves, the melt transitions sharpen, and the melt and crystallization temperatures overall increase.[7e-g],[76a],[101],[102] Eventually, melting points approaching values recorded for low-density polyethylene (LDPE) (T_m = 105 - 115 °C)[103] are reached for long-chain polyesters like PE-19.19 (T_m = 103 °C) and PE-23.23 (T_m = 107 °C).[7f, g] Further elongation of the methylene sequences as in PE-32.32 and PE-48.48 results in even higher melting temperatures of 113 °C and 120 °C[48d, e] respectively, which actually surpass values recorded for LDPE and approach the melting temperature of linear low-density polyethylene (LLDPE) (T_m = 122 °C).[103] As a result, long-chain polyesters are often referred to as polyethylene mimics or polyethylene-like polymers that bridge the gap between traditional polycondensates and aliphatic polyolefins like polyethylene.[8a],[72b],[104],[105]

Polyamides and Polyurethanes

In contrast, the material properties of aliphatic polyamides and polyurethanes are not determined by comparatively weak Van-der-Waals forces acting between hydrocarbon segments but are instead dominated by the formation of strong hydrogen bonds between amide and urethane groups respectively. Hydrogen bond formation drives crystallization in these materials, which forces the polyamide and polyurethane chains to adapt slightly twisted chain conformations in order to facilitate the formation of the maximum possible amount of hydrogen bonds.[106],[107] As this process is influenced by the orientation and positioning of the involved functional groups along the polymer chains, linear aliphatic polyamides and polyurethanes are both known to adopt different crystal modifications, the so-called α-, β- and γ-forms, in combination with a variety of crystal structures depending on whether the polymer is based on monomers containing an odd- or even-number of carbon atoms or a combination of both.[107-109] In addition, aliphatic polyamides are known for their polymorphism as well as belated changes in their crystal structures being a common occurrence because the initially adopted crystal structure depends heavily on the crystallization conditions and is not always the most thermodynamically stable one.[110] Analysis of PA-23.23 via WAXD has shown that this is also an issue for long-chain polyamides.[111] Because of these phenomena, DSC graphs of aliphatic polyamides often show multiple, broad melting endotherms and their crystallinities rarely exceed 40 % - a fact that suggests that crystallization driven by hydrogen bond formation is less efficient than crystallization induced by van-der-Waals interactions between polyolefin-like hydrocarbon segments. [7e],[110],[112] The formation of hydrogen bonds between functional groups also results in linear aliphatic polyamides and polyurethanes both generally possessing melt and crystallization points well above the melt and crystallization temperatures recorded for polyethylene or aliphatic polyesters, as the extensive data compiled by Stempfle *et al.*[8a] poignantly illustrates. However, because urethane groups contain an additional electron-withdrawing oxygen atom adjacent to the central carbon atom and are therefore less polar than amide groups, the hydrogen bonds formed in aliphatic polyurethanes are weaker and their melting points therefore lower than those of comparable polyamides with a similar functional group density. For example, PA-12.12 melts at 183 °C[91a] while PU-12.12 possesses a melting point of only 122 °C[93] and polyamides based on short-chain monomers like PA-4.2 with a very high functional group density can reach melting temperatures approaching almost 400 °C[8a],[113] while melting points recorded for comparable polyurethanes level out at about 200 °C[8a],[106a],[114] Because of the influence that monomer structure has on hydrogen bond formation, the melting points of linear aliphatic polyamides and

polyurethanes both exhibit a pronounced odd-even effect. However, with incorporation of long-chain monomers into the polycondensate backbone, the effect lessens considerably and eventually becomes all but negligible as the functional group density continues to decrease.[108a],[114] Simultaneously, melt and crystallization temperatures also decrease,[8a],[91a],[108a],[114] with the melting points of polyurethanes based on at least one long-chain monomer like PU-10.18 (T_m = 122 °C)and PU-20.18 (T_m = 123 °C)[65] dropping to values in the range of linear low-density polyethylene (LLDPE) (T_m = 122 °C)[103b] while the long-chain polyamide PA-23.23 still possesses a melting point of T_m = 152 °C.[7e] However, despite the decreasing melting points and unlike with comparable long-chain polyesters, hydrogen bond formation remains the driving force behind crystallization in long-chain polyamides and polyurethanes. A shift towards Van-der-Waals forces-driven crystallization with the adoption of a polyethylene-like orthorhombic crystal structure is not observed for polyamides until the functional group density is lowered to about 35 amide groups per 1000 methylene groups, which can be achieved by copolymerizing amide-functionalized dienes with unfunctionalized dienes via ADMET to obtain a random polyamide that corresponds nominally to regular PA-29.29.[8a],[77],[78] For long-chain polyurethanes, no transition of the crystal structure has been observed yet as the polyurethane with the longest methylene sequences studied so far is PU-32.12, which still crystallizes in a triclinic structure.[109b],[115-117]

In addition, hydrogen bond density influences other important material properties like solvent resistance and, in case of polyamides, moisture absorption. Due to their high concentration of highly polar amide groups, technologically relevant short-chain polyamides like PA-6.6 are well-known for their tendency to absorb moisture from air, which can cause swelling and significantly affect dimensional stability as well as impact various mechanical properties of the material.[118] For example, the stress at yield of PA-6.6 can drop by almost 50 % due to moisture absorption.[119] Short-chain polyamides are also less solvent resistant. Consequently, the incorporation of mid- or long-chain monomers in the polyamide backbone increases solvent resistance and reduces the influence that atmospheric conditions have on mechanical properties, which is why mid-chain polyamides like PA-11 and PA-12 are often utilized in demanding industrial applications like automotive fuel lines, pneumatic airbrake tubing, or electrical cable sheathings.[120] For long-chain polyamides with an even lower density of amide groups, these beneficial effects are enhanced even further, with solvent resistance increasing even more[89] and moisture absorption from air decreasing by 60 % if the methylene segment of even one monomer is elongated by 10 methylene units.[121]

1.4. References

1. a)Natural resources: curse or blessing? Van der Ploeg, F. *Journal of Economic Literature*, **2011,** *49* (2), 366-420; b)*The future of petrochemicals – Towards more sustainable plastics and fertilisers*. Fernandez Pales, A.; Levi, P. International Energy Agency: Paris, **2018**.
2. a)Synthesis of ethylene glycol and terephthalic acid from biomass for producing PET. Pang, J.; Zheng, M.; Sun, R.; Wang, A.; Wang, X.; Zhang, T. *Green Chemistry*, **2016,** *18* (2), 342-359; b)Present and future development in plastics from biomass. Shen, L.; Worrell, E.; Patel, M. *Biofuels, Bioproducts and Biorefining: Innovation for a sustainable economy*, **2010,** *4* (1), 25-40.
3. a)Poly-lactic acid synthesis for application in biomedical devices—A review. Lasprilla, A. J.; Martinez, G. A.; Lunelli, B. H.; Jardini, A. L.; Maciel Filho, R. *Biotechnology advances*, **2012,** *30* (1), 321-328; b)Tsuji, H. Poly(Lactic Acid). In *Bio-Based Plastics: Materials and Applications*, Kabasci, S., (Ed.) Wiley: Chichester, U.K., **2013**, pp 171-239.
4. a)Rilsan (Polyamid 11), Synthese und Eigenschaften. Genas, M. *Angewandte Chemie*, **1962,** *74* (15), 535-540; b)Brehmer, B. Polyamides from Biomass Derived Monomers. In *Bio-Based Plastics: Materials and Applications*, Kabasci, S., (Ed.) Wiley: Chichester, U.K., **2013**, pp 275-294.
5. a)Sustainable polymers from renewable resources. Zhu, Y.; Romain, C.; Williams, C. K. *Nature*, **2016,** *540* (7633), 354-362; b)Current progress on bio-based polymers and their future trends. Babu, R. P.; O'Connor, K.; Seeram, R. *Progress in biomaterials*, **2013,** *2* (1), 1-16; c)Bio-based polymers with performance-advantaged properties. Cywar, R. M.; Rorrer, N. A.; Hoyt, C. B.; Beckham, G. T.; Chen, E. Y.-X. *Nature Reviews Materials*, **2022,** *7* (2), 83-103; d)Polymers from renewable resources: a challenge for the future of macromolecular materials. Gandini, A. *Macromolecules*, **2008,** *41* (24), 9491-9504.
6. Catalytic isomerizing ω-functionalization of fatty acids. Goldbach, V.; Roesle, P.; Mecking, S. *ACS Catalysis*, **2015,** *5* (10), 5951-5972.
7. a)Dicarboxylic acid esters from the carbonylation of unsaturated esters under mild conditions. Jiménez-Rodriguez, C.; Eastham, G. R.; Cole-Hamilton, D. J. *Inorganic Chemistry Communications*, **2005,** *8* (10), 878-881; b)Highly selective formation of linear esters from terminal and internal alkenes catalysed by palladium complexes of bis-(di-tert-butylphosphinomethyl) benzene. Jiménez-Rodriguez, C.; Foster, D. F.; Eastham, G. R.; Cole-Hamilton, D. J. *Chemical communications*, **2004,** (15), 1720-1721; c)Highly selective formation of unsaturated esters or cascade reactions to α, ω-diesters by the methoxycarbonylation of alkynes catalysed by

palladium complexes of 1, 2-bis (ditertbutylphosphinomethyl) benzene. Núñez-Magro, A. A.; Robb, L.-M.; Pogorzelec, P. J.; Slawin, A. M.; Eastham, G. R.; Cole-Hamilton, D. J. *Chemical Science*, **2010,** *1* (6), 723-730; d)Mechanistic features of isomerizing alkoxycarbonylation of methyl oleate. Roesle, P.; Dürr, C. J.; Möller, H. M.; Cavallo, L.; Caporaso, L.; Mecking, S. *Journal of the American Chemical Society*, **2012,** *134* (42), 17696-17703; e)Long-chain linear C_{19} and C_{23} monomers and polycondensates from unsaturated fatty acid esters. Stempfle, F.; Quinzler, D.; Heckler, I.; Mecking, S. *Macromolecules*, **2011,** *44* (11), 4159-4166; f)Linear semicrystalline polyesters from fatty acids by complete feedstock molecule utilization. Quinzler, D.; Mecking, S. *Angewandte Chemie International Edition*, **2010,** *49* (25), 4306-4308; g)Linear semicrystalline polyesters from fatty acids by complete feedstock molecule utilization. Quinzler, D.; Mecking, S. *Angewandte Chemie*, **2010,** *122* (25), 4402-4404.

8. a)Long-chain aliphatic polymers to bridge the gap between semicrystalline polyolefins and traditional polycondensates. Stempfle, F.; Ortmann, P.; Mecking, S. *Chemical reviews*, **2016,** *116* (7), 4597-4641; b)Long-chain aliphatic polyesters from plant oils for injection molding, film extrusion and electrospinning. Stempfle, F.; Ritter, B. S.; Mülhaupt, R.; Mecking, S. *Green Chemistry*, **2014,** *16* (4), 2008-2014; c)Plant oil-based long-chain C_{26} monomers and their polymers. Vilela, C.; Silvestre, A. J.; Meier, M. A. *Macromolecular Chemistry and Physics*, **2012,** *213* (21), 2220-2227; d)Self-metathesis of fatty acid methyl esters: full conversion by choosing the appropriate plant oil. Mutlu, H.; Hofsäß, R.; Montenegro, R. E.; Meier, M. A. *Rsc Advances*, **2013,** *3* (15), 4927-4934.
9. a)Long-Chain Polyacetals From Plant Oils. Chikkali, S.; Stempfle, F.; Mecking, S. *Macromolecular rapid communications*, **2012,** *33* (13), 1126-1129; b)Physical properties and hydrolytic degradability of polyethylene-like polyacetals and polycarbonates. Ortmann, P.; Heckler, I.; Mecking, S. *Green Chemistry*, **2014,** *16* (4), 1816-1827.
10. Which polyesters can mimic polyethylene? Stempfle, F.; Ortmann, P.; Mecking, S. *Macromolecular rapid communications*, **2013,** *34* (1), 47-50.
11. a)Drobny, J. G., *Handbook of Thermoplastic Elastomers*. William Andrew Publishing: Norwich, New York, **2007**; b)*Elastic linear copolyesters*. Snyder, M. D. (DuPont), U.S. Patent 2,623,031 (A), **1952**.
12. *TPE Market by Type (SBC, TPU, TPO, TPV, COPE, PEBA), End Use Industry (Automotive, Building&Construction, Footwear, Wire&Cable, Medical, Engineering), Region (North America, Europe,*

APAC, South America, MEA) - Global Forecast to 2026. MarketsAndMarkets Inc.: Northbrook, U.S., **2021**.

13. Ouhadi, T.; Abdou-Sabet, T.; Wussow, H.-G.; Ryan, L. M.; Plummer, L.; Baumann, F. E.; Lohmar, J.; F, V. H.; Malet, F. L. G. Thermoplastic Elastomers. In *Ullmann's Encyclopedia of Industrial Chemistry*, Gerhartz, W.; Elvers, B., (Eds.), Wiley-VCH: Weinheim, Germany, **2000**, pp 1-40.
14. a)Thermally reversible polymer systems by cyclopentadienylation. II. The synthesis of cyclopentadiene-containing polymers. Kennedy, J. P.; Castner, K. F. *Journal of Polymer Science: Polymer Chemistry Edition*, **1979,** *17* (7), 2055-2070; b)A review of thermally controlled covalent bond formation in polymer chemistry. Engle, L.; Wagener, K. *Journal of Macromolecular Science, Part C: Polymer Reviews*, **1993,** *33* (3), 239-257.
15. a)Tant, M. R.; Mauritz, K. A.; Wilkes, G. L., Eds. *Ionomers: Synthesis, Structure, Properties and Applications*. Chapman & Hall: London, U.K., **1997**; b)Ionic thermoplastic elastomers: a review. Antony, P.; De, S. K. *Journal of Macromolecular Science, Part C: Polymer Reviews*, **2001,** *41* (1-2), 41-77.
16. a)Thermoplastic elastomers. Holden, G.; Bishop, E.; Legge, N. R. *Journal of Polymer Science Part C: Polymer Symposia*, **1969,** *26*, 37-57; b)Structure-Property Relationships for Styrene-Diene Thermoplastic Elastomers. Morton, M.; McGrath, J. E.; Juliano, P. C. *Journal of Polymer Science Part C: Polymer Symposia*, **1969,** *26*, 99-115.
17. a)Novel thermoplastic elastomers. I. Synthesis and characterization of star-block copolymers of PSt-b-PIB arms emanating from cyclosiloxane cores. Shim, J. S.; Asthana, S.; Omura, N.; Kennedy, J. P. *Journal of Polymer Science Part A: Polymer Chemistry*, **1998,** *36* (17), 2997-3012; b)Mechanical properties of star block polymer thermoplastic elastomers with glassy and crystalline end blocks. Burns, A. B.; Register, R. A. *Macromolecules*, **2016,** *49* (24), 9521-9530.
18. a)The ATRP Synthesis of the Potential Thermoplastic Elastomer Poly (methyl methacrylate)–b-(lauryl methacrylate)-b-(methyl methacrylate) Hitherto Unrealized by Ionic Polymerization. Chatterjee, D. P.; Mandal, B. M. *Macromolecular Symposia*, **2006,** *240*, 224-231; b)Synthesis, morphology and mechanical properties of linear triblock copolymers based on poly (α-methylene-γ-butyrolactone). Mosnáček, J.; Yoon, J. A.; Juhari, A.; Koynov, K.; Matyjaszewski, K. *Polymer*, **2009,** *50* (9), 2087-2094.
19. a)Legge, N. R.; Holden, G.; Schroeder, H., *Thermoplastic elastomers: A comprehensive review*. Carl Hansser Verlag: New York, USA, **1987**; b)Block copolymers: Copolymerization of ethylene

terephthalate and polyoxyethylene glycols. Coleman, D. *Journal of Polymer Science*, **1954,** *14* (73), 15-28; c)Witsiepe, W. Segmented Polyester Thermoplastic Elastomers. In *ACS Advances in Chemistry*, Platzer, N. A. J., (Ed.) ACS Advances in Chemistry, Vol. 129: *Polymerization Reactions and New Polymers*, ACS Publications: **1973**, pp 39-66.

20. Über neuartige hochelastische Stoffe „Vulcollan". Bayer, O.; Müller, E.; Petersen, S.; Piepenbrink, H. F.; Windemuth, E. *Angewandte Chemie*, **1950,** *62* (3), 57-66.
21. Synthese et caracterisation de copolycondensats sequences poly (amide-seq-ether)—I. Synthese et etude de divers oligomeres ω, ω'difonctionnels du poly (amide-11). Deleens, G.; Foy, P.; Marechal, E. *European Polymer Journal*, **1977,** *13* (5), 337-342.
22. a)Morphology of segmented polyester thermoplastic elastomers. Cella, R. J. *Journal of Polymer Science: Polymer Symposia*, **1973,** *42*, 727-740; b)Maréchal, E. Creation and Development of Thermoplastic Elastomers, and Their Position Among Organic Materials. In *Handbook of Condensation Thermoplastic Elastomers*, Fakirov, S., (Ed.) Wiley-VCH: Weinheim, Germany, **2005**; c)Maréchal, E. Polycondensation Reactions in Thermoplastic Elastomer Chemistry: State of the Art, Trends, and Future Developments. In *Handbook of Condensation Thermoplastic Elastomers*, Fakirov, S., (Ed.) Wiley-VCH: Weinheim, Germany, **2005**.
23. The crystal structure of polyethylene terephthalate. Daubeny, R. d. P.; Bunn, C. W.; Brown, C. *Proceedings of the Royal Society of London. Series A. Mathematical and Physical Sciences*, **1954,** *226* (1167), 531-542.
24. Sustainable elastomers from renewable biomass. Wang, Z.; Yuan, L.; Tang, C. *Accounts of chemical research*, **2017,** *50* (7), 1762-1773.
25. a)Renewable-Resource Thermoplastic Elastomers Based on Polylactide and Polymenthide. Wanamaker, C. L.; O'Leary, L. E.; Lynd, N. A.; Hillmyer, M. A.; Tolman, W. B. *Biomacromolecules*, **2007,** *8* (11), 3634-3640; b)Polylactide–poly (6-methyl-ε-caprolactone)–polylactide thermoplastic elastomers. Martello, M. T.; Hillmyer, M. A. *Macromolecules*, **2011,** *44* (21), 8537-8545; c)Thermoplastic elastomers derived from menthide and tulipalin A. Shin, J.; Lee, Y.; Tolman, W. B.; Hillmyer, M. A. *Biomacromolecules*, **2012,** *13* (11), 3833-3840; d)Sustainable thermoplastic elastomers derived from fatty acids. Wang, S.; Vajjala Kesava, S.; Gomez, E. D.; Robertson, M. L. *Macromolecules*, **2013,** *46* (18), 7202-7212; e)Aliphatic polyester block polymers: renewable, degradable, and sustainable. Hillmyer, M. A.; Tolman, W. B. *Accounts of chemical research*, **2014,** *47* (8), 2390-2396.

26. New approaches to producing polyols from biomass. Gómez-Jiménez-Aberasturi, O.; Ochoa-Gómez, J. R. *Journal of Chemical Technology & Biotechnology*, **2017,** *92* (4), 705-711.

27. a)Recent advances in vegetable oil-based polyurethanes. Pfister, D. P.; Xia, Y.; Larock, R. C. *ChemSusChem*, **2011,** *4* (6), 703-717; b)Plant oils as platform chemicals for polyurethane synthesis: current state-of-the-art. Lligadas, G.; Ronda, J. C.; Galia, M.; Cádiz, V. *Biomacromolecules*, **2010,** *11* (11), 2825-2835.

28. Morphology and properties of thermoplastic polyurethanes with dangling chains in ricinoleate-based soft segments. Xu, Y.; Petrovic, Z.; Das, S.; Wilkes, G. L. *Polymer*, **2008,** *49* (19), 4248-4258.

29. Rani, G. U.; Sharma, S., Biopolymers, Bioplastics and Biodegradables: An Introduction. In *Encyclopedia of Materials: Plastics and Polymers*, 1 ed.; Hashmi, M. S. J., Ed. Elsevier Science: Amsterdam, Netherlands, **2022**; Vol. 2, pp 474-486.

30. a)Succinate production in Escherichia coli. Thakker, C.; Martínez, I.; San, K. Y.; Bennett, G. N. *Biotechnology journal*, **2012,** *7* (2), 213-224; b)Technological advancements in valorization of second generation (2G) feedstocks for bio-based succinic acid production. Narisetty, V.; Okibe, M. C.; Amulya, K.; Jokodola, E. O.; Coulon, F.; Tyagi, V. K.; Lens, P. N.; Parameswaran, B.; Kumar, V. *Bioresource Technology*, **2022**, 127513.

31. Thermal characterization and crystallization kinetics of polyester polyols derived from adipic acid and bio-based succinic acid with 1, 4-butanediol and 1, 6-hexanediol. Schrock, A. K.; Hamilton, H. S.; Johnson, N. D.; del Rosario, C.; Thompson, B.; Ulrich, K.; Coggio, W. D. *Polymer*, **2016,** *101*, 233-240.

32. a)Catalytic conversion of cellulosic biomass to ethylene glycol: Effects of inorganic impurities in biomass. Pang, J.; Zheng, M.; Sun, R.; Song, L.; Wang, A.; Wang, X.; Zhang, T. *Bioresource Technology*, **2015,** *175*, 424-429; b)*Hydrogenolysis of polyols to ethylene glycol in nonaqueous solvents.* Tanikella, M. S. S. R. (DuPont), U.S. Patent 4,404,411 (A), **1983**.

33. a)*Process for the biological production of 1,3-propanediol.* Emptage, M.; S, H.; Laffend, L.; Pucci, J. (DuPont), International Patent: WO 2001012833 (A2), **2001**; b)Production of 1, 3-propanediol from glycerol by Clostridium acetobutylicum and other Clostridium species. Forsberg, C. W. *Applied and environmental microbiology*, **1987,** *53* (4), 639-643.

34. a)Synthetic methods for the preparation of 1, 3-propanediol. Kraus, G. A. *CLEAN–Soil, Air, Water*, **2008,** *36* (8), 648-651; b)Metabolic engineering of Escherichia coli for direct production of 1, 4-butanediol. Yim, H.; Haselbeck, R.; Niu, W.; Pujol-Baxley, C.; Burgard, A.; Boldt, J.;

Khandurina, J.; Trawick, J. D.; Osterhout, R. E.; Stephen, R. *Nature chemical biology*, **2011,** *7* (7), 445-452; c)3-Hydroxypropionaldehyde: applications and perspectives of biotechnological production. Vollenweider, S.; Lacroix, C. *Applied microbiology and biotechnology*, **2004,** *64* (1), 16-27.

35. Press release by Clariant of February 2, 2022. https://www.clariant.com/de/Corporate/News/2022/02/Clariant-launches-100-biobased-surfactants-range-driving-the-transition-towards-renewable-carbon; accessed on February 17, 2022.
36. a)*Genetically engineered Escherichia coli containing nonspecific dehydratase yghD and dha regulon for the biological production of 1,3-propane-diol with high titer*. Emptage, M.; Haynie, S. L.; Laffend, L. A.; Pucci, J. P.; Whited, G. (DuPont), U. S. Patent 6,514,733 (B1), **2003**; b)UCST and LCST phase behavior of poly (trimethylene ether) glycol in water. Lee, H. N.; Rosen, B. M.; Fenyvesi, G.; Sunkara, H. B. *Journal of Polymer Science Part A: Polymer Chemistry*, **2012,** *50* (20), 4311-4315; c)A Detailed Polymerization Model for Cerenol® Polyols. Mueller, P. A.; Murphy, E. R.; Rajagopalan, B.; Congalidis, J. P.; Minter, A. R. *Macromolecular Symposia*, **2011,** *302* (1), 56-68; d)Synthesis and characterization of polyurethanes from epoxidized methyl oleate based polyether polyols as renewable resources. Lligadas, G.; Ronda, J.; Galia, M.; Biermann, U.; Metzger, J. *Journal of Polymer Science Part A: Polymer Chemistry*, **2006,** *44* (1), 634-645; e)Sunkara, H. B.; Miller, R. W. *"DuPont™ Cerenol™ - A New Family of High Performance Polyether glycols"*, Fifth Annual World Congress on Industrial Biotechnology & Bioprocessing, Chicago, April 27–30, **2008**.
37. Press release by BASF of March 5, 2015. https://www.basf.com/us/en/media/news-releases/2015/03/P-US-14-29.html.; accessed on February 10, 2022.
38. *Cerenol™—DuPont Polyether Glycol Made from 1,3-Propanediol (PDO)*. Pavone, A. IHS Chemical: Process Economics Program Review 2013-03 IHS Markit: **2013**.
39. a)Green and sustainable manufacture of chemicals from biomass: state of the art. Sheldon, R. A. *Green Chemistry*, **2014,** *16* (3), 950-963; b)Hydroxymethylfurfural, a versatile platform chemical made from renewable resources. Van Putten, R.-J.; Van Der Waal, J. C.; De Jong, E.; Rasrendra, C. B.; Heeres, H. J.; de Vries, J. G. *Chemical reviews*, **2013,** *113* (3), 1499-1597.
40. a)Microstructure and Mechanical/Elastic Performance of Biobased Poly (Butylene Furanoate)–Block–Poly (Ethylene Oxide) Copolymers: Effect of the Flexible Segment Length. Kwiatkowska, M.; Kowalczyk, I.; Kwiatkowski, K.; Zubkiewicz, A. *Polymers*, **2020,** *12* (2), 271;

b)Production of bio-based 2, 5-furan dicarboxylate polyesters: Recent progress and critical aspects in their synthesis and thermal properties. Papageorgiou, G. Z.; Papageorgiou, D. G.; Terzopoulou, Z.; Bikiaris, D. N. *European Polymer Journal*, **2016,** *83*, 202-229; c)Synthesis and characterization of bio-based poly (butylene furandicarboxylate)-b-poly (tetramethylene glycol) copolymers. Zhou, W.; Zhang, Y.; Xu, Y.; Wang, P.; Gao, L.; Zhang, W.; Ji, J. *Polymer degradation and stability*, **2014,** *109*, 21-26.

41. a)Production, chemistry, and commercial applications of various chemicals from castor oil. Naughton, F. C. *Journal of the American Oil Chemists' Society*, **1974,** *51* (3), 65-71; b)Castor oil as a renewable resource for the chemical industry. Mutlu, H.; Meier, M. A. *European Journal of Lipid Science and Technology*, **2010,** *112* (1), 10-30.
42. Organic reactions in strong alkalis-III: Fission of keto-and hydroxy-acids. Dytham, R.; Weedon, B. *Tetrahedron*, **1960,** *8* (3-4), 246-260.
43. a)Niaounakis, M., *Biopolymers: applications and trends*. William Andrew Publishing: Norwich, New York, **2015**; b)Solid state structure–property behavior of semicrystalline poly (ether-block-amide) PEBAX® thermoplastic elastomers. Sheth, J. P.; Xu, J.; Wilkes, G. L. *Polymer*, **2003,** *44* (3), 743-756.
44. a)*Method of Making Azelaic Acid.* Goebel, C. G.; Brown, A. C.; Oehlschlaeger, H. F.; Rolfes, R. P. (Emery Industries, Inc.), U.S. Patent 2,813,113 (A), **1957**; b)Verhé, R. G. Industrial Products from Lipids and Proteins. In *Renewable Bioresources: Scope and Modification for Non-Food Applications*, Stevens, C. V.; Verhé, R. G., (Eds.), Wiley: Chichester, U.K., **2004**, p 208−250; c)Ozonolysis of unsaturated fatty acids: I. Ozonolysis of oleic acid. Ackman, R. G.; Retson, M.; Gallay, L.; Vandenheuvel, F. *Canadian Journal of Chemistry*, **1961,** *39* (10), 1956-1963; d)Natural fats and oils—renewable raw materials for the chemical industry. Baumann, H.; Bühler, M.; Fochem, H.; Hirsinger, F.; Zoebelein, H.; Falbe, J. *Angewandte Chemie International Edition in English*, **1988,** *27* (1), 41-62; e)Lipids as renewable resources: current state of chemical and biotechnological conversion and diversification. Metzger, J. O.; Bornscheuer, U. *Applied microbiology and biotechnology*, **2006,** *71* (1), 13-22; f)Plant oil renewable resources as green alternatives in polymer science. Meier, M. A.; Metzger, J. O.; Schubert, U. S. *Chemical Society Reviews*, **2007,** *36* (11), 1788-1802.
45. a)Hydrogen peroxide as an oxidant in biomass-to-chemical processes of industrial interest. Teong, S. P.; Li, X.; Zhang, Y. *Green Chemistry*, **2019,** *21* (21), 5753-5780; b)Synthesis of azelaic acid from vegetable oil-based feedstocks. Köckritz, A.; Martin, A. *European Journal of Lipid*

Science and Technology, **2011,** *113* (1), 83-91; c)Chemically catalyzed oxidative cleavage of unsaturated fatty acids and their derivatives into valuable products for industrial applications: a review and perspective. Kerenkan, A. E.; Béland, F.; Do, T.-O. *Catalysis Science & Technology*, **2016,** *6* (4), 971-987; d)Oxidative cleavage of fatty acid derivatives for monomer synthesis. Soutelo-Maria, A.; Dubois, J.-L.; Couturier, J.-L.; Cravotto, G. *Catalysts*, **2018,** *8* (10), 464.

46. A versatile process for the syntheses of very long chain alkanes, functionalised derivatives and some branched chain hydrocarbons. Brooke, G. M.; Burnett, S.; Mohammed, S.; Proctor, D.; Whiting, M. C. *Journal of the Chemical Society, Perkin Transactions 1*, **1996,** (13), 1635-1645.

47. a)Fermentative Herstellung der α, ω-Dicarbonsäure 1, 18-Oktadecendisäure als Grundbaustein für biobasierte Kunststoffe. Zibek, S.; Wagner, W.; Hirth, T.; Rupp, S.; Huf, S. *Chemie Ingenieur Technik*, **2009,** *81* (11), 1797-1808; b)Lipid biotechnology: Industrially relevant production processes. Schörken, U.; Kempers, P. *European Journal of Lipid Science and Technology*, **2009,** *111* (7), 627-645; c)Biotechnological synthesis of long-chain dicarboxylic acids as building blocks for polymers. Huf, S.; Krügener, S.; Hirth, T.; Rupp, S.; Zibek, S. *European Journal of Lipid Science and Technology*, **2011,** *113* (5), 548-561; d)Lu, W.; Ness, J. E.; Xie, W.; Zhang, X.; Liu, F.; Cai, J.; Minshull, J.; Gross, R. A. Biosynthesis of monomers for plastics from renewable oils. In *Biobased Monomers, Polymers, and Materials*, ACS Publications: **2012**, pp 77-90; e)*Biosynthetic Routes to Long-Chain a,ω-Hydroxyacids, Diacids and their Conversion to Oligomers and Polymers.* Gross, R. A.; Lu, W.; Ness, J.; Minshull, J. (Polytechnic Institute of New York University), International Patent: WO 2011008232, **2011**; f)Biosynthesis of Monomers for Plastics from Renewable Oils. Lu, W.; Ness, J. E.; Xie, W.; Zhang, X.; Minshull, J.; Gross, R. A. *Journal of the American Chemical Society*, **2010,** *132* (43), 15451–15455.

48. a)Refining of plant oils to chemicals by olefin metathesis. Chikkali, S.; Mecking, S. *Angewandte Chemie International Edition*, **2012,** *51* (24), 5802-5808; b)Metathesis of unsaturated fatty acids: Synthesis of long-chain unsaturated α, ω-dicarboxylic acids. Ngo, H. L.; Jones, K.; Foglia, T. A. *Journal of the American Oil Chemists' Society*, **2006,** *83* (7), 629-634; c)Stempfle, F.; Roesle, P.; Mecking, S. Long-Chain Polyesters via Chemical Catalytic Conversions of Fatty Acid Ester. In *Biobased Monomers, Polymers, and Materials*, Gross, R. A.; Smith, P. B., (Eds.), ACS Symposium Series, Vol. 1105, ACS Publishing: Washington, D.C., **2012**, pp 151-164; d)Chain multiplication of fatty acids to precise telechelic polyethylene. Witt, T.; Häußler, M.; Kulpa, S.; Mecking, S. *Angewandte Chemie*, **2017,** *129* (26), 7697-7702; e)Chain Multiplication of Fatty Acids to Precise

Telechelic Polyethylene. Witt, T.; Häußler, M.; Kulpa, S.; Mecking, S. *Angewandte Chemie International Edition*, **2017,** *56* (26), 7589-7594.

49. a)Isomerizing hydroformylation of fatty acid esters: Formation of ω-aldehydes. Behr, A.; Obst, D.; Westfechtel, A. *European Journal of Lipid Science and Technology*, **2005,** *107* (4), 213-219; b)Linear selective isomerization/hydroformylation of unsaturated fatty acid methyl esters: a bimetallic approach. Gaide, T.; Bianga, J.; Schlipköter, K.; Behr, A.; Vorholt, A. J. *ACS Catalysis*, **2017,** *7* (6), 4163-4171.
50. a)Isomerizing-hydroboration of the monounsaturated fatty acid ester methyl oleate. Ghebreyessus, K. Y.; Angelici, R. J. *Organometallics*, **2006,** *25* (12), 3040-3044; b)An efficient and recyclable catalytic system comprising nano-iridium (0) and a pyridinium salt of nido-carboranyldiphosphine for the synthesis of one-dimensional boronate esters via hydroboration reaction. Zhu, Y.; Jang, S. H. A.; Tham, Y. H.; Algin, O. B.; Maguire, J. A.; Hosmane, N. S. *Organometallics*, **2012,** *31* (7), 2589-2596.
51. a)Hydrosilylation of long chain unsaturated fatty acid esters. Saghian, N.; Gertner, D. *Journal of the American Oil Chemists Society*, **1974,** *51* (8), 363-367; b)Iridium-catalysed isomerising trialkylsilylation of methyl oleate. Huber, T.; Firlbeck, D.; Riepl, H. M. *Journal of Organometallic Chemistry*, **2013,** *744*, 144-148.
52. a)Polymer precursors from catalytic reactions of natural oils. Furst, M. R.; Le Goff, R.; Quinzler, D.; Mecking, S.; Botting, C. H.; Cole-Hamilton, D. J. *Green Chemistry*, **2012,** *14* (2), 472-477; b)α, ω-Functionalized C_{19} Monomers. Walther, G.; Deutsch, J.; Martin, A.; Baumann, F. E.; Fridag, D.; Franke, R.; Köckritz, A. *ChemSusChem*, **2011,** *4* (8), 1052-1054.
53. a)Synthetic polyester from algae oil. Roesle, P.; Stempfle, F.; Hess, S. K.; Zimmerer, J.; Río Bártulos, C.; Lepetit, B.; Eckert, A.; Kroth, P. G.; Mecking, S. *Angewandte Chemie International Edition*, **2014,** *53* (26), 6800-6804; b)Valorization of unconventional lipids from microalgae or tall oil via a selective dual catalysis one-pot approach. Hess, S. K.; Schunck, N. S.; Goldbach, V.; Ewe, D.; Kroth, P. G.; Mecking, S. *Journal of the American Chemical Society*, **2017,** *139* (38), 13487-13491; c)Production of chemicals from microalgae lipids–status and perspectives. Hess, S. K.; Lepetit, B.; Kroth, P. G.; Mecking, S. *European Journal of Lipid Science and Technology*, **2018,** *120* (1), 1700152.
54. a)Van Leeuwen, P. W. N. M.; Chadwick, J. C., *Carbonylation Reactions. Homogeneous Catalysts: Activity − Stability − Deactivation*. Wiley-VCH: Weinheim, Germany, **2011**; b)Beller, M., Ed. *Catalytic Carbonylation Reactions*. 1 ed.; Topics in Organometallic Chemistry, Vol. 18, Springer:

Heidelberg, **2006**; c)A computational study of the methanolysis of palladium–acyl bonds. Donald, S. M.; Macgregor, S. A.; Settels, V.; Cole-Hamilton, D. J.; Eastham, G. R. *Chemical communications*, **2007,** (6), 562-564.

55. Harris, B., Acrylics for the Future. In *Ingenia*, **2010**; Vol. 45, pp 18-23.
56. Highly active and selective catalysts for the production of methyl propanoate via the methoxycarbonylation of ethene. Clegg, W.; Elsegood, M. R.; Eastham, G. R.; Tooze, R. P.; Wang, X. L.; Whiston, K. *Chemical communications*, **1999,** (18), 1877-1878.
57. Tandem isomerisation–carbonylation catalysis: highly active palladium (II) catalysts for the selective methoxycarbonylation of internal alkenes to linear esters. Pugh, R. I.; Drent, E.; Pringle, P. G. *Chemical communications*, **2001,** (16), 1476-1477.
58. A comprehensive mechanistic picture of the isomerizing alkoxycarbonylation of plant oils. Roesle, P.; Caporaso, L.; Schnitte, M.; Goldbach, V.; Cavallo, L.; Mecking, S. *Journal of the American Chemical Society*, **2014,** *136* (48), 16871-16881.
59. Polymerisable di-and triesters from Tall Oil Fatty Acids and related compounds. Furst, M. R.; Seidensticker, T.; Cole-Hamilton, D. J. *Green Chemistry*, **2013,** *15* (5), 1218-1225.
60. Catalyst activity and selectivity in the isomerising alkoxycarbonylation of methyl oleate. Christl, J. T.; Roesle, P.; Stempfle, F.; Wucher, P.; Göttker-Schnetmann, I.; Müller, G.; Mecking, S. *Chemistry – A European Journal*, **2013,** *19* (50), 17131-17140.
61. a)Hydroesterification of methyl 10-undecenoate in thermomorphic multicomponent solvent systems—Process development for the synthesis of sustainable polymer precursors. Gaide, T.; Behr, A.; Arns, A.; Benski, F.; Vorholt, A. J. *Chemical Engineering and Processing: Process Intensification*, **2016,** *99*, 197-204; b)Selective product crystallization for concurrent product separation and catalyst recycling in the isomerizing methoxycarbonylation of methyl oleate. Herrmann, N.; Kȍhnke, K.; Seidensticker, T. *ACS Sustainable Chemistry & Engineering*, **2020,** *8* (29), 10633-10638.
62. From sunflower oil toward 1, 19-diester: Mechanistic elucidation. Walther, G.; Knöpke, L. R.; Rabeah, J.; Chęciński, M. P.; Jiao, H.; Bentrup, U.; Brückner, A.; Martin, A.; Köckritz, A. *Journal of catalysis*, **2013,** *297*, 44-55.
63. Mechanism and control of the palladium catalyzed alkoxycarbonylation of oleochemicals from sustainable sources. Jameel, F.; Kohls, E.; Stein, M. *ChemCatChem*, **2019,** *11* (19), 4894-4906.

64. Dihydrogen reduction of carboxylic esters to alcohols under the catalysis of homogeneous ruthenium complexes: high efficiency and unprecedented chemoselectivity. Saudan, L. A.; Saudan, C. M.; Debieux, C.; Wyss, P. *Angewandte Chemie*, **2007,** *119* (39), 7617-7620.

65. Renewable Non-Isocyanate Based Thermoplastic Polyurethanes via Polycondensation of Dimethyl Carbamate Monomers with Diols. Unverferth, M.; Kreye, O.; Prohammer, A.; Meier, M. A. *Macromolecular rapid communications*, **2013,** *34* (19), 1569-1574.

66. Introducing catalytic lossen rearrangements: sustainable access to carbamates and amines. Kreye, O.; Wald, S.; Meier, M. A. *Advanced Synthesis & Catalysis*, **2013,** *355* (1), 81-86.

67. Novel long chain unsaturated diisocyanate from fatty acid: synthesis, characterization, and application in bio-based polyurethane. Hojabri, L.; Kong, X.; Narine, S. S. *Journal of Polymer Science Part A: Polymer Chemistry*, **2010,** *48* (15), 3302-3310.

68. a)Kricheldorf, H., *Polycondensation: History and New Results*. Springer: Heidelberg, Germany, **2013**; b)Elias, H.-G., *Macromolecules*. Vol. 1: *Chemical Structures and Syntheses*, Wiley-VCH: Weinheim, **2005**.

69. Synthesis of polycaprolactone: a review. Labet, M.; Thielemans, W. *Chemical Society Reviews*, **2009,** *38* (12), 3484-3504.

70. a)Ring-opening polymerization—an introductory review. Nuyken, O.; Pask, S. D. *Polymers*, **2013,** *5* (2), 361-403; b)Dubois, P.; Coulembier, O.; Raquez, J.-M., Eds. *Handbook of ring-opening polymerization*. Wiley-VCH: Weinheim, **2009**.

71. a)Pepels, M. P. F. *Exploring the Potential of Polymacrolactones as Polyethylene-Mimicks*. Ph.D. Thesis, Eindhoven Unversity of Technology, Eindhoven, Netherlands, **2015**; b)Anionic ring-opening polymerization of macrocyclic esters. Nomura, R.; Ueno, A.; Endo, T. *Macromolecules*, **1994,** *27* (2), 620-621.

72. a)Anionic polymerization of pentadecanolide. A new route to a potentially biodegradable aliphatic polyester. Jedliński, Z.; Juzwa, M.; Adamus, G.; Kowalczuk, M.; Montaudo, M. *Macromolecular Chemistry and Physics*, **1996,** *197* (9), 2923-2929; b)Catalytic ring-opening polymerization of renewable macrolactones to high molecular weight polyethylene-like polymers. Van Der Meulen, I.; Gubbels, E.; Huijser, S.; Sablong, R.; Koning, C. E.; Heise, A.; Duchateau, R. *Macromolecules*, **2011,** *44* (11), 4301-4305; c)*Process for preparing a polyester*. Van der Meulen, I.; Huijser, S.; Gubbels, E.; Heise, A.; Duchateau, R.; Koning, C. E. (Saudi Basic Industries Corporation), U.S. Patent 8,933,190 (B2), **2015**; d)Mimicking (linear) low-density polyethylenes using modified polymacrolactones. Pepels, M. P.; Koeken, R. A.; van der Linden,

S. J.; Heise, A.; Duchateau, R. *Macromolecules*, **2015,** *48* (14), 4779-4792; e)Controlled ring-opening polymerization of ω-pentadecalactone with yttrium isopropoxide as an initiator. Zhong, Z.; Dijkstra, P. J.; Feijen, J. *Macromolecular Chemistry and Physics*, **2000,** *201* (12), 1329-1333.

73. Changes in the chemical composition of essential oil of Angelica archangelica L. roots during storage. Nivinskiene, O.; Butkiene, R.; Mockutë, D. *Chemija (Vilnius)*, **2003,** *14* (1), 52-56.

74. a)Ring-Opening Copolymerization of (R)-β-Butyrolactone with Macrolide: A New Series of Poly(Hydroxyalkanoate)s. Hori, Y.; Hongo, H.; Hagiwara, T. *Macromolecules*, **1999,** *32* (10), 3537-3539; b)Kinetic investigation on the catalytic ring-opening (co) polymerization of (macro) lactones using aluminum salen catalysts. Pepels, M.; Bouyahyi, M.; Heise, A.; Duchateau, R. *Macromolecules*, **2013,** *46* (11), 4324-4334; c)Metal-based catalysts for controlled ring-opening polymerization of macrolactones: high molecular weight and well-defined copolymer architectures. Bouyahyi, M.; Duchateau, R. *Macromolecules*, **2014,** *47* (2), 517-524; d)Ring-opening polymerization of ω-6-hexadecenlactone by a salicylaldiminato aluminum complex: A route to semicrystalline and functional poly(ester)s. Fuoco, T.; Meduri, A.; Lamberti, M.; Venditto, V.; Pellecchia, C.; Pappalardo, D. *Polymer Chemistry*, **2015,** *6* (10), 1727-1740; e)Large-ring lactones from plant oils. Witt, T.; Mecking, S. *Green Chemistry*, **2013,** *15* (9), 2361-2364.

75. a)*Verfahren zur Herstellung von Polylaurinlactam.* Dachs, K.; Kunde, J.; Metzger, H.; Wilhelm, H. (BASF), DE 1,239,473, **1962**; b)The polymerization of dodecalactam. Shein, T. I.; Vlasova, L. N. *Polymer Science U.S.S.R.*, **1964,** *5* (4), 564-569.

76. a)Long-spaced aliphatic polyesters. Ortmann, P.; Mecking, S. *Macromolecules*, **2013,** *46* (18), 7213-7218; b)Acyclic diene metathesis (ADMET) polymerization. Synthesis of an unsaturated polyester. Bauch, C. G.; Wagener, K. B.; Boncella, J. M. *Die Makromolekulare Chemie, Rapid Communications*, **1991,** *12* (7), 413-417; c)Acyclic diene metathesis (ADMET) polymerization of allyl undec-10-enoate and some related esters. Hall, A. J.; Hodge, P.; Kamau, S. D.; Ben-Haida, A. *Journal of Organometallic Chemistry*, **2006,** *691* (24-25), 5431-5437.

77. Bio-Based Aliphatic Polyurethanes Through ADMET Polymerization in Bulk and Green Solvent. Lebarbé, T.; More, A. S.; Sane, P. S.; Grau, E.; Alfos, C.; Cramail, H. *Macromolecular rapid communications*, **2014,** *35* (4), 479-483.

78. Long-spaced polyamides: elucidating the gap between polyethylene crystallinity and hydrogen bonding. Ortmann, P.; Lemke, T. A.; Mecking, S. *Macromolecules*, **2015,** *48* (5), 1463-1472.

79. a)Direct synthesis of polyamides via catalytic dehydrogenation of diols and diamines. Zeng, H.; Guan, Z. *Journal of the American Chemical Society*, **2011,** *133* (5), 1159-1161; b)Synthesis of polyamides from diols and diamines with liberation of H_2. Gnanaprakasam, B.; Balaraman, E.; Gunanathan, C.; Milstein, D. *Journal of Polymer Science Part A: Polymer Chemistry*, **2012,** *50* (9), 1755-1765.

80. Fundamental principles of condensation polymerization. Flory, P. J. *Chemical reviews*, **1946,** *39* (1), 137-197.

81. Polymers and polyfunctionality. Carothers, W. H. *Transactions of the Faraday Society*, **1936,** *32*, 39-49.

82. a)Schwaderer, J. B. *Ruthenium Catalysed Amination of Bio-Based Diols - Building Blocks for Polyamides from Renewables*. Master Thesis, University of Konstanz, Konstanz, Germany, **2016**; b)Walter, J. *Polyamides from Renewable Resources*. Master Thesis, University of Konstanz, Konstanz, Germany, **2015**; c)Diamines for Polymer Materials via Direct Amination of Lipid- and Lignocellulose-based Alcohols with NH_3. Pingen, D.; Schwaderer, J. B.; Walter, J.; Wen, J.; Murray, G.; Vogt, D.; Mecking, S. *ChemCatChem*, **2018,** *10* (14), 3027-3033.

83. Fradet, A.; Tessier, M. Polyesters. In *Synthetic methods in step-growth polymers*, Rogers, M. E.; Long, T. E., (Eds.), Wiley Interscience: Hoboken, New Jersey, **2003**, pp 17-134.

84. Préparation d'acides polyméthylène-dicarboniques de 11 à 19 atomes de carbone et de quelques-uns de leurs dérivés. Chuit, P. *Helvetica Chimica Acta*, **1926,** *9* (1), 264-278.

85. Stempfle, F. *Aliphatic Polyester Materials from Polycondensation of Seed- and Algae Oil-Based Long-Chain Monomers*. Ph.D. Thesis, University of Konstanz, Konstanz, Germany, **2015**.

86. Structure–properties relationship of fatty acid-based thermoplastics as synthetic polymer mimics. Maisonneuve, L.; Lebarbé, T.; Grau, E.; Cramail, H. *Polymer Chemistry*, **2013,** *4* (22), 5472-5517.

87. Köpnick, H.; Schmidt, M.; Brügging, W.; Rüter, J.; Kaminsky, W. Polyesters. In *Ullmann's Encyclopedia of Industrial Chemistry*, Gerhartz, W. E., B., (Ed.) Wiley-VCH: Weinheim, **2000**.

88. Aliphatic long-chain C_{20} polyesters from olefin metathesis. Trzaskowski, J.; Quinzler, D.; Bährle, C.; Mecking, S. *Macromolecular rapid communications*, **2011,** *32* (17), 1352-1356.

89. Synthesis and characterization of polyamides containing octadecanedioic acid: Nylon-2, 18, nylon-3, 18, nylon-4, 18, nylon-6, 18, nylon-8, 18, nylon-9, 18, and nylon-12, 18. Bennett, C.; Mathias, L. J. *Journal of Polymer Science Part A: Polymer Chemistry*, **2005,** *43* (5), 936-945.

90. Redefining polyamide property profiles via renewable long-chain aliphatic segments: Towards impact resistance and low water absorption. Nguyen, P. H.; Spoljaric, S.; Seppälä, J. *European Polymer Journal*, **2018,** *109*, 16-25.

91. a)Polyamides having long methylene chain units. Saotome, K.; Komoto, H. *Journal of Polymer Science Part A-1: Polymer Chemistry*, **1966,** *4* (6), 1463-1473; b)Preparation and characterization of a series of polyamides with long alkylene segments: Nylons 12.20, 10.20, s.20, 6.20, 4.20 and 2.20. Huang, Y.; Li, W.; Yan, D. *Polymer Bulletin*, **2002,** *49* (2), 111-118; c)Synthesis and characterization of nylons based on hexadecane diacid. Li, W.; Yan, D. *Journal of applied polymer science*, **2003,** *88* (10), 2462-2467; d)Polyamides X. 34: A new class of polyamides with long alkane segments. Ehrenstein, M.; Smith, P.; Weder, C. *Macromolecular Chemistry and Physics*, **2003,** *204* (13), 1599-1606; e)Synthesis and characterization of polyamides X.18. Cui, X.; Li, W.; Yan, D.; Yuan, C.; Di Silvestro, G. *Journal of applied polymer science*, **2005,** *98* (4), 1565-1571.

92. Adam, N.; Avar, G.; Blankenheim, H.; Friederichs, W.; Giersig, M.; Weigand, E.; Halfmann, M.; Wittbecker, F.-W.; Larimer, D.-R.; Maier, U.; Meyer-Ahrens, S.; Noble, K.-L.; Wussow, H.-G. Polyurethanes. In *Ullmann's Encyclopedia of Industrial Chemistry*, Gerhartz, W.; Elvers, B., (Eds.), Wiley-VCH: Weinheim, **2000**.

93. Synthesis and characterization of polyethylene-like polyurethanes derived from long-chain, aliphatic α, ω-diols. McKiernan, R. L.; Gido, S. P.; Penelle, J. *Polymer*, **2002,** *43* (10), 3007-3017.

94. a)Polyurethanes and polyureas having long methylene chain units. Saotome, K.; Komoto, H. *Journal of Polymer Science Part A1: Polymer Chemistry*, **1967,** *5* (1), 119-126; b)Novel fatty acid based di-isocyanates towards the synthesis of thermoplastic polyurethanes. More, A. S.; Lebarbé, T.; Maisonneuve, L.; Gadenne, B.; Alfos, C.; Cramail, H. *European Polymer Journal*, **2013,** *49* (4), 823-833.

95. Chemistry of the production of organic isocyanates. Twitchett, H. *Chemical Society Reviews*, **1974,** *3* (2), 209-230.

96. a)Sustainable routes to polyurethane precursors. Kreye, O.; Mutlu, H.; Meier, M. A. *Green Chemistry*, **2013,** *15* (6), 1431-1455; b)Plant-oil-based polyamides and polyurethanes: Toward sustainable nitrogen-containing thermoplastic materials. Meier, M. A. *Macromolecular rapid communications*, **2019,** *40* (1), 1800524; c)Isocyanate-free routes to polyurethanes and poly(hydroxy urethane)s. Maisonneuve, L.; Lamarzelle, O.; Rix, E.; Grau, E.; Cramail, H. *Chemical reviews*, **2015,** *115* (22), 12407-12439.

97. Kohan, M. I.; Mestemacher, S. A.; Pagilagan, R. U.; Redmond, K. Polyamides. In *Ullmann's Encyclopedia of Industrial Chemistry*, Gerhartz, W.; Elvers, B., (Eds.), Wiley-VCH: Weinheim, **2000**.

98. Zhang, C. Biodegradable Polyesters: Synthesis, Properties, Applications. In *Biodegradable Polyesters*, Fakirov, S., (Ed.) Wiley-VCH: Weinheim, Germany, **2015**.

99. a)Crystallization in High Polymers. V. Dependence of Melting Temperatures of Polyesters and Polyamides on Composition and Molecular Weight. Evans, R. D.; Mighton, H. R.; Flory, P. J. *Journal of the American Chemical Society*, **1950,** *72* (5), 2018-2028; b)Korshak, V. V.; Vinogradova, S. V., *Polyesters*. Pergamon Press: Oxford, U.K., **1965**; c)Mandelkern, L.; Alamo, R. G. Thermodynamic Quantities Governing Melting In *Physical Properties of Polymers Handbook*, Mark, J. E., (Ed.) Springer: Heidelberg, Germany, **2007**, pp 165-186.

100. a)Ishioka, R.; Kitakuni, E.; Y., I. Aliphatic Polyesters: "Bionolle". In *Biopolymers*, Steinbüchel, A.; Doi, Y., (Eds.), Vol. 4, Wiley-VCH: Weinheim, **2002**, pp 275-297; b)Thermodynamics of the phase behaviour of poly (vinyl chloride)/aliphatic polyester blends. Woo, E.; Barlow, J.; Paul, D. *Polymer*, **1985,** *26* (5), 763-773; c)Substrate specificities in hydrolysis of polyhydroxyalkanoates by microbial esterases. Mukai, K.; Sema, Y.; Tomita, K. *Biotechnology letters*, **1993,** *15* (6), 601-604.

101. From polyethylene to polyester: influence of ester groups on the physical properties. Pepels, M. P.; Hansen, M. R.; Goossens, H.; Duchateau, R. *Macromolecules*, **2013,** *46* (19), 7668-7677.

102. Encoding crystal microstructure and chain folding in the chemical structure of synthetic polymers. De Ten Hove, C. L. F.; Penelle, J.; Ivanov, D. A.; Jonas, A. M. *Nature materials*, **2004,** *3* (1), 33-37.

103. a)Whiteley, K. S. Polyolefins. In *Ullmann's Encyclopedia of Industrial Chemistry*, Gerhartz, W. E., B., (Ed.) Wiley-VCH: Weinheim, Germany, **2000**; b)Peacock, A. J., *Handbook of Polyethylene - Structures, Properties and Applications*. CRC Press: Boca Raton, Florida, USA, **2000**.

104. Polyethylene like polymers. Aliphatic polyesters of dodecanedioic acid: 1. Synthesis and properties. Barbiroli, G.; Lorenzetti, C.; Berti, C.; Fiorini, M.; Manaresi, P. *European Polymer Journal*, **2003,** *39* (4), 655-661.

105. Nature's polyethylene. Cole-Hamilton, D. J. *Angewandte Chemie International Edition*, **2010,** *49* (46), 8564-8566.

106. a)Polymer constitution and fiber properties. Hill, R.; Walker, E. *Journal of Polymer Science*, **1948,** *3* (5), 609-630; b)Extents of hydrogen bonding in polyamides and polyurethanes. Trifan, D. S.;

Terenzi, J. F. *Journal of Polymer Science*, **1958,** *28* (117), 443-445; c)Über Wasserstofffbrücken in Polyamiden. Bessler, V. E.; Bier, G. *Die Makromolekulare Chemie: Macromolecular Chemistry and Physics*, **1969,** *122* (1), 30-37; d)Hydrogen bonding in polyamides. Schroeder, L.; Cooper, S. L. *Journal of Applied Physics*, **1976,** *47* (10), 4310-4317.

107. Structural studies on linear polyurethanes. II. Crystal and molecular structures of aliphatic polyurethanes from trimethylene diisocyanate, and tetra-and hexa-methylene glycols. Saito, Y.; Hara, K.; Kinoshita, S. *Polymer Journal*, **1982,** *14* (1), 19-31.
108. a)Aharoni, S. M., *n-Nylons: Their Synthesis, Structure and Properties*. Wiley-VCH: Weinheim, Germany, **1997**; b)An investigation of the structures of polyamide series. Kinoshita, Y. *Die Makromolekulare Chemie: Macromolecular Chemistry and Physics*, **1959,** *33* (1), 1-20; c)Solid-state deformation of polyethylene and nylon and its effects on their structure and morphology. Perkins, W. G.; Porter, R. S. *Journal of Materials Science*, **1977,** *12* (12), 2355-2388; d)The crystal structure of polyheptamethylene pimelamide (nylon 77). Kinoshita, Y. *Die Makromolekulare Chemie: Macromolecular Chemistry and Physics*, **1959,** *33* (1), 21-31; e)Investigation on odd-odd nylons based on undecanedioic acid: 1. Synthesis and characterization. Cui, X.; Li, W.; Yan, D. *Polymer international*, **2004,** *53* (11), 1729-1734.
109. a)Structural studies on polyurethane fibers. I. Crystal and molecular structures of aliphatic polyurethanes from hexamethylene diisocyanate and some linear glycols. Saito, Y.; Nansai, S.; Kinoshita, S. *Polymer Journal*, **1972,** *3* (2), 113-121; b)An overview on 12-polyurethane: synthesis, structure and crystallization. Fernández, C.; Bermúdez, M.; Versteegen, R.; Meijer, E.; Vancso, G. J.; Muñoz-Guerra, S. *European Polymer Journal*, **2010,** *46* (11), 2089-2098.
110. Studies on crystallization of high polymers by differential thermal analysis. Inoue, M. *Journal of Polymer Science Part A: General Papers*, **1963,** *1* (8), 2697-2709.
111. Quinzler, D. *Linear Semicrystalline Polyesters and Polyamides from Plant Oil Fatty Acids via Catalytic Alkoxycarbonylation*. Ph.D. Thesis, University of Konstanz, Konstanz, Germany, **2014**.
112. Synthesis and characterization of nylon 18.18 and nylon 18 adamantane. Bennett, C.; Kaya, E.; Sikes, A. M.; Jarrett, W. L.; Mathias, L. J. *Journal of Polymer Science Part A: Polymer Chemistry*, **2009,** *47* (17), 4409-4419.
113. Preparation and some properties of nylon-4, 2. Gaymans, R.; Venkatraman, V.; Schuijer, J. *Journal of Polymer Science: Polymer Chemistry Edition*, **1984,** *22* (6), 1373-1382.
114. Synthesis and thermal properties of [n]-polyurethanes. Neffgen, S.; Kušan, J.; Fey, T.; Keul, H.; Höcker, H. *Macromolecular Chemistry and Physics*, **2000,** *201* (16), 2108-2114.

115. Influence of hydrogen bonding on the crystallization behavior of semicrystalline polyurethanes. McKiernan, R. L.; Heintz, A. M.; Hsu, S. L.; Atkins, E. D.; Penelle, J.; Gido, S. P. *Macromolecules*, **2002,** *35* (18), 6970-6974.

116. Structure of 22, 12-polyurethane in chain-folded lamellar crystals. McKiernan, R. L.; Sikorski, P.; Atkins, E. D.; Gido, S. P.; Penelle, J. *Macromolecules*, **2002,** *35* (22), 8433-8439.

117. Compared structure and morphology of nylon-12 and 10-polyurethane lamellar crystals. Fernández, C.; Bermúdez, M.; Alla, A.; Muñoz-Guerra, S.; Tocha, E.; Vancso, G. J. *Polymer*, **2011,** *52* (7), 1515-1522.

118. Ehrenstein, G. W., *Polymeric Materials - Structure, Properties, Applications*. Carl Hanser Verlag: Munich, Germany, **2012**.

119. Elias, H.-G., *Macromolecules*. Vol. 3: *Physical Structures and Properties*, Wiley-VCH: Weinheim, **2005**.

120. a)Example of industrial valorisation of derivative products of Castor oil. Borg, P.; Lê, G.; Lebrun, S.; Pées, B. *Oléagineux, Corps gras, Lipides*, **2009,** *16* (4-5-6), 211-214; b)Nylon-12-preparation, properties, and applications. Griehl, W.; Ruestem, D. *Industrial & Engineering Chemistry*, **1970,** *62* (3), 16-22.

121. a)New polyamides with long alkane segments: nylon 6.24 and 6.34. Ehrenstein, M.; Dellsperger, S.; Kocher, C.; Stutzmann, N.; Weder, C.; Smith, P. *Polymer*, **2000,** *41* (10), 3531-3539; b)Synthesis of copolyamides containing octadecanedioic acid: An investigation of nylon 6/6, 18 in various ratios. Bennett, C.; Zeng, J.; Kumar, S.; Mathias, L. J. *Journal of applied polymer science*, **2006,** *99* (5), 2062-2067.

2. Objectives

At present, monomers derived from fossil feedstocks are the basis for the production of the majority of polymers. This includes thermoplastic elastomers (TPEs), a versatile class of engineering plastics that combine the thermal processability of thermoplastics with the elastomeric properties of vulcanized rubber by relying on physical forces like crystallite formation for crosslinking instead of the generation of irreversible covalent bonds between polymer chains. Unlike conventional rubbers, they therefore possess distinct melting points above which they can be processed as thermoplastics. A commercially relevant class of TPEs constitute segmented polycondensates and polyaddition products in which short crystallizable polyamide, polyurethane, or polyester hard blocks repeatedly alternate with amorphous polyether soft segments. Crystallization of the hard blocks driven by *e.g.* hydrogen bond formation results in the generation of high-melting crystalline hard domains that remain dispersed within a low-melting amorphous soft matrix, thus causing microphase separation in the final product and the generation of a TPE.

In this thesis the potential of novel linear long-chain polycondensation monomers to serve as building blocks for the generation of a new type of aliphatic hard segments with reduced functional group density in all-renewable segmented copolymer TPEs is explored. Starting point was the conversion of plant oil-derived unsaturated fatty acid esters into linear long-chain C_{19} and C_{23} α,ω-diesters using the catalytic process of isomerizing alkoxycarbonylation. Existing reaction protocols were optimized and upscaled in addition to new multi-step synthesis routes being developed to eventually gain access to a variety of suitable linear long-chain α,ω-functionalized compounds in polymerization grade purity (≥ 99 %). This included the first time synthesis of 1,19-nonadecane diisocyanate and 1,23-tricosane diisocyanate as well as the identification of reaction parameters pivotal to increasing the selectivity for the conversion of long-chain α,ω-diazides into the corresponding long-chain α,ω-diamines via catalytic hydrogenation over Pd/C.

Copolymerization of the thus obtained different types of linear long-chain polycondensation monomers with a sugar-derived oligomeric poly(1,3-propanediol) polyether macrodiol of varying molecular weight yielded several series of all-renewable segmented copolymer TPEs based on all-aliphatic long-chain polyester, polyurethane, or polyamide hard segments. Suitable one- or two-step polycondensation and polyaddition protocols respectively were developed for the different types of

polymerization system to eventually obtain copolymers with number average molecular weights in the range of several 10^4 g mol^{-1}.

The effect of elongated aliphatic hydrocarbon segments consisting of up to 23 crystallizable methylene units being incorporated into the hard blocks on the material properties of different types of copolymer TPEs was studied. This included an investigation of the crystallization behavior, phase separation, thermal properties, ductility, and elastomeric behavior, as well as water absorption in case of polyamide-based materials. Special attention was paid to the potential of the long methylene sequences imparting polyethylene-like crystallinity.

3. Thermoplastic Copolyester Elastomers Based on Long-Chain Aliphatic Hard Segments

3.1. Introduction

Thermoplastic polyester elastomers, or thermoplastic copolyester elastomers (TPCs), are segmented copolymer TPEs in which short crystallizable polyester hard blocks alternate with thermodynamically incompatible amorphous polyether or polyester soft blocks. The most common representatives of this type of TPE are petroleum-based, partly aromatic polyester-polyether block copolymers, especially materials based on terephthalic acid-derived, crystallizable poly(butylene terephthalate) hard blocks in combination with amorphous polyether soft blocks (**Figure 3.1**).

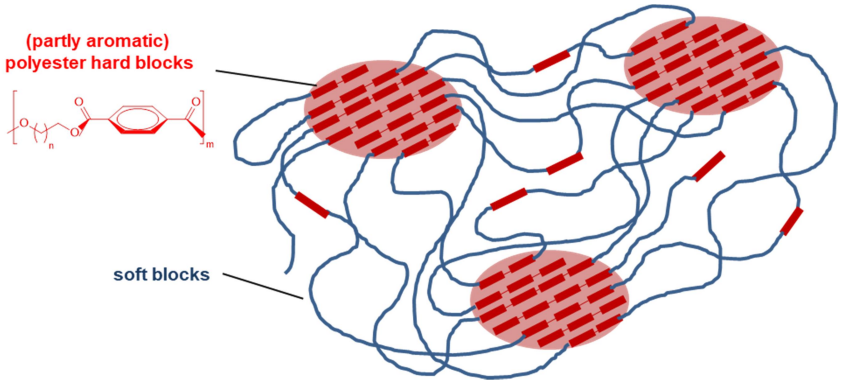

Figure 3.1: Schematic representation of the morphology of typical thermoplastic copolyester elastomers based on partly aromatic polyester hard blocks.

These partly aromatic materials are characterized by high strength, high elasticity, as well as excellent dynamic properties and creep resistance.[1],[2],[3] As a result, they find widespread application in such diverse and demanding areas as the automotive industry in the form of composites,[2],[4] as laminated films in the production of sports and rain wear,[2],[5] but also as surgical drapes and transdermal patches in the medical field.[2],[6] Physical crosslinking in these materials is provided by (semi)crystalline hard domains comprised of polyester blocks that owe their excellent crystallization ability and consequently high melt and crystallization points to the incorporation of aromatic rings into the linear polyester backbone. In contrast, exclusively aliphatic polyester sequences based on currently available short- and mid-chain aliphatic dicarboxylic acids and diols are typically not

suitable to serve as hard blocks in TPCs as their short methylene sequences lack the cohesive force necessary to drive crystallization and provide the material with sufficient physical crosslinking. As a result, all-aliphatic TPCs tend to suffer from low degrees of crystallinity as well as low melt and crystallization points that impede thermoplastic processing and render the final product unsuitable for most everyday applications.[1],[2],[3] However, as outlined in previous chapters, modern catalytic synthesis methods like olefin metathesis[7] and isomerizing alkoxycarbonylation[8] now allow for the preparation of linear long-chain aliphatic α,ω-dicarboxylic acids and diols from plant oils that incorporate the entire hydrocarbon chain of the fatty acid substrate into the final product. Aliphatic polyesters derived from these novel long-chain compounds not only have the advantage of being entirely renewable resource-based but also have been shown to possess a polyethylene-like crystal structure and high degrees of crystallinity.[9],[10],[11] Consequently, the melting points of these aliphatic polyesters are unusually high and approach values recorded for polyethylene, which allows for them to be processed using standard thermoplastic processing techniques like injection molding. [9],[12]

Here, the utility of these novel long-chain compounds to serve as monomers in the generation of high melting, all-aliphatic polyester hard segments in thermoplastic copolyester elastomers is demonstrated and the influence of the length of the monomer methylene sequence on the material properties is investigated. In addition, commonly used, fossil fuel-derived PTMG is replaced by renewable PPDO as the polyether soft segment to increase the degree of sustainability of the obtained materials to 100%.

3.2. Results and Discussion

3.2.1. Synthesis of long-chain thermoplastic copolyester elastomers

As polyester blocks are susceptible to transesterification under polymerization conditions, segmented thermoplastic copolyester elastomers are typically synthesized in a one-step melt polycondensation procedure reminiscent of the synthesis approaches employed to produce classic A_2+B_2-type polyester thermoplastics.[2],[13] Thereby, the macrodiol soft segment directly reacts with the difunctionalized monomers that serve as precursors of the polyester hard blocks to produce a multi-component copolymer in which the monomer units are statistically distributed.[14] This typically involves either the direct esterification of dicarboxylic acid and diol monomers in an A_2+B_2-type polycondensation reaction or polymerization via transesterification catalyzed by *e.g.* a titanium alkoxide.[2],[3],[15] In context of polyesters based on plant oil-derived linear long-chain aliphatic monomers, the direct esterification approach has proven to be feasible for the synthesis of various thermoplastic materials,[16],[17] but transesterification has been shown to overall be the more practical synthesis method[9],[10],[18],[19] and was therefore chosen as the method of choice in this work.

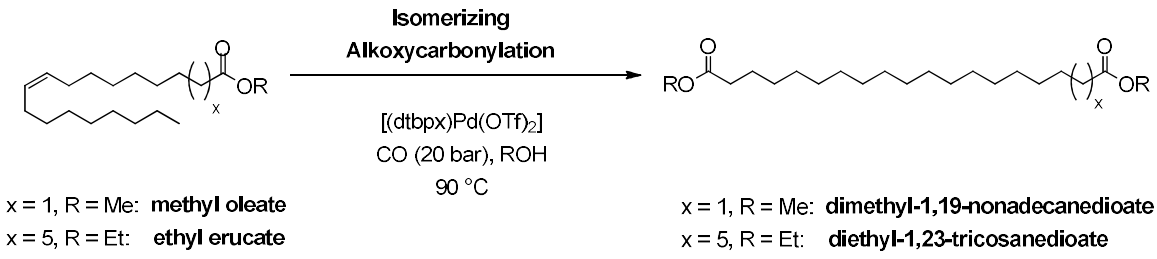

Scheme 3.1: Generation of linear long-chain α,ω-diesters from unsaturated fatty acid esters via isomerizing alkoxycarbonylation.

The necessary linear long-chain α,ω-diesters dimethyl 1,19-nonadecanedioate and diethyl 1,23-tricosanedioate were prepared from methyl oleate and ethyl erucate respectively using isomerizing alkoxycarbonylation (**Scheme 3.1**) (cf. **Chapter 1.2**).[8],[10],[20],[21] As Goldbach *et al.*[22] have recently demonstrated that the defined catalyst precursor [(dtbpx)Pd(OTf)$_2$] is also capable of facilitating isomerizing hydroxycarbonylation reactions, the reaction procedure for the synthesis of dimethyl 1,19-nonadecanedioate as reported in literature[23] was simplified by replacing dried methanol and ethanol respectively with the respective purified alcohol containing still up to 0.2 % water as a solvent and reagent (**Table 3.1**). The results showed that small amounts of water have no pronounced negative effect on the reaction: Under otherwise identical reaction conditions the

conversion of high oleic acid sunflower oil methyl ester in purified methanol (99.9 %) yielded 81 % of pure dimethyl 1,19-nonadecanedioate (**Table 3.1**, **entry 2**) compared to a 83 % yield isolated when freshly distilled and dried methanol was used (**Table 3.1**, **entry 1**). Similarly, replacing absolute ethanol with purified ethanol (99.8 %) in the synthesis of diethyl 1,23-tricosanedioate[23] from technical grade ethyl erucate resulted in no notable decrease in product yield, with the simplified reaction procedure yielding 65 % of the desired diester (**Table 3.1**, **entry 4**) instead of 67 % when absolute ethanol was used (**Table 3.1**, **entry 3**). In addition, the synthesis of dimethyl 1,19-nonadecanedioate could be further upscaled, allowing for the preparation of the desired product on a scale of almost 200 g instead of the 100 g scale so far reported in literature,[12] without a notable decrease in selectivity or overall conversion being observed (**Table 3.1**, **entry 5**). Subsequent hydrogenation of the thus obtained long-chain α,ω-diesters with $LiAlH_4$[9] afforded the corresponding α,ω-diols 1,19-nonadecandiol and 1,23-tricosandiol in polycondensation grade purity.

Table 3.1: Synthesis of dimethyl 1,19-nonadecanedioate[a] and diethyl 1,23-tricosanedioate[b] via isomerizing alkoxycarbonylation.

entry	substrate	H_2O content	isolated yield of pure product
1	methyl oleate	-	34.6 g (83 %)
2	methyl oleate	0.01 %	33.9 g (81 %)
3	ethyl erucate	-	28.6 g (67 %)
4	ethyl erucate	0.02 %	27.5 g (65 %)
5 [c]	methyl oleate	-	193.2 g (74 %)

a) conditions: 120 mmol substrate, 0.26 mmol [(dtbpx)Pd(OTf)$_2$], 120 ml MeOH, 20 bar CO, 90 °C, 120 h. b) conditions: 100 mmol substrate, 0.26 mmol [(dtbpx)Pd(OTf)$_2$], 120 ml EtOH, 20 bar CO, 90 °C, 120 h. c) conditions: 730 mmol substrate, 0.95 mmol [(dtbpx)Pd(OTf)$_2$], 500 ml MeOH, 20 bar CO, 90 °C, 120 h.

For the synthesis of entirely aliphatic and renewable resource-based TPCs, the obtained fatty acid-derived linear long-chain C_{19} and C_{23} α,ω-diesters and α,ω-diols were employed as hard monomers to form all-aliphatic crystallizable polyester hard blocks, while corn-derived dihydroxyl-terminated PPDO with an average molecular weight of M_n = 1000 g mol^{-1} or 2000 g mol^{-1} ($PPDO_{1000}$ and $PPDO_{2000}$) respectively served as a macrodiol to generate amorphous soft blocks. Copolymerization of the hard and soft monomers in different ratios in a one-step melt polycondensation process yielded a series of all-aliphatic segmented poly(ester-ether) block copolymers of varying composition in which the soft macrodiol content ranged from 29 wt.% to 87.% (**Table 3.2, entry 1-16**). Average

molecular weights of the obtained copolymers ranged from M_n = 2.0 to 5.2 x 10^4 g mol^{-1} according to end group analysis from ^{1}H NMR spectroscopy. These results were qualitatively confirmed by GPC analysis which also showed a polydispersity index of about 2, indicating a well behaved molecular weight distribution. Though, it has to be noted that GPC analysis *vs.* polystyrene standards typically overestimates the molecular weights of aliphatic polymers up to a factor of two.

Table 3.2: Poly(ether-ester) block copolymers based on crystallizable aliphatic long-chain polyester hard segments. [a)]

entry	polymer [b)]	diacid [eq.]	diol (1) [eq.]	diol (2) [eq.]	$M_{n,NMR}$ [c)] [g mol^{-1}]	$M_{n,GPC}$ [d)] [g mol^{-1}]	M_w/M_n [d)]
1	TPC-C_{19}PPDO$_{1000}$-76wt%	4 (C_{19})	-	4 (PPDO$_{1000}$)	3.9 × 10^4	5.9 × 10^4	1.9
2	TPC-C_{19}PPDO$_{1000}$-66wt%	4 (C_{19})	1 (C_{19})	3 (PPDO$_{1000}$)	4.0 × 10^4	7.1 × 10^4	1.9
3	TPC-C_{19}PPDO$_{1000}$-53wt%	4 (C_{19})	2 (C_{19})	2 (PPDO$_{1000}$)	3.0 × 10^4	6.8 × 10^4	2.0
4	TPC-C_{19}PPDO$_{1000}$-32wt%	4 (C_{19})	3 (C_{19})	1 (PPDO$_{1000}$)	4.3 × 10^4	7.6 × 10^4	2.2
5	TPC-C_{19}PPDO$_{2000}$-87wt%	4 (C_{19})	-	4 (PPDO$_{2000}$)	3.3 × 10^4	6.3 × 10^4	1.9
6	TPC-C_{19}PPDO$_{2000}$-80wt%	4 (C_{19})	1 (C_{19})	3 (PPDO$_{2000}$)	2.8 × 10^4	6.7 × 10^4	1.9
7	TPC-C_{19}PPDO$_{2000}$-69wt%	4 (C_{19})	2 (C_{19})	2 (PPDO$_{2000}$)	2.8 × 10^4	5.8 × 10^4	2.0
8	TPC-C_{19}PPDO$_{2000}$-49wt%	4 (C_{19})	3 (C_{19})	1 (PPDO$_{2000}$)	3.5 × 10^4	6.4 × 10^4	2.0
9	TPC-C_{23}PPDO$_{1000}$-73wt%	4 (C_{23})	-	4 (PPDO$_{1000}$)	5.2 × 10^4	7.1 × 10^4	1.8
10	TPC-C_{23}PPDO$_{1000}$-62wt%	4 (C_{23})	1 (C_{23})	3 (PPDO$_{1000}$)	2.8 × 10^4	6.1 × 10^4	2.0
11	TPC-C_{23}PPDO$_{1000}$-48wt%	4 (C_{23})	2 (C_{23})	2 (PPDO$_{1000}$)	2.4 × 10^4	5.9 × 10^4	1.8
12	TPC-C_{23}PPDO$_{1000}$-29wt%	4 (C_{23})	3 (C_{23})	1 (PPDO$_{1000}$)	2.0 × 10^4	n.d.	n.d.
13	TPC-C_{23}PPDO$_{2000}$-85wt%	4 (C_{23})	-	4 (PPDO$_{2000}$)	3.7 × 10^4	6.7 × 10^4	1.9
14	TPC-C_{23}PPDO$_{2000}$-77wt%	4 (C_{23})	1 (C_{23})	3 (PPDO$_{2000}$)	2.9 × 10^4	6.4 × 10^4	1.9
15	TPC-C_{23}PPDO$_{2000}$-65wt%	4 (C_{23})	2 (C_{23})	2 (PPDO$_{2000}$)	1.9 × 10^4	4.3 × 10^4	2.2
16	TPC-C_{23}PPDO$_{2000}$-45wt%	4 (C_{23})	3 (C_{23})	1 (PPDO$_{2000}$)	3.0 × 10^4	n.d.	n.d.
17	TPC-C_{12}PPDO$_{2000}$-62wt%	7 (C_{12})	5 (C_{12})	2 (PPDO$_{2000}$)	6.3 × 10^4	11.5 × 10^4	2.0
18	TPC-C_{12}PTMG$_{2000}$-62wt%	7 (C_{12})	5 (C_{12})	2 (PTMG$_{2000}$)	5.3 × 10^4	5.5× 10^4	1.9

a) melt polycondensation of 10 mmol of α,ω-diester with respective comonomers in the presence of 0.05 mol% of N,N'-di-2-naphthyl-1,4-phenylenediamine and 0.16 mol% of $Ti(OBu)_4$. b) specifications regarding wt.% referring to polyether (diol 2) content. c) Determined by end-group analysis from ^{1}H NMR spectroscopy. d) Determined by GPC in THF at 50 °C *vs.* polystyrene standards.

In order to be able to quantify the impact that methylene sequence length in the polyester hard blocks has on material properties, an additional all-aliphatic poly(ether-ester) block copolymer based on polyester hard blocks derived from commercially available mid-chain dimethyl 1,12-dodecanedioate and 1,12-dodecanediol was prepared The resulting partly renewable copolyester

TPC-C_{12}PPDO$_{2000}$-62wt% (**Table 3.2, entry 17**) with an average molecular weight of M_n = 6.3 x 10^4 g mol^{-1} according to ^{1}H NMR spectroscopy was designed to possess a similar block length distribution and hard to soft phase ratio as the erucic acid-derived long-chain TPC-C_{23}PPDO$_{2000}$-65wt% (**Table 3.2, entry 15**), with the weight fraction of the PPDO$_{2000}$ macrodiol accounting for 62 wt.% and 65 wt.% respectively. The major difference between the two copolyesters apart from the length of the methylene sequences in the aliphatic hard blocks is the fact that the shortest possible hard block, an isolated diacid repeat unit, is only half as long for the mid-chain monomer-based TPC-C_{12}PPDO$_{2000}$-62wt% as for its long-chain analog. However, a statistical evaluation of the block length distribution showed that these shortest possible blocks constitute only a relatively small portion of the hard segments in both materials (**Figure 3.2**).

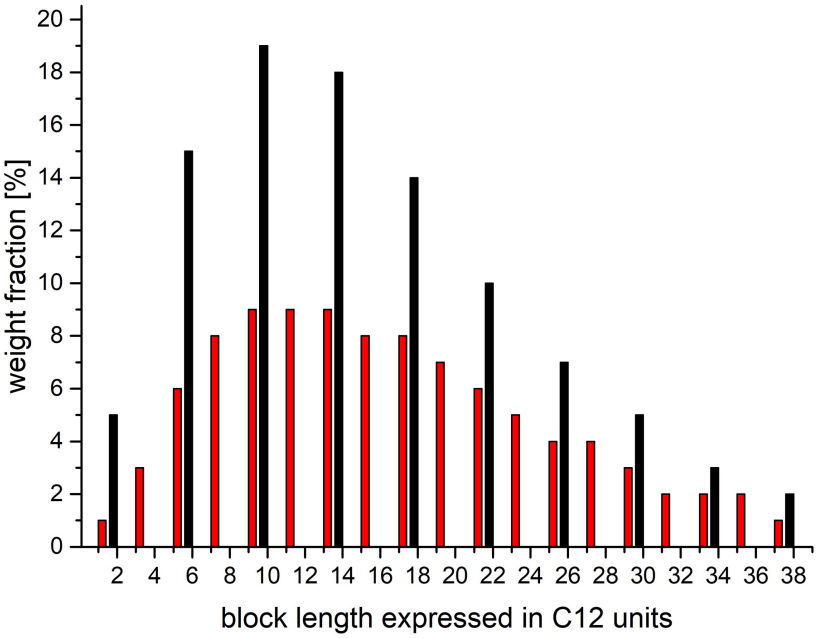

Figure 3.2. Block length distribution expressed on C_{12}-basis for copolyesters of C_{24} dicarboxylic acid with C_{24} diol and 25 mol% polyether (black) and for copolyester of C_{12} dicarboxylic acid with C_{12} diol and 14.3 mol% polyether (red), i.e. isolated acid repeat unit: n =1 (C_{12}) and n = 2 (C_{24}).

Similarly, TPC-C_{12}PTMG$_{2000}$-62wt% (**Table 3.1, entry 18**) in which renewable PPDO$_{2000}$ was replaced with a petroleum-derived PTMG$_{2000}$ polyether macrodiol of the same average molecular weight was synthesized to investigate the influence that the polyether soft phase has on the material properties of the final product.

3.2.2. Morphology of long-chain thermoplastic copolyester elastomers

The morphology of the synthesized long-chain TPCs, exemplified by TPC-C_{23}PPDO$_{2000}$-65wt%, was investigated using wide-angle X-ray diffraction (WAXD). The resulting diffraction pattern (**Figure 3.3**) featured two distinct diffraction peaks at 2θ = 21.4° and 23.8° corresponding to the 110 and 200 reflections of an orthorhombic crystal structure, thereby confirming that TPCs based on plant oil-derived long-chain polyester hard segments crystallize in a polyethylene-like structure, the same as the long-chain aliphatic polyester thermoplastics on which the aliphatic hard segments are based.[9],[11]

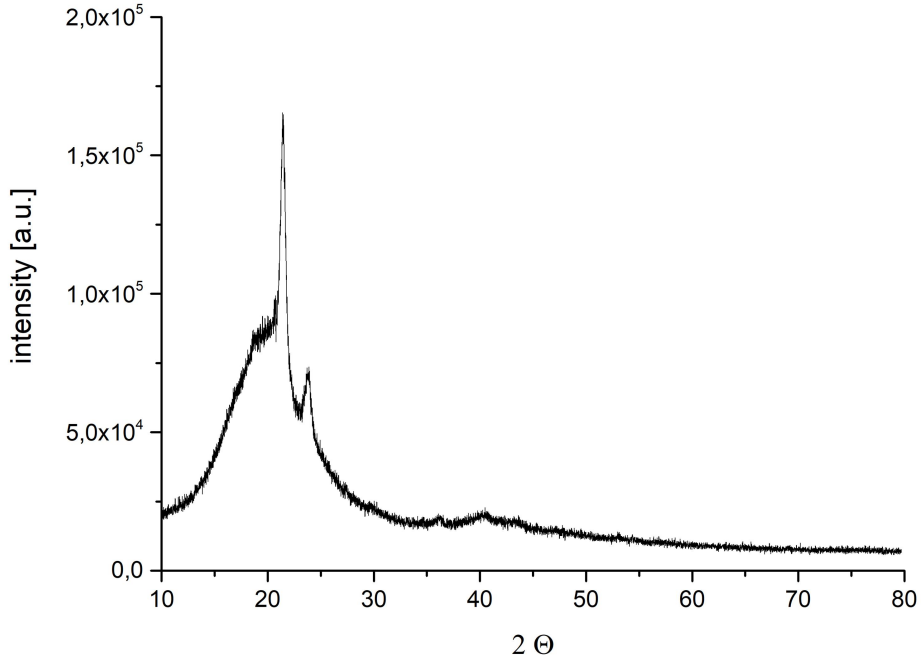

Figure 3.3: WAXD data of TPC-C_{23}PPDO$_{2000}$-65wt%.

The degree of crystallinity calculated for TPC-C_{23}PPDO$_{2000}$-65wt% did not exceed 8 % (**Table 3.3, entry** 1) despite the polyester hard phase accounting for 35 wt.% of the material. Similarly, its mid-chain analog, TPC-C_{12}PPDO$_{2000}$-62wt%, also exhibited a degree of crystallinity of only 9 % (**Table 3.3**, **entry 3**), indicating that the length of the methylene sequences within the aliphatic polyester hard segments did not have a significant effect on the degree of crystallinity. In comparison, replacing PPDO$_{2000}$ with a PTMG macrodiol of similar molecular weight resulted in an increase to 13 % and 15 % respectively for long-chain TPC-C_{23}PTMG$_{2000}$-65wt%[24] (**Table 3.3**, **entry 2**) and its mid-chain analog, TPC-C_{12}PTMG$_{2000}$-62wt% (**Table 3.3**, **entry 4**).

Table 3.3: Degree of crystallinity of different all-aliphatic poly(ether-ester) block copolymers.

entry	polymer	degree of crystallinity χ[a)]
1	TPC-C_{23}PPDO$_{2000}$-65wt%	8 %
2[b)]	TPC-C_{23}PTMG$_{2000}$-65wt%	13 %
3	TPC-C_{12}PPDO$_{2000}$-62wt%	9 %
4	TPC-C_{12}PTMG$_{2000}$-62wt%	15 %

a) calculated by peak deconvolution of recorded WAXD patterns. b) polymer sample provided by F. Stempfle.[24]

3.2.3. Thermal properties of long-chain thermoplastic copolyester elastomers

The thermal properties of the synthesized renewable all-aliphatic poly(ether-ester) block copolymers were investigated using differential scanning calorimetry (DSC) (**Table 3.4**). The thermograms of all studied materials containing PPDO soft segments featured a glass transition point at about T_g = - 65 °C, which corresponds roughly with the glass transitions recorded for pure PPDO$_{1000}$ and PPDO$_{2000}$ at - 71 °C and - 70 °C respectively (**Table 3.4**, **entry 19** and **20**). The difference of about 5 °C suggests that phase separation, while high, was not complete. Glass transition temperatures also remained roughly constant independent of polymer composition, indicating that the ratio of hard to soft phase did not significantly affect phase separation in the studied materials. This is noteworthy as the glass transition points observed for partly aromatic TPCs based on terephthalic acid-derived polyester hard segments rise significantly with increasing hard phase content.[25] Mid-chain monomer-based TPC-C_{12}PPDO$_{2000}$-62wt% exhibited a glass transition in the same temperature range at T_g = - 66 °C (**Table 3.4**, **entry 17**), thereby indicating that phase separation was not significantly affected by the length of the methylene sequences in the aliphatic hard segments. The glass transition of the PTMG polyether soft phase in TPC-C_{12}PTMG$_{2000}$-62wt% (**Table 3.4**, **entry 18**. was not visible in the recorded DSC thermogram.

Table 3.4: Thermal properties of all-aliphatic poly(ether-ester) block copolymers based on crystallizable long-chain polyester hard segments.

entry	Polymer	diacid [eq.]	diol (1) [eq.]	diol (2) [eq.]	T_m [a)] [°C]	T_c [a)] [°C]	T_g [b)] [°C]
1	TPC-C_{19}PPDO$_{1000}$-76wt%	4 (C_{19})	-	4 (PPDO$_{1000}$)	20 c)	7	-65
2	TPC-C_{19}PPDO$_{1000}$-66wt%	4 (C_{19})	1 (C_{19})	3 (PPDO$_{1000}$)	18/62 c)	14/36 c)	-64
3	TPC-C_{19}PPDO$_{1000}$-53wt%	4 (C_{19})	2 (C_{19})	2 (PPDO$_{1000}$)	78	63	-64
4	TPC-C_{19}PPDO$_{1000}$-32wt%	4 (C_{19})	3 (C_{19})	1 (PPDO$_{1000}$)	89	73	-64
5	TPC-C_{19}PPDO$_{2000}$-87wt%	4 (C_{19})	-	4 (PPDO$_{2000}$)	14	-12	-67
6	TPC-C_{19}PPDO$_{2000}$-80wt%	4 (C_{19})	1 (C_{19})	3 (PPDO$_{2000}$)	8/56 c)	29 c)	-66
7	TPC-C_{19}PPDO$_{2000}$-69wt%	4 (C_{19})	2 (C_{19})	2 (PPDO$_{2000}$)	4/74 c)	61	-65
8	TPC-C_{19}PPDO$_{2000}$-49wt%	4 (C_{19})	3 (C_{19})	1 (PPDO$_{2000}$)	89	73	-66
9	TPC-C_{23}PPDO$_{1000}$-73wt%	4 (C_{23})	-	4 (PPDO$_{1000}$)	39c)	25c)	-64
10	TPC-C_{23}PPDO$_{1000}$-62wt%	4 (C_{23})	1 (C_{23})	3 (PPDO$_{1000}$)	45/78c)	38/54c)	-64
11	TPC-C_{23}PPDO$_{1000}$-48wt%	4 (C_{23})	2 (C_{23})	2 (PPDO$_{1000}$)	89	69	-64
12	TPC-C_{23}PPDO$_{1000}$-29wt%	4 (C_{23})	3 (C_{23})	1 (PPDO$_{1000}$)	95	79	-64
13	TPC-C_{23}PPDO$_{2000}$-85wt%	4 (C_{23})	-	4 (PPDO$_{2000}$)	7/24c)	-7/10c)	-64
14	TPC-C_{23}PPDO$_{2000}$-77wt%	4 (C_{23})	1 (C_{23})	3 (PPDO$_{2000}$)	36/77c)	28/49c)	-64
15	TPC-C_{23}PPDO$_{2000}$-65wt%	4 (C_{23})	2 (C_{23})	2 (PPDO$_{2000}$)	86	67	-66
16	TPC-C_{23}PPDO$_{2000}$-45wt%	4 (C_{23})	3 (C_{23})	1 (PPDO$_{2000}$)	94	78	-66
17	TPC-C_{12}PPDO$_{2000}$-62wt%	7 (C_{12})	5 (C_{12})	2 (PPDO$_{2000}$)	62	38	-66
18	TPC-C_{12}PTMG$_{2000}$-62wt%	7 (C_{12})	5 (C_{12})	2 (PTMG$_{2000}$)	17/66c)	1/45c)	n.d.d)
19	PPDO$_{1000}$	-	-	-	19	-	-70
20	PPDO$_{2000}$	-	-	-	14/20	-	-70

a) Determined by DSC with a heating/cooling rate of 10 K min^{-1}. b) Determined by DSC with a heating/cooling rate of 30 K min^{-1}. c) Broad melting and crystallization transitions observed. d) no T_g detectable via DSC

The DSC thermograms recorded for the synthesized TPCs also featured at least one melting point. Upper melting points ranged from 14 °C to 89 °C for poly(ether-ester) block copolymers based on oleic acid-derived PE-19.19 polyester hard segments (**Table 3.4**, **entry 1-8**) and from 24 °C to 96 °C for materials based on erucic acid-derived PE-23.23 polyester blocks (**Table 3.4**, **entry 9-16**). Polycondensation of dimethyl 1,19-nonadecanedioate and diethyl-1,23-trisocanedioate respectively with stoichiometric amounts of a soft PPDO polyether macrodiol yielded polyester-polyether copolymers whose thermal properties were dominated by the low melting polyether soft phase (**Table 3.4**, **entry 1, 5, 9** and **13**), with only the melting point of TPC-C_{23}PPDO$_{1000}$-73wt% at 39 °C (**Table 3.4**, **entry 9**) significantly exceeding room temperature. The very low crystallization temperatures of these materials, which ranged from - 7 °C to 25 °C, also complicated or outright

prevented further processing of the final product via injection molding. In order to obtain TPCs that can be readily processed using standard thermoplastic processing techniques, a partial replacement of the PPDO polyether soft segment with 1,19-nonadicanediol or 1,23-tricosanediol respectively was necessary to increase the average length of the crystallizable polyester hard blocks, thereby increasing Van-der-Waals interactions between the aliphatic segments and improving crystallization conditions. Accordingly, the observed melt and crystallization temperatures rose with increasing 1,19-nonadicanediol and 1,23-tricosanediol content (**Figure 3.4**).

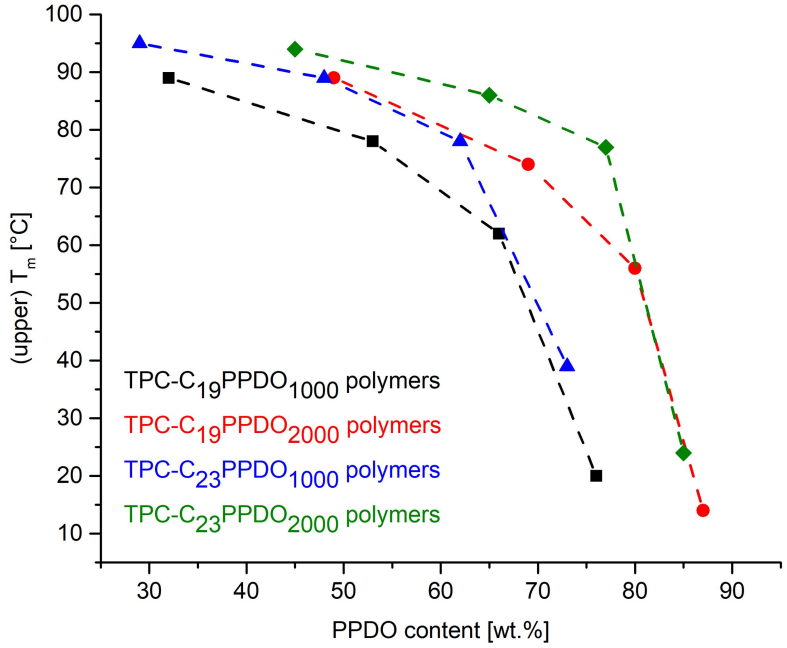

Figure 3.4: Correlation between polymer composition and (upper) melting points of all-aliphatic poly(ether-ester) block copolymers with crystallizable long-chain polyester hard segments.

At the same time, the emergence of a second, increasingly dominating, melt peak related to the formation of crystalline polyester hard domains could be observed in the recorded DSC thermograms (**Figure 3.5** and **3.6,** cf. **Chapter 3.4.5, Figure 3.17 and 3.18**). Melting points of the synthesized TPCs eventually peaked at 89 °C for TPC-C_{19}PPDO$_{1000}$-32wt% and TPC-C_{19}PPDO$_{2000}$-49wt% of the C_{19}-series (**Table 3.4**, **entry 4** and **8**) and at 94 °C and 96 °C respectively for TPC-C_{23}PPDO$_{1000}$-29wt% and TPC-C_{23}PPDO$_{2000}$-45wt% of the C_{23}-series (**Table 3.4**, **entry 12** and **16**), thereby approaching values recorded for the corresponding long-chain polyesters, PE-19,19 and PE-23,23 (T_m = 103 °C and 108 °C).[9] In general, the thermal properties of TPCs containing less than 50 wt.% of PPDO polyether soft phase were completely dominated by the

crystalline polyester hard phase, which corresponds well with previous reports about commercial TPCs based on partly aromatic poly(butylene terephthalate) polyester hard segments.[25],[26]

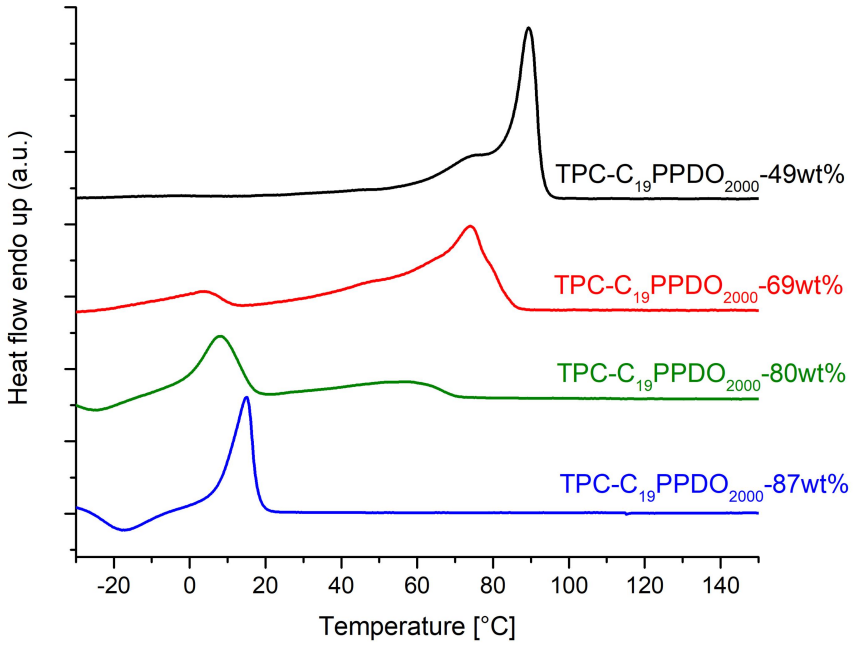

Figure 3.5. DSC thermograms (second heating) of poly(ether-ester) block copolymers based on oleic acid-derived C_{19} monomers and $PPDO_{2000}$.

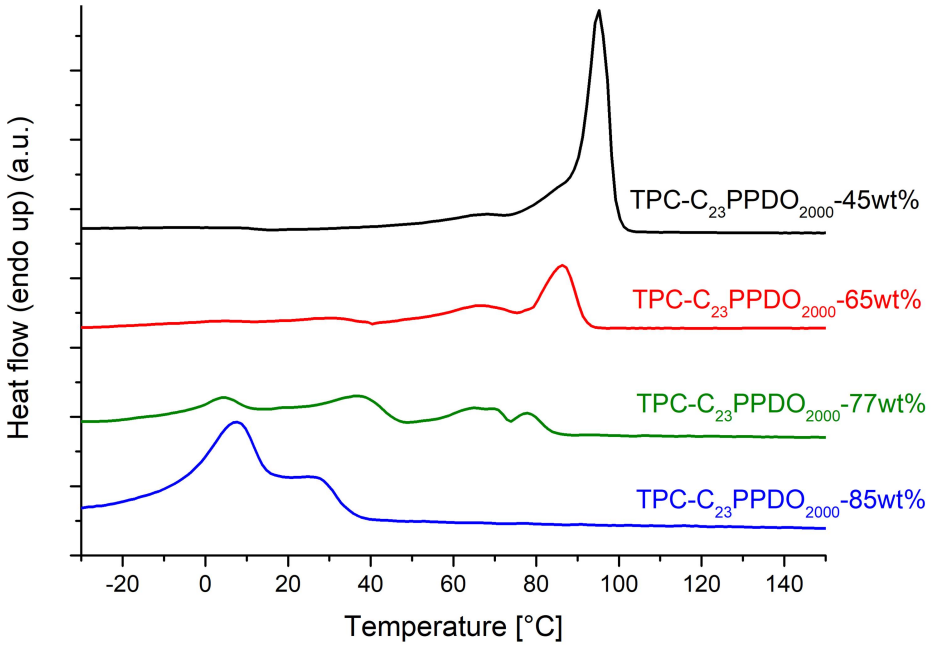

Figure 3.6. DSC thermograms (second heating) of poly(ether-ester) block copolymers based on erucic acid-derived C_{23} monomers and $PPDO_{2000}$.

The thermal properties of TPCs containing less than 50 wt.% of PPDO polyether soft phase were generally dominated by the crystalline polyester hard phase, which corresponds well with previous reports about commercial TPCs based on partly aromatic poly(butylene terephthalate) polyester hard segments.[25],[26] TPCs with polyester hard segments based on erucic acid-derived C_{23} hard monomers (**Table 3.4**, **entry 9-16**)exhibited slightly higher melt and crystallization points than their C_{19} monomer-based counterparts (**Table 3.4**, **entry 1-8**) due to the crystallizable methylene sequences in the PE-23.23 polyester blocks being slightly longer. TPCs based on the $PPDO_{2000}$ macrodiol (**Table 3.4**, **entry 5-8**) generally also exhibited slightly lower melt and crystallization points than comparable poly(ether-ester) copolymers based on shorter $PPDO_{1000}$ polyether soft segments (**Table 3.4**, **entry 13-16**) (**Figure 3.4**).

Direct comparison of the thermal properties of mid-chain monomer-based TPC-$C_{12}PPDO_{2000}$-62wt% (**Table 3.4, entry 17**) with its long-chain analog TPC-$C_{23}PPDO_{2000}$-65wt% (**Table 3.4, entry 15**) revealed a difference in the upper melting point of more than 20 °C, with TPC-$C_{12}PPDO_{2000}$-62wt% melting at a significantly lower temperature of only 62 °C instead of 86 °C recorded for TPC-$C_{23}PPDO_{2000}$-65wt% (**Figure 3.7**). This substantial gap between melting points can be attributed to the additional ester groups incorporated in the aliphatic polymer backbone of TPC-$C_{12}PPDO_{2000}$-62wt% leading to less favorable crystallization conditions as their presence results in a lowering of the cohesion energy between hydrocarbon chains and an increasing likelihood for the occurrence of crystal imperfections.

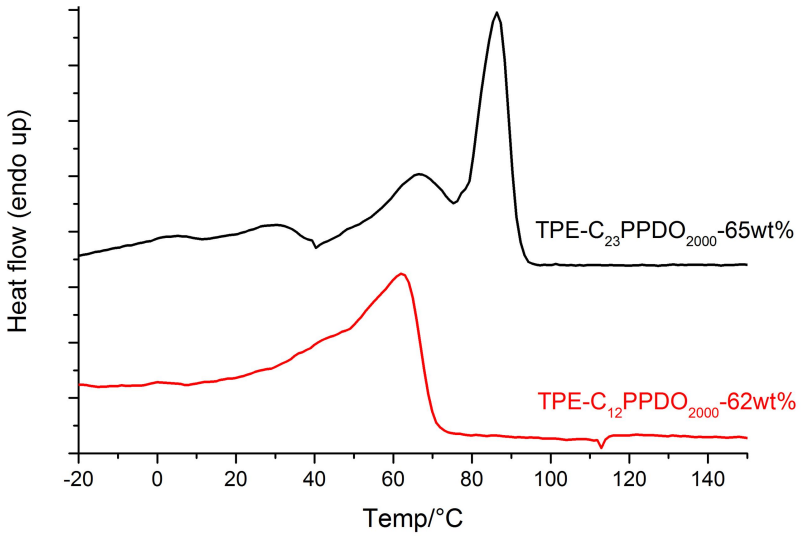

Figure 3.7. DSC thermograms (second heating) of poly(ether-ester) block copolymers based on erucic acid-derived C_{23} monomers and $PPDO_{2000}$.

Replacing $PPDO_{2000}$ with a comparable PTMG polyether macrodiol of the same average molecular weight did not drastically affect the thermal properties, with TPC-$C_{23}PPDO_{2000}$-65wt% (**Table 3.4, entry 15**) possessing the same melting point (T_m = 86 °C) as a PTMG-based analog of otherwise identical composition.[24],[27] For mid-chain TPCs, replacing $PPDO_{2000}$ with $PTMG_{2000}$ resulted in a slight increase in the melting point from 62 °C recorded for TPC-$C_{12}PPDO_{2000}$-62wt% (**Table 3.4, entry 17**) to 66 °C recorded for TPC-$C_{12}PTMG_{2000}$-62wt% (**Table 3.4, entry 18**).

3.2.4. Mechanical properties of long-chain thermoplastic copolyester elastomers

In order to assess the mechanical properties and elastomeric behavior of the synthesized poly(ether-ester) block copolymers, dogbone-shaped test specimen were prepared via piston injection molding and subsequently subjected to tensile tests as well as cyclic hysteresis testing (**Table 3.5**).

Table 3.5: Mechanical properties of all-aliphatic poly(ether-ester) block copolymers based on crystallizable long-chain polyester hard segments.

entry	polymer	diacid [eq.]	diol (1) [eq.]	diol (2) [eq.]	E_t [a),b)] [MPa]	ε_b [a),c)] [%]	residual strain[d)] [%]
1	TPC-$C_{19}PPDO_{1000}$-66wt%	4 (C_{19})	1 (C_{19})	3 ($PPDO_{1000}$)	10	1087	16
2	TPC-$C_{19}PPDO_{1000}$-53wt%	4 (C_{19})	2 (C_{19})	2 ($PPDO_{1000}$)	41	618	19
3	TPC-$C_{19}PPDO_{1000}$-32wt%	4 (C_{19})	3 (C_{19})	1 ($PPDO_{1000}$)	107	58	51
4	TPC-$C_{19}PPDO_{2000}$-80wt%	4 (C_{19})	1 (C_{19})	3 ($PPDO_{2000}$)	3[f)]	>1100[f)]	15
5	TPC-$C_{19}PPDO_{2000}$-69wt%	4 (C_{19})	2 (C_{19})	2 ($PPDO_{2000}$)	19	984	16
6	TPC-$C_{19}PPDO_{2000}$-49wt%	4 (C_{19})	3 (C_{19})	1 ($PPDO_{2000}$)	64	438	26
7	TPC-$C_{23}PPDO_{1000}$-62wt%	4 (C_{23})	1 (C_{23})	3 ($PPDO_{1000}$)	43	462	39
8	TPC-$C_{23}PPDO_{1000}$-48wt%	4 (C_{23})	2 (C_{23})	2 ($PPDO_{1000}$)	57	217	24
9	TPC-$C_{23}PPDO_{1000}$-29wt%	4 (C_{23})	3 (C_{23})	1 ($PPDO_{1000}$)	125	41	57
10	TPC-$C_{23}PPDO_{2000}$-77wt%	4 (C_{23})	1 (C_{23})	3 ($PPDO_{2000}$)	12	>1100	35
11	TPC-$C_{23}PPDO_{2000}$-65wt%	4 (C_{23})	2 (C_{23})	2 ($PPDO_{2000}$)	28	749	15
12	TPC-$C_{23}PPDO_{2000}$-45wt%	4 (C_{23})	3 (C_{23})	1 ($PPDO_{2000}$)	79	405	27
13	TPC-$C_{12}PPDO_{2000}$-62wt%	7 (C_{12})	5 (C_{12})	2 ($PPDO_{2000}$)	22	230	22
14	TPC-$C_{12}PTMG_{2000}$-62wt%	7 (C_{12})	5 (C_{12})	2 ($PTMG_{2000}$)	42	-	25
15[e)]	TPC-$C_{23}PTMG_{2000}$-65wt%[24]	4 (C_{23})	2 (C_{23})	2 ($PTMG_{2000}$)	50	298	30[24)]

a) Tensile tests were performed according to ISO 527/1-2 on type 5A test specimen prepared by injection molding. b) Crosshead speed 1 mm min^{-1}. c) Crosshead speed 500 mm min^{-1}. d) Determined from cyclic hysteresis testing after 10 cycles with a constant strain of 100 % at a crosshead speed of 50 mm min^{-1}. e) Polymer sample supplied by F. Stempfle. f) data collected from a single test specimen.

TPC-C_{19}PPDO$_{1000}$-32wt% and TPC-C_{23}PPDO$_{1000}$-29wt% (**Table 3.5**, **entry 3** and **9**), which both contained only about 30 wt.% of the comparatively low molecular weight PPDO$_{1000}$ macrodiol as a soft segment, showed characteristics usually associated with semi-rigid thermoplastics, including the general shape of the stress-strain curve (**Figure 3.8**). Recorded elongations at break (ε_b) only reached values of 58 % and 41 % respectively while the calculated Young's moduli (E_t) of 107 MPa and 125 MPa exceeded 100 MPa. Replacing PPDO$_{1000}$ with higher molecular weight PPDO$_{2000}$ as the soft segment in TPC-C_{19}PPDO$_{2000}$-49wt% and TPC-C_{23}PPDO$_{2000}$-45wt% (**Table 3.5**, **entry 6** and **12**) resulted in a drop of the Young moduli to values below 100 MPa as well as a drastic improvement in the recorded elongations at break, with test specimen TPC-C_{19}PPDO$_{2000}$-49wt% and TPC-C_{23}PPDO$_{2000}$-45wt% not failing until elongations of more than 400 % were reached. Partial replacement of the hard, fatty acid-derived C_{19} and C_{23} α,ω-diols with increasing amounts of amorphous PPDO$_{1000}$ or PPDO$_{2000}$ polyether soft segment led to changes in the general characteristics of the recorded stress-strain curves to a shape typically associated with thermoplastic elastomers (**Figure 3.8**).

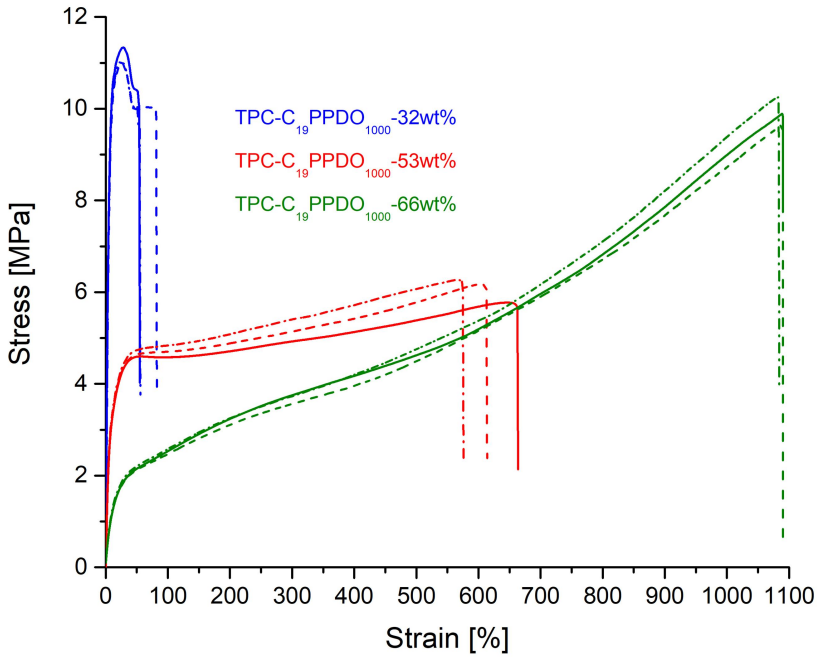

Figure 3.8: Stress-Strain curves of polymers of the TPC-C_{19}PPDO$_{1000}$ series demonstrating the change in curve shape with increasing soft segment content.

Elongations at break also increased drastically with increasing soft phase content (**Table 3.5**) until the ductility of TPC-C_{19}PPDO$_{2000}$-80wt% and TPC-C_{23}PPDO$_{2000}$-77wt% respectively (**Table 3.5, entry 4** and **9**) exceeded the limit of the test apparatus of a maximum elongation of 1100 % (**Figure 3.9**).

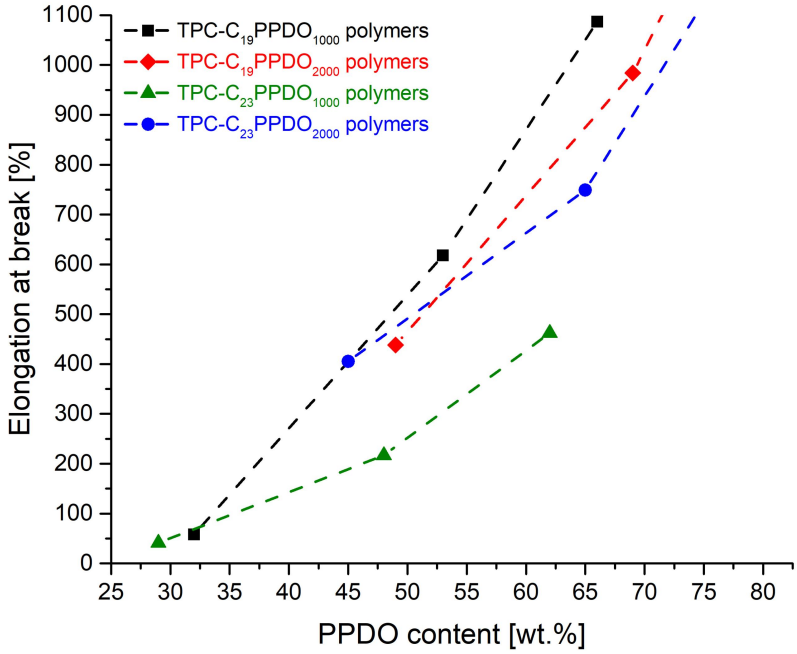

Figure 3.9: Correlation between elongation at break and polymer composition in all-aliphatic TPCs.

Simultaneously, the calculated Young's moduli continuously dropped until values as low as 3 MPa were reached for TPC-C_{19}PPDO$_{2000}$-80wt% (**Table 3.5, entry 4**) (**Figure 3.10**). In addition, TPCs of the C_{19}-series (**Table 3.5, entry 1-6**) generally exhibited higher elongations at break and lower Young's moduli than comparable copolymers of the C_{23}-series with otherwise similar composition (**Table 3.5, entry 7-12**). The same trends could be observed for TPCs containing longer PPDO$_{2000}$ soft segments instead of shorter PPDO$_{1000}$ polyether soft blocks (**Figure 3.9 and 3.10**).

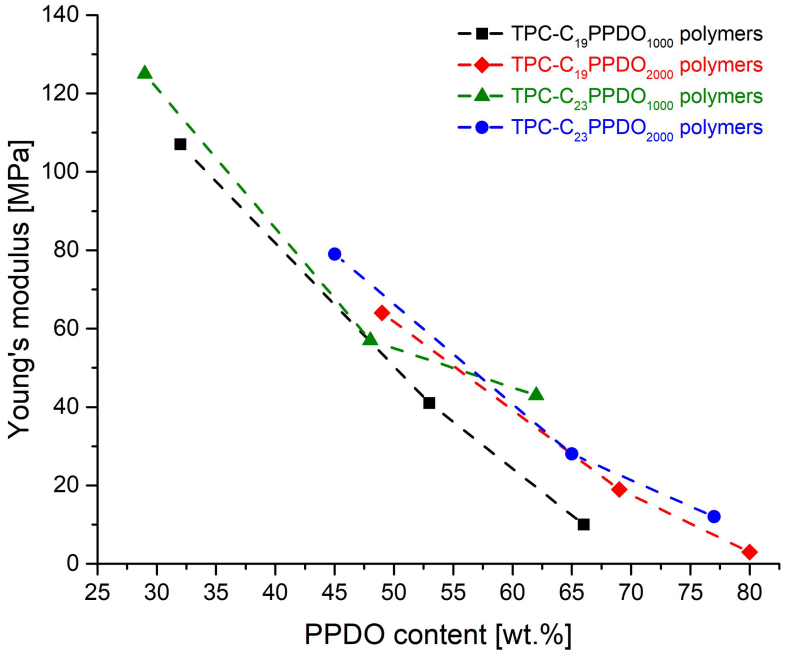

Figure 3.10: Correlation between Young's moduli and polymer composition in all-aliphatic TPCs

Cyclic hysteresis tests were performed on dogbone-shaped test specimen prepared via injection molding in order to assess the elastomeric properties of the synthesized TPCs. The test specimens were repeatedly exposed to consecutive cycles of loading and unloading to a constant strain of 100 % until 100 cycles were completed. During the first couple of cycles, the residual deformation gradually increased and a pronounced hysteresis was observed, however afterwards all studied poly(ether-ester) copolymers exhibited a virtually constant level of recovery which corresponds with the behavior expected for TPEs.[2],[25],[28],[29] After 10 cycles residual strains ranged from 15 % to 57 % depending on polymer composition (**Table 3.5**). For TPCs with polyester hard segments based on oleic acid-derived C_{19} monomers, copolymers with a polyether content higher than 50 wt.% exhibited almost identical, very small permanent sets of about 15 % (**Table 3.5**, **entry 1**, **2**, **4**, and **5**). In contrast, for TPCs with hard segments based on erucic acid-derived C_{23} monomers, a minimum of 24 % and 15 % respectively was observed for materials containing 50 mol % (of total diol) of $PPDO_{1000}$ or $PPDO_{2000}$ (**Table 3.5**, **entry 8** and **11**), indicating this to be an optimum ratio of hard to soft phase for TPCs with polyester hard segments based on C_{23} repeat units. In addition, polymers containing $PPDO_{2000}$ soft segments (**Table 3.5**, **entry 4-6** and **10-12**) generally exhibited better elastomeric behavior and a lower permanent set than corresponding copolymers with the same mol % of shorter $PPDO_{1000}$ soft segments (**Table 3.5**, **entry 1-3** and **7-9**) (**Figure 3.11**).

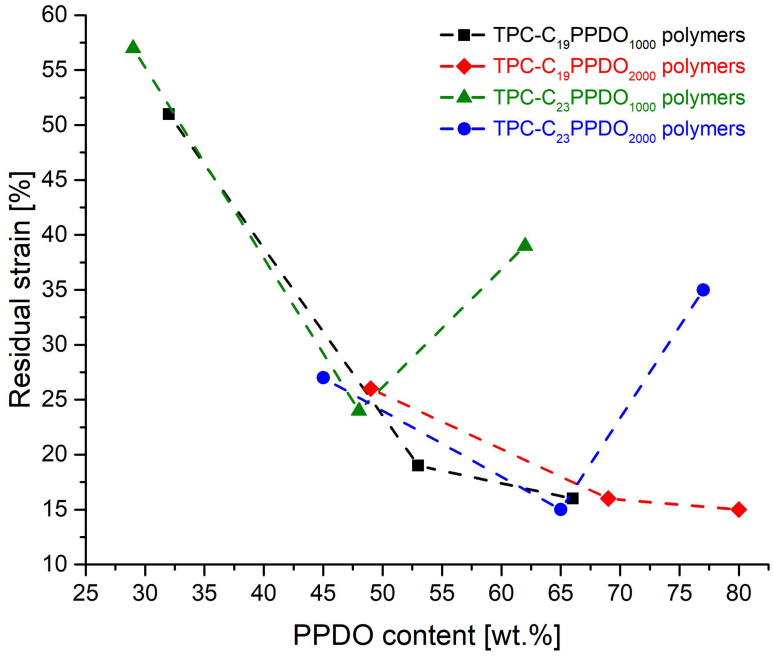

Figure 3.11: Correlation between TPC composition and elastomeric properties.

Analysis of the mechanical properties of TPC-C_{12}PPDO$_{2000}$-62wt% via tensile testing (**Table 3.5**, **entry 13**) revealed that shorter methylene sequences in the aliphatic polyester hard blocks resulted in a slight decrease of the Young's modulus of TPC-C_{12}PPDO$_{2000}$-62wt% (E_t = 22 MPa) when compared to the Young's modulus of its long-chain analog, TPC-C_{23}PPDO$_{2000}$-65wt% (E_t = 28 MPa) (**Table 3.5**, **entry 11**) due to the higher amount of ester groups resulting in a weakening of the cohesion within the crystalline hard domains. Similarly, the elongation at break dropped drastically from 749 % recorded for TPC-C_{23}PPDO$_{2000}$-65wt% to 240 % observed for TPC-C_{12}PPDO$_{2000}$-62wt% (**Figure 3.12**). The shortening of the crystallizable aliphatic segments within the hard blocks also negatively impacted the elastomeric properties, with TPC-C_{12}PPDO$_{2000}$-62wt% exhibiting a residual strain of 22 % after cyclic hysteresis testing (**Table 3.5**, **entry 13**) compared to 15 % recorded for TPC-C_{23}PPDO$_{2000}$-65wt% (**Table 3.5**, **entry 11**) (**Figure 3.13**).

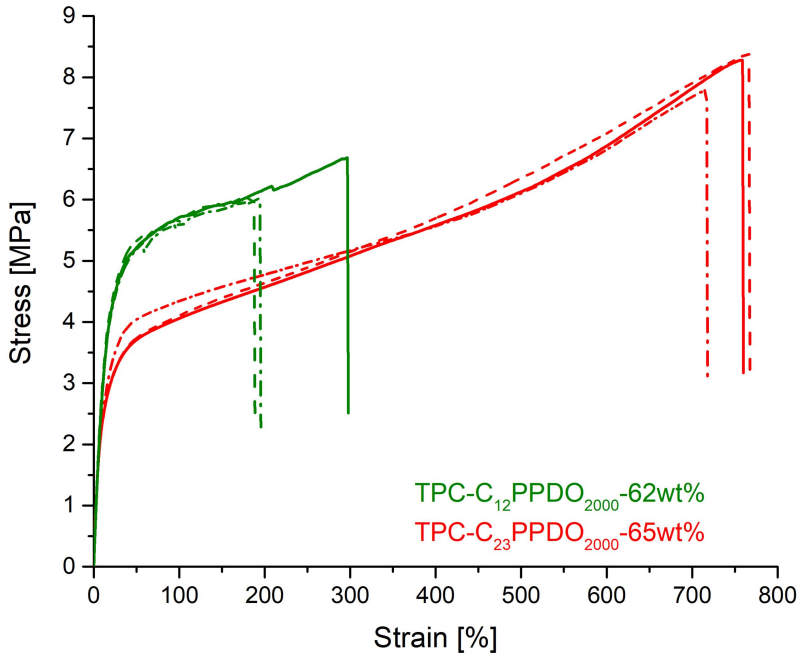

Figure 3.12: Stress-strain curves of TPC-C_{23}PPDO$_{2000}$-65wt% (red) and its mid-chain monomer-based analogue TPC-C_{12}PPDO$_{2000}$-62wt% (green).

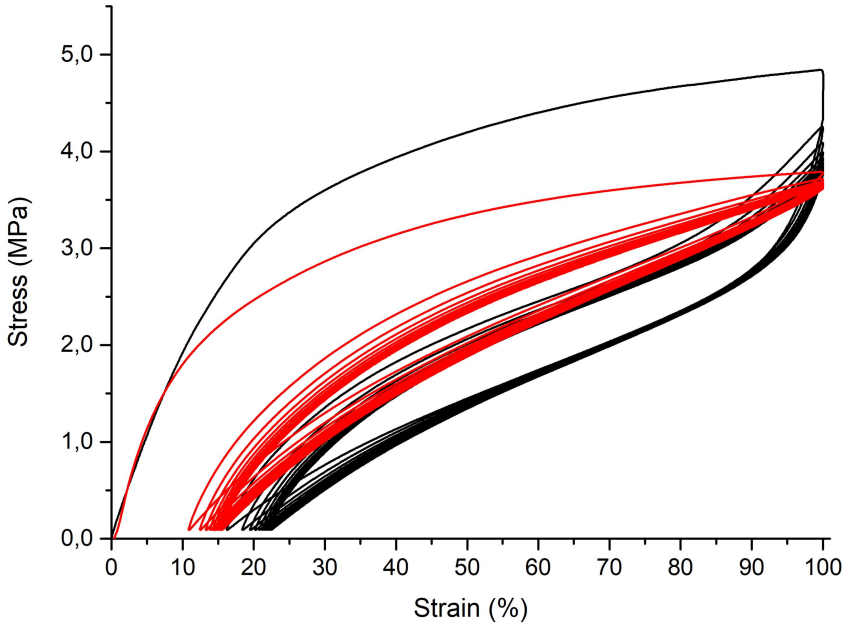

Figure 3.13: Stress–strain curves of the long-chain poly(ether-ester) block copolymer TPC-C_{23}PPDO$_{2000}$-65wt% (red) and its mid-chain analogue, TPC-C_{12}PPDO$_{2000}$-62wt% (black), from cyclic hysteresis testing with a constant strain of 100% (first 10 cycles displayed).

Replacing $PPDO_{2000}$ with $PTMG_{2000}$ as the soft segment in long-chain TPCs resulted in an increase of the Young's modulus from 28 MPa for TPC-$C_{23}PPDO_{2000}$-65wt% (**Table 3.5**, **entry 11**) to 50 MPa for TPC-$C_{23}PTMG_{2000}$-65wt% (**Table 3.5**, **entry 15**), while the elongation at break dropped drastically from 749 % to 298 % (**Figure 3.14**). Simultaneously, the permanent set after hysteresis testing doubled from 15 % to 30 %.[24] A similar trend was observed for their mid-chain analogues TPC-$C_{12}PPDO_{2000}$-62wt% and TPC-$C_{12}PTMG_{2000}$-62wt% (**Table 3.5**, **entry 13** and **14**)in which a replacement of $PPDO_{2000}$ with $PTMG_{2000}$ resulted in a doubling of the Young's modulus from 22 MPa to 42 MPa and the permanent set after cyclic hysteresis testing increased slightly from 22 % to 25 %.

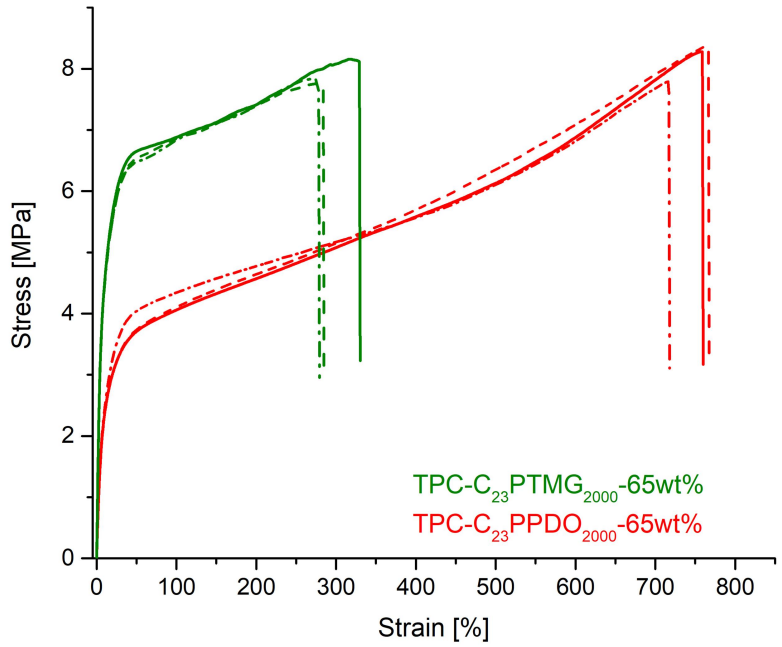

Figure 3.14: Stress-strain curves of TPC-$C_{23}PPDO_{2000}$-65wt% (red) and its analog TPC-$C_{23}PTMG_{2000}$-65wt% (green).

3.3. Conclusion

It could be successfully demonstrated that plant oil-derived linear long-chain aliphatic α,ω-dicarboxylic acids and diols are suitable monomers for the generation of high melting, all-aliphatic polyester hard segments in thermoplastic copolyester elastomers (TPCs), thereby providing an alternative to crystallizable aromatic dicarboxylic acid repeat units typically employed in the polyester hard blocks of commercially available TPCs to achieve sufficiently high melting points. The synthesis of the necessary long-chain C_{19} and C_{23}-diesters from unsaturated fatty acid esters via isomerizing alkoxycarbonylation was successfully simplified by demonstrating that small amounts of water have no significant negative impact on the reaction result. Polycondensation of the thus obtained linear long-chain monomers with an amorphous corn-derived dihydroxyl-terminated poly(1,3-propanediol) macromonomer (PPDO) of varying chain length (1000 vs. 2000 g mol^{-1}) yielded a series of renewable all-aliphatic segmented poly(ester-ether) block copolymers with molecular weights reaching values up to $M_n = 5.2 \times 10^4$ g mol^{-1}. Physical crosslinking in these materials is provided by the long methylene sequences in the hard segments imparting polyethylene-like crystallinity to the polyester hard domains, while the corn-derived, diol-terminated poly(1,3-propanediol) serves as a soft segment. Depending on copolymer composition, melting points reach values of up to 95 °C, which is particularly significant as aliphatic copolyesters based exclusively on readily available short- or mid-chain aliphatic monomers are prone to softening and loss of elastomeric properties upon being exposed to elevated ambient temperatures. Accordingly, DSC analysis of a dodecanedioic acid-based mid-chain poly(ester-ether) block copolymer, TPC-$C_{12}PPDO_{2000}$-62wt%, revealed a relatively low melting point of 66 °C. In contrast, the thermogram of its long-chain analog, TPC-$C_{23}PPDO_{2000}$-65wt%, with a comparable copolyester mass composition and block length distribution featured a melting point at 86 °C, which constitutes an increase in the melting point by 20 °C. In addition, the synthesized long-chain copolymers generally exhibited good ductility and elastomeric behavior if the polyether macromonomer accounted for at least 45 wt.% of the copolymer, with the lowest observed permanent set after cyclic hysteresis testing being as low as 15 %. An especially favorable combination of high melting point, ductility, and shape recovery was observed for TPC-C23PPDO2000-65wt% in which the $PPDO_{2000}$ macrodiol accounted for 65 wt.% (50 mol% of the total diols employed) of the poly(ester-ether) block copolymer. TPCs containing a poly(1,3-propanediol) soft segment instead of a more commonly employed poly(tetramethylene ether) glycol of comparable molecular weight also showed better ductility and elasticity.

3.4. Experimental Section

3.4.1. Materials and general considerations

Unless stated otherwise, all manipulations were carried out under an inert gas atmosphere using standard Schlenk or glovebox techniques. Toluene was distilled from sodium under an inert gas atmosphere. Methanol and ethanol were dried by distillation from Mg/I_2 under a nitrogen atmosphere. Alternatively, methanol p.a. (99.9 %) and ethanol p.a. (99.8 %) obtained from Sigma-Aldrich were degassed prior to use. Toluene was distilled from sodium and THF from sodium/benzophenone. All other solvents were used in technical grade as received.

High oleic sunflower oil methyl ester (Dakolub MB 9001, 92.5 %) was supplied by Dako AG and degassed prior to use. Titanium(IV) butoxide (> 97 %), $LiAlH_4$, and 1,12-dodecanediol (> 99 %) were supplied by Sigma-Aldrich. N,N'-di-2-naphthyl-1,4-phenylenediamine (> 96 %), dimethyl dodecanedioate (> 99 %), and ethyl erucate (> 90 %) were purchased from TCI Europe, and in case of the latter degassed prior to use. Poly(1,3-propanediol) (Cerenol®) with a number average molecular mass of M_n = 1000 g mol^{-1} and M_n = 2000 g mol^{-1} kindly donated by Allessa GmbH and poly(tetramethylene glycol) with a number average molecular mass of M_n = 2000 g mol^{-1} kindly donated by BASF were molten at 40 °C and degassed prior to use. Carbon monoxide (3.7) and hydrogen (5.0) were supplied by Air Liquide. [Pd(dtbpx)$(OTf)_2$] was prepared according to a reported procedure[10] and available in the work group. Samples of TPC-C_{23}PTMG$_{2000}$-65wt%[24] were available in the work group.

NMR spectra were recorded on a Varian Inova 400, a Bruker Avance 400 or on a Bruker Avance DRX 600 spectrometer. ^{1}H and ^{13}C chemical shifts were referenced to the solvent signals. Acquired data was processed and analyzed using MestReNova software.

DSC analyses were performed on a Netzsch Phoenix 204 F1 instrument with a heating and cooling rate, respectively, of 10 K min^{-1} in a temperature range of -50 to 160 °C for melt and crystallization transitions. Data reported is from second heating cycles. Glass transitions were determined at a heating rate of 30 K min^{-1} in a temperature range of -100 to 160 °C.

Gel permeation chromatography (GPC) measurements were carried out on a Polymer Laboratories PL-GPC 50 with two PLgel 5 µm MIXED-C columns in THF at 50 °C against polystyrene standards with refractive index detection.

Tensile testing was performed on dogbone-shaped sample bars (75 × 12.5 × 2 mm^3; ISO 527-2, type 5A) which were prepared using a HAAKE Minijet II (Thermo Scientific) piston injection molder.

0.1 wt.-% of N,N'-di-2naphthyl-1,4-phenylenediamine were employed as a stabilizer. After preconditioning the samples overnight, tensile tests were performed on a Zwick 1446 Retroline tC II instrument according to ISO 527 (crosshead speed 500 mm min^{-1}, with a determination of the Young modulus at a crosshead speed of 1 mm min^{-1} at elongations < 10 %). The Zwick test Xpert software version 11.0 was used to collect and analyze the data. Young's modulus, yield stress, yield strain, tensile stress at break and tensile strain at break were obtained by averaging the data from several test specimens.

Cyclic hysteresis tests were performed on dogbone-shaped sample bars (75 × 12.5 × 2 mm^3; ISO 527-2, type 5A). The test specimens were repeatedly exposed to consecutive cycles of loading and unloading to a constant strain of 100% with a constant crosshead speed of 50 mm min^{-1}. The recovery was measured by observing the residual strain after 10 cycles using Zwick test Xpert software version 11.0 and the OriginPro software.

Wide angle X-Ray diffraction was performed on a Bruker AXS D8 Advance diffractometer using CuK_{α_1} radiation. Diffraction patterns were recorded in the range 10 to 60 degrees 2θ, at a temperature of 25 °C. Degrees of crystallinity were calculated using the OriginPro2015 software as the ratio between the area corresponding to the crystalline reflections and the total area of the WAXD pattern after applying a deconvolution fitting routine.

3.4.2. Monomer Synthesis

Synthesis of dimethyl 1,19-nonadecanedioate

The isomerizing alkoxycarbonylation of methyl oleate was carried out analogous to a reported procedure[23] in a mechanically stirred 300 ml stainless steel pressure reactor equipped with a glass inlay, a mechanical stirrer, and a heating/cooling jacket supplied with a thermostat controlled by a thermocouple dipping into the reaction mixture. The apparatus was heated to 50 °C and purged with nitrogen several times prior to use. Methyl oleate (40 ml, Dakolub MB 9001, 92.5 %) and 205 mg (0.257 mmol, 0.002 eq.) of the catalyst precursor [(dtbpx)Pd$(OTf)_2$] were dissolved in 120 ml of dry or p.a grade methanol under a nitrogen atmosphere and the solution cannula transferred into the reactor. The sealed reactor was then pressurized with 20 bar CO and heated to 90 °C. Constant pressure was maintained during the next 90 h by periodic replenishing of CO. Afterwards, the reactor was cooled down to room temperature and vented. The precipitated crude product was dissolved by adding dichloromethane, and remaining solid palladium residues were removed by

subsequent filtration over a Buchner funnel and 2 cm of silica gel. Removal of the solvent and subsequent repeated recrystallization from methanol and n-heptane yielded pure dimethyl 1,19-nonadecanedioate (34.6 g, 97.0 mmol, 83 % yield (dry solvent) or 33.9 g, 95.1 mmol, 81 % yield (p.a. grade solvent) respectively) as a gleaming white solid.

Upscaled synthesis of dimethyl 1,19-nonadecanedioate

The upscaled synthesis of dimethyl 1,19-nonadecanedioate was carried out analogous to a reported procedure, [12] whereby methyl oleate (220 ml, Dakolub MB 9001, 92.5 %) was dissolved in 450 ml of dry methanol under a nitrogen atmosphere and cannula transferred into a 1.1 l stainless steel pressure reactor equipped with a mechanical stirrer and a heating/cooling jacket supplied with a thermostat controlled by a thermocouple dipping into the reaction mixture. A solution of 0.760 g (0.95 mmol) [(dtbpx)Pd(OTf)$_2$] in additional 50 ml of dry methanol were added while the reactor was being preheated to 60 °C. The sealed reactor was then pressurized with 20 bar CO and heated to 90 °C. Constant pressure was maintained during the next 92 h by periodic replenishing of CO. Afterwards, the reactor was cooled down to room temperature and vented. The precipitated crude product was dissolved by adding dichloromethane, and remaining solid palladium residues were removed by subsequent filtration over a Buchner funnel and 2 cm of silica gel. Removal of the solvent and subsequent repeated recrystallization from methanol and n-heptane yielded pure dimethyl 1,19-nonadecanedioate (179.7 g, 0.504 mol, 73 % yield) as a gleaming white solid.

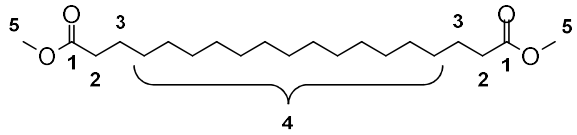

^{1}H NMR ($CDCl_3$, 25 °C, 400 MHz**)**: δ 3.65 (s, 6H, H-5), 2.29 (t, $^3J_{H-H}$ = 7.6 Hz, 4H, H-2), 1.67-1.56 (m, 4H, H-3), 1.35-1.20 (m, 26H, H-4) ppm.

^{13}C{^{1}H} NMR ($CDCl_3$, 25 °C, 101 MHz): δ 174.5 (s, C-1), 51.6 (s, C-5), 34.3 (s, C-2), 30.2-29.2 (C-4), 25.1 (s, C-3) ppm.

Synthesis of diethyl 1,23-tricosanedioate

Diethyl 1,23-tricosanedioate was prepared from ethyl erucate in an isomerizing alkoxycarbonylation reaction analogous to the procedure described above.[23] The conversion of technical grade ethyl erucate (40 ml, > 90 %) in 120 ml of dry ethanol followed by repeated recrystallization from methanol yielded pure diethyl 1,23-tricosanedioate as a gleaming white solid in a yield of 67 % (28.6 g, 64.9 mmol) or of 65 % (27.5 g, 62.4 mmol) if p.a. grade ethanol (99.8 %) was employed as a solvent and reactant instead of dry ethanol.

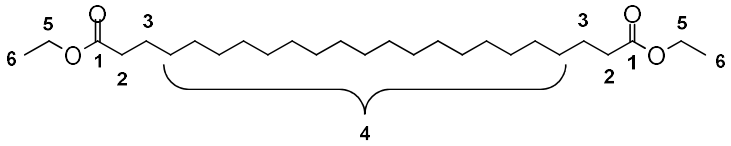

^{1}H NMR ($CDCl_3$, 25 °C, 400 MHz): δ 4.11 (q, $^{3}J_{H\text{-}H}$ = 7.1 Hz, 6H, H-5), 2.28 (t, $^{3}J_{H\text{-}H}$ = 7.6 Hz, 4H, H-2), 1.65 - 1.57 (m, 4H, H-3), 1.31 - 1.19 (m, 40H, H-4 and H-6) ppm.

^{13}C{^{1}H} NMR ($CDCl_3$, 25 °C, 101 MHz): δ 174.1 (C-1), 60.3 (C-5), 34.5 (C-2), 29.8 - 29.3 (C-4), 25.2 (C-3), 14.4 (C-6) ppm.

Synthesis of nonadecane-1,19-diol

Reduction of dimethyl 1,19-nonadecandioate was carried out analogous to a procedure reported in literature.[12] Dimethyl 1,19-nonadecanedioate (27.0 g, 75.7 mmol) was dissolved in 350 ml of dry THF. The resulting solution was slowly added to a stirred suspension of $LiAlH_4$ (8.0 g, 210.8 mmol) in 500 ml of dry THF at 0 °C. The reaction mixture was heated to reflux for 1 h, allowed to cool down, and then stirred over night at room temperature. The reaction was quenched by slowly adding 10 ml of water, followed by the addition of 10 ml of a 15 % aqueous solution of NaOH and another 15 ml of water. The resulting white suspension was heated to 40 °C before being filtrated over a Buchner funnel. The solvent was then removed from the filtrate *in vacuo* to yield the crude product which was recrystallized from chloroform to yield pure 1,19-nonadecanediol as a white solid (21.4 g, 71.2 mmol, 95 %).

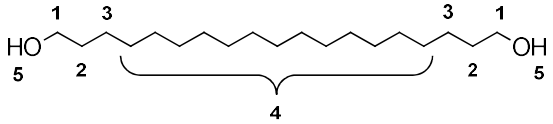

^{1}H NMR ($CDCl_3$, 50 °C, 400 Hz): δ 3.64 (t, $^{3}J_{H\text{-}H}$ = 6.6 Hz, 4H, H-1), 1.57 (quint, $^{3}J_{H\text{-}H}$ = 6.7 Hz, 4H, H-2), 1.42–1.25 (m, 30H), 1.18 (br. s, 2H, H-5 [=OH])

^{13}C{^{1}H} NMR ($CDCl_3$, 50 °C, 101 MHz): δ 63.3 (C-1), 33.1 (C-2), 29.8-19.6 (C-4) 25.9 (C-3).

Synthesis of tricosane-1,23-diol

The reduction of diethyl 1,23-tricosanedioate (25.0 g, 56.8 mmol) with $LiAlH_4$ (5.9 g, 156.1 mmol) was carried out analogously to the procedure described above for its 1,19-analgoue,[12] and after repeated recrystallization of the crude product from chloroform yielded pure tricosane-1,23-diol as a white solid in a yield of 92 % (18.6 g, 52.2 mmol).

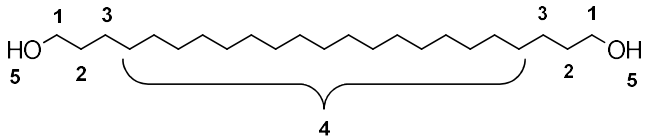

^{1}H NMR ($CDCl_3$, 50 °C, 400 MHz): δ 3.64 (t, $^{3}J_{H\text{-}H}$ = 6.6 Hz, Hz, 4H, H-1), 1.57 (quint, $^{3}J_{H\text{-}H}$ = 6.7 Hz, 4H, H-2), 1.41-1.25 (m, 38H, H-3 and H-4), 1.20 (br. s, 2H, H-5 [=OH]).

^{13}C{1H} NMR ($CDCl_3$, 50 °C, 101 MHz): δ 63.3 (C-1), 33.1 (C-2), 29.9-29.6 (C-4), 26.0 (C-3).

3.4.3. General polymerization procedure

Polycondensation reactions were carried out under inert gas atmosphere in a 100 mL two-necked Schlenk tube equipped with a helical full screw mechanical stirrer. The apparatus was heated with an aluminum block equipped with a thermocouple to control the temperature. The desired amount of monomers (the amount of α,ω-diester was set to 10 mmol) was weighed in and degassed. After adding 0.05 mol% of N,N'-di-2-naphthyl-1,4-phenylenediamine, the mixture was heated to 120 °C and the reaction started by adding 0.6 ml of a 0.028 M solution of $Ti(Bu)_4$ in toluene. The temperature was raised by 10 K every 45 minutes until a temperature of 180 °C was reached, at which point vacuum was applied to remove volatiles. The polymer melt was then stirred overnight at 200 °C to yield the desired product.

3.4.4. Molecular weight determination by ^{1}H NMR spectroscopy

Molecular weights determined from ^{1}H NMR spectra via end group analysis were calculated using the following formula:

$$M_n = DP_n \cdot M_0 = \frac{\int E_4}{\frac{1}{3}\int E_1 + \frac{1}{2}\int E_2 + \frac{1}{2}\int E_3} \cdot M_0, \qquad \text{for } C_{19} \text{ monomer-based TPCs}$$

and

$$M_n = DP_n \cdot M_0 = \frac{\int E_4}{\frac{1}{2}\int E_1 + \frac{1}{2}\int E_2 + \frac{1}{2}\int E_3} \cdot M_0, \qquad \text{for } C_{23} \text{ monomer-based TPCs}$$

The degree of polymerization (DP_n) was defined as the ratio of the signal intensities of the internal methylene group in alpha position to the carbonyl group of the fatty acid-derived diacid repeat unit (E_4, 2.28 ppm, 2H, **Figure 3.15**: **signal e**) and the weighted sum of the signals corresponding to the theoretically possible end groups. These end groups include a methyl ester end group (E_1, 3.61 ppm, 3H) or ethyl ester end group (E_1, 4.11 ppm 2H) respectively and the methylene groups adjacent to a terminal hydroxyl group belonging to either a fatty acid-derived diol (E_2, 3.64 ppm, 2H) or a PPDO polyether segment. (E_3, 3.76 ppm, 2H, **Figure 3.15: signal c**).

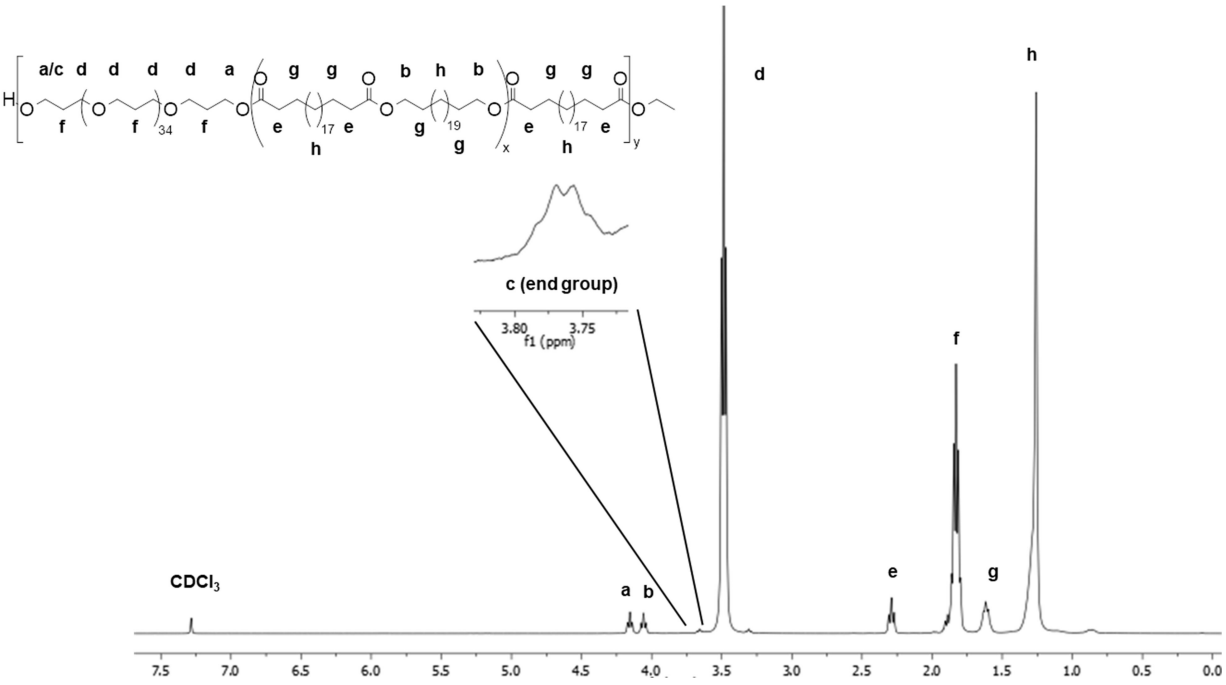

Figure 3.15: ^{1}H NMR (400 MHz, $CDCl_3$, 25°C) of TPC-$C_{23}PPDO_{2000}$-65wt%. Insert shows enlargement of the end group region.

3.4.5. DSC analysis

DSC analyses were performed on a Netzsch Phoenix 204 F1 instrument with a heating and cooling rate, respectively, of 10 K min^{-1} in a temperature range of -50 to 160 °C for melt and crystallization transitions. Data reported is from second heating cycles.

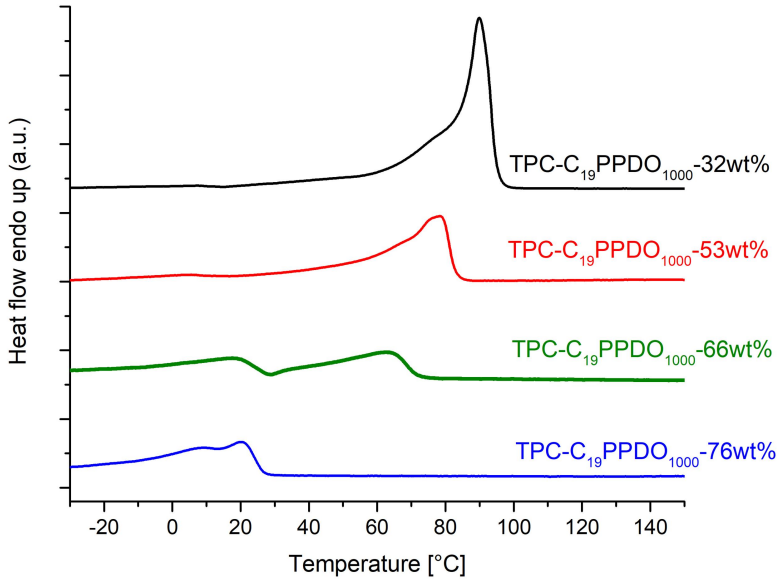

Figure 3.16. DSC thermograms (second heating) of poly(ether-ester) block copolymers based on oleic acid-derived C_{19} monomers and $PPDO_{1000}$

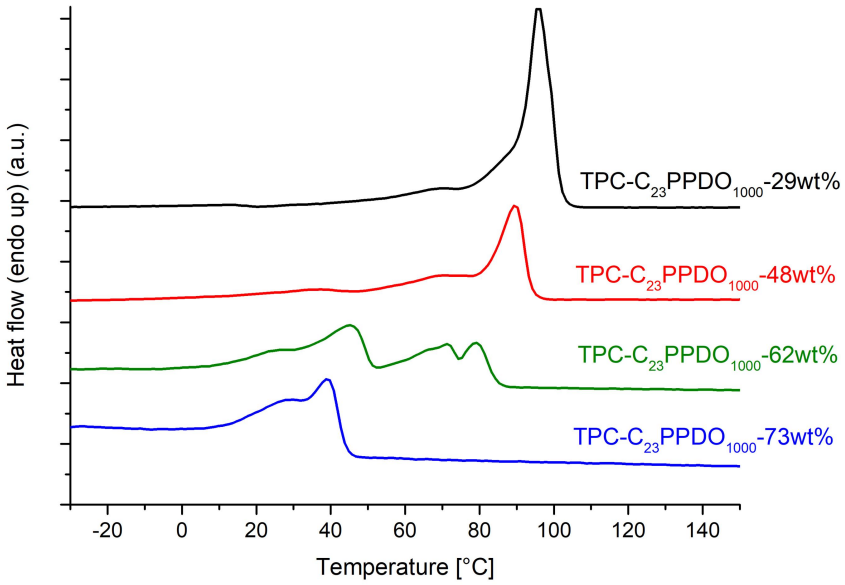

Figure 3.17. DSC thermograms (second heating) of poly(ether-ester) block copolymers based on erucic acid-derived C_{23} monomers and $PPDO_{1000}$

3.5. References

1. Roslaniec, Z. Polyester Thermoplastic Elastomers: Synthesis, Properties, and Some Applications. In *Handbook of Condensation Thermoplastic Elastomers*, Fakirov, S., (Ed.) Wiley-VCH: Weinheim, Germany, **2005**.
2. Ouhadi, T.; Abdou-Sabet, T.; Wussow, H.-G.; Ryan, L. M.; Plummer, L.; Baumann, F. E.; Lohmar, J.; F, V. H.; Malet, F. L. G. Thermoplastic Elastomers. In *Ullmann's Encyclopedia of Industrial Chemistry*, Gerhartz, W.; Elvers, B., (Eds.), Wiley-VCH: Weinheim, Germany, **2000**, pp 1-40.
3. Drobny, J. G., *Handbook of Thermoplastic Elastomers*. William Andrew Publishing: Norwich, New York, **2007**.
4. Advancing technology to spur big growth for plastic composites during the '80s. Mock, J. A. *Plastics Engineering*, **1983,** *39* (2), 13-19.
5. *Flexible layered product.* Vrouenraets, C. M. F.; Sikkema, D. J. (AKZO), U.S. Patent 4,493,870 (A), **1983**.
6. Elastomers for biomedical applications. Yoda, R. *Journal of Biomaterials Science, Polymer Edition*, **1998,** *9* (6), 561-626.
7. a)Metathesis of unsaturated fatty acids: Synthesis of long-chain unsaturated α, ω-dicarboxylic acids. Ngo, H. L.; Jones, K.; Foglia, T. A. *Journal of the American Oil Chemists' Society*, **2006,** *83* (7), 629-634; b)High turnover numbers with ruthenium-based metathesis catalysts. Dinger, M. B.; Mol, J. C. *Advanced Synthesis & Catalysis*, **2002,** *344* (6-7), 671-677.
8. a)Dicarboxylic acid esters from the carbonylation of unsaturated esters under mild conditions. Jiménez-Rodriguez, C.; Eastham, G. R.; Cole-Hamilton, D. J. *Inorganic Chemistry Communications*, **2005,** *8* (10), 878-881; b)Mechanistic features of isomerizing alkoxycarbonylation of methyl oleate. Roesle, P.; Dürr, C. J.; Möller, H. M.; Cavallo, L.; Caporaso, L.; Mecking, S. *Journal of the American Chemical Society*, **2012,** *134* (42), 17696-17703.
9. a)Linear semicrystalline polyesters from fatty acids by complete feedstock molecule utilization. Quinzler, D.; Mecking, S. *Angewandte Chemie International Edition*, **2010,** *49* (25), 4306-4308; b)Linear semicrystalline polyesters from fatty acids by complete feedstock molecule utilization. Quinzler, D.; Mecking, S. *Angewandte Chemie*, **2010,** *122* (25), 4402-4404.
10. Long-chain linear C_{19} and C_{23} monomers and polycondensates from unsaturated fatty acid esters. Stempfle, F.; Quinzler, D.; Heckler, I.; Mecking, S. *Macromolecules*, **2011,** *44* (11), 4159-4166.

11. Which polyesters can mimic polyethylene? Stempfle, F.; Ortmann, P.; Mecking, S. *Macromolecular rapid communications*, **2013,** *34* (1), 47-50.
12. Long-chain aliphatic polyesters from plant oils for injection molding, film extrusion and electrospinning. Stempfle, F.; Ritter, B. S.; Mülhaupt, R.; Mecking, S. *Green Chemistry*, **2014,** *16* (4), 2008-2014.
13. a)Maréchal, E. Creation and Development of Thermoplastic Elastomers, and Their Position Among Organic Materials. In *Handbook of Condensation Thermoplastic Elastomers*, Fakirov, S., (Ed.) Wiley-VCH: Weinheim, Germany, **2005**; b)Maréchal, E. Polycondensation Reactions in Thermoplastic Elastomer Chemistry: State of the Art, Trends, and Future Developments. In *Handbook of Condensation Thermoplastic Elastomers*, Fakirov, S., (Ed.) Wiley-VCH: Weinheim, Germany, **2005**.
14. Block-frequency distribution of copolymers. Frensdorff, H. *Macromolecules*, **1971,** *4* (4), 369-375.
15. Segmented polyether ester copolymers—A new generation of high performance thermoplastic elastomers. Hoeschele, G. *Polymer Engineering & Science*, **1974,** *14* (12), 848-852.
16. Aliphatic long-chain C_{20} polyesters from olefin metathesis. Trzaskowski, J.; Quinzler, D.; Bährle, C.; Mecking, S. *Macromolecular rapid communications*, **2011,** *32* (17), 1352-1356.
17. Plant oil-based long-chain C_{26} monomers and their polymers. Vilela, C.; Silvestre, A. J.; Meier, M. A. *Macromolecular Chemistry and Physics*, **2012,** *213* (21), 2220-2227.
18. Structure–properties relationship of fatty acid-based thermoplastics as synthetic polymer mimics. Maisonneuve, L.; Lebarbé, T.; Grau, E.; Cramail, H. *Polymer Chemistry*, **2013,** *4* (22), 5472-5517.
19. Long-chain aliphatic polymers to bridge the gap between semicrystalline polyolefins and traditional polycondensates. Stempfle, F.; Ortmann, P.; Mecking, S. *Chemical reviews*, **2016,** *116* (7), 4597-4641.
20. Highly selective formation of linear esters from terminal and internal alkenes catalysed by palladium complexes of bis-(di-tert-butylphosphinomethyl) benzene. Jiménez-Rodriguez, C.; Foster, D. F.; Eastham, G. R.; Cole-Hamilton, D. J. *Chemical communications*, **2004,** (15), 1720-1721.
21. Highly selective formation of unsaturated esters or cascade reactions to α, ω-diesters by the methoxycarbonylation of alkynes catalysed by palladium complexes of 1, 2-bis (ditertbutylphosphinomethyl) benzene. Núñez-Magro, A. A.; Robb, L.-M.; Pogorzelec, P. J.; Slawin, A. M.; Eastham, G. R.; Cole-Hamilton, D. J. *Chemical Science*, **2010,** *1* (6), 723-730.

22. Single-step access to long-chain α, ω-dicarboxylic acids by isomerizing hydroxycarbonylation of unsaturated fatty acids. Goldbach, V.; Falivene, L.; Caporaso, L.; Cavallo, L.; Mecking, S. *ACS Catalysis*, **2016,** *6* (12), 8229-8238.
23. Large-ring lactones from plant oils. Witt, T.; Mecking, S. *Green Chemistry*, **2013,** *15* (9), 2361-2364.
24. Stempfle, F. *Aliphatic Polyester Materials from Polycondensation of Seed- and Algae Oil-Based Long-Chain Monomers*. Ph.D. Thesis, University of Konstanz, Konstanz, Germany, **2015**.
25. Morphology of segmented polyester thermoplastic elastomers. Cella, R. J. *Journal of Polymer Science: Polymer Symposia*, **1973,** *42*, 727-740.
26. Poly (tetramethylene ether glycol)/Poly (butylene terephthalate) segmented block copolymers: Effects of composition and thermal treatment on thermal and physical properties. Choi, K.-C.; Lee, E.-K.; Choi, S.-Y. *Journal of Industrial and Engineering Chemistry*, **2003,** *9* (5), 518-525.
27. Thermoplastic polyester elastomers based on long-chain crystallizable aliphatic hard segments. Stempfle, F.; Schemmer, B.; Oechsle, A.-L.; Mecking, S. *Polymer Chemistry*, **2015,** *6* (40), 7133-7137.
28. Holden, G.; Kricheldorf, H. R.; Quirk, R. P., *Thermoplastic Elastomers*. Hanser: Munich, Germany, **2004**.
29. NMR investigations of in-situ stretched block copolymers of poly (butylene terephthalate) and poly (tetramethylene oxide). Schmidt, A.; Veeman, W. S.; Litvinov, V. M.; Gabriëlse, W. *Macromolecules*, **1998,** *31* (5), 1652-1660.

4. Thermoplastic Polyurethane Elastomers Based on Long-Chain Aliphatic Hard Segments

4.1. Introduction

Thermoplastic polyurethane elastomers (TPUs) constitute another group of commercially important thermoplastic elastomers. They describe a class of linear segmented copolymers in which relatively long, flexible polyester or polyether soft segments alternate with rigid, high melting polyurethane hard segments. TPUs are versatile materials that are generally characterized by good thermal properties, high strength, and excellent resistance towards abrasion, oil, and many other solvents.[1] Accordingly, they find application in a variety of areas but are especially prevalent in the production of *e.g.* shoes, automotive parts, seals, electrical plugs, and medical devices where these properties are especially advantageous.[1a] Defining feature of TPUs and polyurethanes in general, is the presence of urethane groups in the polymer backbone. These urethane groups self-associate via the formation of intermolecular hydrogen bonds, thereby providing physical crosslinking between the polyurethane hard segments. The thermodynamic incompatibility of the urethane-rich, polar polyurethane hard blocks with the comparatively apolar soft blocks results in microphase separation, with nano scale hard segment domains being dispersed within a continuous soft segment matrix (**Figure 4.1**).[2]

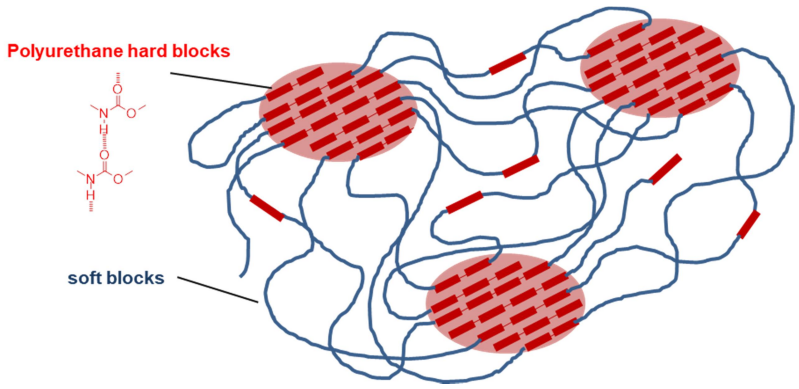

Figure 4.1: Schematic representation of the morphology of thermoplastic polyurethane elastomers.

Typically, the macromonomers serving as soft segments are relatively long and flexible polyester or polyether macrodiols like *e.g.* polycaprolactone or poly(tetramethylene glycol) with a molecular weight of about 1.000 to 3000 g mol^{-1} that impart flexibility and ductility in the polymer. The high-

melting polyurethane hard blocks that dominate the thermal properties and also serve as the load bearing phase are usually generated by polyaddition of aromatic diisocyanates like 4,4'-diphenyl-methane diisocyanate (MDI) with short aliphatic diols like 1,4-butanediol (**Scheme 4.1, a**).[1a],[3] Aromatic diisocyanates are used in most commercial TPUs to improve mechanical properties. In contrast, all-aliphatic TPUs based on *e.g.* isophorone diisocyanate or 1,6-hexane diisocyanate (HDI) stand out due to their optical clarity and high UV-light and thermal stability (**Scheme 4.1, b**).[1a],[4],[5]

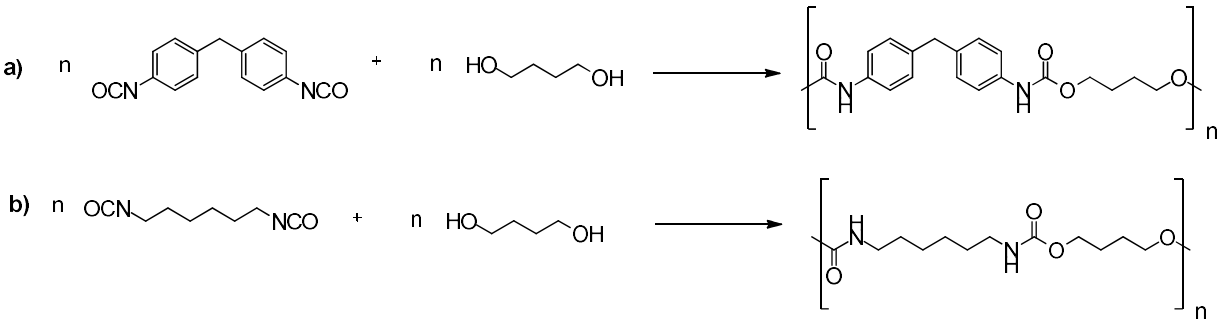

Scheme 4.1: Generation of aromatic (a) and aliphatic (b) polyurethane hard blocks via polyaddition of diisocyanate and diol monomers.

In this context, linear long-chain aliphatic diisocyanates are of interest as they provide access to a novel kind of all-aliphatic TPUs with reduced hydrogen bond density in the polyurethane hard domains and consequently new sets of material properties. However, while the synthesis of some long-chain diisocyanates up to 1,20-eicosane diisocyanate (C_{20}) has been reported in the past,[6],[7],[8] only mid-chain diisocyanates are commercially available at the moment. But thanks to the development of new biotechnological[9] and chemical catalytic processes like olefin metathesis[10] and isomerizing alkoxycarbonylation,[11] a series of novel linear long-chain α,ω-difunctionalized compounds has recently become accessible from common seed[12],[13],[14] and algae oils.[15] This includes some long-chain aliphatic dicarbamates[16] and (unsaturated) diisocyanates[17], containing up to 18 methylene units. However, the synthesis and purification of these compounds remains a challenge, especially if sustainability and safety concerns regarding the involvement of highly toxic phosgene are taken into consideration.[18] The utilization of long-chain polyurethane precursors in the generation of all-aliphatic TPUs has also not yet been investigated. Therefore, in this thesis a new synthesis route for the preparation of novel linear long-chain diisocyanates derived from renewable oleic acid and erucic acid ester substrates is developed and their utility for the generation of hard blocks in all-renewable all-aliphatic thermoplastic polyurethane elastomers is demonstrated.

4.2. Results and Discussion

4.2.1. Synthesis of long-chain α,ω-diisocyanates via nucleophilic substitution

To this day, the standard way to synthesize organic diisocyanate compounds involves the treatment of the corresponding diamines with highly toxic phosgene.[19] In case of short-chain aliphatic diisocyanates, this is typically coupled with the immediate removal of the volatile and highly reactive product from the reaction mixture via distillation to avoid further conversion into urea compounds. However, for long-chain α,ω-diisocyanates with their higher molecular weights and boiling points, this is not feasible. In order to be able to access 1,19-nonadecane diisocyanate and 1,23-tricosane diisocyanate respectively, a synthesis procedure was developed that avoided the involvement of diamine substrates and other starting materials capable of reacting with the respective desired product. Instead, isocyanate groups were generated from bromide functionalities via a nucleophilic substitution reaction with potassium cyanate (**Scheme 4.2**).[20],[21] Compared to rearrangement reactions which have already been successfully used in the past to prepare linear aliphatic diisocyanates[17],[22],[23] as well as dicarbamates[16] from fatty acid-derived long-chain compounds, this method also had the advantage of avoiding a shortening of the fatty acid hydrocarbon chain.

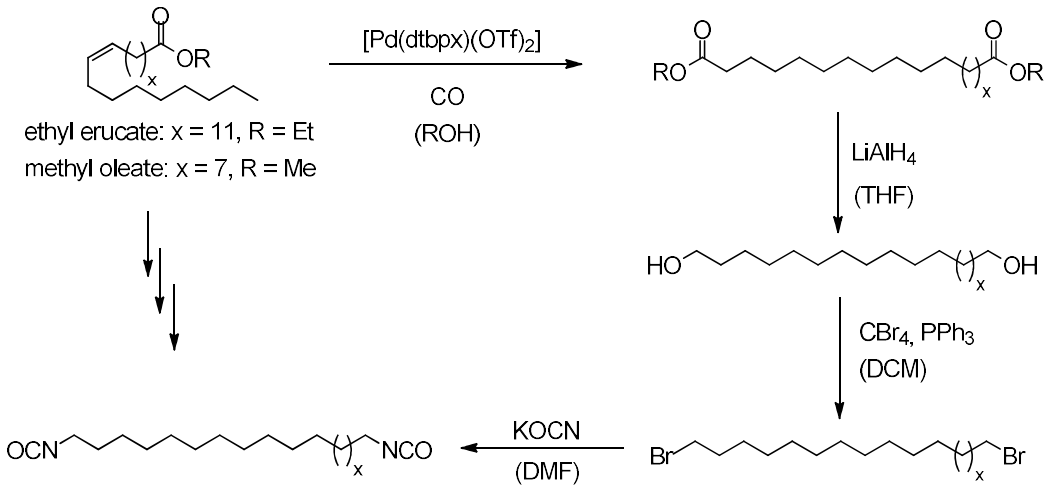

Scheme 4.2: Multistep synthesis of fatty acid-based 1,19-nonadecane diisocyanate (x = 7) and 1,23-tricosane diisocyanate (x = 11).

The necessary linear long-chain dibromo substrates, 1,19-dibromononadecane and 1,23-dibromotricosane, were prepared in a multistep synthesis procedure starting with the isomerizing alkoxycarbonylation of methyl oleate and ethyl erucate respectively. The thus obtained

diesters dimethyl 1,19-nonadecanedioate and diethyl 1,23-tricosandioate (cf. **Chapter 3.2.1**)[24] were reduced with $LiAlH_4$ to the corresponding long-chain diols[25] which were then converted into the aforementioned dibromo compounds via an Apple II reaction (**Scheme 4.2**).[15a] Subsequent treatment of 1,19-dibromononadecane and 1,23-dibromotricosane respectively with excess amounts of potassium cyanate in DMF yielded the corresponding long-chain diisocyanates, 1,19-nonadecane diisocyanate and 1,23-tricosane diisocyanate. Though, in order to be able to obtain the desired products in sufficient amounts and in polycondensation grade purity optimization of the reaction conditions (**Table 4.1**) and the work-up procedure (cf. **Chapter 5.4.2**) proved to be necessary.

Table 4.1: Synthesis of 1,19-nonadecanediisocyanate via nucleophilic substitution. [a]

entry	dibromo substrate	cyanate salt	solvent	temp. [°C]	time	substrate conversion [%]	yield [%]	crude product composition [f] [%]	
								isocyanate groups	isocyanurate groups
1	C_6	KOCN	DMF	140	7 h	100	>100[b]	34	39
2	C_{19}	KOCN	DMF	140	7 h	100	- [l]	- [l]	- [l]
3	C_{19}	KOCN	DMF	140	3 h	100	36	50	45
4	C_{19}	KOCN	DMF	140	30 min	100	97[b]	75	16
5	C_{19}	KOCN	DMF	140	20 min	100	81[b]	87[c]	9[c]
6	C_{19}	KOCN	DMF	120	1 h	100	93[b]	81	15
7[d]	C_{19}	KOCN	DMF	120	40 min	100	58	89	5
8	C_{19}	KOCN	DMF	120	30 min	100	54	91	4
9[e]	C_{19}	KOCN	DMF	120	20 min	91	60	81	3
10	C_{19}	KOCN	DMF	120	15 min	96	65	81	3
11[d]	C_{19}	KOCN	DMF	100	30 min	98	38	91	4
12[d]	C_{19}	KOCN	DMF/ toluene	120	30 min	40	70	36	-
13[d]	C_{19}	KOCN	DMF/ toluene	120	90 min	86	55	76	2
14[d]	C_{19}	KOCN	DMF/ toluene	120	2 h	93	38	80	4
15[d]	C_{19}	KOCN	MeCN	100	30 min	0	-	-	-
16[d]	C_{19}	KOCN	DMSO	120	30 min	100	13[g]	19	30
17[d]	C_{19}	AgOCN	DMF	120	30 min	76	10	16	-[i]
18[d]	C_{19}	KOCN[h]	DMF	120	30 min	100	- [l]	- [l]	- [l]
19	C_{19}[k]	KOCN	DMF	120	15 min	100	- [l]	- [l]	- [l]

a) Standard reaction conditions: 1 g (2.36 mmol) of aliphatic dibromide in 17 ml of hot DMF was treated with 5 eq. (952 mg, 77.7 mmol) of KOCN. b) contained substantial amounts of inorganic salts, insoluble polyisocyanurate and/or solvent; c) combined results from two product fractions, d) 250 mg (0.59 mmol) of C_{19}-dibromide in 7 ml of hot DMF was treated with 5 eq. (238 mg, 2.93 mmol) of potassium cyanate. e) 1,25 g C_{19}-dibromide in 20 ml DFM, f) according to ^{1}H NMR spectroscopy. g) insoluble fraction comprised of polyisocyanurate not included. h) 100 mol% of 18-crown-6 ether in relation to KOCN added. i) 39% of 1,19-nonadecane dicyanate formed as additional side product, k) 1,19-nonadecane dimesylate used as educt. l) reaction yielded insoluble polymeric material.

The obtained crude products were analyzed using ^{1}H NMR spectroscopy (**Figure 4.2**) which identified isocyanurate compounds (δ = 3.86, m) generated via isocyanate (δ = 3.29, t) trimerization to be the major side products formed during the course of the reaction (**Scheme 4.3**).

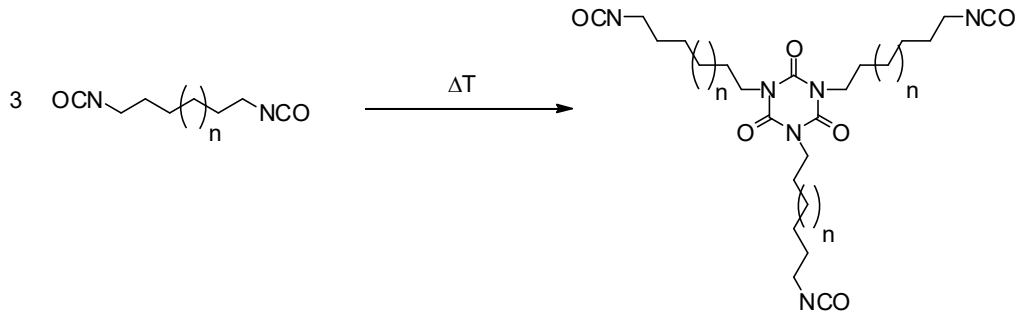

Scheme 4.3: Isocyanurate formation via trimerization of aliphatic diisocyanates (n =1 for 1,6-hexamethylene diisocyanate, n = 14 for 1,19-nonadecane diisocyanate.

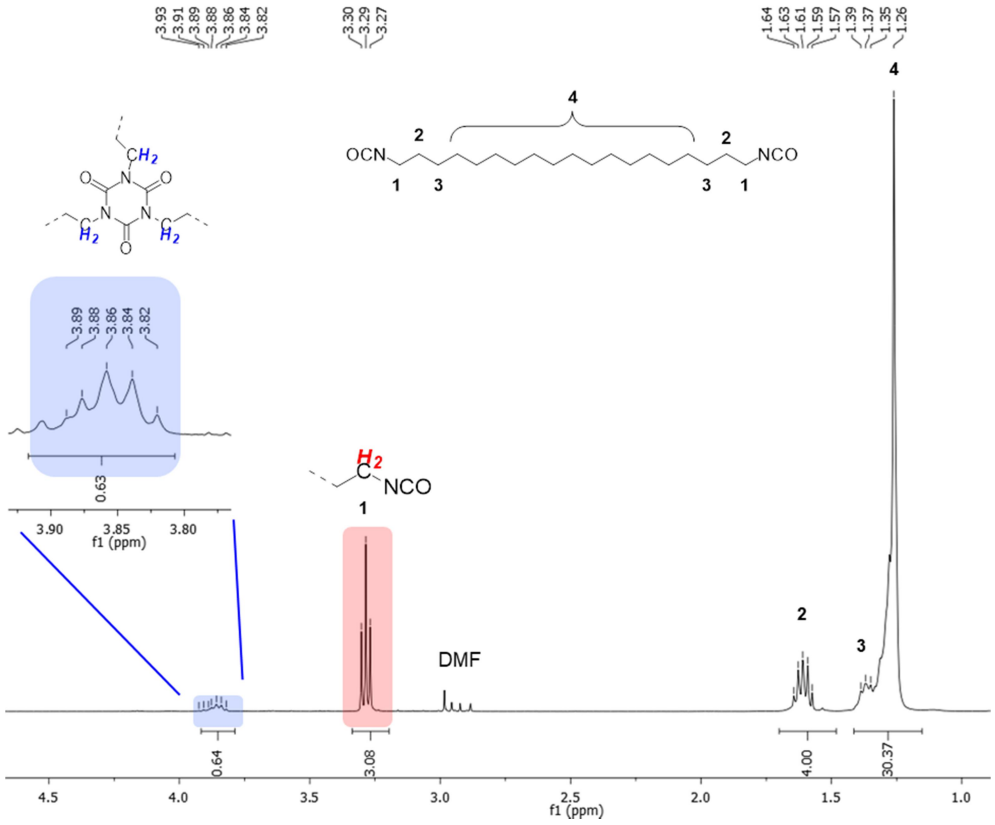

Figure 4.2: Exemplary 1H NMR spectrum (400 MHz, CDCl3, RT) of the crude product obtained from the treatment of 1,19-dibromononadecane with KOCN in DMF (Table 4.1, entry 4). Signals corresponding to methylene groups adjacent to isocyanate groups (red) and isocyanurate groups (blue) highlighted.

Long-chain 1,19-nonadecane diisocyanate, with its long flexible hydrocarbon backbone, revealed itself to be highly susceptible to trimerization and ultimately self-polymerization. Treating 1,19-dibromononadecane with KOCN at 140 °C for 7 hours resulted in the formation of an insoluble polymer most likely comprised of highly crosslinked polyisocyanurate (**Table 4.1, entry 2)**. In contrast, the soluble crude product obtained from the conversion of short-chain 1,6-dibromohexane under identical conditions consisted of a complicated product mixture that still contained about 34 % isocyanate functionalities in addition to 39 % of isocyanurate groups (**Table 4.1, entry 1)**. No substantial amounts of insoluble polyisocyanurate were formed. In order to reduce to amount trimerization products being generated during the synthesis of 1,19-nonadecane diisocyanate, the reaction time was incrementally reduced from 7 h to 20 min (**Table 4.1**, **entry 2–5**), which resulted in the isocyanurate content in the crude product dropping from 100 % to 9 %. Lowering the reaction temperature to 120 °C (**Table 4.1**, **entry 6–10**) and 100 °C (**Table 4.1**, **entry 11**) respectively reduced to amount of isocyanurate groups being formed even further to 5 % or less if the reaction time did not exceed 40 min. Simultaneously, the content of isocyanate functionalities increased until isocyanate groups accounted for up to 91 % of all functional groups present in the crude product, indicating that at reduced temperatures and reaction times the main product being formed is 1,19-nonadecane diisocyanate. Optimum results were obtained after 30 min. at a temperature of 120 °C (**Table 4.1**, **entry 8**) (**Figure 4.3**). Further reduction of either the reaction temperature to 100 °C (**Table 4.1**, **entry 11**) or of the reaction time to 20 min (**Table 4.1**, **entry 9**) or 15 min (**Table 4.1**, **entry 10**) did not improve the ratio of isocyanurate to isocyanate groups any further, instead substrate conversion remained incomplete.

It also has to be noted that with improving crude product composition the nominal yield of the isolated soluble product fraction decreased from values approaching or even exceeding 100 % (**Table 4.1**, **entry 4-6** and **2**) to values ranging from 38 % to 65 % (**Table 4.1**, **entry 7-11**). However, this has to be taken with a grain of salt as, especially for reactions in which large amounts of polyisocyanurate or isocyanurate side products were formed, an efficiently removal of solvent and potassium salt residues from the product mixture was impossible, therefore resulting in nominal crude product yields being inflated and selectivities being impossible to determine accurately.

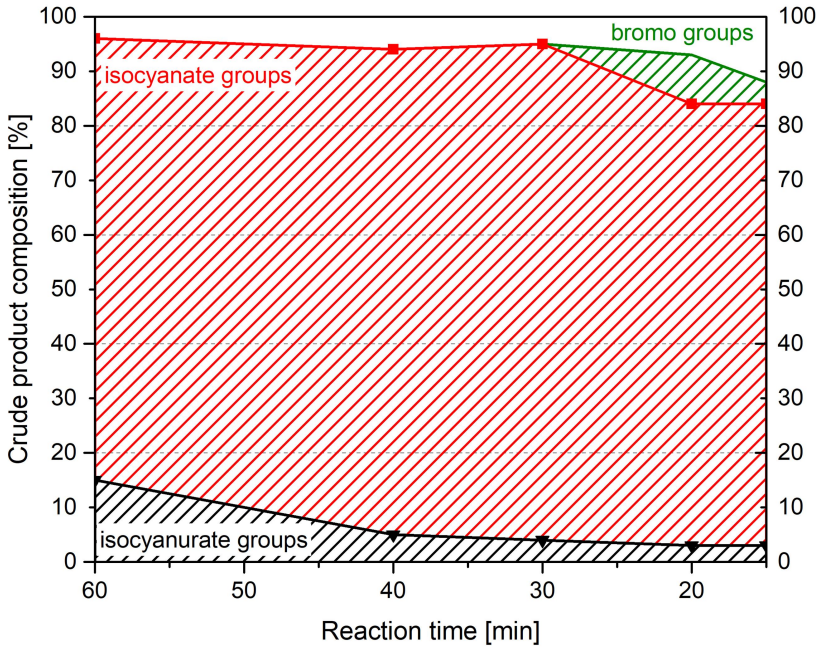

Figure 4.3: Correlation between reaction time and crude product composition for the synthesis of 1,19-dnonadecane diisocyanate in DMF at 120 °C (**Table 4.1, entry 6-10**). Cumulative depiction of functional group content: isocyanurate groups (black), isocyanate groups (red), bromide groups (green).

The effect of different solvents on the reaction result was also explored: No reaction took place if DMF was replaced by acetonitrile (MeCN) (**Table 4.1**, **entry 15**), while DMSO (**Table 4.1**, **entry 16**) was found to facilitate trimerization and self-polymerization, with the reaction yielding mostly insoluble polyisocyanurate in addition to a small amount of a soluble, low molecular weight oligoisocyanurate product fraction. Employing a less polar DMF/toluene mixture (ratio 1:1) significantly slowed down the nucleophilic substitution reaction, with full conversion not being reached even after the reaction time was successively extended from 30 min (40 %) to 2 hours (93 %) (**Table 4.1**, **entry 12-14**). And while the formation isocyanurate groups was also delayed under these conditions, the isocyanurate contamination increased in unison with conversion of 1,19-dibromononadecane, overall resulting in no improvement of selectivity for the desired product. Addition of stoichiometric amounts (in relation to potassium cyanate) of 18-crown-6 ether[26] to increase the concentration of dissolved cyanate anions (**Table 4.1**, **entry 18**) led to almost immediate precipitation of insoluble polyisocyanurate. No soluble product fraction containing the desired product could be isolated. Similarly, employing 1,19-nonadecane dimesylate (**Table 4.1**, **entry 19**) instead of 1,19-dibromononadecane as the starting material in an attempt to exploit the higher

susceptibility of mesylate groups to nucleophilic substitution[27] also resulted in immediate polymer precipitation. No diisocyanate containing product fraction could be isolated. Replacing potassium cyanate with silver cyanate as the metal cyanate salt (**Table 4.1**, **entry 17**) successfully prohibited diisocyanate trimerization. However, substrate conversion only reached a value of 76 %. Analysis of the crude product via ^{1}H NMR spectroscopy also revealed the formation of an additional cyanate side product, with cyanate functionalities accounting for 39 % of the functional groups present in the crude product. At the same time the content of isocyanate functionalities dropped to 16 %.

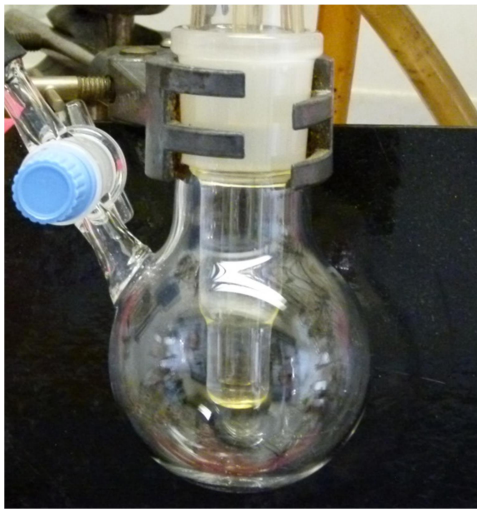

Figure 4.4: Cooling finger used for the purification of long-chain aliphatic diisocyanates via distillation.

In order to isolate the synthesized long-chain diisocyanates in polycondensation grade purity, distillation was required. Boiling points at a pressure of 0.06 mbar were determined to be 130°C for 1,19-nonadecane diisocyanate and 140 °C for 1,23-tricosane diisocyanate. But as both diisocyanates continued to trimerize and decompose upon being exposed to high temperatures for extended periods of time, standard distillation equipment proved to be inadequate. Instead, a custom-designed sublimation apparatus equipped with a cooling finger needed to be employed (**Figure 4.4**). However, due to the limited size and design of the apparatus the amount of 1,19-nonadecane diisocyanate and 1,23-nonadeance diisocyanate that could be distilled was limited to roughly 1 g of pure product per batch. Overall, optimization of the reaction conditions as well as the work-up procedure (cf. **Chapter 4.4.2**) allowed for the synthesis of pure 1,19-nonadecane diisocyanate and 1,23-nonadeance diisocyanate from their respective corresponding dibromo compounds to be upscaled to a scale of

about 1 g of product (**Table 4.2**), with the limiting factor being the size of the distillation apparatus. The yield of pure 1,19-nonadecane diisocyanate could be increased to about 35 % independent of the batch size (but within the limits of the distillation apparatus) (**Table 4.2**, **entry 1-4**), which for a batch size of 4 g of 1,19-dibromononadecane translates to 1.17 g of the desired product (**Table 4.2**, **entry 4**). Similarly, 1,23-tricosane diisocyanate was successfully prepared from 1,23-dibromo-tricosane, with subsequent distillation at 140 °C and 0.06 mbar yielding the desired product in polycondensation grade purity in yields of up to 40 % (**Table 4.2**, **entry 5**). Upscaling to a batch size of to 2.7 g of educt made it possible to obtain up to 0.89 g of pure product without the overall yield suffering (**Table 4.2**, **entry 6**).

Table 4.2: Upscaling of the synthesis of 1,19-nonadecane diisocyanate and 1,23-tricosane diisocyanate. [a)]

entry	diisocyanate	batch size [b)]	yield [c)]
1	C_{19}	1.0 g	0.28 g (34 %)
2	C_{19}	2.0 g	0.51 g (35 %)
3	C_{19}	3.0 g	0.86 g (35 %)
4	C_{19}	4.0 g	1.17 g (36 %)
5	C_{23}	2.0 g	0.67 g (40 %)
6	C_{23}	2.7 g	0.89 g (39 %)

a) reaction conditions: 17 ml DMF/1 gram substrate, 120 °C, 35 min. b) referring to amount of dibromo substrate. c) referring to purified diisocyanate product.

The structure of the distilled long-chain diisocyanates was confirmed via ATR-FTIR and NMR spectroscopy. The recorded FTIR spectra showed strong absorption bands at about 2260 cm^{-1} (**Figure 4.5**) characteristic for N=C=O stretching vibrations of an isocyanate group. Similarly, ^{13}C and $^{1}H,^{13}C$ HMBC NMR spectra showed a resonance at about δ = 122 ppm, which corresponds well with the carbon atom of an isocyanate group (**Figure 4.7** and cf. **Chapter 4.4.2, Figure 4.22, 4.24** and **4.25)**, while the recorded ^{1}H NMR spectra further confirmed that the desired diisocyanates were isolated in purities exceeding 98 % (**Figure 4.6** and cf. **Chapter 4.4.2, Figure 4.23**).

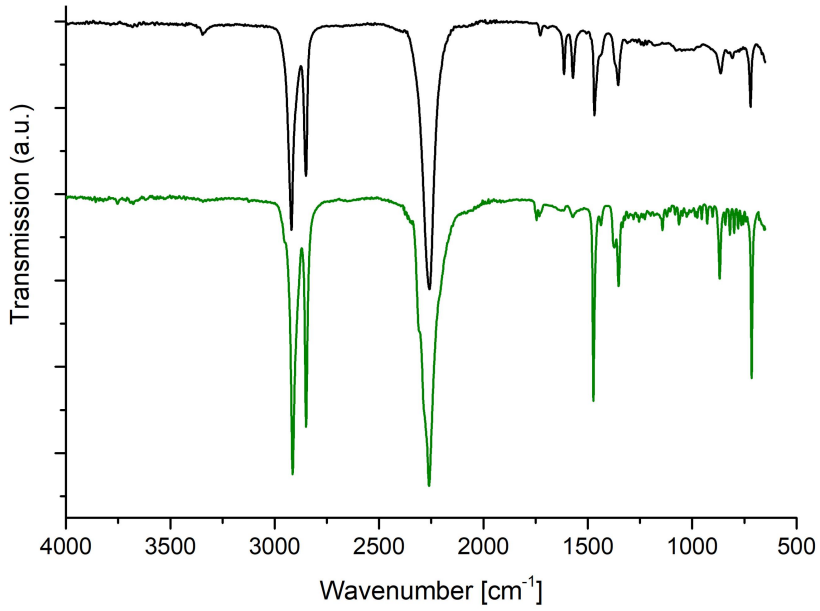

Figure 4.5: FTIR spectra of 1,19-nonadecane diisocyanate (black) and 1,23-tricosane diisocyanate (green).

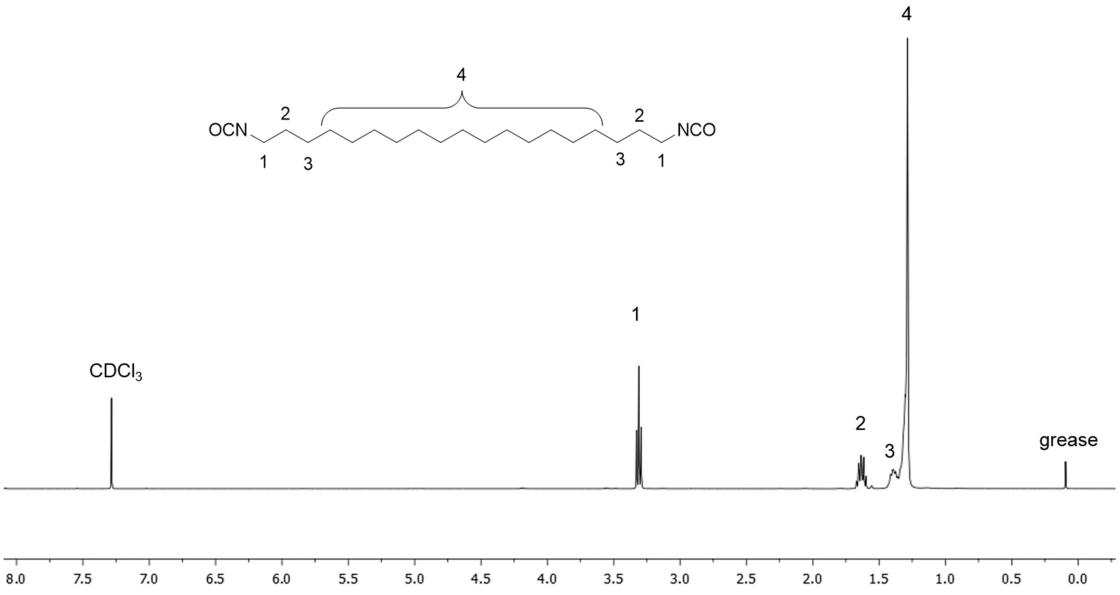

Figure 4.6: ^{1}H NMR spectrum ($CDCl_3$, 400 MHz) of 1,19-nonadecane diisocyanate.

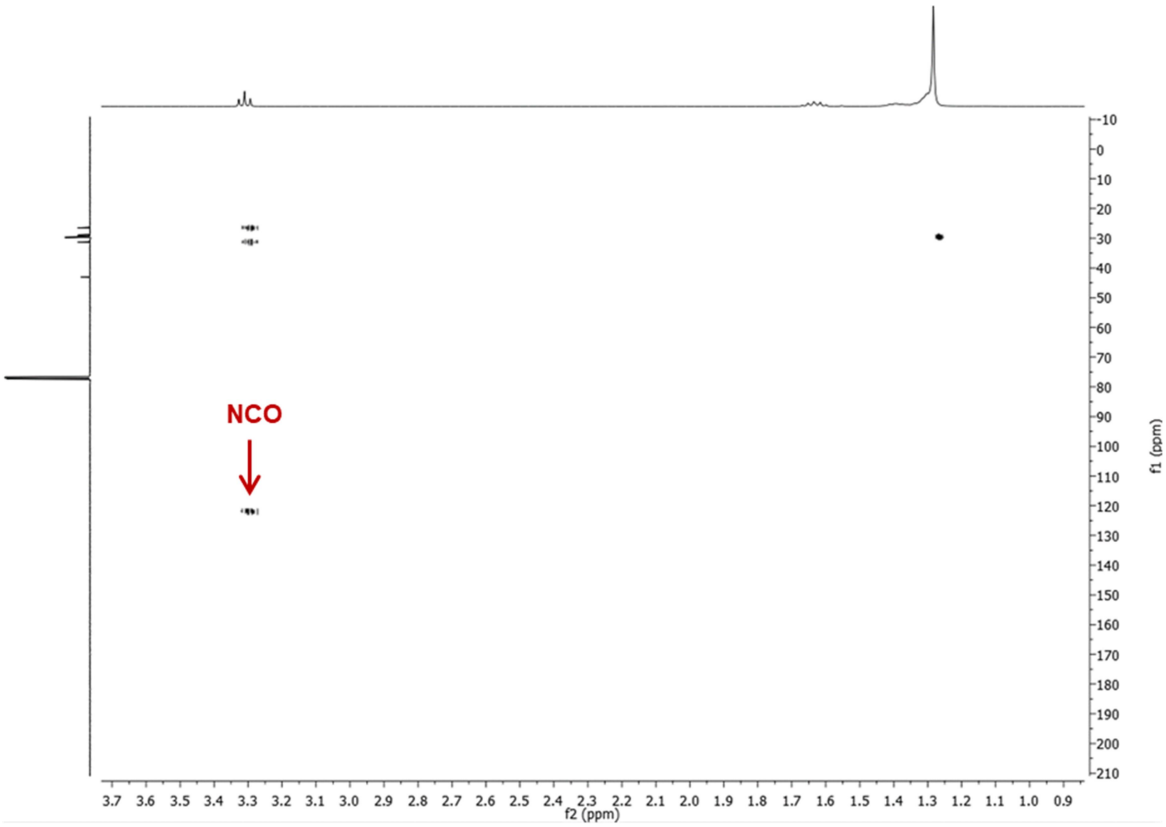

Figure 4.7: $^{1}H,^{13}C$ HMBC NMR spectrum ($CDCl_3$, 400 MHz, 101 MHz) of 1,19-nonadecane diisocyanate.

4.2.2. Synthesis of long-chain thermoplastic polyurethane elastomers

Thermoplastic polyurethane elastomers from the polyaddition of diisocyanates and diols are most commonly prepared via melt polyaddition either in a one-step or two-step prepolymer procedure. The latter involves the generation of an isocyanate-terminated prepolymer from the reaction of the diisocyanate monomer with the amorphous macrodiol before the diol chain extender is added.[1] Alternatively, solution polymerization in polar organic solvents like e.g. dimethylformamide, dimethylacetamide or sulfolane which are capable of dissolving a wide variety of polyurethane hard and polyether and polyester soft segments can also be employed.[1a],[28] The number of steps involved in the polymerization can have an effect on the material properties of the obtained TPU as the block length distribution of the hard blocks and therefore polymer morphology is directly affected.[29] In addition, it has to be noted that according to Flory statistics[30] the high molecular weights necessary to ensure chain entanglement are only achieved if the ratio of isocyanate to alcohol functionalities does not drop below 0.97, even in the later stages of the reaction, making the two-step approach less

reliable due to the increased chance for isocyanate decomposition. An excess of free isocyanate groups during the prepolymer phase can also result in the formation of undesirable allophanat and biuret groups.[1],[31]

Table 4.3: Synthesis of segmented poly(urethane-ether) block copolymers based on long-chain and mid-chain aliphatic polyurethane hard segments. [a)]

entry	polymer	mol-% $PPDO_{2000}$ of total diol	solvent	M_n[b)] (NMR)	M_n[c)] (GPC)	M_w/M_n[c)]
1	TPU-$C_{19}PPDO_{2000}$-85wt%	100 %	DMF	3.1×10^4	5.1×10^4	1.5
2	TPU-$C_{19}PPDO_{2000}$-78wt%	75 %	TCE	3.2×10^4	4.5×10^4	1.7
3	TPU-$C_{19}PPDO_{2000}$-67wt%	50 %	TCE	3.9×10^4	4.2×10^4	1.6
4	TPU-$C_{23}PPDO_{2000}$-83wt%	100 %	TCE	5.0×10^4	5.7×10^4	1.7
5	TPU-$C_{23}PPDO_{2000}$-75wt%	75 %	TCE	3.0×10^4	3.9×10^4	1.7
6	TPU-$C_{23}PPDO_{2000}$-63wt%	50 %	TCE	3.3×10^4	4.1×10^4	1.7
7	TPU-$C_{12}PPDO_{2000}$-59wt%	29 %	TCE	6.7×10^4	-	-
8	PU-19.19	-	TCE	-	0.6×10^4 [d)]	1.8 [d)]
9	PU-23.23	-	TCE	-	0.3×10^4 [d)]	1.8 [d)]

a) solution polymerization at 80°C with 0.5 mol % of DBTDL. b) determined by end-group analysis from ^{1}H NMR spectroscopy. c) Determined by GPC in THF at 50 °C versus polystyrene standards. d) Determined by GPC in 1,2,4-trichlorobenzene at 160 °C versus polyethylene standards.

In order to prepare novel segmented TPUs based on all-aliphatic long-chain polyurethane hard segments, fatty acid-derived 1,19-nonadecane diisocyanate and 1,23-tricosane diisocyanate were copolymerized with varying amounts of the corresponding long-chain diols and renewable polyether $PPDO_{2000}$ in a one-step polyaddition reaction. Because melt polymerization proved to be unsuitable for polyaddition systems containing a high-melting long-chain diol, a solution polymerization procedure was developed that yielded a series of high molecular weight segmented poly(urethane-ether) block copolymers whose $PPDO_{2000}$ polyether soft segment content ranged from 63 to 85 wt.% (**Table 4.3, entry 1-6)**. Catalytic amounts of dibutyltin dilaurate (DBTDL) were added to the reaction mixture to facilitate polyaddition and compensate for the relatively low reactivity of aliphatic diisocyanates compared to their aromatic counterparts. Because solubility of the emerging poly(urethane-ether) block copolymers in DMF was found to decrease drastically with increasing polyurethane hard block content, 1,1,2,2-tetrachloroethane (TCE) was employed as the solvent for all three component polyaddition systems. This way, segmented long-chain poly(urethane-ether) block copolymers with a number average molecular weight ranging from 3.0 x 10^4 to

5.0 x 10^4 g mol^{-1} according to ^{1}H NMR spectroscopy could be obtained. These results were qualitatively confirmed using GPC analysis, which also revealed a well behaved molecular weight distribution M_w/M_n of around 1.7 for all synthesized TPUs. In addition, solution polymerization of 1,19-nonadecane diisocyanate and 1,23-nonadecane diisocyanate respectively with equimolar amounts of their corresponding long-chain diols in TCE yielded the long-chain polyurethanes PU-19.19 and PU-23.23 (**Table 4.3**, **entry 8** and 9), though number average molecular weights of these thermoplastics remained limited to 0.6 x 10^4 g mol^{-1} and 0.3 x 10^4 g mol^{-1} respectively according to GPC analysis due to recurring solubility issues during polymerization.

In order to further assess the effect that methylene sequence length and urethane group density in aliphatic polyurethane hard segments have on the material properties of TPUs, another segmented all-aliphatic poly(urethane-ether) block copolymer, TPU-C_{12}PPDO$_{2000}$-59wt%, based on mid-chain 1,12-diisocyanatododecane and 1,12-dodecanediol was prepared (**Table 4.3**, **entry 7**). TPU-C_{12}PPDO$_{2000}$-59wt% possessed a comparable weight fraction of soft PPDO$_{2000}$ polyether diol as its long-chain analog, TPU-C_{23}PPDO$_{2000}$-63wt% (**Table 4.3, entry 6**) in combination with almost identical block length distributions and a similar chain microstructure. The only major difference was that the shortest hard block, *i.e.* an isolated diisocyanate repeat unit, in the long-chain monomer-based TPU-C_{23}PPDO$_{2000}$-63wt% was about twice as long (C_{23}) as in its mid-chain analog TPU-C_{12}PPDO$_{2000}$-59wt% (C_{12}) (cf. **Chapter 3.2.2, Figure 3.2)**. The number average molecular weight of TPU-C_{12}PPDO$_{2000}$-59wt% was determined to be 6.7 × 10^4 g mol^{-1} according to ^{1}H NMR spectroscopy.

4.2.3. Morphology of long-chain thermoplastic polyurethane elastomers

As is typical for aliphatic TPUs, the obtained long-chain poly(urethane-ether) block copolymers were transparent and became more opaque the more the hard segment content increased (**Figure 4.8**).

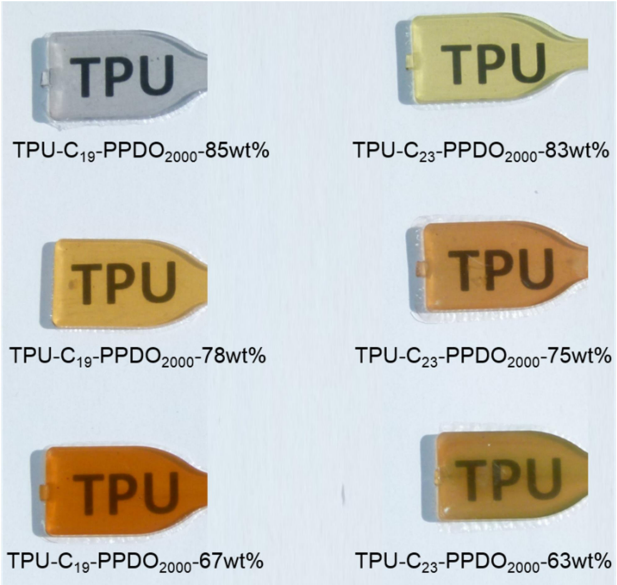

Figure 4.8: Photography of injection molded test specimens of TPUs based on C_{19} and C_{23} long-chain monomers (discoloration due to injection molding).

ATR-FTIR spectroscopy was used to further investigate the composition of the synthesized TPUs as well as to determine their relative degree of phase separation as both factors directly influence mechanical properties. The obtained FTIR spectra (cf. **Chapter 4.4.5, Figure 4.28** and **4.29**) showed no isocyanate peaks at about 2260 cm^{-1}, thereby confirming that conversion of the isocyanate functionalities was complete. Instead, the amide and carbonyl regions featured distinct absorption bands at 3334 cm^{-1}, 1723 cm^{-1}, and 1683 cm^{-1} respectively, thereby confirming the formation of urethane groups (**Figure 4.9** and **4.10**). The carbonyl signals of TPU-C_{12}PPDO$_{2000}$-59wt% appeared at slightly lower absorption frequencies of 1720 cm^{-1} and 1680 cm^{-1} respectively due to small structural differences (cf. **Chapter 4.4.5, Figure 4.30**).

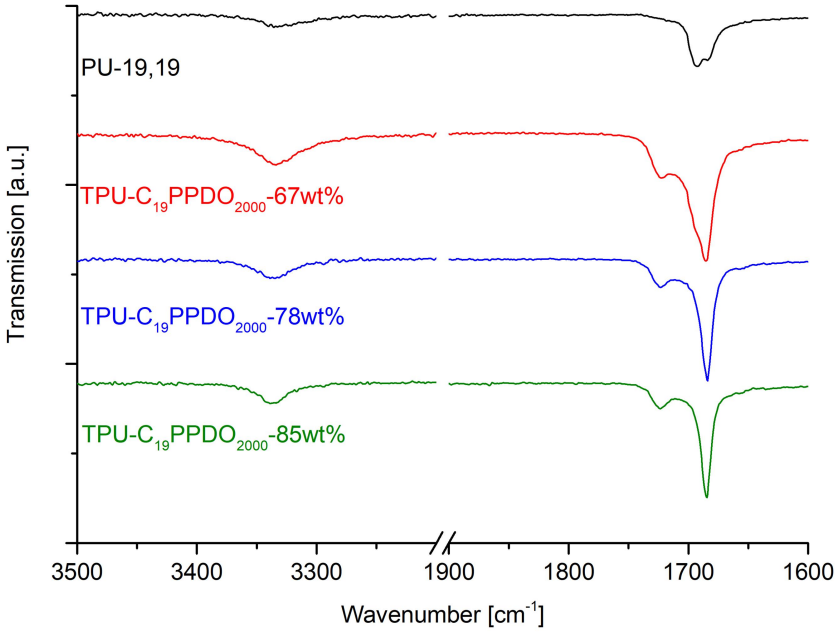

Figure 4.9: Amide and carbonyl regions of the FTIR spectra of PU-19.19 and thermoplastic polyurethane elastomers based on long-chain aliphatic C_{19} monomers.

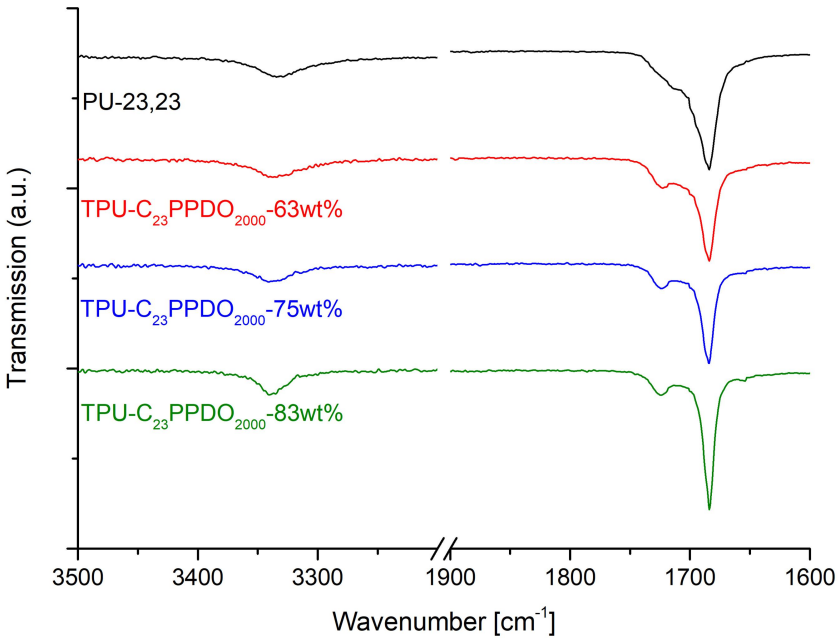

Figure 4.10: Amide and carbonyl regions of the FTIR spectra of PU-23.23 and thermoplastic polyurethane elastomers based on long-chain aliphatic C_{23} monomers.

The shift of the amide band to 3334 cm^{-1} in combination with the absence of further amide bands at about 3400 cm^{-1} suggested the presence of only hydrogen bonded amide hydrogen atoms in all TPUs. But as urethane amide groups can form hydrogen bonds with urethane carbonyl groups - thereby leading to the formation of hard domains and phase separation - as well as with oxygen atoms of ether groups of the soft phase - thereby leading to phase mixing - this data alone was not sufficient to make a definitive statement about the degree of phase separation. Instead, a closer inspection of the signals in the carbonyl regions at 1723 cm^{-1} and 1683 cm^{-1} was required. The latter compared well with a value of 1685 cm^{-1} previously reported for carbonyl groups that are organized and strongly hydrogen bonded with amide groups and whose vibrational motions are restricted accordingly, resulting in a shift to a lower absorption frequency.[32] Additional absorption bands relating to carbonyl groups not involved in any hydrogen bonding would be expected to appear at about 1730 cm^{-1}, while the absorption bands of carbonyl groups bound by poorly ordered hydrogen bonds appear at about 1710 cm^{-1}.[3a],[32] Accordingly, the carbonyl band at 1723 cm^{-1} can be assigned to non-hydrogen bonded carbonyl groups, with minor deviations from literature values being attributed to differences in the structure of the hard segment components.

With increasing content of hard segments, the carbonyl band at 1683 cm^{-1} started to broaden and further analysis via peak deconvolution suggested the presence of an additional overlapping absorption band at about 1702 cm^{-1} which can be attributed to the presence of poorly ordered hydrogen bonds. This indicates the formation of larger hard domains with imperfect hydrogen bonding, especially for TPU-C_{23}PPDO$_{2000}$-63wt% and TPU-C_{19}PPDO$_{2000}$-67wt% with the highest hard phase content of all synthesized materials. For the thermoplastics PU-19,19 and PU-23,23 broad absorption bands at 1693 cm^{-1} and 1685 cm^{-1} were observed, suggesting overlapping of multiple signals (**Figure 4.9** and **4.10**).

In order to obtain a quantitative measure of the relative amounts of different carbonyl groups present and to determine the extent of phase separation, the carbonyl regime of the FTIR spectra was quantitatively analyzed by peak deconvolution of the carbonyl absorption bands. The percentage of each carbonyl signal was obtained by comparing the specific peak areas with the total peak area (**Table 4.4**). The results indicated that only about 15 % of the carbonyl groups in all synthesized long-chain TPUs remained unbound, thereby implying a high degree of phase separation of about 85 % regardless of the copolymer composition (**Table 4.4, entry 1-6**). In comparison, in TPUs based on aromatic or cycloaliphatic polyurethane hard segments similar degrees of phase separation are generally only reached after annealing.[32b],[33] Accordingly, a quantitative analysis of the

FTIR spectrum of the mid-chain monomer-based analog TPU-C_{12}PPDO$_{2000}$-59wt% (cf. **Chapter 4.4.5, Figure 4.30**) revealed a much lower degree of phase separation of only 56% (**Table 4.4, entry 7**), indicating that increased chain flexibility due to longer methylene sequences in long-chain monomer-based TPUs promotes hydrogen bond formation and phase separation.

Table 4.4: Quantitative analysis of the carbonyl region of FTIR spectra recorded for all-aliphatic TPUs by peak deconvolution.

		peak area [%]	
entry	**polymer**	free C=O groups (1723 cm^{-1})	H-bonded C=O groups (1702 cm^{-1}+ 1685 cm^{-1})
1	TPU-C_{19}PPDO$_{2000}$-85wt%	13	87
2	TPU-C_{19}PPDO$_{2000}$-78wt%	13	87
3	TPU-C_{19}PPDO$_{2000}$-67wt%	14	86
4	TPU-C_{23}PPDO$_{2000}$-83wt%	15	85
5	TPU-C_{23}PPDO$_{2000}$-75wt%	15	85
6	TPU-C_{23}PPDO$_{2000}$-63wt%	13	87
7	TPU-C_{12}PPDO$_{2000}$-59wt%	44[a)]	56[b)]

a) Signal at 1720 cm^{-1}. b) Signal at 1680 cm^{-1}

In addition, the crystalline solid state structure of the studied novel long-chain polyurethanes was further elucidated using WAXD. While polyesters based on long-chain aliphatic monomers crystallize in the polyethylene-like orthorhombic structure due to crystallization being driven by Van-der-Waals interactions between the long hydrocarbon segments with ester groups being incorporated in the all-trans hydrocarbon crystal lattice as defects,[34] the crystalline structure of long-chain polyurethanes is typically still dominated by the formation of intermolecular hydrogen bonds between urethane groups.[8],[35] Accordingly, WAXD diffraction patterns recorded for PU-19,19 and PU-23,23 (**Figure 4.11**) as well as corresponding TPUs (**Figure 4.12**) displayed peaks at 2θ angles of 19.6°, 21.1° and 23.6°, which correspond to d-spacings of 4.5 Å, 4.2 Å and 3.8 Å respectively. These results do not concur with an orthorhombic diffraction pattern and d-spacings (4.1 Å (d_{110}) and 3.7 Å (d_{200})).[36] Instead, the d-spacings of the two observed prominent diffraction peaks at 19.6° and 23.6° appeared to be related to the two characteristic reflection peaks (4.4 Å (d_{100}) and 3.7 Å (d_{010})) typically seen for even-even polyamides or polyurethanes in a triclinic crystal phase.[37] In addition, the weaker diffraction peak at 21.1° (4.2 Å) corresponds well with a pseudohexagonal phase, thereby indicating an overall crystal structure composed of a mixture of triclinic and pseudohexagonal cells.

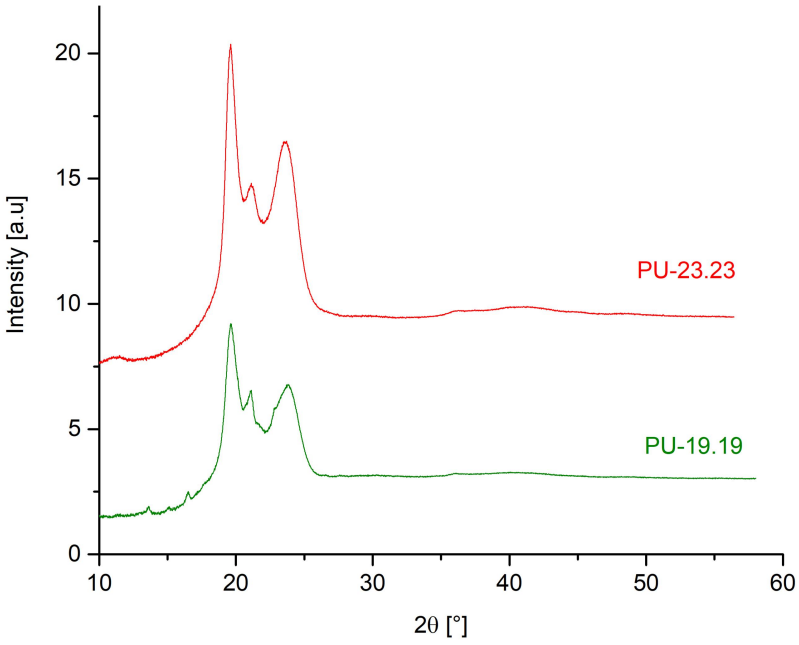

Figure 4.11: WAXD pattern of PU-19.19 (green) and PU-23.23 (red).

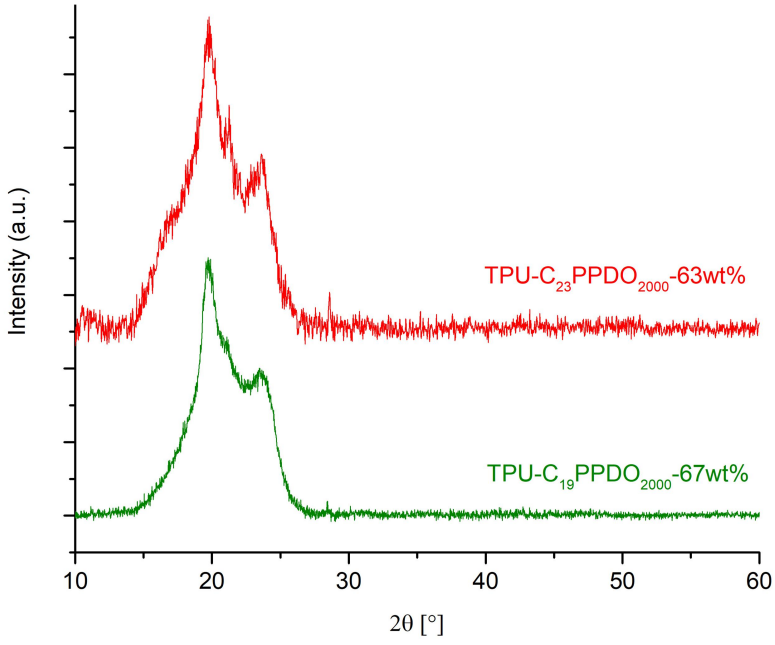

Figure 4.12: WAXD pattern of TPU-C_{19}PPDO$_{2000}$-67wt% (green) and TPUC_{23}PPDO$_{2000}$-63wt% (red).

Similar results have in the past been reported for aliphatic polyurethanes derived from short-chain diisocyanates and long-chain diols.[35b] Overall, analysis of the WAX diffraction patterns revealed that

despite the long methylene sequences hydrogen bonding remained the driving factor for crystallization and no polyethylene-like crystal structure was adopted.

4.2.4. Thermal properties of long-chain thermoplastic polyurethane elastomers

DSC thermograms recorded for the synthesized all-aliphatic long-chain TPUs feature two melting points, a lower melting point relating to the PPDO polyether soft phase in the range of -6 °C to 1 °C and a high melting point in the range of 62 °C to 116 °C correlating to the semi-crystalline polyurethane hard domains (**Table 4.5, Figure 4.14** and **4.15**). Partial replacement of the polyether macromonomer by 1,19-nonadecanediol or 1,23-tricosanediol respectively resulted in a significant increase of the melt temperatures of the polyurethane hard phase, with the values recorded for upper melting points rising from 62 °C to 109 °C for C_{19} monomer-based TPUs (**Table 4.5, entry 1-3**) and from 76 °C to 116 °C for C_{23} monomer-based TPUs (**Table 4.5, entry5-7**), thereby increasingly approaching the melting points of the corresponding homopolymers PU-19.19 (T_m = 132 °C) and PU-23.23 (T_m = 122 °C) respectively (**Table 4.5**, **entry 4** and **8**) (**Figure 4.13**).

Table 4.5: Thermal properties of polyurethanes and polyurethane-polyether block copolymers based on long- and mid-chain aliphatic hard segments.

entry	polymer	mol-% $PPDO_{2000}$ of total diol	T_m [a)]	T_c [a)]	T_g [b)]
			[°C]	[°C]	[°C]
1	TPU-$C_{19}PPDO_{2000}$-85wt%	100 %	-1/62	-18/32	-66
2	TPU-$C_{19}PPDO_{2000}$-78wt%	75 %	-6/97	-23/68	-68
3	TPU-$C_{19}PPDO_{2000}$-67wt%	50 %	-6/109	-31/78	-68
4	PU-19.19	-	132[c)]	106	-
5	TPU-$C_{23}PPDO_{2000}$-83wt%	100 %	1/76	-13/60	-68
6	TPU-$C_{23}PPDO_{2000}$-75wt%	75 %	-4/102	-18/78	-69
7	TPU-$C_{23}PPDO_{2000}$-63wt%	50 %	-6/116	-20/89	-69
8	PU-23.23	-	122[c)]	103	-
9	TPU-$C_{12}PPDO_{2000}$-59wt%	29 %	-6/129	-38/86	-66

a) Determined by DSC with a heating/cooling rate of 10 K min^{-1}. b) Determined by DSC with a heating rate of 30 K min^{-1}. c) Upper melting point.

In contrast, the melting temperatures of PU-19.19 and PU-23.23 were determined by their hydrogen bond density. Though, as with other known long-chain aliphatic polyurethanes,[16],[38] the melting points of both, PU-19.19 as well as PU-23.23, did not exceed the melting point of linear polyethylene

(T_m = 135 °C)[39] despite the presence of hydrogen bonds, a phenomenon that is typically attributed to undisturbed crystallization driven by van-der-Waals interactions being more efficient.[14],[40] The appearance of two melting points in the thermograms of both thermoplastics can be explained by the low molecular weight of the studied polymer samples.

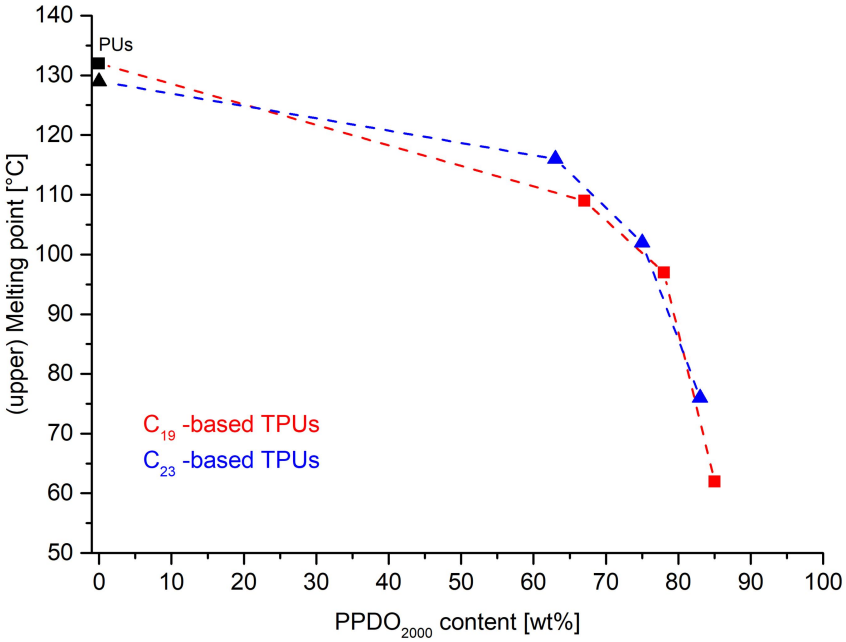

Figure 4.13: Correlation between TPU composition and (upper) melting point.

In addition, increasing polyurethane hard phase content in the synthesized long-chain TPUs also resulted in a sharpening of the associated melting peaks in the recorded DSC thermograms (**Figure 4.14** and **Figure 4.15**). In contrast, lower melting points relating to the polyether soft phase decreased slightly with increasing hard phase content but otherwise remained mostly unaffected by changes in the overall polymer composition. The same was found to be true for glass transition points which could be observed at about -68 °C for all synthesized TPUs. This minimal deviation from the glass transition point of pure $PPDO_{2000}$ (T_g = -70°C) confirmed a high degree of phase separation independent of polymer composition.

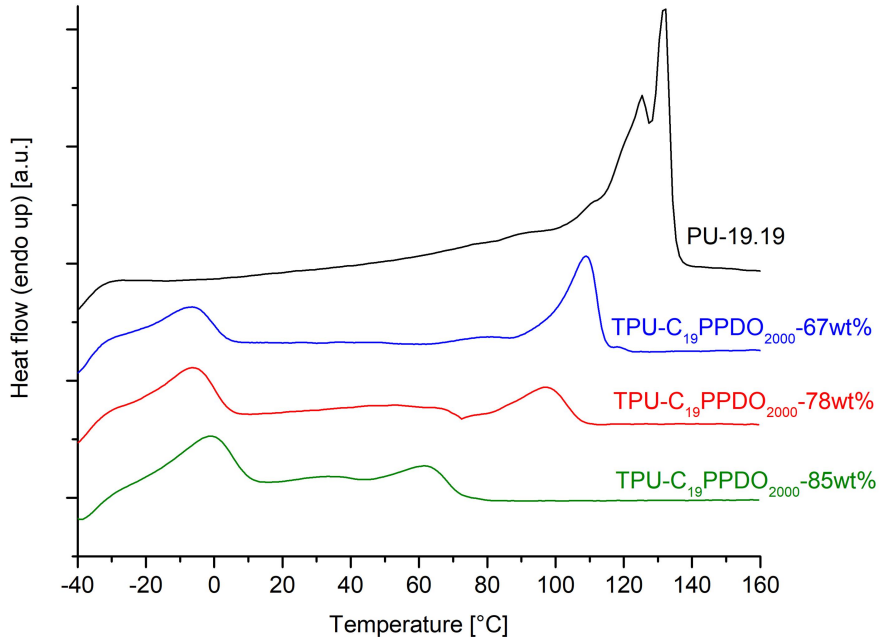

Figure 4.14: DSC thermograms (second heating) of PU-19.19 and polyurethane-polyether copolymers based on C_{19} monomers.

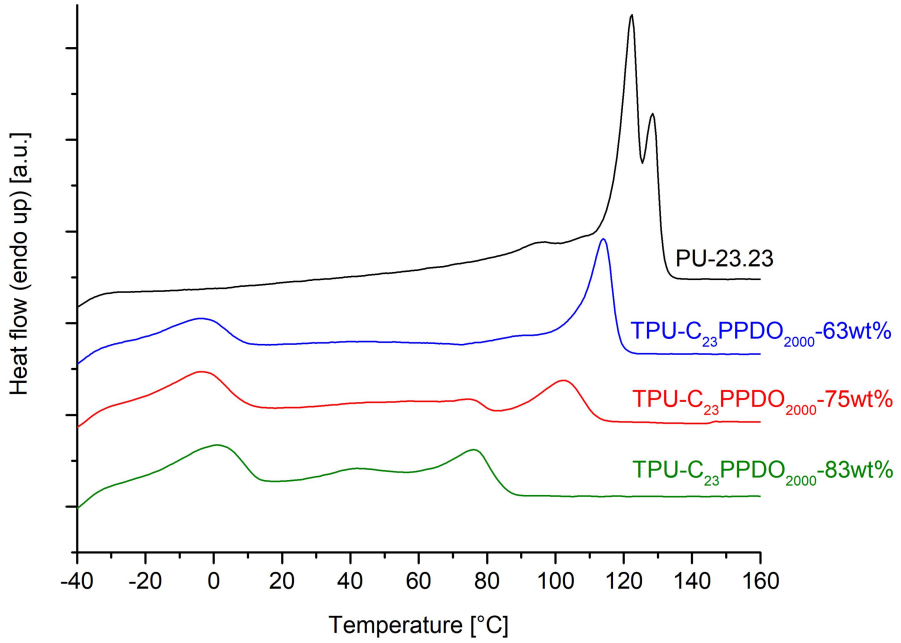

Figure 4.15: DSC thermograms (second heating) of PU-23.23 and polyurethane-polyether copolymers based on C_{23} monomers.

Comparison of the thermal properties of long-chain TPU-$C_{23}PPDO_{2000}$-63wt% with its mid-chain analogue, TPU-$C_{12}PPDO_{2000}$-59wt% (**Table 4.5**, **entry 9**), revealed an increase in the melting point by 13 °C from 116 °C to 129 °C for TPU-$C_{12}PPDO_{2000}$-59wt% (**Figure 4.16**), which can be attributed to the higher concentration of urethane groups and therefore higher hydrogen bond density in TPU-$C_{12}PPDO_{2000}$-59wt% as well as the odd-even effect.

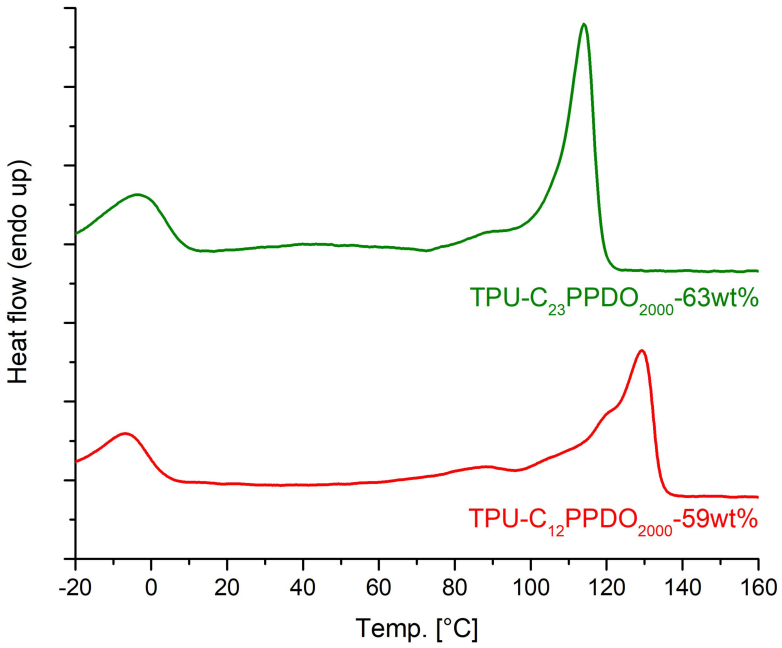

Figure 4.16: DSC thermograms (second heating) of TPU-$C_{23}PPDO_{2000}$-63wt% (green) and its mid-chain analogue, TPU-$C_{12}PPDO_{2000}$-59wt% (red).

4.2.5. Mechanical properties of long-chain thermoplastic polyurethane elastomers

Injection molding was successfully used to prepare dog-bone shaped test specimen suitable to perform tensile tests, thereby proving that all synthesized segmented polyurethane materials can be processed using standard thermoplastic processing techniques. Subsequent tensile tests revealed that all prepared TPUs show ductile behavior and exhibit sufficient elongation at break (> 250 %) to qualify as TPEs, with elongations at break increasing to values up to 470 % with increasing polyether soft phase content (**Table 4.6, entry 1-6**). In addition, segmented TPUs with hard segments based on 1,23-tricosane diisocyanate and 1,23-tricosanediol instead of the corresponding C_{19} monomers generally exhibited a lower elongation at break, except for TPUs with a very high hard phase content,

TPU-C_{19}PPDO$_{2000}$-67wt% and TPU-C_{23}PPDO$_{2000}$-63wt%, which exhibited similar elongations at break within the error margin of the measuring method (**Table 4.6, entry 3** and **6**) (**Figure 4.17**).

Table 4.6: Mechanical properties of poly(urethane-ether) block copolymers based on long- and mid-chain aliphatic polyurethane hard segments.

entry	polymer	Young's modulus [a),b] [MPa]	elongation at break [a),c)] [%]	residual strain [d)] [%]
1	TPU-C_{19}PPDO$_{2000}$-85wt%	17	470	26
2	TPU-C_{19}PPDO$_{2000}$-78wt%	22	450	33
3	TPU-C_{19}PPDO$_{2000}$-67wt%	24	270	31
4	TPU-C_{23}PPDO$_{2000}$-83wt%	21	440	32
5	TPU-C_{23}PPDO$_{2000}$-75wt%	21	270	39
6	TPU-C_{23}PPDO$_{2000}$-63wt%	36	282	37
7	TPU-C_{12}PPDO$_{2000}$-59wt%	39	650	29

a) Tensile tests according to ISO 527/1-2, specimen type 5A prepared by injection molding. b) Crosshead speed 1 mm min^{-1}. c) Crosshead speed 500 mm min^{-1}. d) Determined from cyclic hysteresis experiments after 10 cycles at an elongation of 100 % with a crosshead speed of 50 mm min^{-1}.

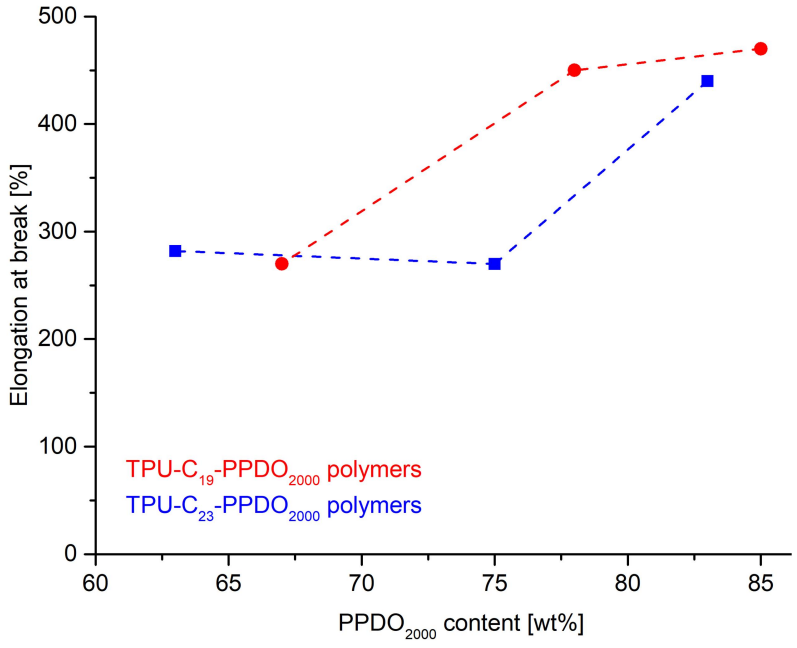

Figure 4.17: Correlation between polymer composition and elongation at break in aliphatic long-chain TPUs.

As expected, Young moduli decreased with increasing content of polyether soft segment for both polymer series, with calculated values for E_t ranging from 17 to 24 MPa for C_{19}-containing TPUs and 21 to 36 MPa (**Table 4.6, entry 1-3**) for C_{23}-containing polymers (**Table 4.6, entry 4-6)** **(Figure 4.18**).

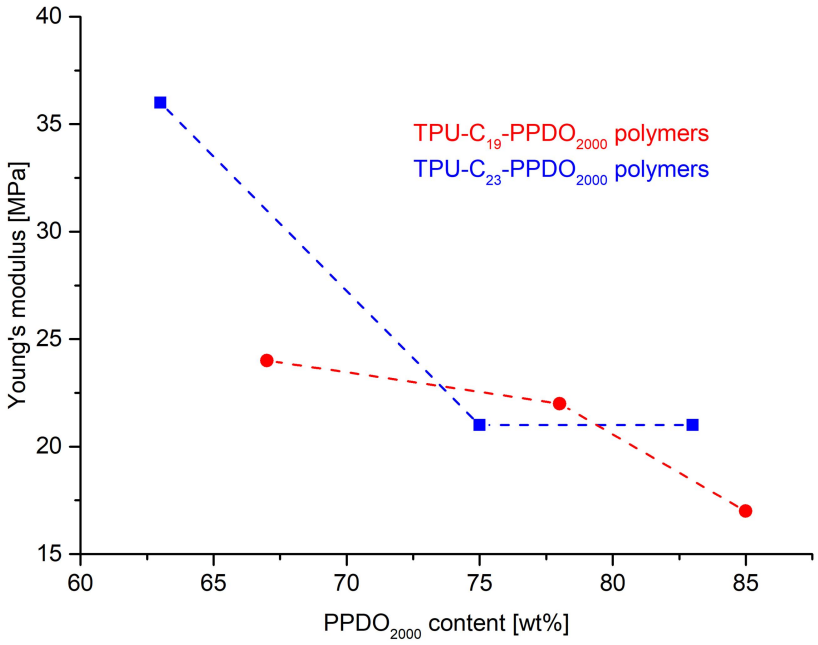

Figure 4.18: Correlation between Young's modulus and polymer composition in aliphatic long-chain TPUs

Comparison of TPU-C_{23}PPDO$_{2000}$-63wt% (**Table 4.6**, **entry 6**) with its mid-chain analog TPU-C_{12}PPDO$_{2000}$-59wt% (**Table 4.6**, **entry 7**) showed that halving the length of the methylene sequences in the PU hard segments has no significant effect on the Young's modulus, with TPU-C_{12}PPDO$_{2000}$-59wt% exhibiting only a slightly higher Young's modulus of 39 MPa than the long-chain TPU-C_{23}PPDO$_{2000}$-63wt% (E_t = 36 MPa). In contrast, the ductility improved drastically, with the elongation at break increasing from 280 % for TPU-C_{23}PPDO$_{2000}$-63wt% to 650 % for TPU-C_{12}PPDO$_{2000}$-59wt% (**Figure 4.19**). This increase in ductility could not be explained with the odd-even effect but has to be attributed to increased hydrogen bond density in the polyurethane hard domains.[41]

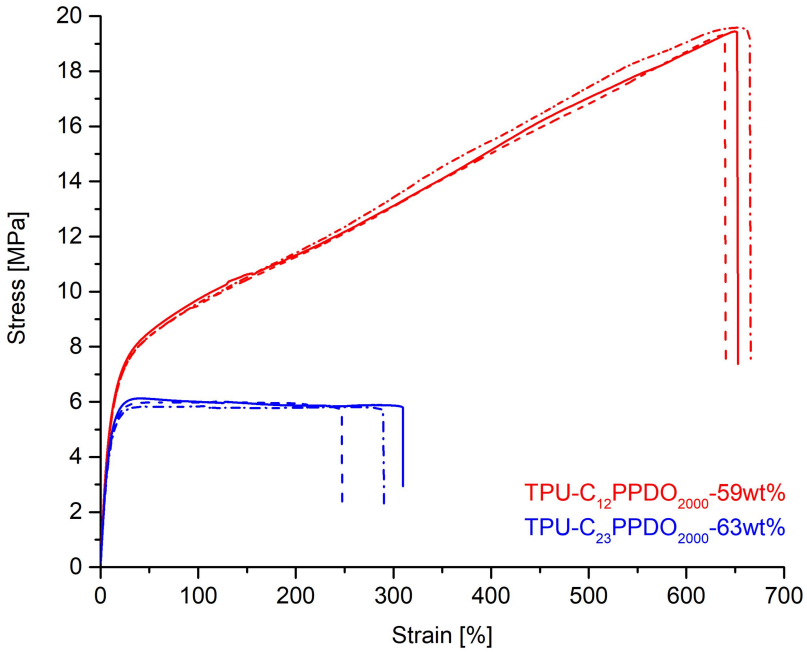

Figure 4.19: Stress-strain curves of long-chain TPU-C_{23}PPDO$_{2000}$-63wt% (blue) and its mid-chain analog TPU-C_{12}PPDO$_{2000}$-59wt% (red).

In order to assess the elastic properties of the polyurethane-polyether copolymers cyclic hysteresis tests were performed. Test specimens were repeatedly exposed to consecutive cycles of loading to a constant strain of 100% and unloading. After the first few cycles, where hysteresis is observed and the residual deformation gradually increases, all TPUs exhibit a virtually constant level of recovery. This behavior is typical of thermoplastic elastomers[1a],[2] and can be ascribed to the adoption of a largely constant structure after an initial change in morphology with alignment of the polymer microstructure.[42] For the segmented polyurethane-polyether copolymers studied here, elastomeric behavior is observed for all synthesized materials and residual strains after 10 cycles range between 26 % and 33 % for C_{19}–based copolymers (**Table 4.6, entry 1-3**) and between 32 % and 39 % for C_{23} copolymers (**Table 4.6, entry 4-6**) (**Figure 4.20**). For both polymer series the observed residual strain differs only slightly with varying content of hard and soft segment, though the highest level of recovery is observed for polymers without a long-chain diol as an additional component contributing to the crystalline phase. Comparison of TPU-C_{23}PPDO$_{2000}$-63wt% with the mid-chain analog TPU-C_{12}PPDO$_{2000}$-59wt% showed that doubling the hydrogen bond density in the hard domains by replacing C_{23} monomer with C_{12} monomers results in improved elastic behavior with a decrease of the observed residual strain from 37 % to 29 % (**Table 4.6, entry 6** and **7**, **Figure 4.21**).

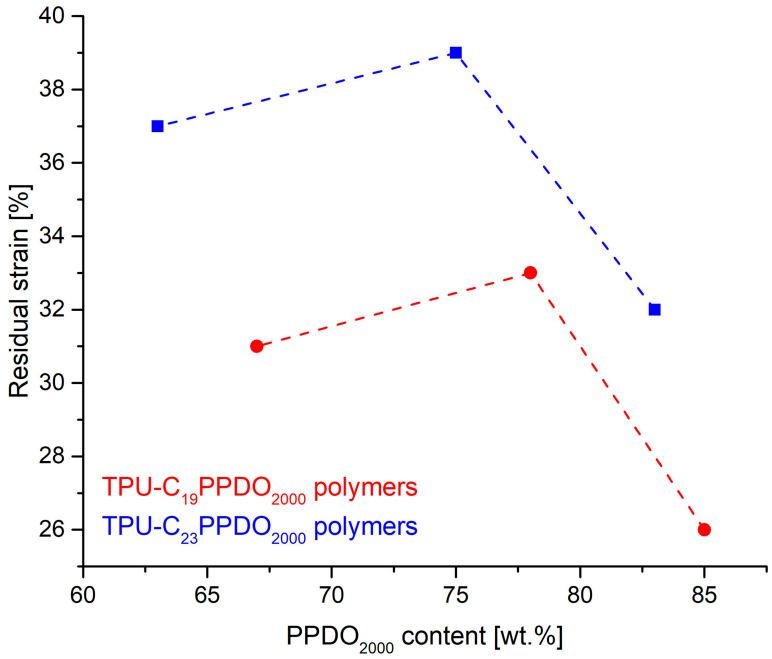

Figure 4.20: Correlation between polymer composition and elastomeric behavior in aliphatic long-chain TPUs (Residual strain given after 10 cycles of cyclic hysteresis testing).

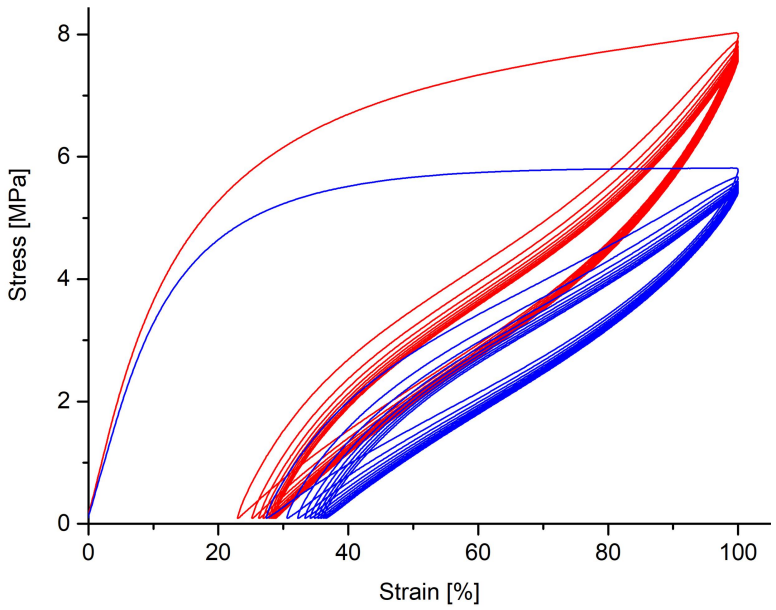

Figure 4.21: Stress–strain curves recorded from cyclic tensile tests with a constant strain of 100 % for TPU-C_{23}PPDO$_{2000}$-63wt% (blue) and its mid-chain analog TPU-C_{12}PPDO$_{2000}$-59wt% (red) (10 cycles displayed).

4.3. Conclusion

In summary, starting from plant-oil derived oleic acid and erucic acid esters, the two novel linear long-chain diisocyanates 1,19-nonadecane diisocyanate and 1,23-tricosane diisocyanate could be successfully synthesized via nucleophilic substitution. Optimization of the reaction conditions and the work-up procedure made it possible to increase the yields to 36 % and 40 % respectively and obtain both monomers on a 1 g scale and in polycondensation grade purity. Polyaddition of these bio-based long-chain diisocyanates and their corresponding long-chain diols with diol-terminated $PPDO_{2000}$ yielded entirely bio-based, transparent polyurethane-polyether copolymers with molecular weights up to $M_n = 5.0 \times 10^4$ g mol^{-1}. The long-chain aliphatic polyurethane hard segments provide physical crosslinking via hydrogen bonding, resulting in melting points reaching values of up to 116 °C and in these thermoplastic materials exhibiting elastomeric behavior, therefore qualifying as thermoplastic elastomers. A particularly high degree of shape recovery was observed if no additional long-chain diol chain extender was incorporated into the material. Analysis of the synthesized materials via FTIR spectroscopy revealed a well-separated microphase morphology and strongly hydrogen bonded hard segments. In addition, comparison to an analogous mid-chain monomer based polyurethane-polyether copolymer showed that employing long-chain aliphatic compounds as monomers for the generation of polyurethane hard segments with a relatively low density of urethane groups and consequently hydrogen bonds resulted in lower melting points and decreased ductility as well as in an decrease of elasticity but promoted phase separation.

4.4. Experimental Section

4.4.1. Materials and general considerations

Unless stated otherwise, all manipulations were carried out under an inert gas atmosphere using standard Schlenk or glovebox techniques. Methylene chloride was distilled from CaH_2. DMF, DMSO, MeCN, and 1,1,2,2-tetrachloroethane were dried over molecular sieves (3 Å). n-Heptane (Emplura® 99 %) was purchased from Merck and methanol (99.8 %) from Sigma-Aldrich. All other solvents were used in technical grade as received. Tetrabromomethane (98 %) and dibutyltin dilaurate (98 %) were purchased from ABCR, triphenylphosphine (99 %) from Acros Organics, potassium cyanate (96 %), silver cyanate (99 %), and 18-crown-6 (>99 %) from Sigma Aldrich, and N,N'-di-2-naphthyl-1,4-phenylenediamine (>96 %) from TCI Europe. Poly(1,3-propanediol) with a number average molecular mass of M_n = 2000 g mol^{-1} was kindly donated by Allessa GmbH and was degassed prior to use. Dimethyl 1,19-nonadecanedioate, diethyl 1,23-tricosanedioate, as well as the corresponding long-chain diols 1,19-nonadecanediol and 1,23-tricosanediol were prepared as described previously (cf. **Chapter 3.4.2**).

NMR spectra were recorded on a Varian Inova 400 and a Bruker Avance 400 spectrometer.^{1}H and ^{13}C chemical shifts were referenced to the solvent signals.

DSC analyses were performed on a Netzsch Phoenix 204 F1 instrument. Melt and crystallization transitions were determined at a heating and cooling rate of 10 K min^{-1} respectively in a temperature range of −50 to 160 °C. All data reported is from second heating cycles. Glass transition points were determined at a heating rate of 30 K min^{-1} in a temperature range of -100 to 160 °C.

Gel permeation chromatography (GPC) measurements were carried out on a Polymer Laboratories PLGPC 50 with two PLgel 5 μm MIXED-C columns in THF at 50 °C against polystyrene standards with refractive index detection or on a Polymer Laboratories 220 instrument equipped with Olexis columns with differential refractive index, viscosity, and light-scattering (15° and 90°) detectors in 1,2,4-trichlorobenzene at 160 °C against linear polyethylene standards.

Tensile testing was performed on dogbone-shaped sample bars (75 × 12.5 × 2 mm^3; ISO 527-2, type 5A) which were prepared using a HAAKE Minijet II (Thermo Scientific) piston injection molder. 0.1 wt.% of N,N'-di-2naphthyl-1,4-phenylenediamine were employed as a stabilizer. After preconditioning the samples overnight, tensile tests were performed on a Zwick 1446 Retroline tC II instrument according to ISO 527 (crosshead speed 500 mm min^{-1}, with a determination of the Young's modulus at a crosshead speed of 1 mm min^{-1}). The Zwick test Xpert software version 11.0

was used to collect and analyze the data. Young's modulus, yield stress, yield strain, tensile stress at break and tensile strain at break were obtained by averaging the data from several test specimens.

Cyclic hysteresis tests were performed on dogbone-shaped sample bars (75 × 12.5 × 2 mm^3; ISO 527-2, type 5A). The test specimens were repeatedly exposed to consecutive cycles of loading and unloading to a constant strain of 100 % with a constant crosshead speed of 50 mm min^{-1}. The recovery was measured by observing the residual strain after 10 cycles.

Attenuated total reflection Fourier transform infrared (ATR-FTIR) spectra were recorded on a PerkinElmer Spectrum100 FTIR Spectrometer equipped with a Universal ATR Sampling Accessory. FTIR scans were collected on injection molded dogbone-shaped sample bars (75 × 12.5 × 2 mm^3; ISO 527-2, type 5A). The frequency range covered was from 4000 to 650 cm^{-1} by averaging 32 scans at a resolution of 2 cm^{-1}.

Wide angle X-Ray diffraction spectra (WAXD) were recorded on a Bruker AXS D8 Advance diffractometer using $CuK_{\alpha 1}$ radiation. Diffraction patterns were recorded in the range 10 to 60 degrees 2θ, at 25 °C. Polymer samples for WAXD were prepared by precipitation from THF.

4.4.2. Monomer synthesis

Synthesis of 1,19-dibromononadecane

The synthesis of 1,19-dibromononadecane was carried out analogous to a reported procedure.[15a] 1,19-Nonadecanediol (11.4 g, 37.9 mmol) and CBr_4 (31.4 g, 94.8 mmol) were suspended in 500 mL methylene chloride and triphenylphosphine (26.9 g, 102.4 mmol) was slowly added as a solid over the course of 30 min. The yellow solution was then heated to 50 °C for 1 h and afterwards stirred overnight at room temperature. Then, 100 mL methanol and 10 mL water were added and the solution stirred for another 10 min. The solvent was then removed to obtain a beige solid, which was dissolved in 200 mL n-pentane and methanol. After extraction with pentane (3 x 200 mL), the combined pentane phases were washed once with 200 ml of water before the solvent was removed to yield the solid off-white crude product. Column chromatography with methylene chloride and subsequent crystallization from ethanol/ethyl acetate (4:1) yielded 14.5 g of the desired product as a white solid (34.0 mmol, 88 %).

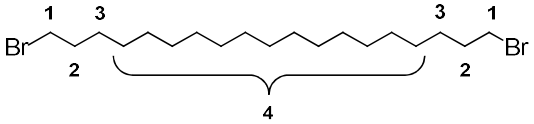

^{1}H NMR ($CDCl_3$, 25 °C, 400 MHz) δ 3.41 (t, $^{3}J_{H-H}$ = 7.0 Hz, 4H, H-1), 1.85 (quint, $^{3}J_{H-H}$ = 7.0 Hz, 4H, H-2), 1.42 (quint, $^{3}J_{H-H}$ = 7.0 Hz, 4H, H-3), 1.35 - 1.21 (m, 26H, H-4) ppm.

^{13}C NMR (101 MHz, 25 °C, $CDCl_3$) δ 34.2 (C-1), 33.0 (C-2), 29.8 - 29.6 (C-4), 28.9 (C-4), 28.3 (C-3) ppm.

Synthesis of 1,23-dibromotricosane

1,23-Dibromonotricosane was synthesized analogous to the procedure described above.[15a] Starting from 1,23-tricosanediol (10 g, 28.0 mmol), the desired product was obtained in a yield of 94 % (12.7 g, 26.3 mmol) as a white solid

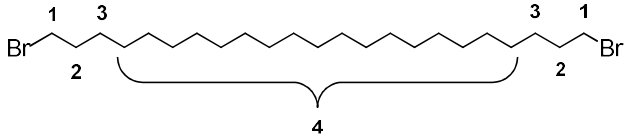

^{1}H NMR ($CDCl_3$, 25 °C, 400 MHz) δ 3.41 (t, $^{3}J_{H-H}$ = 7.0 Hz, 4H, H-1), 1.85 (quint., $^{3}J_{H-H}$ = 7.0 Hz, 4H, H-2), 1.42 (quint, $^{3}J_{H-H}$ = 7.0 Hz, 4H, H-3), 1.35 - 1.21 (m, 34H, H-4) ppm.

^{13}C NMR (101 MHz, 25 °C, $CDCl_3$) δ 34.2 (C-1), 33.0 (C-2), 29.9 - 29.6 (C-4), 28.3 (C-3) ppm.

General procedure for optimization experiments regarding the preparation of 1,19-nonadecane diisocyanate

1,19-Dibromononadecane (1 g, 2.36 mmol) was dissolved in 17 ml of solvent and the solution heated to the desired temperature. An excess of inorganic cyanate salt (5 eq.) was added and the suspension stirred for the desired time. Afterwards, the mixture was cooled down rapidly using a cold water bath. Organic products were extracted with n-heptane (3 x 50 ml) and the combined n-heptane phases were washed with DMF before residual inorganic salts and insoluble polymeric byproducts were removed by filtration over a Whatman filter. Subsequent removal of the solvent yielded the crude product as an off-white, wax-like solid.

Synthesis of 1,19-nonadecane diisocyanate

1,19-Dibromononadecane (3.0 g, 7.0 mmol) was dissolved in 50 ml of DMF and the solution heated to 120 °C. Potassium cyanate (2.9 g, 35.2 mmol, 5 eq.) was added and the resulting suspension stirred at 120 °C for 35 min. After rapid cooling down to room temperature, the reaction mixture was extracted with n-heptane (3 x 100 ml) and the combined n-heptane phases washed with cold water. After drying over $MgSO_4$, filtration and removing of the solvent, the crude product was distilled using a sublimation apparatus with a cold finger (130 °C, 0.06 mbar) to give 860 mg (2.5 mmol, 35 %) of the desired product as a white solid.

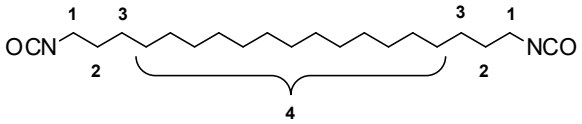

^{1}H NMR ($CDCl_3$, 25 °C, 400 MHz) δ 3.29 (t, $^{3}J_{H\text{-}H}$ = 6.7 Hz, 4H, H-1), 1.61 (quint, $^{3}J_{H\text{-}H}$ = 6.7 Hz, 4H, H-2), 1.41 - 1.33 (m, 4H, H-3), 1.33 – 1.21 (m, 26H, H-4) (cf. **Chapter 4.2.2**, **Figure 4.6**) ppm.
^{13}C NMR (101 MHz, 25 °C, $CDCl_3$) δ 122.1 (NCO), 43.1 (C-1), 31.4 (C-2), 29.8 - 29.6 (C-4), 29.1 (C-4), 26.7 (C-3) ppm.

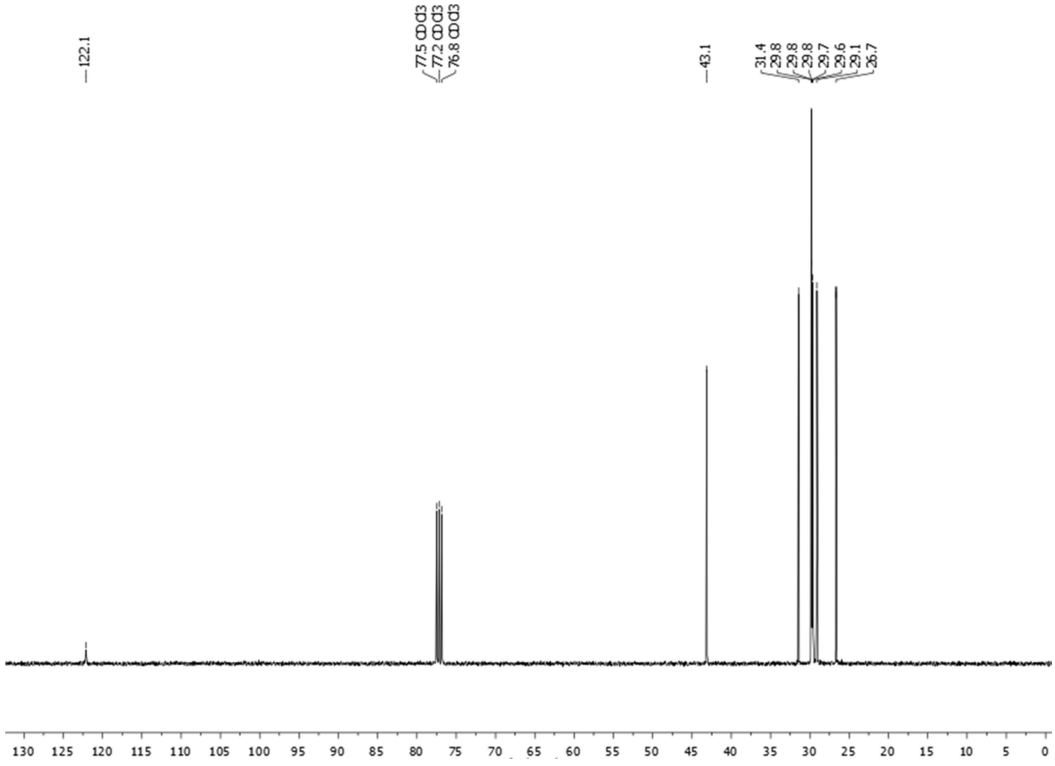

Figure 4.22: ^{13}C NMR spectrum ($CDCl_3$, 25 °C, 101 MHz) of 1,19-nonadecane diisocyanate.

Synthesis of 1,23-tricosane diisocyanate

1,23-Tricosane diisocyanate was prepared analogous to the aforementioned procedure starting from 1,23-dibromotricosane (2.0 g, 4.1 mmol). The desired product was isolated by distillation (140 °C, 0.06 mbar) to yield 672 mg (1.6 mmol, 40 %) of pure 1,23-tricosane diisocyanate as a white solid.

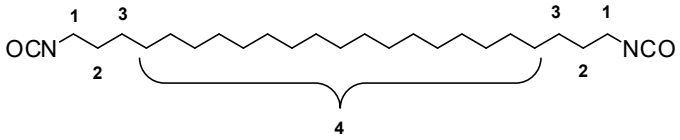

^{1}H NMR ($CDCl_3$, 25 °C, 400 MHz) δ 3.29 (t, $^{3}J_{H-H}$ = 6.7 Hz, 4H, H-1), 1.61 (quint, $^{3}J_{H-H}$ = 6.7 Hz, 4H, H-2), 1.42 – 1.33 (m, 4H, H-3), 1.33 – 1.21 (m, 34H, H-4) ppm.

^{13}C NMR (101 MHz, $CDCl_3$) δ 122.1 (NCO), 43.1 (C-1), 31.4 (C-2), 29.8 - 29.6 (C-4), 29.1 (C-4), 26.7 (C-3) ppm.

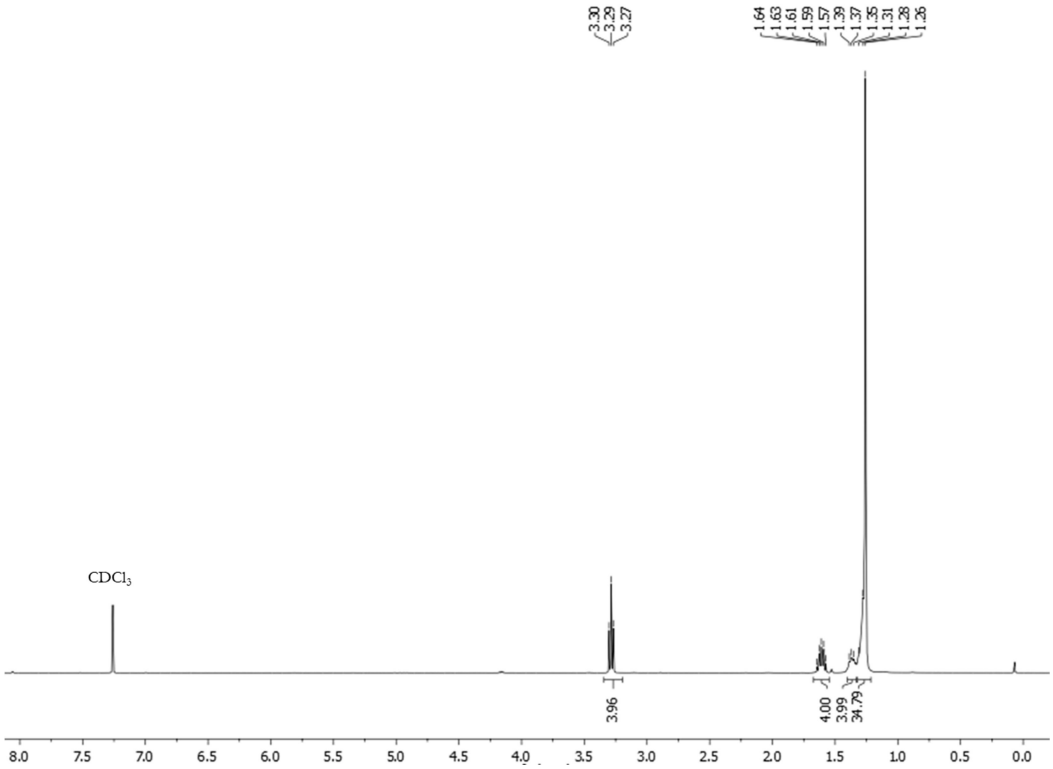

Figure 4.23:^{1}H NMR spectrum ($CDCl_3$, 25 °C, 400 MHz) of 1,23-tricosane diisocyanate.

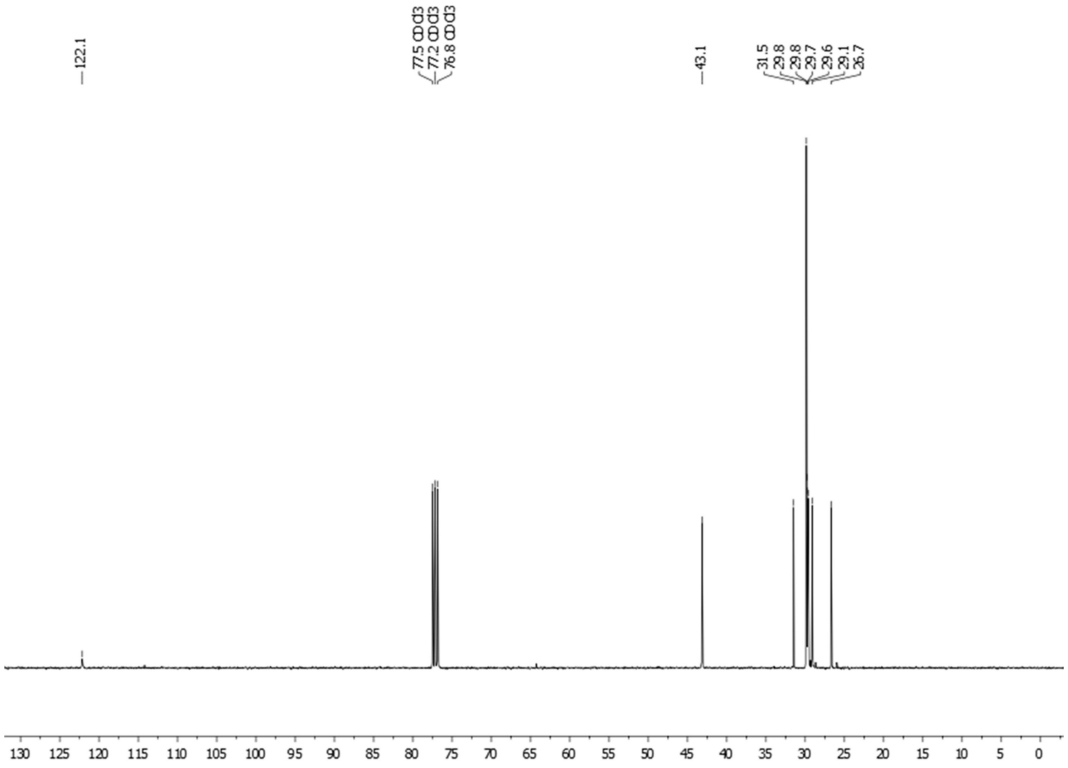

Figure 4.24:[13]C NMR spectrum ($CDCl_3$, 25 °C, 101 MHz) of 1,23-tricosane diisocyanate.

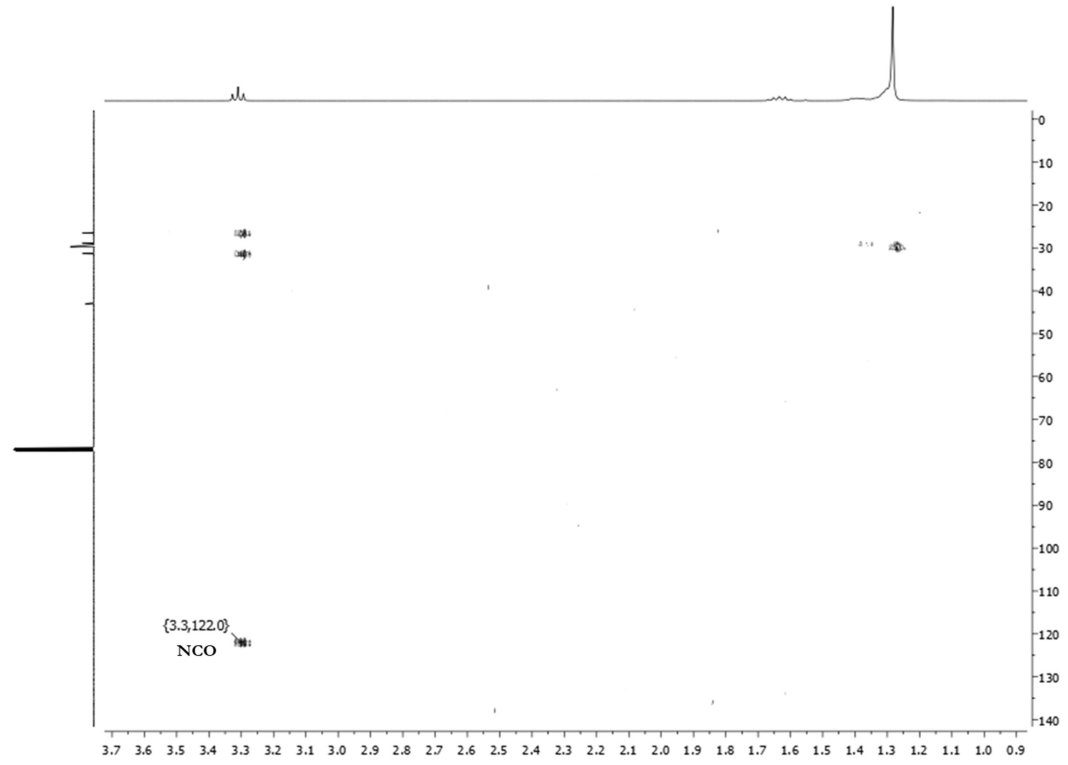

Figure 4.25: [1]H, [13]C HMBC NMR spectrum ($CDCl_3$, 25 °C, 101 MHz) of 1,23-tricosane diisocyanate.

4.4.3. Polymer synthesis

General procedure for solution polyaddition experiments

Freshly distilled α,ω-diisocyanate (2.4 mmol) and the other monomers were weighed in a 100 ml two-neck Schlenk flask equipped with a magnetic stirrer. The mixture was degassed and dissolved in 20 ml of 1,1,2,2-tetrachloroethane or DMF respectively. Then 0.5 mol% of dibutyltin dilaurate were added and the solution was heated to 80 °C using an aluminum block equipped with a thermocouple to control the temperature. After stirring for 24 h, the reaction was stopped by adding 5 ml of dried methanol and stirring the mixture for another 15 min. The polymer was then precipitated by pouring the reaction mixture into methanol. After filtration, the white rubber-like polymer was dried *in vacuo* at 50°C for 48 h. Any remaining solvent residues were removed from the polymer melt by applying vacuum.

4.4.4. Molecular weight determination by ^{1}H NMR spectroscopy

Molecular weights determined from ^{1}H NMR spectra via end group analysis were calculated using the following formula:

$$M_n = DP_n \cdot M_0 = \frac{\int E_4}{\frac{1}{3}\int E_1 + \frac{1}{2}\int E_2 + \frac{1}{2}\int E_3} \cdot M_0$$

The degree of polymerization (DP_n) was defined as the ratio of the signal intensities of the internal methylene group of the fatty acid-derived dicarbamate repeat unit in alpha position to the urethane group (E_4, 3.15 ppm, 2H, **Figure 4.25** and **4.26**: **Signal g**) and the weighted sum of the signals corresponding to possible end groups. These theoretically possible end groups include a methyl carbamate end group (E_1, 3.68 ppm, 3H) formed by the reaction of excess isocyanate groups with methanol at the end of the polymerization procedure. However, in reality only methylene groups adjacent to a terminal hydroxyl group belonging to either the fatty acid-derived diol (E_2, 3.64 ppm, 2H) or a $PPDO_{2000}$ polyether segment (E_3, 3.76 ppm, 2H, **Figure 4.25** and **4.26**: **Signal e**) were visible in the recorded ^{1}H NMR spectra.

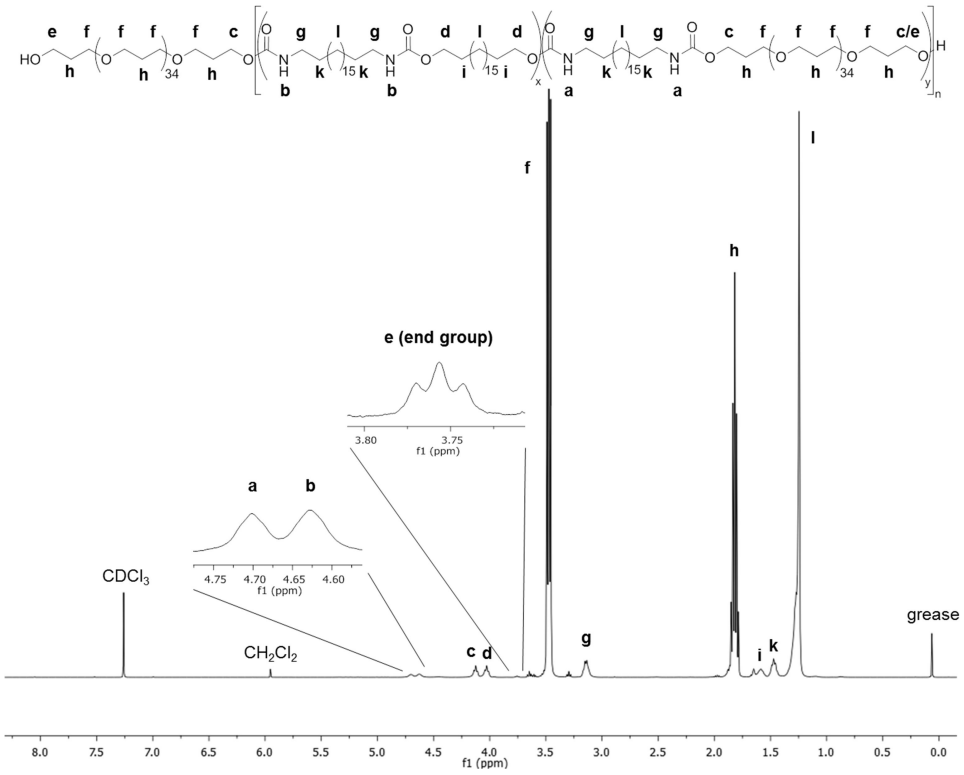

Figure 4.26: ^{1}H NMR spectrum ($CDCl_3$, 400 MHz) of TPU-C_{19}PPDO$_{2000}$-65wt%.

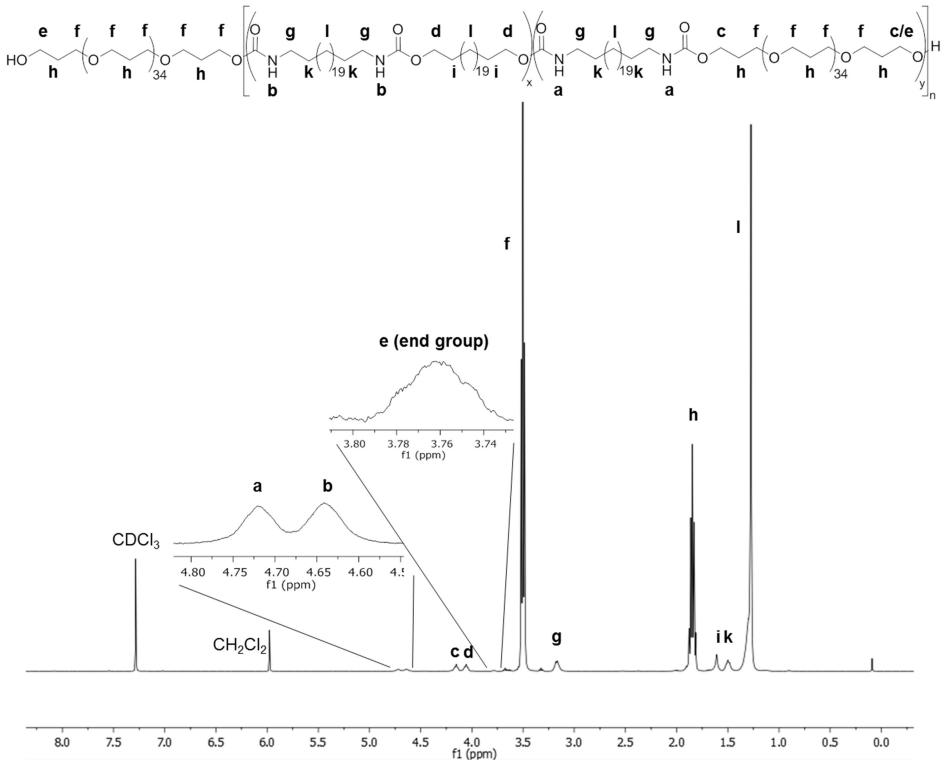

Figure 4.27: ^{1}H NMR spectrum ($CDCl_3$, 400 MHz) of TPU-C_{23}PPDO$_{2000}$-63wt%.

4.4.5. FTIR spectroscopy

Attenuated total reflection Fourier transform infrared (ATR-FTIR) spectra were recorded on a PerkinElmer Spectrum100 FTIR Spectrometer equipped with a Universal ATR Sampling Accessory. FTIR scans were collected on injection molded dogbone-shaped sample bars (75 × 12.5 × 2 mm^3; ISO 527-2, type 5A). The frequency range covered was from 4000 to 650 cm^{-1} by averaging 32 scans at a resolution of 2 cm^{-1}.

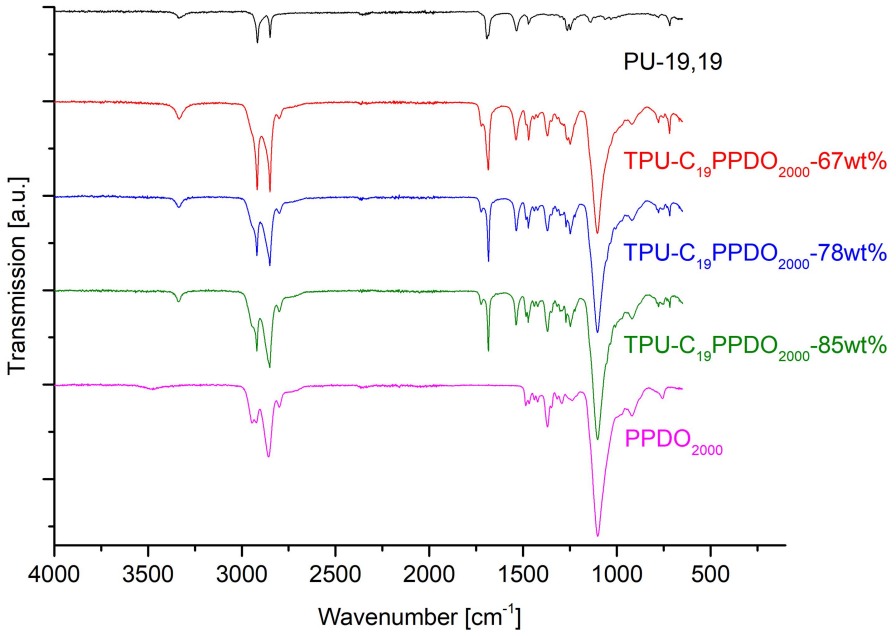

Figure 4.28: FTIR spectra of $PPDO_{2000}$, PU-19.19 and poly(urethane-ether) block copolymers based on long-chain C_{19} monomers.

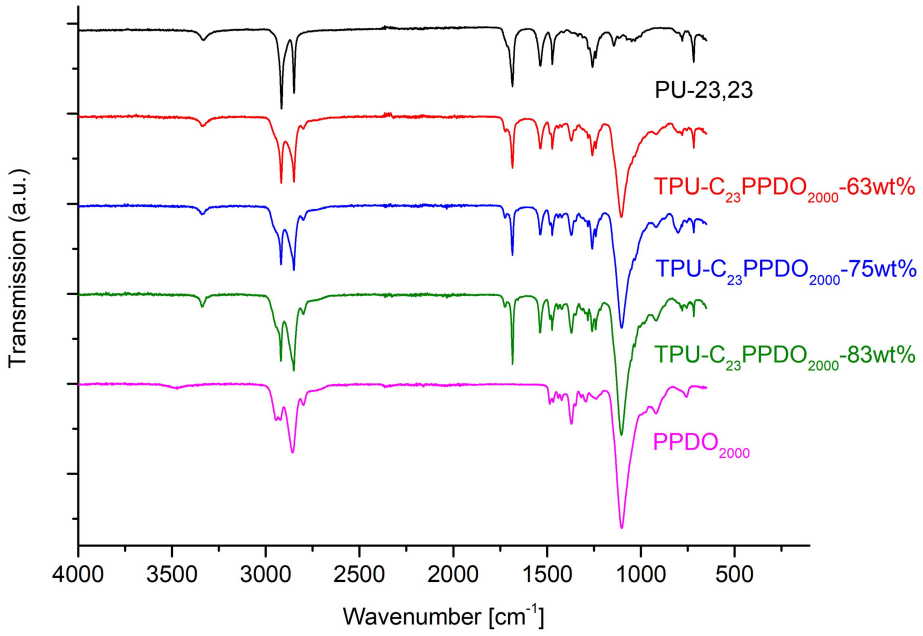

Figure 4.29: FTIR spectra of $PPDO_{2000}$, PU-23.23 and poly(urethane-ether) block copolymers based on long-chain C_{23} monomers.

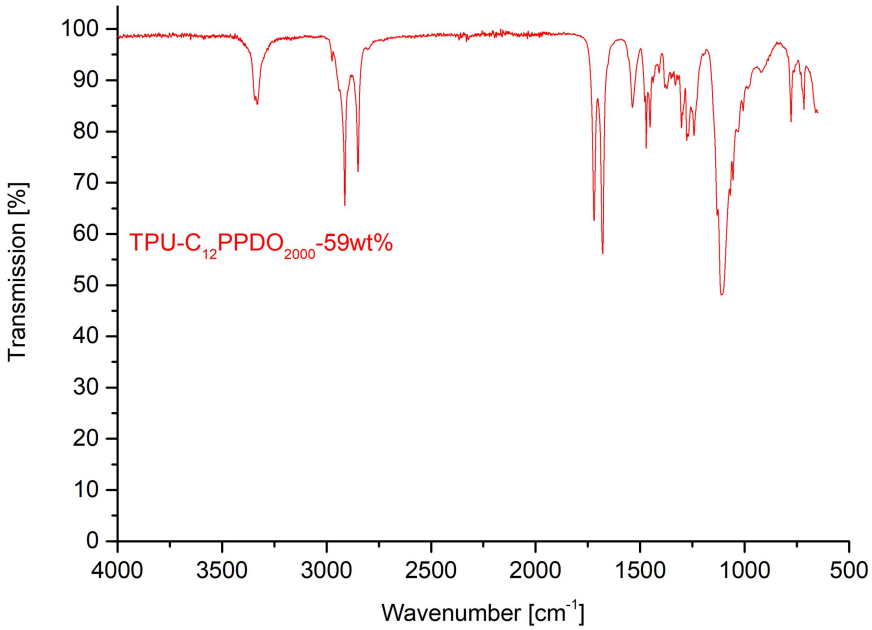

Figure 4.30: FTIR spectra of TPU-$C_{12}PPDO_{2000}$-59wt% based on mid-chain C_{12} monomers.

4.5. References

1. a)Ouhadi, T.; Abdou-Sabet, T.; Wussow, H.-G.; Ryan, L. M.; Plummer, L.; Baumann, F. E.; Lohmar, J.; F, V. H.; Malet, F. L. G. Thermoplastic Elastomers. In *Ullmann's Encyclopedia of Industrial Chemistry*, Gerhartz, W.; Elvers, B., (Eds.), Wiley-VCH: Weinheim, Germany, **2000**, pp 1-40; b)Drobny, J. G., *Handbook of Thermoplastic Elastomers*. William Andrew Publishing: Norwich, New York, **2007**.
2. Holden, G.; Kricheldorf, H. R.; Quirk, R. P., *Thermoplastic Elastomers*. Hanser: Munich, Germany, **2004**.
3. a)Polyurethane elastomers. Petrović, Z. S.; Ferguson, J. *Progress in Polymer Science*, **1991,** *16* (5), 695-836; b)Synthesis methods, chemical structures and phase structures of linear polyurethanes. Properties and applications of linear polyurethanes in polyurethane elastomers, copolymers and ionomers. Król, P. *Progress in materials science*, **2007,** *52* (6), 915-1015; c)The structure, microphase-separated morphology, and property of polyurethanes and polyureas. He, Y.; Xie, D.; Zhang, X. *Journal of Materials Science*, **2014,** *49* (21), 7339-7352.
4. Thermal stability and flame retardancy of polyurethanes. Chattopadhyay, D.; Webster, D. C. *Progress in Polymer Science*, **2009,** *34* (10), 1068-1133.
5. a)Randall, D.; Lee, S., *The Polyurethanes Book*. Wiley VCH: Weinheim, Germany, **2003**; b)Hepburn, C., *Polyurethane Elastomers*. Springer: Heidelberg, Germany, **2012**.
6. Modification of nylon 66 with diisocyanates and diacid chlorides. I. Chemical reaction. Perry, E.; Savory, J. *Journal of applied polymer science*, **1967,** *11* (12), 2473-2483.
7. a)Syntheses of Many Membered Cyclic Ureas. IV. Syntheses of Hendecamethylene-, Tridecamethylene-, and Pentadecamethylene-diisocyanate. Syntheses of 14-, 16- and 18-Membered Cyclic Ureas by the Reaction of these Diisocyanates with Water. Iwakura, Y.; Uno, K. *Nippon Kagaku Zasshi*, **1957,** *78* (10), 1511-1516; b)Syntheses of Many Membered Cyclic Ureas. III. Syntheses of Dodecamethylene-, Tetradecamethylene-and Hexadecamethylene-diisocyanate. Syntheses of 15-, 17-, 19-Membered Cyclic Ureas by the Reaction of these Diisocyanates with Water. Iwakura, Y.; Uno, K. *Nippon Kagaku Zasshi*, **1957,** *78* (10), 1507-1510.
8. Long-chain aliphatic polymers to bridge the gap between semicrystalline polyolefins and traditional polycondensates. Stempfle, F.; Ortmann, P.; Mecking, S. *Chemical reviews*, **2016,** *116* (7), 4597-4641.

9. a)Lipid biotechnology: Industrially relevant production processes. Schörken, U.; Kempers, P. *European Journal of Lipid Science and Technology*, **2009,** *111* (7), 627-645; b)Biocatalytic and fermentative production of α, ω-bifunctional polymer precursors. Schaffer, S.; Haas, T. *Organic Process Research & Development*, **2014,** *18* (6), 752-766; c)Biosynthesis of Monomers for Plastics from Renewable Oils. Lu, W.; Ness, J. E.; Xie, W.; Zhang, X.; Minshull, J.; Gross, R. A. *Journal of the American Chemical Society*, **2010,** *132* (43), 15451–15455.
10. a)High turnover numbers with ruthenium-based metathesis catalysts. Dinger, M. B.; Mol, J. C. *Advanced Synthesis & Catalysis*, **2002,** *344* (6-7), 671-677; b)Metathesis of unsaturated fatty acids: Synthesis of long-chain unsaturated α, ω-dicarboxylic acids. Ngo, H. L.; Jones, K.; Foglia, T. A. *Journal of the American Oil Chemists' Society*, **2006,** *83* (7), 629-634.
11. a)Dicarboxylic acid esters from the carbonylation of unsaturated esters under mild conditions. Jiménez-Rodriguez, C.; Eastham, G. R.; Cole-Hamilton, D. J. *Inorganic Chemistry Communications*, **2005,** *8* (10), 878-881; b)Mechanistic features of isomerizing alkoxycarbonylation of methyl oleate. Roesle, P.; Dürr, C. J.; Möller, H. M.; Cavallo, L.; Caporaso, L.; Mecking, S. *Journal of the American Chemical Society*, **2012,** *134* (42), 17696-17703.
12. Polymer precursors from catalytic reactions of natural oils. Furst, M. R.; Le Goff, R.; Quinzler, D.; Mecking, S.; Botting, C. H.; Cole-Hamilton, D. J. *Green Chemistry*, **2012,** *14* (2), 472-477.
13. α, ω-Functionalized C_{19} Monomers. Walther, G.; Deutsch, J.; Martin, A.; Baumann, F. E.; Fridag, D.; Franke, R.; Köckritz, A. *ChemSusChem*, **2011,** *4* (8), 1052-1054.
14. Long-chain linear C_{19} and C_{23} monomers and polycondensates from unsaturated fatty acid esters. Stempfle, F.; Quinzler, D.; Heckler, I.; Mecking, S. *Macromolecules*, **2011,** *44* (11), 4159-4166.
15. a)Synthetic polyester from algae oil. Roesle, P.; Stempfle, F.; Hess, S. K.; Zimmerer, J.; Río Bártulos, C.; Lepetit, B.; Eckert, A.; Kroth, P. G.; Mecking, S. *Angewandte Chemie International Edition*, **2014,** *53* (26), 6800-6804; b)Valorization of unconventional lipids from microalgae or tall oil via a selective dual catalysis one-pot approach. Hess, S. K.; Schunck, N. S.; Goldbach, V.; Ewe, D.; Kroth, P. G.; Mecking, S. *Journal of the American Chemical Society*, **2017,** *139* (38), 13487-13491; c)Production of chemicals from microalgae lipids–status and perspectives. Hess, S. K.; Lepetit, B.; Kroth, P. G.; Mecking, S. *European Journal of Lipid Science and Technology*, **2018,** *120* (1), 1700152.

16. Renewable Non-Isocyanate Based Thermoplastic Polyurethanes via Polycondensation of Dimethyl Carbamate Monomers with Diols. Unverferth, M.; Kreye, O.; Prohammer, A.; Meier, M. A. *Macromolecular rapid communications*, **2013,** *34* (19), 1569-1574.
17. Novel long chain unsaturated diisocyanate from fatty acid: synthesis, characterization, and application in bio-based polyurethane. Hojabri, L.; Kong, X.; Narine, S. S. *Journal of Polymer Science Part A: Polymer Chemistry*, **2010,** *48* (15), 3302-3310.
18. a)Plant-oil-based polyamides and polyurethanes: Toward sustainable nitrogen-containing thermoplastic materials. Meier, M. A. *Macromolecular rapid communications*, **2019,** *40* (1), 1800524; b)Sustainable routes to polyurethane precursors. Kreye, O.; Mutlu, H.; Meier, M. A. *Green Chemistry*, **2013,** *15* (6), 1431-1455.
19. Chemistry of the production of organic isocyanates. Twitchett, H. *Chemical Society Reviews*, **1974,** *3* (2), 209-230.
20. *Preparation of organic isocyanates*. Schaeffer, W. D. (Union Oil Company of California), U. S. Patent 3,017,420, **1962**.
21. New synthesis of amino acids from halogenated carboxylic esters. Effenberger, F.; Drauz, K. *Angewandte Chemie International Edition*, **1979,** *18* (6), 474-476.
22. Novel fatty acid based di-isocyanates towards the synthesis of thermoplastic polyurethanes. More, A. S.; Lebarbé, T.; Maisonneuve, L.; Gadenne, B.; Alfos, C.; Cramail, H. *European Polymer Journal*, **2013,** *49* (4), 823-833.
23. A fully bio-based waterborne polyurethane dispersion from vegetable oils: From synthesis of precursors by thiol-ene reaction to study of final material. Fu, C.; Zheng, Z.; Yang, Z.; Chen, Y.; Shen, L. *Progress in Organic Coatings*, **2014,** *77* (1), 53-60.
24. Long-chain aliphatic polyesters from plant oils for injection molding, film extrusion and electrospinning. Stempfle, F.; Ritter, B. S.; Mülhaupt, R.; Mecking, S. *Green Chemistry*, **2014,** *16* (4), 2008-2014.
25. a)Linear semicrystalline polyesters from fatty acids by complete feedstock molecule utilization. Quinzler, D.; Mecking, S. *Angewandte Chemie*, **2010,** *122* (25), 4402-4404; b)Linear semicrystalline polyesters from fatty acids by complete feedstock molecule utilization. Quinzler, D.; Mecking, S. *Angewandte Chemie International Edition*, **2010,** *49* (25), 4306-4308.
26. Chemistry of naked anions. III. Reactions of the 18-crown-6 complex of potassium cyanide with organic substrates in aprotic organic solvents. Cook, F. L.; Bowers, C. W.; Liotta, C. L. *The Journal of Organic Chemistry*, **1974,** *39* (23), 3416-3418.

27. Smith, M. B.; March, J., *March's Advanced Organic Chemistry: Reactions, Mechanisms, and Structure*. 6 ed.; Wiley VCH: Hoboken, New Jersey, USA, **2007**.

28. Adam, N.; Avar, G.; Blankenheim, H.; Friederichs, W.; Giersig, M.; Weigand, E.; Halfmann, M.; Wittbecker, F.-W.; Larimer, D.-R.; Maier, U.; Meyer-Ahrens, S.; Noble, K.-L.; Wussow, H.-G. Polyurethanes. In *Ullmann's Encyclopedia of Industrial Chemistry*, Gerhartz, W.; Elvers, B., (Eds.), Wiley-VCH: Weinheim, **2000**.

29. a)Properties of polyether-polyurethane block copolymers: effects of hard segment length distribution. Miller, J. A.; Lin, S. B.; Hwang, K. K.; Wu, K.; Gibson, P.; Cooper, S. L. *Macromolecules*, **1985,** *18* (1), 32-44; b)Structure property studies of polyester- and polyether-based MDI–BD segmented polyurethanes: Effect of one- vs. two- stage polymerization conditions. Abouzahr, S.; Wilkes, G. L. *Journal of applied polymer science*, **1984,** *29* (9), 2695-2711.

30. Fundamental principles of condensation polymerization. Flory, P. J. *Chemical reviews*, **1946,** *39* (1), 137-197.

31. Überwachung der Produkteigenschatten während der Herstellung linearer Polyurethanelastomere. Maass, H.-J.; Wiegleb, K.; Michalke, K.; Eberhardt, P.; Techritz, K. *Plaste und Kautschuk*, **1987,** *34* (7), 251-254.

32. a)Morphology control of segmented polyurethanes by crystallization of hard and soft segments. Hood, M. A.; Wang, B.; Sands, J. M.; La Scala, J. J.; Beyer, F. L.; Li, C. Y. *Polymer*, **2010,** *51* (10), 2191-2198; b)FTIR investigation of the influence of diisocyanate symmetry on the morphology development in model segmented polyurethanes. Yilgor, I.; Yilgor, E.; Guler, I. G.; Ward, T. C.; Wilkes, G. L. *Polymer*, **2006,** *47* (11), 4105-4114.

33. a)A comparison of phase organization of model segmented polyurethanes with different intersegment compatibilities. Hernandez, R.; Weksler, J.; Padsalgikar, A.; Choi, T.; Angelo, E.; Lin, J.; Xu, L.-C.; Siedlecki, C. A.; Runt, J. *Macromolecules*, **2008,** *41* (24), 9767-9776; b)Critical parameters in designing segmented polyurethanes and their effect on morphology and properties: A comprehensive review. Yilgör, I.; Yilgör, E.; Wilkes, G. L. *Polymer*, **2015,** *58*, A1-A36.

34. a)Long-spaced aliphatic polyesters. Ortmann, P.; Mecking, S. *Macromolecules*, **2013,** *46* (18), 7213-7218; b)Aliphatic long-chain C_{20} polyesters from olefin metathesis. Trzaskowski, J.; Quinzler, D.; Bährle, C.; Mecking, S. *Macromolecular rapid communications*, **2011,** *32* (17), 1352-1356; c)Encoding crystal microstructure and chain folding in the chemical structure of

synthetic polymers. De Ten Hove, C. L. F.; Penelle, J.; Ivanov, D. A.; Jonas, A. M. *Nature materials*, **2004,** *3* (1), 33-37.

35. a)Structural studies on linear polyurethanes. II. Crystal and molecular structures of aliphatic polyurethanes from trimethylene diisocyanate, and tetra-and hexa-methylene glycols. Saito, Y.; Hara, K.; Kinoshita, S. *Polymer Journal*, **1982,** *14* (1), 19-31; b)Influence of hydrogen bonding on the crystallization behavior of semicrystalline polyurethanes. McKiernan, R. L.; Heintz, A. M.; Hsu, S. L.; Atkins, E. D.; Penelle, J.; Gido, S. P. *Macromolecules*, **2002,** *35* (18), 6970-6974; c)Crystallization behavior of strongly interacting chains. Heintz, A. M.; McKiernan, R. L.; Gido, S. P.; Penelle, J.; Hsu, S. L.; Sasaki, S.; Takahara, A.; Kajiyama, T. *Macromolecules*, **2002,** *35* (8), 3117-3125.
36. The crystal structure of long-chain normal paraffin hydrocarbons. The "shape" of the< CH2 group. Bunn, C. W. *Transactions of the Faraday Society*, **1939,** *35*, 482-491.
37. The crystal structures of two polyamides ('nylons'). Bunn, C. W.; Garner, E.; Bragg, W. L. *Proceedings of the Royal Society of London. Series A. Mathematical and Physical Sciences*, **1947,** *189* (1016), 39-68.
38. Synthesis and characterization of polyethylene-like polyurethanes derived from long-chain, aliphatic α, ω-diols. McKiernan, R. L.; Gido, S. P.; Penelle, J. *Polymer*, **2002,** *43* (10), 3007-3017.
39. Acyclic diene metathesis (ADMET) polymerization. Synthesis of perfectly linear polyethylene. O'Gara, J. E.; Wagener, K. B.; Hahn, S. F. *Die Makromolekulare Chemie, Rapid Communications*, **1993,** *14* (10), 657-662.
40. Synthesis and characterization of nylon 18.18 and nylon 18 adamantane. Bennett, C.; Kaya, E.; Sikes, A. M.; Jarrett, W. L.; Mathias, L. J. *Journal of Polymer Science Part A: Polymer Chemistry*, **2009,** *47* (17), 4409-4419.
41. Fatty acid-derived diisocyanate and biobased polyurethane produced from vegetable oil: synthesis, polymerization, and characterization. Hojabri, L.; Kong, X.; Narine, S. S. *Biomacromolecules*, **2009,** *10* (4), 884-891.
42. NMR investigations of in-situ stretched block copolymers of poly (butylene terephthalate) and poly (tetramethylene oxide). Schmidt, A.; Veeman, W. S.; Litvinov, V. M.; Gabriëlse, W. *Macromolecules*, **1998,** *31* (5), 1652-1660.

5. Thermoplastic Polyamide Elastomers Based on Long-Chain Aliphatic Polyamide Hard Segments

5.1. Introduction

Thermoplastic polyamide elastomers (TPAs) are a group of segmented thermoplastic elastomers based on typically aliphatic polyamide hard segments that, depending on the exact chemical composition of the employed soft and hard blocks, can be further divided into poly(ester amide)s (PEAs), poly(ester-*b*-ether-*b*-amide)s (PEEAs), poly(carbonate ester amides (PCEAs), and poly(ether-*b*-amide)s (PEBAs).[1],[2] Physical crosslinking in in these materials is provided by the formation of strong hydrogen bonds between amide groups of the glassy or semi-crystalline polyamide hard domains, while the amorphous polyether, polycarbonate, and/or polyester soft segments generate a continuous soft matrix, thereby imparting flexibility and elastomeric properties to the material.[1] For PEBAs and PEEAs, the continuous soft matrix is typically comprised of a polyether macrodiol like poly(ethylene glycol) (PEG), poly(propylene glycol) (PPG), or poly(tetramethylene glycol) (PTMG)[2a],[3] (M_n = 400 to 3000 g mol^{-1})[1],[4] which is linked to the carboxylic acid-terminated aliphatic polyamide hard blocks (M_n = 800 to 5000 g mol^{-1})[1],[4] via the formation of ester groups.[1],[2],[5],[6] PEEAs additionally contain short polyester sequences that affect the morphology of the final product. Depending on the chemical structure, block length, and resulting degree of solubility of these polyester segments in the aliphatic or aromatic polyamide hard phase and/or the polyether soft phase, this third type of block can help to stabilize the biphasic morphology of the PEEA or generate a separate third polyester phase, thereby creating a more complex overall morphology, though very short oligoester segments generally tend to remain (at least partly) dissolved in the polyether soft matrix independent on whether they are based on an aromatic or aliphatic dicarboxylic acid (**Figure 5.1**).[2b],[6]Polyamide blocks employed as hard segments are typically aliphatic and most commonly comprised of short PA-6,[2a],[7] PA-6.6,[2a] PA-11,[2a],[8] or PA-12[2a] sequences, though copolyamides like PA-10,12,[2a],[9] of different short- or mid-chain dicarboxylic acids and diamines as well as partly aromatic polyaramid and polyterepthalamide[6] sequences are also known to be suitable to serve as crystallizable polyamide hard segments.

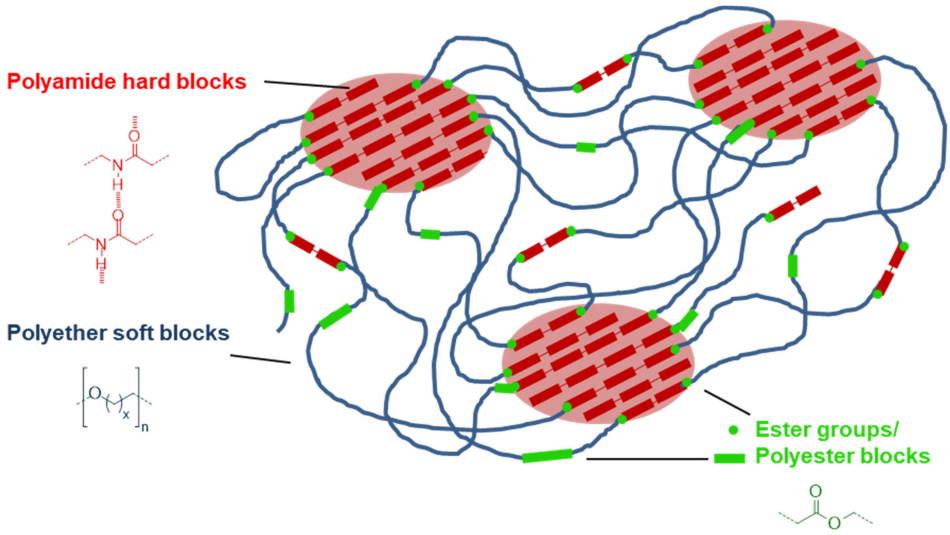

Figure 5.1: Schematic representation of the morphology of a segmented thermoplastic poly(ester-*b*-ether-*b*-amide) terpolymer (PEEA) with polyester blocks (partly) soluble in the polyether soft matrix.

Compared to other types of segmented TPEs, the synthesis of TPAs like PEBAs and PEEAs differs in so far as it typically requires not only the generation of the namesake amide groups to form polyamide hard blocks but also the generation of ester groups to link the different types of hard and soft blocks together and, in case of PEEAs, produce additional polyester segments. Consequently, the most commonly employed synthesis approaches involve two- or even three-step polycondensation procedures comprised of a polyamidation and at least one (trans-)esterification step (**Scheme 5.1**). For TPAs based on A_2+B_2-type polyamide hard segments, in the first step the diamine reacts with an excess of the dicarboxylic acid in a melt polyamidation reaction to form a dicarboxylic-acid terminated polyamide prepolymer (M_n = 800 - 5000 g mol^{-1})[1],[4] (**Scheme 5.1, step 1)** which, in the second step, undergoes a melt polycondensation with the polyether macrodiol (M_n = 400 = 3000 g mol^{-1})[1],[4] at high temperatures and low pressure to generate a segmented multiblock PEBA copolymer (**Scheme 5.1, step 2)**.[10],[11],[12] For the synthesis of PEEAs, an additional dicarboxylic acid and diol chain extender can be added to the reaction mixture during this esterification step to simultaneously introduce polyester blocks into the copolymer and produce a segmented poly(ester-*b*-ether-*b*-amide) terpolymer. Though alternatively, a third dedicated transesterification step can be added to the overall procedure(**Scheme 5.1, step 3)**.[2b] In order to facilitate the formation of ester linkages, catalysts like titanium alkoxides are often added to the reaction mixture during the esterification and/or transesterification step.[13]

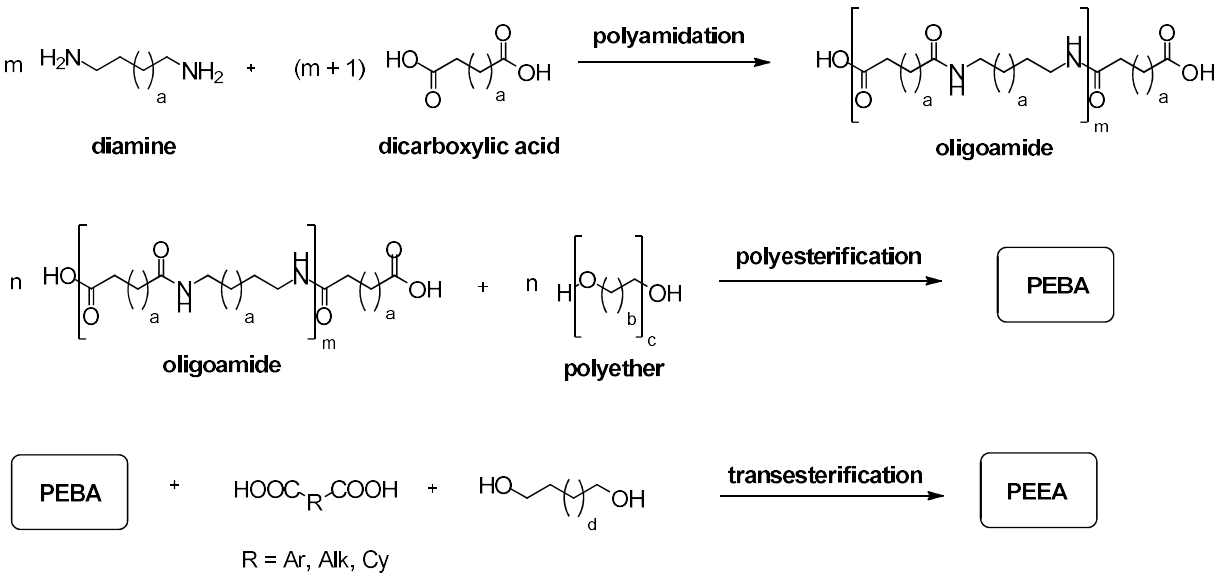

Scheme 5.1: Schematic representation of the multi-step synthesis of PEBAs and PEEAs.

Compared to similar TPUs and TPCs, TPAs generally possess significantly higher melting points due to the high polarity and density of the amide groups present in the polyamide hard segments resulting in the formation of a vast number of very strong hydrogen bonds in the final product.[1],[2a],[4] TPAs in general are also known for their excellent low-temperature flexibility, easy processability, lightweight, chemical resistance, as well as good thermal stability and mechanical properties, which put them in the upper range of quality among TPEs.[2a],[6] Accordingly, TPAs find application in such diverse areas as athletic footwear,[1],[5] small-diameter medical tubing,[5],[14] seals and pneumatic hoses in the automotive and transportation industry,[1],[2a],[5] gas-separation membranes,[5],[15] breathable films,[5],[16] and permanent antistatic agents.[5],[17] However, the polar nature of commonly employed short-chain aliphatic polyamides like PA-6 or PA-6.6 also increases the hydrophilicity of the final product, especially if the elastomeric soft phase is based on a comparably hydrophilic polyether like PEG. As a result, many commercially available PEBAs and PEEAs exhibit an increased tendency to absorb water, a characteristic that can negatively impact other material properties like the Young's modulus and tensile strength.[2a],[18],[19] However, thanks to the development of new catalytic methods like isomerizing alkoxycarbonylation,[20] long-chain α,ω- dicarboxylic acids and diamines have recently become available from plant oils, thereby providing access to novel long-chain aliphatic polyamides with reduced amide group density and overall polarity[21],[22] and opening up the possibility to synthesize a new type of renewable long-chain TPAs with a new set of material properties.

5.2. Results and Discussion

5.2.1. Synthesis of long-chain aliphatic α,ω-diamines

Although linear aliphatic α,ω-diamines like hexamethylene-1,6-diamine are produced on a large industrial scale, the selective synthesis of this type of polycondensation monomers remains a challenge as terminal primary amine groups tend to be highly reactive and commonly employed synthesis routes are prone to side reactions. For example, the catalytic hydrogenation of hexamethylene-1,6-dinitrile, as it is performed in the chemical industry, to produce hexamethylene-1,6-diamine also always results in the formation of secondary amines as a side product.[23] In regards to the preparation of long-chain aliphatic α,ω-diamines from plant oils, this is especially problematic as the removal of secondary amine and nitrile side products to isolate the desired long-chain compounds in polycondensation grade purity has proven to be difficult or outright impossible in the past.[24],[25] In addition, the classic dinitrile route as described for hexamethylene-1,6-diamine has been shown to be an impractical approach due to solubility issues associated with linear long-chain α,ω-dinitriles.[26] Consequently, alternative synthesis routes have been explored in the past. This includes the direct amination of 1,19-nonadecanediol and 1,23-tricosanediol initiated by a ruthenium pincer complex to generate 1,19-nonadecane diamine as well as 1,23-tricosane diamine on a laboratory scale.[27],[28] However, this approach requires elaborate equipment and even under optimized reaction conditions yields a product that typically contains around 5 % of nitrile side products that are impossible to separate from the desired diamine.[24] As an alternative, linear long-chain α,ω-diamines can also be generated via a multistep synthesis route ending with the heterogeneous catalytic hydrogenation of the corresponding linear long-chain α,ω-diazides over palladium on charcoal (Pd/C) (**Scheme 5.2**).[21],[26],[29] However, though this approach has been used to synthesize 1,19-nonadecane diamine and 1,23-tricosane diamine in polymerization grade purity in the past,[21],[26] more recent results suggest that this approach is also highly susceptible to the formation of the aforementioned impossible to remove side products,[25] warranting further investigation especially in regards to the upscaling of the reaction.

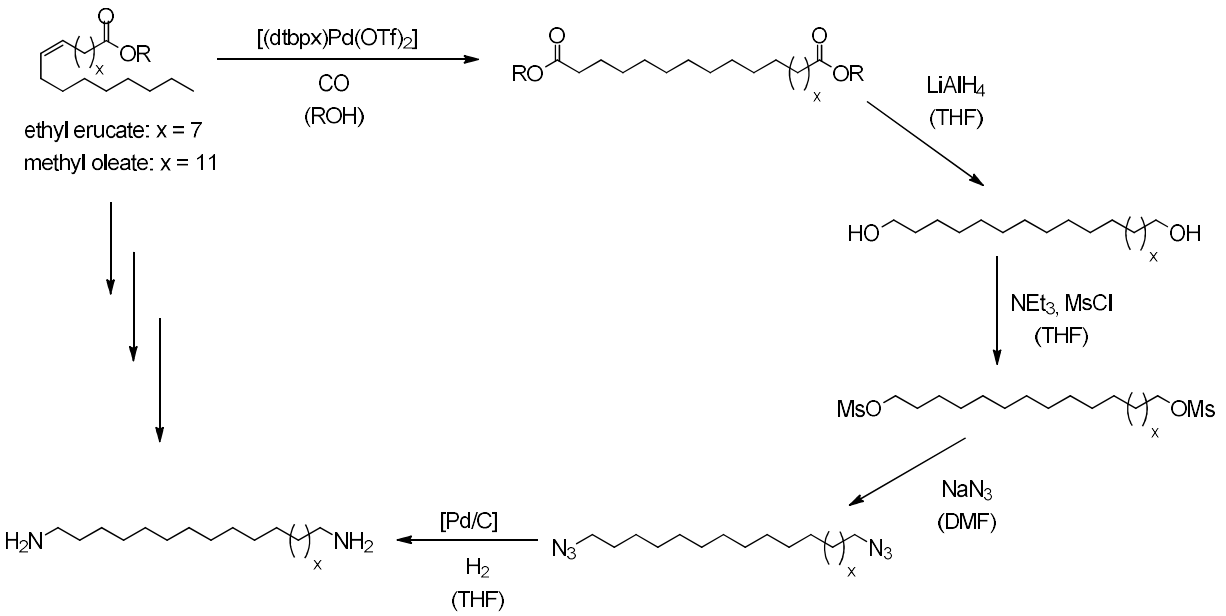

Scheme 5.2: Multistep synthesis of long-chain aliphatic diamines from unsaturated fatty acid esters via catalytic hydrogenation of diazides over Pd/C.

1,19-Nonadecane diazide and 1,23-tricosane diazide were prepared in accordance with literature via a multistep synthesis route starting from methyl oleate and ethyl erucate respectively (**Scheme 5.2**).[21] After isomerizing alkoxycarbonylation and subsequent reduction of the obtained linear long-chain C_{19} and C_{23} diesters to the corresponding diols, the hydroxyl functionalities were transformed into mesylate groups using triethylamine and methanesulfonyl chloride in an optimized reaction procedure that allowed for upscaling of the reaction and avoided product decomposition during the final recrystallization step. Subsequent treatment of the obtained long-chain α,ω-dimesylates with sodium azide yielded the desired linear long-chain α,ω-diazides via a nucleophilic substitution reaction. This way, 1,19-nonadecane diazide and 1,23-tricosane diazide could be obtained on a 20 g scale in yields of 95 % and 89 % respectively.

Subsequent experiments regarding the heterogeneous catalytic hydrogenation of 1,19-nonadecane diazide over Pd/C (10.wt.%) confirmed the formation of varying amounts of different side products depending on the employed reaction conditions, while overall product yield remained mostly unaffected and varied only slightly between 80 to 88 % (**Table 5.1**). Substrate conversions and exact crude product compositions were determined using ^{1}H NMR spectroscopy, which identified nitrile and secondary amine groups as the main functionalities being formed in addition to the desired primary amine groups (**Figure 5.2**).

Table 5.1: Catalytic hydrogenation of 1,19-nonadecane diazide. [a)]

entry	diazide conc.	Pd/C [b)]	H_2	solvent (ratio)	yield [c)]	crude product composition [d)]		
						prim. amine	sec. amine	nitrile
1	0.4 M	10 wt.%	20 bar	THF	84 %	74 %	7 %	19 %
2	0.2 M	10 wt.%	20 bar	THF	88 %	> 98 %	< 1 %	< 1 %
3	0.1 M	10 wt.%	20 bar	THF	81 %	100 %	0 %	0 %
4	0.4 M	10 wt.%	20 bar	THF/AcOH (6:1)	n.d.[e)]	77 %	2 %	21 %
5	0.4 M	5 wt.%	10 bar	THF/AcOH (6:1)	n.d. [e)]	88 %	1 %	11 %
6	0.4 M	5 wt.%	20 bar	THF/AcOH (6:1)	n.d. [e)]	83 %	4 %	13 %
7	0.4 M	2.5 wt.%	20 bar	THF/AcOH (6:1)	n.d. [e)]	94 %	0 %	6 %
8	0.4 M	1 wt.%	20 bar	THF/AcOH (6:1)	n.d. [e)]	12 %[f)]	0 %	0 %
9	0.4 M	2.5 wt.%	10 bar	THF	80 %.	94 %	2 %	4 %
10	0.4 M	2.5 wt.%	30 bar	THF	83 %.	91 %	3 %	6 %

a) standard conditions: 2.85 mmol 1,19-nonadecane diazide (0.4 M), 10 wt.% Pd/C (10 wt.%), 7 ml of solvent, 20 bar H_2, 40 °C, 3 h. b) catalyst loading in reference to the amount of diazide substrate. d) determined via ^{1}H NMR spectroscopy. c) crude product yield after removal of solid Pd and solvent residues. e) crude product retained non negligible amounts acetic acid. f) conversion incomplete, azide groups accounted for 88 % of functional groups in crude product.

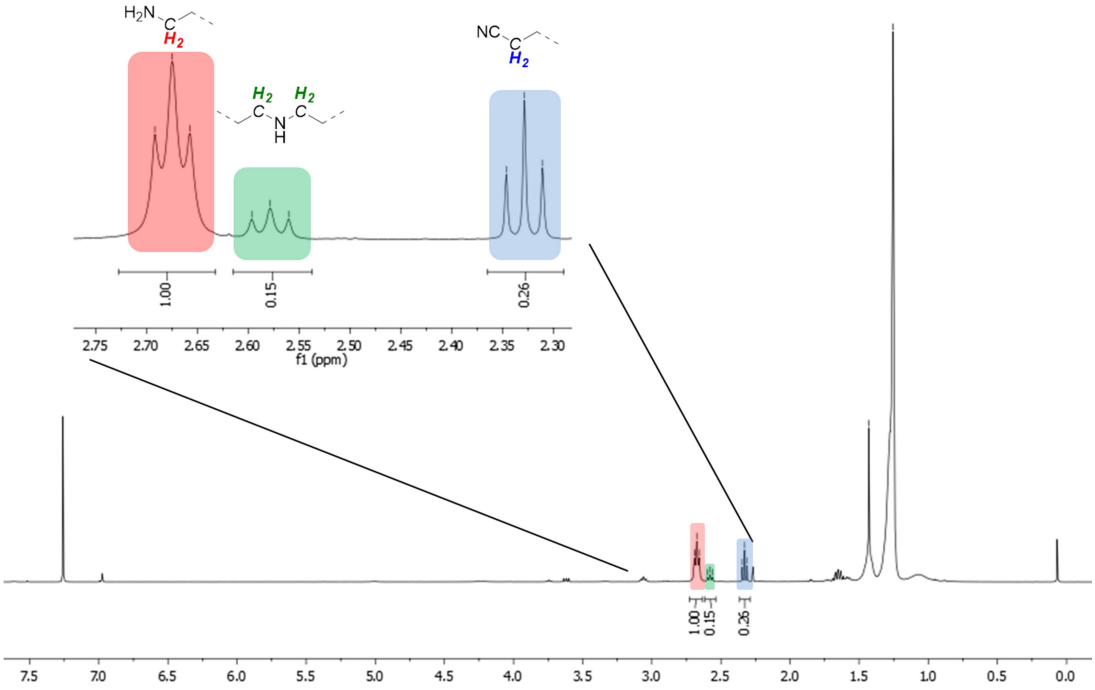

Figure 5.2: ^{1}H-NMR spectrum ($CDCl_3$, 25 °C; 400 MHz) of the product mixture obtained from the catalytic hydrogenation (Pd/C, 10wt.%) of 1,19-nonadecane diazide (0.4 M) in THF (cf. **Table 5.1**, **entry 1**). Region corresponding to the signals of methylene groups in α-position to formed functional groups highlighted.

Substrate concentration and catalyst loading were identified to be the most decisive factors in regards to suppressing the generation of nitrile and secondary amine compounds: A successive reduction of the concentration of 1,19-nonadecane diazide from 0.4 M to 0.2 M and finally 0.1 M (**Table 5.1, entry 1-3**) resulted in the content of nitrile and secondary amine groups in the crude product dropping from 19 % and 7 % respectively to about 1 % each until no traces of either side product could be detected anymore. Similarly, a reduction in the catalyst load from 10 wt.% to 5 wt.% and eventually 2.5 wt.% (**Table 5.1, entry 4, 6, and 7**) had a profound effect on the formation of nitrile groups, with the nitrile content in the crude product dropping from 21 % to 13 % and eventually 6 % in direct correlation to the reduced Pd/C concentration. Reducing the catalyst even further to 1 wt.% resulted in neither nitrile nor secondary amine groups being formed, however under these conditions the reaction remained incomplete, with diazide conversion dropping drastically from 100 % to only 12 % (**Table 5.1, entry 8**).

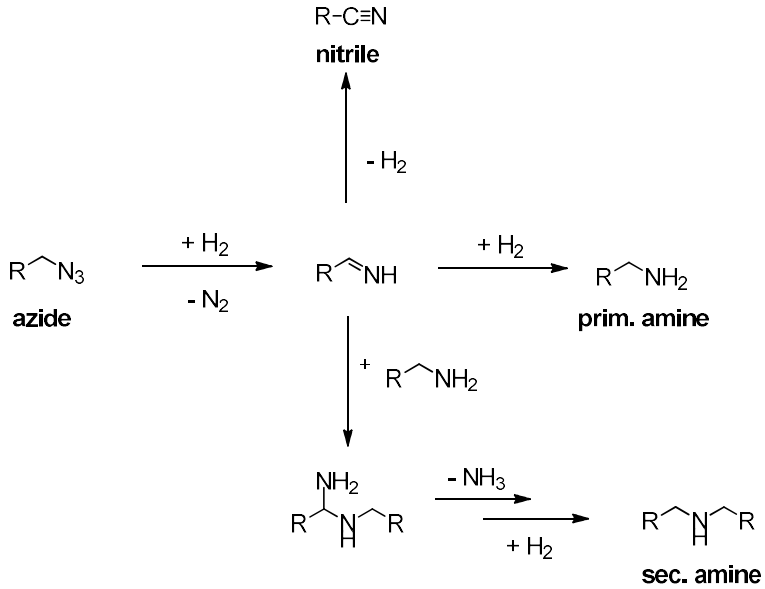

Scheme 5.3: Possible (side) reaction pathways taking place during the catalytic hydrogenation of organic azides over Pd/C (R = alkyl).

In an attempt to further block the reaction pathway leading to the formation of secondary amine (**Scheme 5.3**) and make diamine synthesis at higher substrate concentrations possible, THF was partly replaced with AcOH as the solvent (**Table 5.1, entry 4-8)**. At a THF to AcOH ratio of 6:1, the amount of secondary amine groups being formed dropped from 7 % in pure THF (**Table 5.1, entry 1)** to 2 % (**Table 5.1, entry 4**) if otherwise standard conditions were applied. In combination

with a reduction of the catalyst load from 10 wt.% (**Table 5.1, entry 4)** to 2.5 wt.% (**Table 5.1, entry 7**), the formation of secondary amines could thus be suppressed altogether, however residues of AcOH proved to be difficult to remove, impeded product purification via recrystallization, and the formation of nitrile groups remained unaffected. Additional attempts to promote the reaction pathway leading to the generation of amine groups (**Scheme 5.3**) by increasing the hydrogen pressure had no noticeable positive effect on raw product composition. Counterintuitively, increasing the hydrogen pressure from 10 bar to 20 bar (**Table 5.1, entry 5** and **6)** or from 10 bar to 30 bar (**Table 5.1, entry 9** and **10)** even resulted in slightly more side products being formed independent of changes in solvent composition and catalyst load, with the primary amine content dropping from 88 to 83 % and from 94 to 91 % respectively.

Table 5.2: Upscaling of the synthesis of 1,19-nonadecane diamine via catalytic hydrogenation. [a)]

entry	batch size	diazide conc.	Pd/C [b)]	Yield [c)]	product composition [d)]		
					prim. amine	sec. amine	nitrile
1	2,5 g	0.1M	5 wt.%	94 %	98 %	2 %	0 %
2	5 g	0.2 M	5 wt.%	85 %	98 %	2 %	< 1 %
3	5 g	0.2 M	2.5 wt.%	87 %	99 %	1 %	< 1 %
4	10 g	0.2 M[e)]	2.5 wt.%	85 %	99 %	1 %	< 1 %

a) 1,19-nonadecane diazide in 70 ml of THF, 40 °C, 3h, 20 bar of H_2, Pd/C (10 wt.%). b) catalyst loading in reference to the amount of diazide substrate employed. c) yield after recrystallization from n-heptane. d) determined via ^{1}H NMR spectroscopy. e) 140 ml THF.

With these results in mind, the reaction was incrementally upscaled to un ultimate batch size of 10 g of 1,19-nonadecane diazide, with substrate concentrations in THF not exceeding 0.2 M and the catalyst load being ultimately reduced from 5 wt.% to 2.5 wt.% (**Table 5.2**). Initially, doubling the batch size from 2.5 g to 5.0 g of diazide with a simultaneous increase in substrate concentration from 0.1 M to 0.2 M resulted in the product yield dropping from 94 % to 85 % (**Table 5.2, entry 1** and **2**). However, further upscaling to a batch size of 10 g of 1,19-nonadecane diazide had no additional impact on the yield of pure 1,19-nonadecane diamine (**Table 5.2, entry 3**). Simultaneously, neither upscaling nor an increase in substrate concentration did significantly affect selectivity, with all product batches containing 1-2 % of secondary amine as well as traces (< 1 %) of nitrile compounds, the only exception being the smallest batch size of 2.5 g substrate (**Table 5.2, entry 1**). Reduction of the catalyst load from 5 wt.% (**Table 5.2, entry 1** and **2**) to 2.5 wt.% (**Table 5.2, entry 3** and **4**) resulted in a slight improvement in product purity, with the secondary amine content dropping from

2 % to 1 % thereby yielding several grams of 1,19-nonadecane diamine in a polycondensation grade purity of 99 % (**Table 5.2, entry 4**). Further upscaling of the reaction was prohibited by the size of the available reactor.

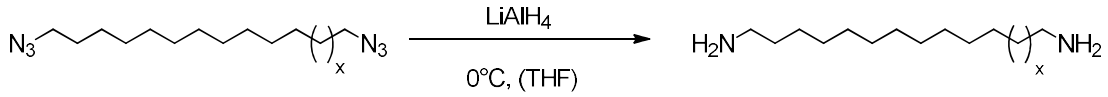

Scheme 5.4: Synthesis of 1,19-nonadecane diamine (x = 7) and 1,23-tricosane diamine (x = 11) via diazide reduction with $LiAlH_4$.

In an alternative approach, 10 g batches of 1,19-nonadecane diazide and 1,23-tricosane diazide respectively were successfully converted into corresponding 1,19-nonadecane diamine and 1,23-tricosane diamine using stoichiometric amounts of the inorganic hydride $LiAlH_4$. Despite previous reports indicating this synthesis approach only yielding negligible amounts of the desired product,[25] the reaction was found to be selective. After recrystallization from n-heptane, both long-chain α,ω-diamines could be isolated in yields of 92 % and 90 % respectively. ^{1}H NMR spectroscopy confirmed that both α,ω-diamines were obtained in polycondensation grade purity of > 99 % (**Figure 5.3** and **5.4**). Further upscaling of the reaction procedure was prohibited due to the volatile nature of the reaction which included decelerated gas evolution, a sudden, strong heat development, and a solidification of the reaction mixture due to the formation of a lithium amine salt network. These issues could be partly mitigated by careful monitoring of the reaction temperature and by working in high dilution (100-150 ml of solvent per gram of diazide) but safety concerns remained.

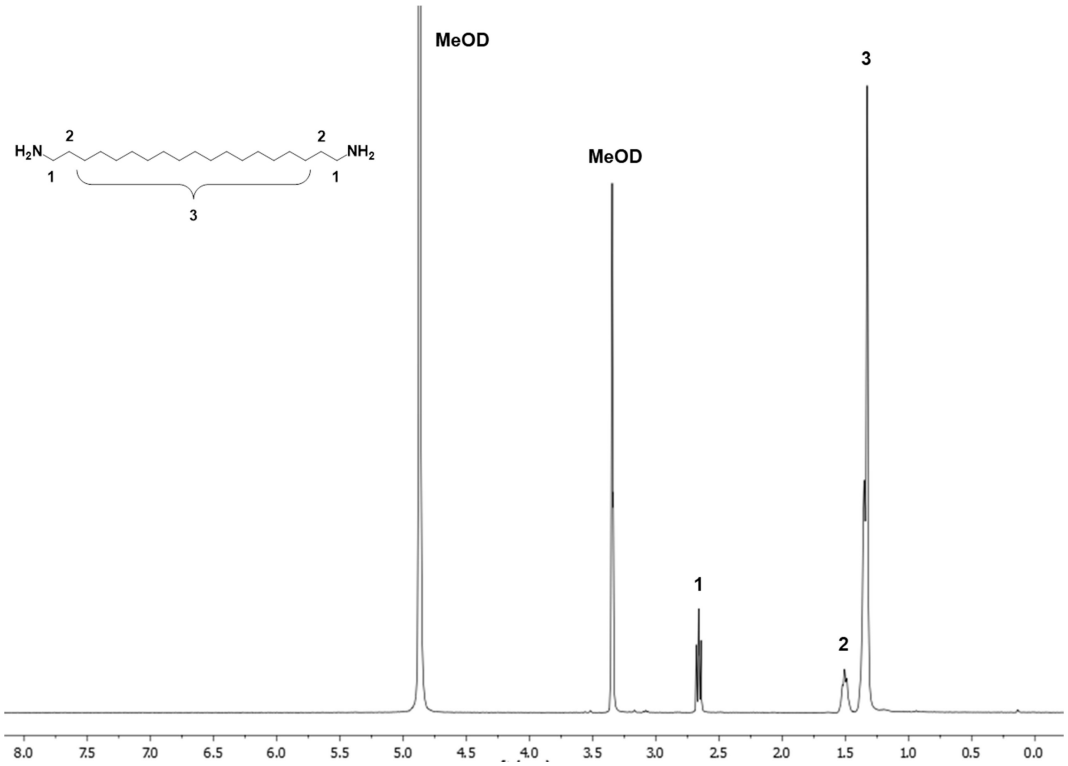

Figure 5.3: ^{1}H NMR spectrum (MeOD, 25 °C, 400 MHz) of 1,19-nonadecane diamine.

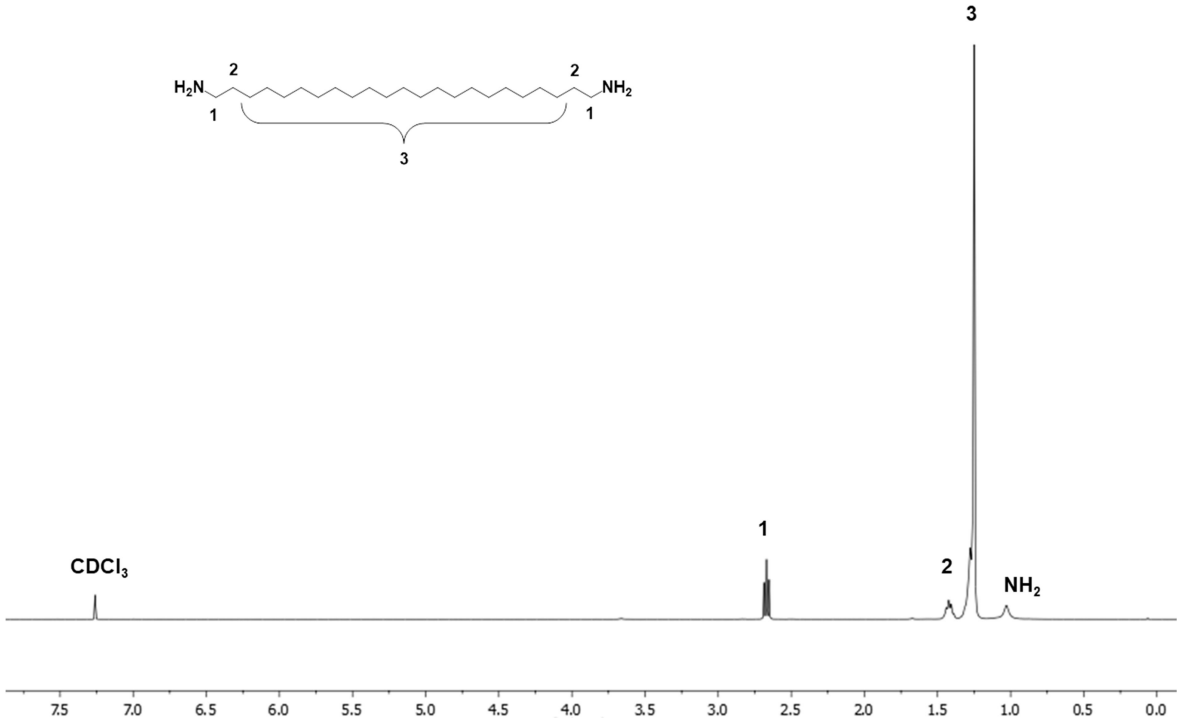

Figure 5.4: ^{1}H NMR spectrum ($CDCl_3$, 25 °C; 400 MHz) of 1,23-tricosane diamine.

5.2.2. Synthesis of long-chain thermoplastic PEEA elastomers

Compared to other segmented copolymer TPEs prepared via polycondensation or polyaddition reactions, TPAs typically differ in so far as their synthesis involves the generation of more than one type of functional group because the hydroxyl-terminated polyether macrodiols that are most commonly employed as soft segments are not compatible with the formation of amide linkages. Consequently, PEBAs and PEEAs are typically synthesized in a sequential two- or three-step polycondensation approach consisting of a polyamidation step and at least one (trans)esterification step.[2b],[10],[11],[12] Though it is theoretically possible to synthesize PEBAs and PEEAs in a single-step one-pot procedure,[11],[30],[31] single-step polycondensation requires for the employed monomers to be highly reactive as is the case for *e.g.* caprolactam but not for long-chain aliphatic α,ω-diamines and α,ω-dicarboxylic acids.[10] Consequently, in this work the two-step approach was employed which also affected the block length distribution in the generated PA-19.19 and PA-23.23 hard blocks (**Figure 5.5**) and resulted in on average shorter polyamide hard segments compared to the polyester and polyurethane hard blocks formed during the one-step synthesis of comparable segmented long-chain TPCs and TPUs with a similar hard to soft phase ratio (cf. **Chapter 3.2.1** and **4.2.2**).[32]

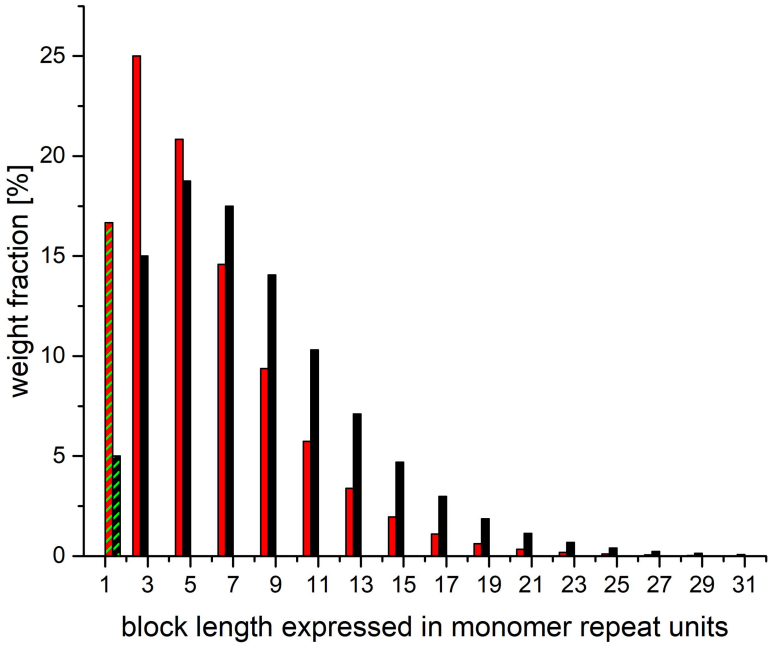

Figure 5.5. Block length distributions in A_2+B_2-type polyamide hard segments for segmented TPAs with a dicarboxylic acid to diamine ratio of 2:1 and 25 mol% polyether soft phase synthesized in a one-step (black) or two-step (red) polycondensation procedure (expressed in hard monomer repeat units), including isolated diacid repeat unit (n = 1) (slashed green).

In addition, the relatively large excess of α,ω-dicarboxylic acid employed during the synthesis of oligomeric PA-19.19 and PA-23.23 prepolymers resulted in not converted excess 1,19-nonadecanedioic acid and 1,23-tricosanedioic acid respectively accounting for 4 to 45 wt.% of the polyamidation product (**Table 5.3**) and the eventual formation of a PEEA containing isolated long-chain diester units in addition to the long-chain polyamide hard blocks and polyether $PPDO_{2000}$ soft segments.

Table 5.3: Synthesis of long- and mid-chain monomer-based oligoamide prepolymers via melt polycondensation [a)]

entry	oligoamide	monomers	NH_2/COOH ratio	M_n [b)] [g mol^{-1}]	free α,ω-diacid content
1	PA-19.19-1/4	C_{19}	1:4	525[d)]	45 wt.%
2	PA-19.19-2/4	C_{19}	2:4	919	17 wt.%
3	PA-19.19-3/4	C_{19}	3:4	2101[d)]	4 wt.%
4	PA-23.23-1/4	C_{23}	1:4	620	45 wt.%
5	PA-23.23-2/4	C_{23}	2:4	1087	17 wt.%
6	PA-23.23-3/4	C_{23}	3:4	2494[d)]	4 wt.%
7[c)]	PA-12.12-5/7	C_{12}	5:7	1216	5 wt.%

a) reaction conditions: 200 °C, 1 atm. N_2, 2h; followed by 2h under vacuum. b) according to ^{1}H NMR end group analysis including excess α,ω-diacid. c) 80 °C, 1 atm. N_2 for 2h followed by 15 min at 200 °C and 1 atm. N_2 alternating with 15 min at RT and vacuum, repeat for 4 h. d) ^{1}H NMR signals overlap.

1,19-Nonadecane diamine and 1,23-tricosane diamine respectively were copolymerized with excess amounts of their corresponding long-chain α,ω-dicarboxylic acids obtained from the alkaline hydrolysis of the corresponding long-chain diesters[21] to generate a series of carboxylic acid-terminated PA-19.19 and PA-23.23 oligomers with number average molecular weights ranging from 525 g mol^{-1} to 2494 g mol^{-1} (**Table 5.3**). Excess free α,ω-dicarboxylic acid accounted for 45 wt.% to 4 wt.% of the reaction product. Polyamidation reactions were carried out in melt at 200 °C but unlike for polyamidation systems based on more volatile aliphatic short- or mid-chain monomers[30] the application of additional nitrogen or steam pressure during the beginning stages of the reaction was not necessary as the comparatively high molecular weights of the employed C_{19} and C_{23} diamines and dicarboxylic acids prevented unwanted monomer evaporation under the applied conditions.

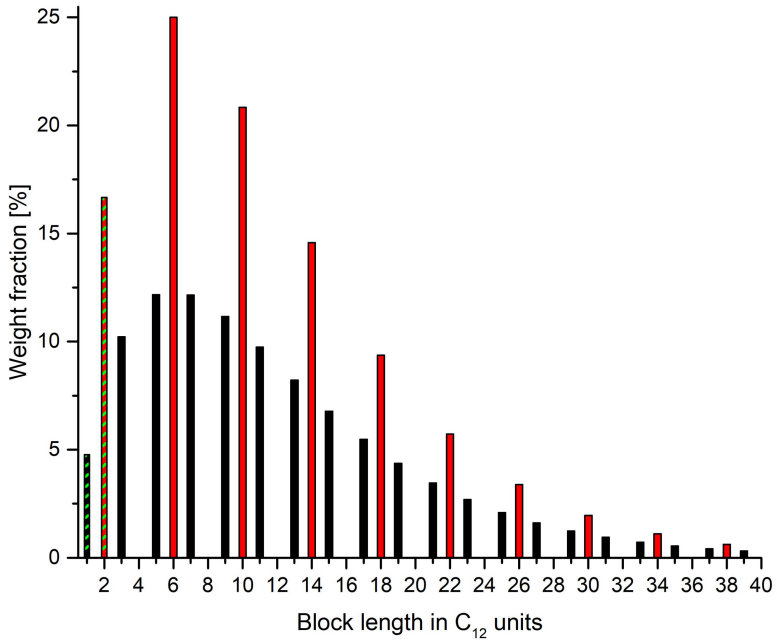

Figure 5.6 Polyamide block length distributions expressed on C_{12}-basis for oligoamides based on C_{24} dicarboxylic acid and C_{24} diamine in a ratio of 2:1 (PA-23.23-2/4) (red) and for oligoamides based on C_{12} dicarboxylic acid and C_{12} diamine in a ratio of 7/5 (PA-12.12-5/7) (black), i.e. isolated acid repeat unit: n = 1 (C_{12}, slashed green) and n = 2 (C_{24}, slashed green); acid-diamine-acid: n = 3 (C_{12}) and n = 6 (C_{24}) etc.

In order to further assess the effect that methylene sequence length and hydrogen bond density in the polyamide hard segments have on the material properties of all-aliphatic TPAs, an additional carboxylic acid-terminated PA-12.12 oligomer PA-12.12-5/7 based on mid-chain 1,12-dodecanediamine and 1,12-dodecanedioic acid was prepared using the same reaction procedure with an adjusted temperature and pressure protocol (**Table 5.3**, **entry 7**). The average molecular weight (M_n = 1216 g mol^{-1}) and block length distribution of PA-12.12-5/7 were comparable to those of its long-chain erucic acid-derived analog PA-23.23-2/4 (M_n = 1087 g mol^{-1}, **Table 5.3**, **entry 5**), though it has to be noted that the respective excess free α,ω-dicarboxylic acid accounted for only 5 wt.% of PA-12.12-5/7 but for 17 wt.% of PA-23.23-2/4 (**Figure 5.6**). When possible the composition and molecular weights were confirmed via ^{1}H NMR spectroscopy.

Table 5.4: Polymerization conditions, polymer compositions, and molecular weights of segmented poly(ester-*b*-ether-*b*-amide) copolymers based on long-chain and mid-chain aliphatic polyamide hard segments .[a)]

entry	polymer	oligoamide macro-monomer	PEEA composition			M_n [b)] (NMR) [g mol^{-1}]
			PA	isol. diester units	$PPDO_{2000}$	
1[c)]	TPA-$C_{19}PPDO_{2000}$-79wt%	PA-19.19-1/4	12 wt.%	9 wt.%	79 wt.%	7.9 x 10^4
2	TPA-$C_{19}PPDO_{2000}$-68wt%	PA-19.19-2/4	27 wt.%	5 wt.-%	68 wt.%	2.8 x 10^4
3[d)]	TPA-$C_{19}PPDO_{2000}$-49wt%	PA-19.19-3/4	49 wt.%	2 wt.%	49 wt.%	n.d.[e)]
4[c)]	TPA-$C_{23}PPDO_{2000}$-76wt%	PA-23.23-1/4	13 wt.%	11 wt.%	76 wt.%	7.9 x 10^4
5	TPA-$C_{23}PPDO_{2000}$-65wt%	PA-23.23-2/4	29 wt.%	6 wt.%	65 wt.%	9.8 x 10^4
6[d)]	TPA-$C_{23}PPDO_{2000}$-45wt%	PA-23.23-3/4	53 wt.%	2 wt.%	45 wt.%	16.4 x 10^4
7	TPA-$C_{12}PPDO_{2000}$-62wt%	PA-12.12-5/7	36 wt.%	2 wt.%	62 wt.%	3.8 x 10^4

a) melt polycondensation of 2 mmol of the respective oligoamide prepolymer with 2 mmol of $PPDO_{2000}$ in a 100 ml two-necked Schlenk tube equipped with a helical full screw agitator in the presence of 0.1 mol% of $Ti(OBu)_4$ and 0.1 wt.% of N,N'-di-2-naphthyl-1,4-phenylenediamine. b) determined by end-group analysis from ^{1}H NMR spectroscopy. c) melt polycondensation of 3 mmol of oligoamide prepolymer and 3 mmol of $PPDO_{2000}$. d) melt polycondensation of 1.5 mmol of oligoamide prepolymer and 1.5 mmol of $PPDO_{2000}$. e) not determined due to insolubility

In the second polyesterification step, the synthesized carboxylic acid-terminated PA-19.19, PA-23.23, and PA-12.12 prepolymers were copolymerized with equimolar amounts of renewable $PPDO_{2000}$ polyether macrodiol in a melt polycondensation procedure facilitated by catalytic amounts of $Ti(OBu)_4$ to prepare high molecular weight poly(ester-*b*-ether-*b*-amide) copolymers (**Table 5.4**). As the investigated polymerization systems revealed themselves to be susceptible to shear-thickening and the Weissenberg effect ("rod-climbing effect"),[33] extensive optimization of the applied reaction conditions, including in relation to different batch sizes, was necessary to ensure effective mixing and avoid the occurrence of temperature gradients within the emerging polymer melt. This included using mechanical stirrers with different agitator geometries as well as the development of dynamic stirring speed and temperature protocols that accounted for the thermodynamic incompatibility of the oligoamide and polyether macromonomers as well as the increasing viscosity of the emerging polymer melt during the course of the reaction. For smaller batch sizes of about 3 g of polymer, the utilization of a helical double ribbon agitator proved to yield the best results, however after upscaling of the reaction to batches of 5 g polymer or more a full screw helical agitator was required to obtain PEEAs of high molecular weight. (**Table 5.4**) (**Figure 5.7**).

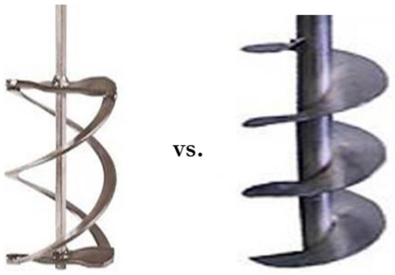

Figure 5.7: Image of a helical double ribbon agitator (left) and a full screw helical agitator blade (right).

In this way, a series of entirely renewable, all-aliphatic long-chain PEEAs with molecular weights ranging from 2.8×10^4 to 16.4×10^4 g mol^{-1} according to end group analysis from ^{1}H NMR spectroscopy were obtained as opaque, off-white materials (**Table 5.4, entry 1-6**). The content of $PPDO_{2000}$ polyether soft phase ranged from 45 wt.% to 79 wt.% depending on the average block length and molecular weight of the employed PA-19.19, PA-23.23 or PA-12.12 oligoamide prepolymers. Isolated aliphatic diester repeat units accounted for a maximum 11 wt.% of the final product. In addition, a mid-chain monomer-derived analog to long-chain TPA-$C_{23}PPDO_{2000}$-65wt% (**Table 5.4, entry 5**), TPA-$C_{12}PPDO_{2000}$-62wt% (**Table 5.4, entry 7**) based on the PA-12.12-5/7 polyamidation product (**Table 5.3, entry 7**) was also prepared to more accurately assess the influence that the methylene sequence length and hydrogen bond density in aliphatic polyamide hard blocks have on the material properties. The number average molecular weight of TPA-$C_{12}PPDO_{2000}$-62wt% was determined to be 3.8×10^4 g mol^{-1} according to ^{1}H NMR spectroscopy. In addition, TPA-$C_{12}PPDO_{2000}$-62wt% possessed a similar block length distribution and overall polymer composition as TPA-$C_{23}PPDO_{2000}$-65wt% (**Figure 5.6)**, with oligoamide segments accounting for 29 wt.% and 36 wt.%, and isolated diester repeat units accounting for 2 wt.% and 6 wt.% of the respective PEEA (**Table 5.4**, **entry 7** and **5**).

5.2.3. Morphology of long-chain thermoplastic PEEA elastomers

As the morphology of TPAs influences their mechanical properties, the microphase structure of PEEA copolymers based on PA-19.19, PA-23.23, and PA-12.12 hard segments was further investigated using ATR-FTIR spectroscopy to determine the relative degree of phase separation and further elucidate hydrogen bond formation in materials based on different aliphatic polyamide hard segments but with similar overall polymer composition. Accordingly, FTIR spectra were recorded for TPA-C_{12}PPDO$_{2000}$-62wt%, TPA-C_{19}PPDO$_{2000}$-68wt%, and TPA-C_{23}PPDO$_{2000}$-65wt% (**Figure 5.8**).

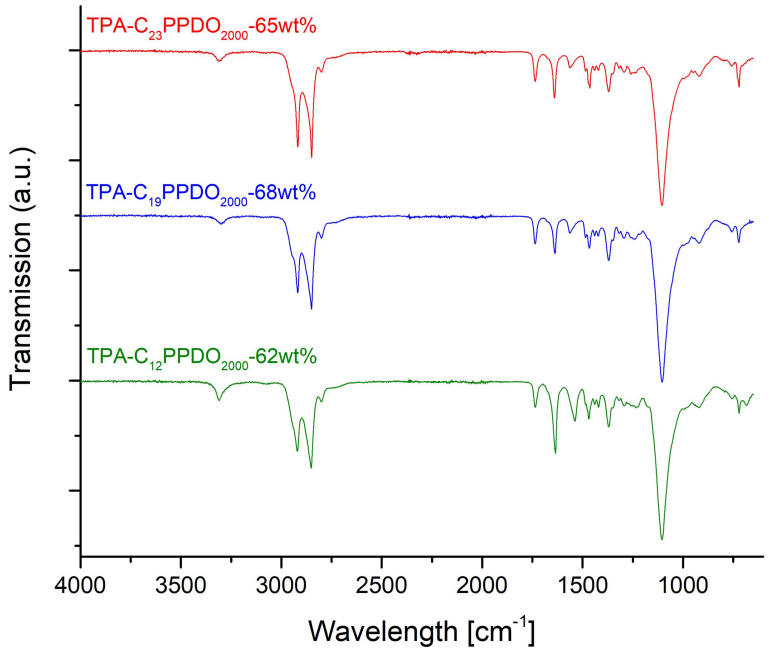

Figure 5.8: FTIR spectra of thermoplastic PEEA elastomers TPA-C_{12}PPDO$_{2000}$-62wt% (green), TPA-C_{19}PPDO$_{2000}$-68wt% (blue), and TPA-C_{23}PPDO$_{2000}$-65wt% (red) based on C_{12}, C_{19}, and C_{23} hard monomers.

The amide and carbonyl regions of the obtained spectra (**Figure 5.9**) all showed a series of distinct absorption bands around 3310 cm^{-1} and 1637 cm^{-1} associated with the presence of amide groups in addition to a signal at 1735 cm^{-1} that can be attributed to ester groups, thereby further confirming the general PEEA structure.[34] Furthermore, the absence of any type of signal at about 3450 cm^{-1} associated with free amide hydrogens in combination with the shift of the N-H stretching signal to 3310 cm^{-1} suggested that close to 100 % of amide hydrogens were hydrogen-bonded.[34],[35] The deviation from literature values given for highly ordered hydrogen bonds (3295 cm^{-1}) as well as

disordered hydrogen bonds (3336 cm^{-1}) in PA-12.12-based TPAs[34] indicated a mixture of both types of hydrogen bonds being present, which is not unusual for materials based on aliphatic semi-crystalline or amorphous polyamides.[35]

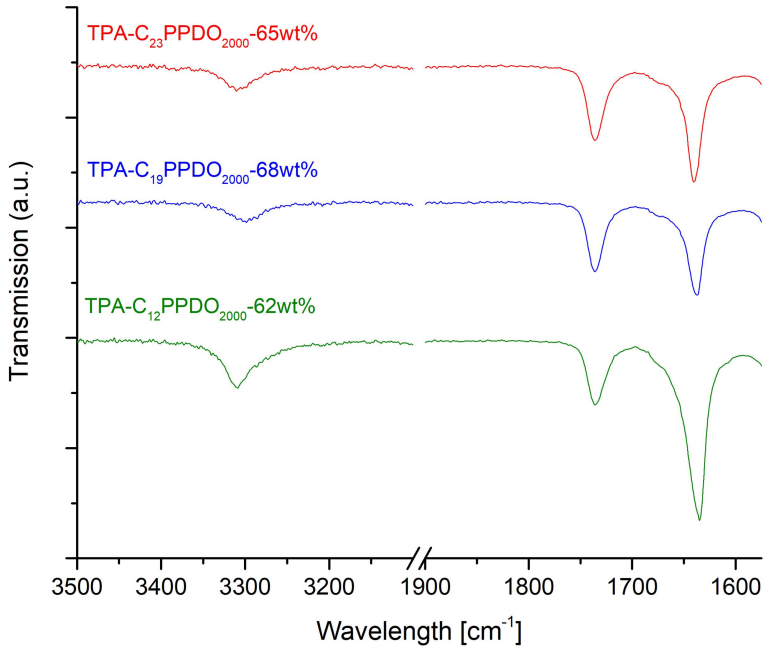

Figure 5.9: Amide and carbonyl regions of the FTIR spectra of thermoplastic PEEA elastomers with similar overall composition based on C_{12} (green), C_{19} (blue), and C_{23} (red) hard monomers.

However, amide hydrogens can not only form hydrogen bonds with amide carbonyls of the oligoamide hard segments but also with the carbonyl groups of ester linkages as well as with ether groups of the $PPDO_{2000}$ soft segments. Therefore, N-H stretching data alone is not sufficient to make a definitive statement about the degree of phase separation. Instead a closer inspection of the carbonyl region of the recorded IR spectra was necessary, which revealed the presence of intensive absorption bands at about 1735 cm^{-1} and 1635 cm^{-1}, with the latter possessing a weak shoulder in the range of 1670 to 1675 cm^{-1}. The distinct signal at 1735 cm^{-1} could be attributed to the presence of non-hydrogen bonded carbonyl groups of the ester functionalities, thereby confirming that neither ester linkages of the polyamide blocks nor of the isolated diester units participate in any type of hydrogen bonding.[34],[36],[37] In contrast, the amide carbonyl region was dominated by an intensive absorption band at about 1635 cm^{-1} to 1640 cm^{-1} associated with the C=O stretching of hydrogen-bonded amide carbonyl groups. The shift of the signal corresponded well with the value of 1638 cm^{-1}

given in literature for carbonyl groups of aliphatic polyamides involved in the formation of highly ordered hydrogen bonds. Peak deconvolution also suggested the presence of additional smaller overlapping signals at slightly higher absorption frequencies at roughly 1650 cm^{-1} that can be attributed to the presence of disordered hydrogen bonds. The weak shoulder appearing at a shift of 1670 cm^{-1} to 1675 cm^{-1} also suggested the presence of a small amount of non-hydrogen bonded amide carbonyl groups, thereby indicating that phase separation was high but not complete.[34] Minor deviations of observed signals from values cited in literature could be attributed to differences in the structure of the aliphatic hard segment components and to differences in the thermal history of the studied polymer samples.

In order to obtain a quantitative measure of the relative amounts of free and hydrogen-bonded amide carbonyl groups and determine the extent of phase separation, the amide carbonyl region of the recorded FTIR spectra was further analyzed using peak deconvolution of the corresponding absorption bands at about 1672 cm^{-1} and 1640 cm^{-1} respectively. The percentage of each carbonyl signal was obtained by comparing the specific peak areas of free and hydrogen-bonded amide carbonyl signals with the total peak area (**Table 5.5**). The results revealed that free amide carbonyl groups account for only 4 to 5 % of the total amide carbonyls independent of the length of the methylene sequences in the aliphatic polyamide hard segments, thereby suggesting that the studied aliphatic PEEAs possess a high degree of phase separation of about 95 % regardless of the chain length of the linear aliphatic α,ω-diamines and α,ω-dicarboxylic acid on which the polyamide hard blocks are based.

Table 5.5: Quantitative analysis of the amide carbonyl region of FTIR spectra of all-aliphatic PEEAs by peak deconvolution.

entry	polymer	peak area [%]	
		free amide C=O groups (ca. 1672 cm^{-1})	**H-bonded amide C=O groups [a] (ca. 1640 cm^{-1})**
1	TPA-C_{12}PPDO$_{2000}$-62wt%	4	96
2	TPA-C_{19}PPDO$_{2000}$-68wt%	4	96
3	TPA-C_{23}PPDO$_{2000}$-65wt%	5	95

a) Combined area of multiple overlapping peaks correlating to hydrogen bonds of different states of order.

A closer look at the aliphatic region of the recorded FTIR spectra (**Figure 5.10**) confirmed the general crystalline nature of the polyamide hard domains in all studied TPAs, as all recorded FTIR spectra featured a distinct, sharp absorption bands at 720 cm^{-1} which is characteristic for the C-H rocking of methylene groups within the crystalline regions of aliphatic polyamides.[34] The FTIR spectrum of TPA-C_{12}PPDO$_{2000}$-62wt% also featured a broad amide V absorption band at 683 cm^{-1}, indicating crystallization in the α-form.[38],[39] In contrast, the amide V absorption band in long-chain TPA-C_{19}PPDO$_{2000}$-68wt% and TPA-C_{23}PPDO$_{2000}$-65wt% appeared at 725 cm^{-1} and 728 cm^{-1} respectively as a, in case of TPA-C_{19}PPDO$_{2000}$-68wt% weak shoulder of the C-H rocking signal, thereby suggesting the adoption of a more loosely packed γ-form in polyamide hard domains based on odd-numbered long-chain monomers.[39] The γ-form is generally more likely to appear in polyamides derived from odd-numbered monomers, while aliphatic polyamides based on even-numbered monomers are more likely to adopt the α-form, though with increasing hydrocarbon chain length the γ-form becomes more prevalent depending on crystallization conditions, with PA-12.12 being known to adopting both crystal modifications depending on *e.g.* the thermal history of the studied sample.[22],[40],[41]

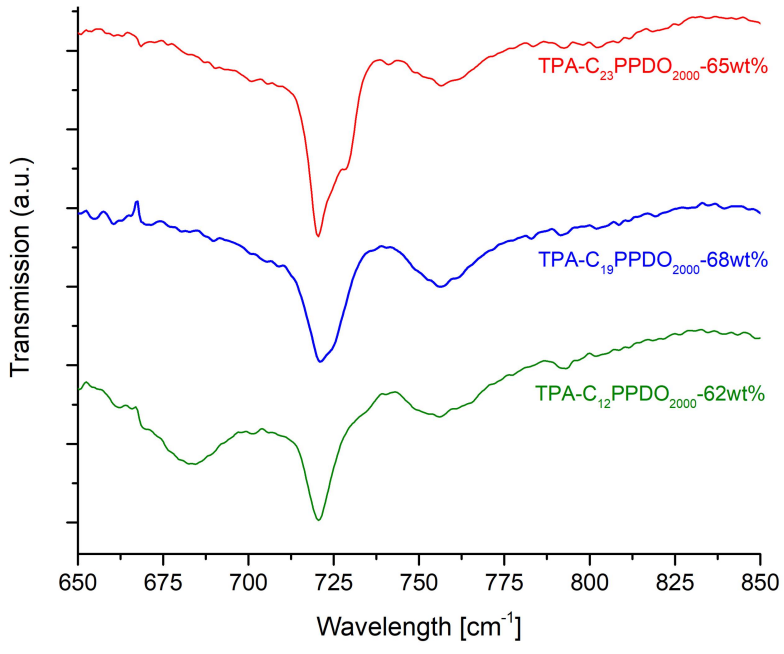

Figure 5.10: Aliphatic region of the FTIR spectra of thermoplastic PEEA elastomers with similar overall composition based on polyamide hard segments derived from C_{12} (green), C_{19} (blue), and C_{23} (red) monomers.

In order to further elucidate the crystalline solid state structure of the synthesized PEEAs and to determine whether isolated aliphatic long-chain diester units are capable of forming a distinct second type of crystalline hard phase or disturb crystallization of the polyamide hard segments, the synthesized PEEAs were further analyzed using wide angle X-ray diffraction. Due to solubility issues, the diffraction patterns were recorded using samples solidified by cooling from the melt instead of samples crystallized from solution, which typically results in the formation of smaller crystals with a higher amount of defects. It also has to be noted that the degree of crystallinity in polyamides generally rarely exceeds 40 %.[42] Aliphatic polyamides are also well known for their polymorphism, with a single sample sometimes containing up to three different crystal phases,[41],[43] a phenomenon that has also been observed for long-chain PA-23.23.[26]

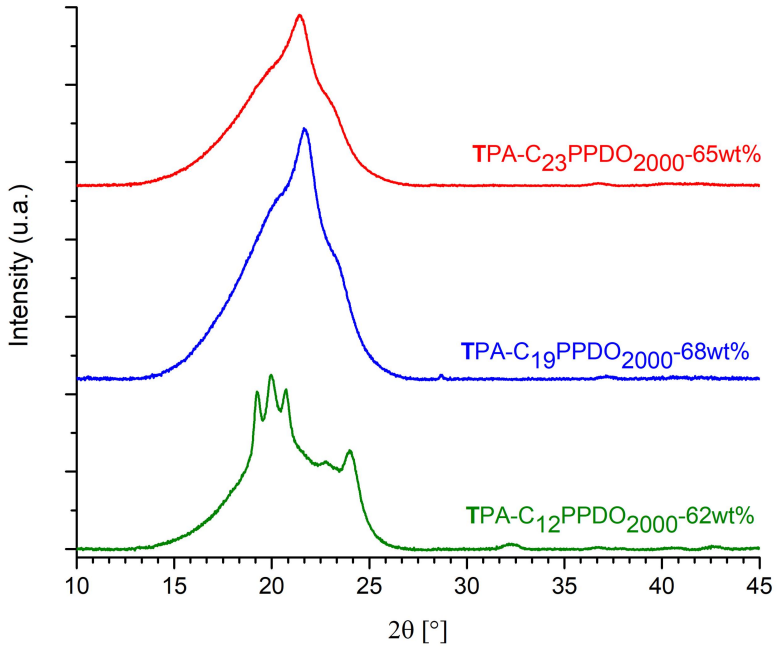

Figure 5.11: WAXD patterns of thermoplastic PEEA elastomers with similar overall composition based on polyamide hard segments derived from C_{12} (green), C_{19} (blue), and C_{23} (red) monomers.

Apart from a large amorphous halo, the diffractograms recorded for long-chain TPA-C_{19}PPDO$_{2000}$-68wt% and TPA-C_{23}PPDO$_{2000}$-65wt% were dominated by a broad diffraction peak appearing at an 2θ angle of about 21.6° and 21.4° respectively (**Figure 5.11**) that corresponds to a d-spacing of 4.1 Å to 4.2 Å and is characteristic for odd-odd numbered aliphatic polyamides crystallizing in the pseudohexagonal γ-modification.[39],[44],[45] Further analysis via peak deconvolution

also strongly suggested the presence of additional overlapping diffraction peaks, thereby indicating that the PA-19.19 and PA-23.23 hard segments in TPA-C_{19}PPDO$_{2000}$-68wt% and TPA-C_{23}PPDO$_{2000}$-65wt% overall adopted a complicated polymorphic structure in which the γ-modification is prevalent. PA-12.12 hard blocks of the mid-chain analog, TPA-C_{12}PPDO$_{2000}$-62wt%, were also found to adopt a polymorphic overall structure, with the WAXD diffraction pattern featuring multiple distinct peaks at 2θ angles of 19.2°, 20.0°, 20.7°, and 23.9° in addition to a broad amorphous halo (**Figure 5.11**). Diffraction peaks appearing at 2θ = 20.0° and 23.9° corresponding to d-spacings of 4.4 Å (d_{100}) and 3.7 Å (d_{010}) respectively were related to the presence of a triclinic α-phase.[39] Neither diffractogram featured the reflection pattern associated with the orthorhombic polyethylene-like crystal structure found in long-chain polyesters[46] and long-chain TPCs (cf. **Chapter 3.2.2, Figure 3.3**), indicating that Van-der-Waals interactions between the methylene sequences of isolated C_{12}, C_{19}, and C_{23} diester units are not strong enough to drive the formation of a second type of crystalline hard phase with polyethylene-like crystallinity.

5.2.4. Thermal properties of long-chain thermoplastic PEEA elastomers

The synthesized long-chain PEEAs were further analyzed using differential scanning calorimetry (DSC) (**Table 5.6**) which revealed the existence of a glass transition between - 71 °C and – 66°C depending on exact polymer composition. Glass transitions generally corresponded well to the glass transition temperature recorded for pure PPDO$_{2000}$, (-70 °C) thereby confirming a high degree of phase separation for all synthesized materials, though a slight increase of the glass transition temperature was observed with increasing polyamide block length and hard phase content, especially for PEEAs based on C_{19} monomers. The recorded DSC thermograms (**Figure 5.12** and **5.13**) also featured at least two melting points for all synthesized long-chain PEEAs. This included a lower melting point correlating to the amorphous polyether soft phase in the range of 0 °C to 9 °C and a upper melting point in the range of 128 °C to 152 °C that can be attributed to the melting of the polyamide hard phase. Additional very broad third, and in case of TPA-C_{23}PPDO$_{2000}$-65wt% (**Table 5.6, entry 5**) even fourth, thermal transitions related to changes in hydrogen bonding and structural transitions taking place within the polymorphic crystalline hard domains[47] were observed between 89 °C and 144 °C for all long-chain PEEAs except TPA-C_{23}PPDO$_{2000}$-45wt% (**Table 5.6, entry 6**). Transition peaks related to polyamide hard blocks were generally also very broad, a commonly observed phenomenon for aliphatic polyamides because state transitions in crystal cells,[47] lamellae

thickening, secondary crystallization,[48] and polymorphism[22],[41],[43] lead to melting peaks not representing a single structural transition but multiple, partly overlapping transition processes.

Table 5.6: Thermal properties of poly(ester-*b*-ether-*b*-amide) copolymers based on long-chain and mid-chain aliphatic polyamide hard segments.

entry	polymer	T_m[a)] [°C]	T_c[a)] [°C]	T_g[b)] [°C]
1	TPA-C_{19}PPDO$_{2000}$-79wt%	5/92/128[c)]	-18/62	-71
2	TPA-C_{19}PPDO$_{2000}$-68wt%	8/89/149[c)]	-7/67/116	-70
3	TPA-C_{19}PPDO$_{2000}$-49wt%	9/144/152[c)]	-10/116	-66
4	TPA-C_{23}PPDO$_{2000}$-76wt%	1/108/136[c)]	-32/70	-68
5	TPA-C_{23}PPDO$_{2000}$-65wt%	0/107/136/144 [c)]	74	-69
6	TPA-C_{23}PPDO$_{2000}$-45wt%	9/143	-9/110	-66
7	TPA-C_{12}PPDO$_{2000}$-62wt%	8/171	-6/131	-70

c) Determined by DSC with a heating/cooling rate of 10 K min^{-1}. b) Determined by DSC with a heating rate of 30 K min^{-1} c) broad melt transitions observed.

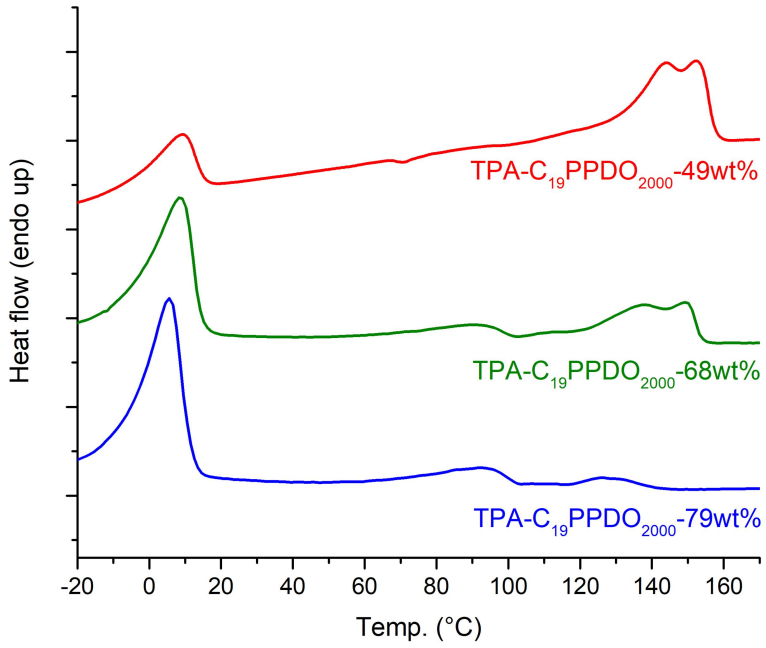

Figure 5.12: DSC thermograms (second heating) of poly(ester-*b*-ether-*b*-amide) copolymers based on oleic acid-derived C_{19} monomers and PPDO$_{2000}$.

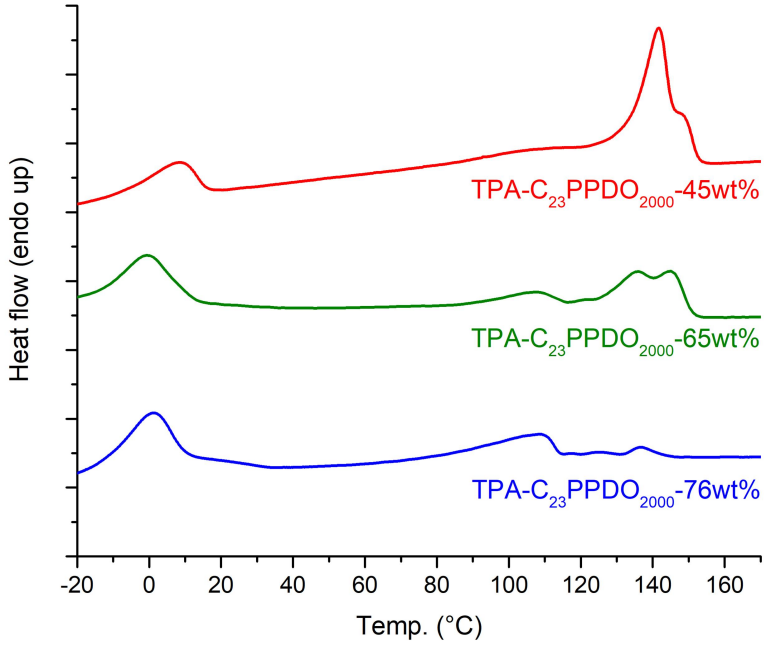

Figure 5.13 DSC thermograms (second heating) of poly(ester-*b*-ether-*b*-amide) copolymers based on erucic acid-derived C_{23} monomers and $PPDO_{2000}$.

As expected, PEEAs with polyamide hard segments based on PA-19.19 (**Table 5.6, entry 1-3**) generally speaking exhibited slightly higher upper melting points than comparable materials based on PA-23.23 (**Table 5.6, entry 4-6**)due to their higher hydrogen bond density. The only exception to this rule were TPA-C_{19}PPDO$_{2000}$-79wt% and TPA-C_{23}PPDO$_{2000}$-76wt% (**Table 5.6, entry 1** and **6**) which both possess a very low overall hard phase content and consequently very short polyamide hard blocks. Due to more favorable crystallization conditions, TPA-C_{23}PPDO$_{2000}$-76wt% exhibited a slightly higher upper melting point of 136 °C compared to 128 °C observed for TPA-C_{23}PPDO$_{2000}$-76wt%. In addition, with increasing block length of the polyamide hard segments and thereby increasing overall content of crystalline hard phase, the upper melting temperatures rose from 128 °C to 152 °C for PEEAs of the C_{19} series and from 136 °C to 144 °C for PEEAs of the C_{23} series, thereby approaching the values recorded for thermoplastic PA-19.19 (T_m = 158 °C)[24b] and PA-23.23 (T_m = 152 °C)[21], with melting peaks associated with the polyamide hard segments becoming increasingly sharper and more dominant (**Figure 5.12** and **5.13**). This can be attributed to crystallization conditions becoming more favorable and the degree of ordering of the hard segment increasing with increasing polyamide block length. The values for the lower melting points corresponding to the melt transitioning of the polyether soft phase were not significantly affected.

Comparison of the thermal properties of long-chain TPA-C_{23}PPDO$_{2000}$-65wt% (**Table 5.6, entry 5**) with its mid-chain monomer-based analog, TPA-C_{12}PPDO$_{2000}$-62wt% (**Table 5.6, entry 7**), showed an increase in the upper melting temperature by almost 30 °C from 144 °C to 171 °C for TPA-C_{12}PPDO$_{2000}$-62wt% due to the shorter methylene sequences resulting in an increase in hydrogen bond density in the polyamide hard domains. In addition, the upper melting point of TPA-C_{12}PPDO$_{2000}$-62wt% appeared as a much sharper peak in the DSC thermogram (**Figure 5.14**). A weak glass transition was detected at -70 °C similar to TPA-C_{23}PPDO$_{2000}$-65wt%.

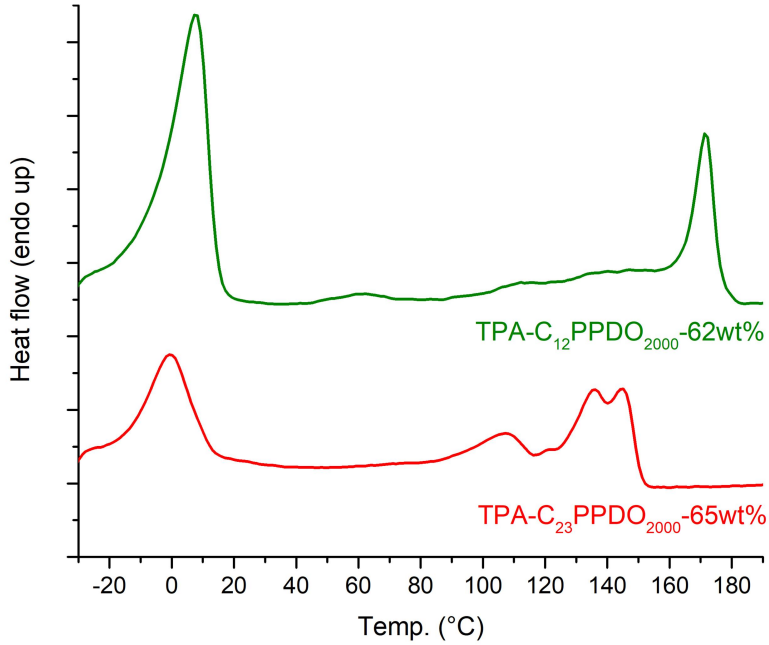

Figure 5.14: DSC thermograms (second heating) of TPA-C_{23}PPDO$_{2000}$-65wt% and its mid-chain-monomer based analog TPA-C_{12}PPDO$_{2000}$-62wt%

5.2.5. Mechanical properties of long-chain thermoplastic PEEA elastomers

In order to investigate the mechanical properties of the synthesized long-chain TPAs, tensile tests were performed on test specimens prepared via injection molding. However, the available test setup and test conditions designed to analyze TPEs, proved to only be applicable to PEEAs with a polyether soft segment content exceeding 50 wt.% (**Table 5.7**). Attempts to perform tensile tests and cyclic hysteresis tests on samples of TPA-C_{19}PPDO$_{2000}$-49wt% and TPA-C_{23}PPDO$_{2000}$-45wt% did not yield any analyzable data (**Table 5.7**, **entry3** and **6**). Accordingly, it had to be concluded that the hard to soft phase ratio in these PEEAs is too high for them to qualify as TPEs,

Table 5.7: Mechanical properties of poly(ester-*b*-ether-*b*-amide) copolymers based on long-chain and mid-chain aliphatic polyamide hard segments.

entry	polymer	Young's modulus [a),b)] [MPa]	elongation at break [a),c)] [%]	residual strain[d)] [%]	nominal residual strain[d)] [%]
1	TPA-C_{19}PPDO$_{2000}$-79wt%	6	193	-	8
2	TPA-C_{19}PPDO$_{2000}$-68wt%	13	404	14	21
3	TPA-C_{19}PPDO$_{2000}$-49wt%	n.d.	n.d.	-	n.d.
4	TPA-C_{23}PPDO$_{2000}$-76wt%	8	170	-	9
5	TPA-C_{23}PPDO$_{2000}$-65wt%	22	114	-	21
6	TPA-C_{23}PPDO$_{2000}$-45wt%	n.d.	n.d.	-	n.d.
7	TPA-C_{12}PPDO$_{2000}$-62wt%	21	353	18	26

a) Tensile tests performed according to ISO 527/1-2, specimen type 5A prepared by injection molding. Given values were obtained by averaging the data from several test specimens. b) crosshead speed 1 mm min^{-1}. c) crosshead speed 500 mm min^{-1}. d) Determined from hysteresis experiments after 10 cycles at an elongation of 100 % with a crosshead speed of 50 mm min^{-1}.

Ductility of the analyzable long-chain PEEAs remained limited, though elongations at break did exceed 100 % (**Table 5.7**, **entry 1, 4,** and **5**) and in case of TPA-C_{19}PPDO$_{2000}$-68wt% even reached a value of 404 % (**Table 5.7**, **entry 2**). Overall, the studied long-chain aliphatic PEEAs failed at considerably lower elongations than comparable long-chain TPCs and TPUs with a similar microphase structure (cf. **Chapter 3.2.3** and **Chapter 4.2.5**). As expected, Young moduli (E_t) seem to increase with increasing hard phase content, with values for E_t increasing from 6 MPa and 8 MPa for TPA-C_{19}PPDO$_{2000}$-79wt% and TPA-C_{23}PPDO$_{2000}$-76wt% respectively (**Table 5.7**, **entry 1** and **4**) to 13 MPa and 22 MPa calculated for TPA-C_{19}PPDO$_{2000}$-68wt% and TPA-C_{23}PPDO$_{2000}$-65wt%

(**Table 5.7**, **entry 2** and **5**). Though, it has to be noted that the available data is too limited to extrapolate a definite trend. The same is true for elongations at break.

Comparison of TPA-C_{23}PPDO$_{2000}$-65wt% (**Table 5.7, entry 5**) to its mid-chain monomer-based analog TPA-C_{12}PPDO$_{2000}$-62wt% (**Table 5.7, entry 7**) revealed that the length of the methylene sequences in the polyamide hard segments had no significant effect on the Young's modulus, with both polymers possessing comparable Young's moduli of 22 MPa and 21 MPa respectively, which lies within the measuring accuracy of the test method. In contrast, replacing PA-23.23 with PA-12.12 hard blocks drastically improved ductility and resulted in an increase of the elongation at break from 170 % for TPA-C_{23}PPDO$_{2000}$-65wt% to 353 % recorded for TPA-C_{12}PPDO$_{2000}$-62wt% (**Figure 5.15**), which cannot be explained by the odd-even effect and has to be attributed to increased hydrogen bond density.

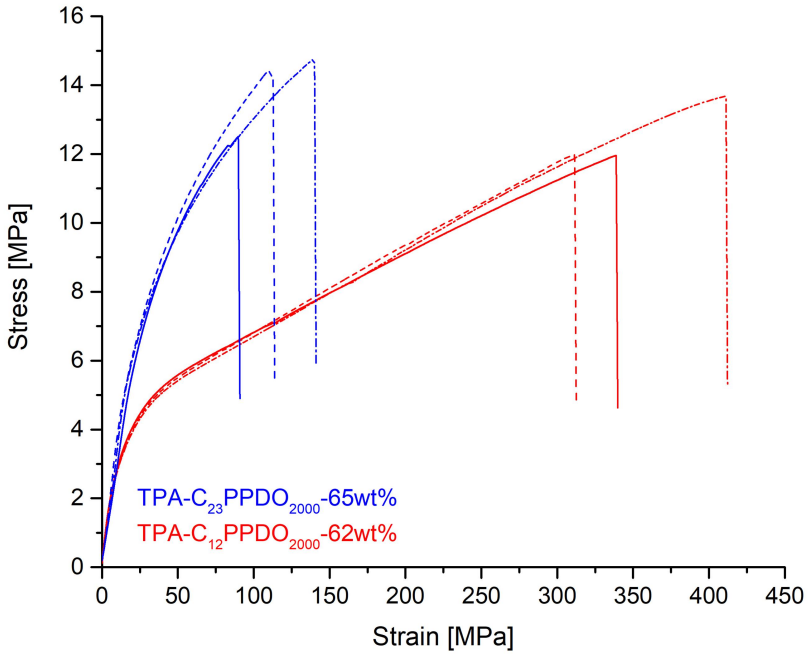

Figure 5.15: Stress-strain curves of long-chain TPA-C_{23}PPDO$_{2000}$-65wt% (blue) and its mid-chain analog TPU-C_{12}PPDO$_{2000}$-62wt% (red).

In order to assess the elastomeric properties of the long-chain PEEA copolymers containing more than 50 wt.% of polyether soft segment, cyclic hysteresis tests were performed using injection molded test specimen which were repeatedly subjected to consecutive cycles of loading to a strain of 100 % and unloading to assess shape recovery (**Table 5.7, entry 1, 2, 4,** and **5**). As expected for TPEs,[1],[2],[10],[49] during the first few cycles hysteresis was observed, with residual deformation

gradually increasing until after approximately 10 cycles a virtually constant level of recovery was reached. However, it has to be noted that it was generally not possible to determine the residual strain using the standard test setup as the mechanical contact extensometer used to measure elongations during standard hysteresis testing proved to be unsuitable for the studied materials. Therefore, the nominal residual strain as a function of the distance between specimen grips was recorded instead. This typically results in the recorded permanent set being distorted towards higher values as exemplified by TPA-C_{19}PPDO$_{2000}$-68wt% (**Table 5.7, entry 2**) whose residual strain was determined to be 14 % compared to a nominal residual strain of 21 %. Values recorded for the nominal residual strain of the studied long-chain PEEAs increased with increasing hard segment content from 8 % to 21 % for PEEAs based on C_{19} monomers (**Table 5.7**, **entry 1** and **2**) and from 9 % to 21 % for copolymers of the C_{23} series (**Table 5.7**, **entry 4** and **5**). Comparison of TPA-C_{23}PPDO$_{2000}$-65wt% (**Table 5.7, entry 5**) with its mid-chain monomer-based analog TPA-C_{12}PPDO$_{2000}$-62wt% (**Table 5.7, entry 7**) revealed a small positive effect of the reduced hydrogen bond density on elasticity, with the long-chain monomer-based PEEA exhibiting a smaller nominal residual strain of 21 % compared to a value of 26 % recorded for its mid-chain monomer-based analog (**Figure 5.16**).

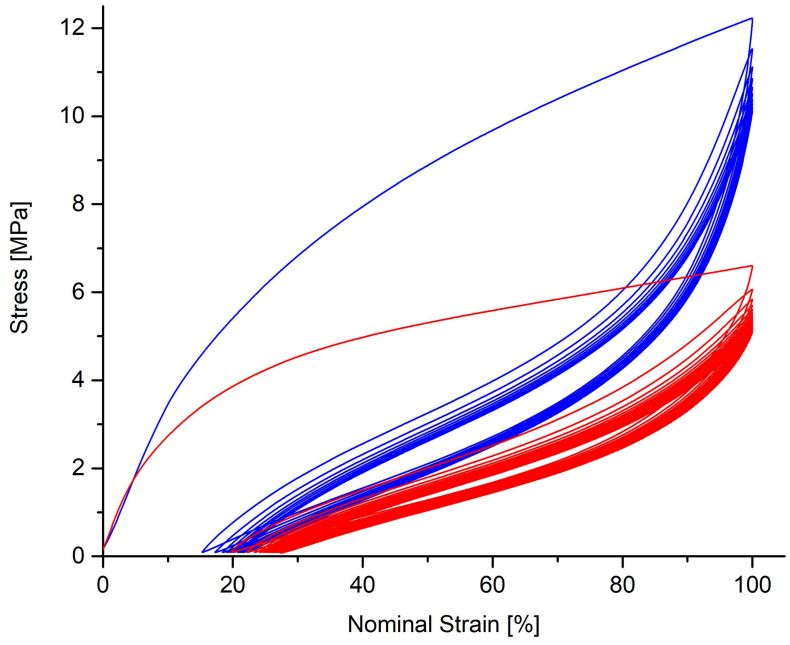

Figure 5.16: Stress–strain curves from cyclic tensile tests with a constant nominal strain of 100% for poly(ester-*b*-ether-*b*-amide) copolymers TPA-C_{23}PPDO$_{2000}$-65wt% (blue) and its mid-chain analog TPA-C_{12}PPDO$_{2000}$-62wt% (red).

5.2.6. Water absorption of long-chain PEEAs

Moisture absorption and subsequent swelling can have a profound impact on the material properties and thermal processability of polymeric materials because of water molecules acting as plasticizers. Polyamides are known to be especially susceptible to this phenomenon due to the highly polar nature of amide groups, with overall amide group and hydrogen bond density directly influencing a polyamide's tendency to absorb moisture from air.[1],[2],[18],[22] Accordingly, aliphatic polyamides based on monomers with longer methylene sequences and therefore a lower overall amide group and hydrogen bond density absorb less water and are therefore generally less affected by humid environments than their more polar short-chain counterparts.[22],[50],[51] For example, while water absorption of mid-chain PA-11 is limited to about 0.25 wt.%, the weight of short-chain PA-6 samples increases by 1.2 wt.% under wet conditions and by up to 9.5 wt.% due to moisture absorption from air depending on air humidity and the test protocol being used.[52]

For TPAs, their tendency to absorb water is not only determined by the chemical structure of their polyamide hard segments but also by the nature of their soft phase. Consequently, literature values can vary widely between different types of TPAs. For example, water absorption for standard PEBAs is typically cited to be about 1.2 wt.%[1] but can range from 0.5 to 5 wt.%[2a] depending on copolymer composition, the hydrophilicity of the polyether soft phase, and the exact test method used. PA-6 or PA-6.6 hard segments as well as highly polar PEG soft segments increase the overall hydrophilicity of the material, while mid-chain polyamides like PA-12 or PA-12.12 and comparatively nonpolar PTMG or polyester soft segments are considered to be hydrophobic blocks.[2] Extremely hydrophilic TPAs can absorb up to 48 wt.% of water.[1]

Table 5.8: Moisture and water absorption of all-renewable poly(ester-*b*-ether-*b*-amide) copolymers based on long-chain and mid-chain aliphatic polyamide hard segments. [a)]

entry	polymer	moisture absorption from air [b)]	water absorption [c)]
1	TPA-C_{23}PPDO$_{2000}$-65wt%	0.19 wt.%	1.2 wt.%
2	TPA-C_{12}PPDO$_{2000}$-62wt%	0.23 wt.%	3.6 wt.% (4.9 wt.%)[d)]

a) absorption tests were performed on injection molded rectangular test specimen (length × width × thickness = 90 × 10 × 1 mm³) that were cut into 30 mm pieces (length × width × thickness = 30 × 10 × 1 mm³). b) determined as weight loss of equilibrated polymer samples after drying under forced-air convection at 50 °C until weight remained stable. c) water absorption under wet conditions determined according to ISO 62 by immersion of test specimens in distilled water at 23 °C for 24 h. d) determined after 4 days of immersion.

In order to determine the amount of water that PEEAs based on long-chain polyamide hard segments and renewable PPDO soft segments can absorb and to quantitatively assess the effect that elongated methylene sequences in aliphatic polyamide hard segments have on hydrophilicity, TPA-C_{23}PPDO$_{2000}$-65wt% (**Table 5.8, entry 1**) as well as its mid-chain monomer-based analog TPA-C_{12}PPDO$_{2000}$-62wt% (**Table 5.8, entry 2**) were subjected to two different type of absorption tests to measure moisture absorption from air as well as water absorption under wet conditions. The ability of the two polymers to absorb moisture from air was determined by measuring the weight loss of equilibrated test specimens prepared via injection molding after having been dried at 50 °C for several days. TPA-C_{12}PPDO$_{2000}$-62wt% lost 0.23 wt.% of its original weight, while its long-chain counterpart lost only 0.19 wt.%, indicating that replacing mid-chain monomers in the polyamide hard segments with long-chain compounds slightly reduces the tendency of aliphatic TPAs with PPDO soft segments to absorb moisture from air over extended periods of time. Similarly, when pre-dried samples of both polymers were immersed in water, the weight of TPA-C_{23}PPDO$_{2000}$-65wt% increased by only 1.2 wt.% after 24 hours, with the weight remaining stable afterwards, even with continued immersion. In contrast, TPA-C_{12}PPDO$_{2000}$-62wt% gained 3.6 wt.% of weight within the first 24 hours and the weight of the immersed specimens only stabilized after four days of immersion, overall resulting in an increase in weight by 4.9 wt.%, which equates to about four times the amount of water being absorbed by TPA-C_{23}PPDO$_{2000}$-65wt%. Overall, the tendency of the synthesized long-chain monomer-derived materials to absorb water can be described as average, though this has also partly to be attributed to the relatively hydrophilic nature of the PPDO$_{2000}$ soft segments, while the moisture absorption from air is relatively low.

5.3. Conclusion

Long-chain, fatty acid-derived 1,19-nonadecane diamine and 1,23-tricosane diamine could be prepared from the corresponding diazides on a 10 g scale and in polycondensation grade purity using either a classic organic synthesis route utilizing $LiAlH_4$ as a reactant or via catalytic reduction with H_2 over Pd/C. In the latter approach, minimization of catalyst load and reduction of the overall substrate concentration were identified as the major factors in the suppression of the formation of secondary amine and nitrile side products that are otherwise impossible to remove from the crude product mixture. This way, pure long-chain diamines could be produced in yields of up to 86 % and then used as monomers for the generation of polyamide hard segments in renewable all-aliphatic thermoplastic poly(ester-*b*-ether-*b*-amide) elastomers. By optimizing the reaction procedure and the used equipment, it was possible to develop a two-step melt polycondensation procedure to synthesize segmented TPAs based on plant-oil derived long-chain monomers and a $PPDO_{2000}$ polyether macrodiol with molecular weights M_n reaching values of up to 16.4 x 10^4 g mol^{-1}. Physical crosslinking in these materials was provided by the selective formation of hydrogen bonds between amide groups of the long-chain aliphatic polyamide hard segments, which also facilitated microphase separation. Accordingly, high degrees of phase separation for the polyamide phase of about 95 % were reached independent of methylene sequence length in the polyamide hard blocks, as was confirmed via FTIR spectroscopy. Further analysis via WAXD also revealed a complicated polymorphic crystal structure dominated by hydrogen bond formation. The isolated 1,19-nonadecane and 1,23-tricosane diester blocks did not form a second distinct crystalline hard phase with a polyethylene-like crystal structure. In addition, the synthesized long-chain TPAs were found to possess several melting points correlating to their polymorphic multiphase morphology, with upper melting points associated with the melting of the crystalline polyamide hard domains ranging from 128 °C to 152 °C depending on the exact copolymer composition. Compared to similar PEEAs based on short-chain aliphatic polyamide hard segments, this constituted a notable reduction in the upper melting temperature due to reduced hydrogen bond density, with the melting point of PA-12.12-based TPA-$C_{12}PPDO_{2000}$-62wt% lying 30 °C above the melting point of analogous long-chain TPA-$C_{23}PPDO_{2000}$-65wt%. Consequently, long-chain PEEAs were easier to process using standard thermoplastic processing techniques like injection molding. The reduced hydrogen bond density in the polyamide hard domains also positively affected the tendency of the investigated materials to absorb water, with TPA-$C_{23}PPDO_{2000}$-65wt% absorbing considerably less water under wet conditions

than its mid-chain monomer-based analog. In addition, the investigation of the mechanical properties confirmed the elastomeric properties of the synthesized long-chain PEEA copolymers, thereby confirming their status as TPEs. Particularly high degrees of shape recovery with nominal permanent sets of only 8 % and 9 % respectively after 10 consecutive cycles of hysteresis testing were observed for TPA-C_{19}PPDO$_{2000}$-79wt% and TPA-C_{23}PPDO$_{2000}$-76wt% which both possessed an especially high polyether content in combination with short polyamide hard blocks and a relatively large content of isolated diester blocks. With increasing polyamide content and block length, which went hand in hand with a decrease in the content of isolated diester blocks, the observed hysteresis during cyclic hysteresis testing increased to about 20 %.. Comparison to the mid-chain monomer based analog TPA-C_{12}PPDO$_{2000}$-62wt% revealed that reducing the amide content by employing long-chain aliphatic monomers for the generation of polyamide hard segments resulted in reduced ductility of the obtained PEEA copolymer but in an increase in elasticity.

5.4. Experimental Section

5.4.1. Materials and general considerations

Unless stated otherwise, all manipulations were carried out under an inert gas atmosphere using standard Schlenk or glovebox techniques. THF was distilled from sodium/benzophenone under inert conditions with the addition of benzophenone. Toluene was distilled from sodium under an inert gas atmosphere, and DMF was dried over molecular sieves (3 Å). Acetic acid was degassed prior to use. All other solvents were used in p.a. or technical grade as received. Hydrogen (5.0) was supplied by Air Liquide. Potassium hydroxide (90 %), triethylamine (99 %), sodium azide (> 90 %), 1,12-diaminododecane (98 %), titanium(IV) tetrabutoxide (> 97 %), toluene p.a. (> 99.5 %) and methanol p.a. (99.8 %) were supplied by Sigma Aldrich. Palladium/charcoal activated (10 %), methane sulfonyl chloride (> 99 %), sodium hydroxide (> 98 %), trifluoroacetic acid (99 %), n-heptane (Emplura® 99 %) were purchased from Merck. $LiAlH_4$, DMF p.a. (> 99.5 %) were obtained from Acros. THF p.a. (> 99 %), 1,12-dodecanedioic acid and acetic acid (> 99.8 %) were purchased from VWR. N,N'-di-2-naphthyl-1,4-phenylenediamine (> 96 %) was supplied by TCI Europe. Poly(trimethylene glycol) with a number average molecular mass of M_n = 2000 g mol^{-1} was kindly donated by Allessa GmbH and was degassed prior to use. All deuterated solvents were supplied by Eurisotop.

NMR spectra were recorded on a Varian Inova 400 and a Bruker Avance 400 spectrometer.^{1}H and ^{13}C chemical shifts were referenced to the solvent signals or. Oligoamide and poly(ester-*b*-ether-*b*-amide) samples were dissolved in $CDCl_3$ with 1 drop of trifluoroacetic acid added, in which case chemical shifts were referenced to the signal of trifluoroacetic acid.

DSC analyses were performed on a Netzsch Phoenix 204 F1 instrument with a heating and cooling rate, respectively, of 10 K min^{-1} in a temperature range of −50 to 160 °C for the detection of melt and crystallization points and 20 K min^{-1} in a temperature range of -100 to 150 °C for the detection of glass transitions. Data reported are from second heating cycles in case of melt and crystallization point analysis.

Tensile tests were performed on dogbone-shaped sample bars (75 × 12.5 × 2 mm3; ISO 527-2, type 5A) which were prepared using a HAAKE Minijet II (Thermo Scientific) piston injection molder. After preconditioning the samples at 80°°C for 2 hours, tensile tests were performed on a Zwick 1446 Retroline tC II instrument according to ISO 527 (crosshead speed 500 mm min^{-1}, with a determination of the Young's modulus at a crosshead speed of 1 mm min^{-1}). The Zwick test Xpert

software version 11.0 was used to collect and analyze the data. Young's modulus, yield stress, yield strain, tensile stress at break and tensile strain at break were obtained by averaging the data from several test specimens. Cyclic hysteresis tests were performed on dogbone-shaped sample bars (75 × 12.5 × 2 mm3; ISO 527-2, type 5A) that were preconditioned at 80°°C for 2 hours. The test specimens were repeatedly exposed to consecutive cycles of loading and unloading to a constant nominal strain of 100 % with a constant crosshead speed of 50 mm min^{-1}. The recovery was measured by observing the nominal residual strain after 10 cycles.

Attenuated total reflection Fourier transform infrared (ATR-FTIR) spectra were recorded on a PerkinElmer Spectrum100 FTIR Spectrometer equipped with a Universal ATR Sampling Accessory. FTIR scans were collected on injection molded dogbone-shaped sample bars (75 × 12.5 × 2 mm^3; ISO 527-2, type 5A) after conditioning overnight. The frequency range covered was from 4000 to 650 cm^{-1} by averaging 32 scans at a resolution of 2 cm^{-1}. The obtained data was analyzed using the OriginPro 2015 software.

Wide angle X-Ray diffraction (WAXD) was performed on a Bruker AXS D8 Advance diffractometer using $CuK_{\alpha 1}$ radiation on samples solidified by cooling from the melt. Diffraction patterns were recorded in the range 10 to 60 degrees 2θ, at 25 °C.

Moisture and water absorption tests were performed on rectangular test specimens (length × width × thickness = 30 × 10 × 1 mm^3) cut from a larger rectangular test specimen prepared via injection molding (length × width × thickness = 90 × 10 × 1 mm^3). In order to determine the moisture absorption from air, the test specimens were allowed to equilibrate and absorb moisture from air for 14 days at ambient temperature before being dried in an oven under forced-air convection at 50 °C and weighed every 24 h until their weight remained stable (+/- 0.1 mg). Water absorption under wet conditions was determined according to DIN EN ISO 62. Pre-dried test specimens were immersed in distilled water (8 ml H_2O per 1 cm^2 specimen surface) at room temperature and weighed every 24 hours until their weight remained stable. Moisture and water absorption values were calculated by averaging the results obtained from three test specimens.

5.4.2. Monomer synthesis

Synthesis of 1,19-nonadecanedioic acid

The synthesis of 1,19-nonadecanedioic acid was carried out analogous to a reported procedure.[21] Potassium hydroxide (34.3 g, 610 mmol) was added to a suspension of dimethyl 1,19-nonadecanediester (21.8 g, 61.1 mmol) in a mixture of 750 ml of methanol and 30 ml of distilled water in a round bottomed flask. The resulting mixture was refluxed for 2 h, after which the mixture was allowed to cool down to room temperature and the solvent was removed *in vacuo*. The obtained white solid was dissolved in 750 ml of distilled water at 50 °C before the solution was acidified to pH = 2 by adding HCl (aq., conc.) to precipitate the desired product. After filtration, the obtained crude product was washed with water and dried *in vacuo* at 50 °C. Remaining water residues were removed via azeotropic distillation of toluene, after which the desired product was recrystallized from hot toluene, yielding 1,19-nonadecanedioic acid as a white powder in a yield of 96 % (18.8 g, 57.2 mmol).

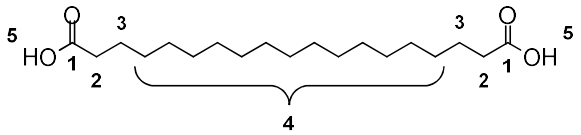

^{1}H NMR (DMSO-d_6, 25 °C, 400 MHz) δ 11.96 (s, 2H, H-5), 2.18 (t, $^{3}J_{H\text{-}H}$ = 7.4 Hz, 4H, H-2), 1.47 (quint, $^{3}J_{H\text{-}H}$ = 7.3 Hz, 4H), 1.32-1.13 (m, 26H, H-4) ppm.

^{13}C NMR (DMSO-d_6, 25 °C, 101 MHz) δ 174.5 (C-1), 33.7 (C-2), 29.0 - 28.5 (C-4), 24.5 (C-3) ppm.

Synthesis of 1,23-tricosanedioic acid

1,23-Tricosanedioic acid was prepared analogous to a previously reported procedure.[21] Potassium hydroxide (20.3 g, 364 mmol) was added to a suspension of dimethyl 1,23-tricosanediester (15.0 g, 36.4 mmol) in a mixture of 500 ml of methanol and 30 ml of distilled water. The resulting mixture was refluxed for 6 h, after which the mixture was allowed to cool down to room temperature and the solvent was removed in vacuo. The obtained white solid was dissolved in 750 ml of distilled water at 50 °C before the solution was acidified to pH = 2 by adding HCl (aq., conc.) to precipitate the dicarboxylic acid. After filtration, the obtained crude product was washed with water and dried in vacuo at 50 °C. Remaining water residues were removed via azeotropic distillation of toluene, after

which the desired product was recrystallized from hot toluene, yielding 1,19-nonadecanedioic acid as a white powder in a yield of 91 % (12.8 g, 33.2 mmol).

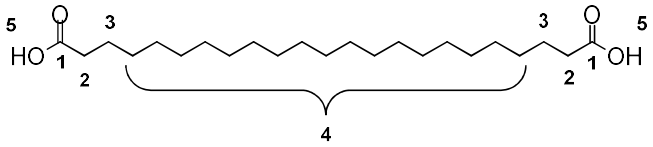

^{1}H NMR (DMSO-d_6, 25 °C, 400 MHz) δ 11.96 (s, 2H, H-5), 2.18 (t, $^{3}J_{H-H}$ = 7.3 Hz, 4H, H-2), 1.48 (quint., $^{3}J_{H-H}$ = 7.3 Hz, 4H, H-3), 1.30 – 1.18 (m, 34H, H-4) ppm.

^{13}C NMR (DMSO-d_6, 25 °C, 101 MHz) δ 174.5 (C-1), 33.6 (C-2), 29.0 - 28.5 (C-4), 24.5 (C-3) ppm.

Synthesis of 1,19-nonadecane dimesylate

1,19-Nonadecane dimesylate was prepared analogous to a previously reported procedure.[21] In a two-necked round bottomed flask, triethylamine (30.3 g, 299 mmol) and 1,19-nonadecanediol (18.0 g, 59.9 mmol) were dissolved in 250 ml of THF at 50 °C. Mesyl chloride (20.6 g, 180 mmol) was added dropwise via a syringe, resulting in the precipitation of a white solid. The obtained suspension was stirred at 50 °C for 3 h during which the color slowly changed to first yellow and then orange until the mixture eventually turned a dark red. After stirring at room temperature for another 12 hours, 500 ml of dichloromethane were added and the resulting red solution was successively washed with water (500 ml), 2 M HCl (500 ml), water (500 ml), saturated $NaHCO_3$ solution (400 ml), and water (500 ml) to remove byproducts. The washed organic phase was dried over $MgSO_4$ and the solvent removed in vacuo. Recrystallization from acetone yielded pure 1,19-nonadecane dimesylate as a glittering off-white solid in a yield of 88 % (24.1 g, 52.7 mmol).

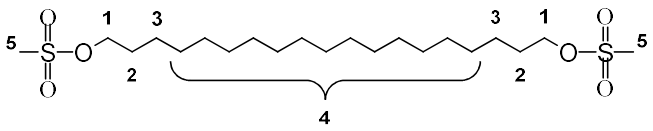

^{1}H NMR ($CDCl_3$, 25 °C, 400 MHz) δ 4.22 (t, $^{3}J_{H-H}$ = 6.6 Hz, 4H, H-1), 3.00 (s, 6H, H-5), 1.81 - 1.65 (m, 4H, H-2), 1.39 (quint., $^{3}J_{H-H}$ = 7.3, 6.9 Hz, 4H, H-3), 1.35 – 1.15 (m, 26H, H-4) ppm.

^{13}C NMR ($CDCl_3$, 25 °C, 101 MHz) δ 70.3 (C-1), 37.5 (C-5), 29.8-29.3 (C-4), 29.2 (C-2), 25.6 (C-3) ppm).

Synthesis of 1,23-tricosane dimesylate

1,23-Tricosane dimesylate was prepared analogous to a previously reported procedure.[21] In a three-necked round bottomed flask, triethylamine (26.2 g, 259 mmol) and 1,23-tricosanediol (18.5 g, 51.9 mmol) were dissolved in 500 ml of THF at 55 °C. A solution of mesyl chloride (17.8 g, 155 mmol) in 40 ml of THF was added dropwise via a dropping funnel, resulting in the precipitation of a white solid. The suspension was stirred at 55 °C for 3 h, during which the color slowly changed to first yellow and then orange until the mixture eventually turned a dark red. After stirring at room temperature for another 12 hours, 400 ml of dichloromethane were added and the resulting red solution was successively washed with water (700 ml), 2 M HCl (700 ml), water (700 ml), saturated $NaHCO_3$ solution (500 ml), and water (700 ml) to remove byproducts. The washed organic phase was dried over $MgSO_4$ and the solvent removed in vacuo. Recrystallization from acetone yielded pure 1,23-tricosane dimesylate as a glittering off-white solid in a yield of 86 % (22.9 g, 44.7 mmol).

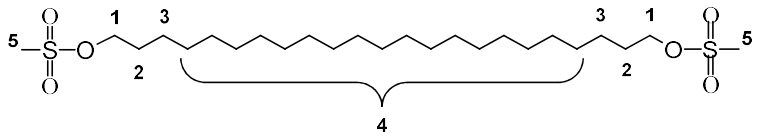

^{1}H NMR ($CDCl_3$, 25 °C, 400 MHz) δ 4.22 (t, $^3J_{H\text{-}H}$ = 6.6 Hz, 4H, H-1), 3.00 (s, 6H, H-5), 1.74 (quint., $^3J_{H\text{-}H}$ = 6.6 Hz, 4H, H-2), 1.44 – 1.35 (m, 4H, H-3), 1.34 – 1.19 (m, 34H, H-4) ppm.

^{13}C NMR ($CDCl_3$, 25 °C, 101 MHz) δ 70.4 (C-1), 37.5 (C-5), 29.8 – 29.3 (C-4), 29.2 (C-2), 25.5 (C-3) ppm.

Synthesis of 1,19-nonadecane diazide

1,19-Nonadecane diazide was prepared analogous to a previously reported procedure.[21] In a two-necked round bottomed flask, a suspension of 1,19-nonadecane dimesylate (27.8 g, 60,9 mmol) in 400 ml of DMF was heated to 65 °C, resulting in the formation of an orange solution before NaN_3 (19.8 g, 304 mmol) was added. The mixture was then stirred at 85 °C for 3.5 h before being allowed to cool down and stirred for another 12 h at room temperature. After the addition of 200 ml of distilled water, the DMF-water phase was extracted three times with 400 ml of n-heptane. The combined organic phases were then successively washed with saturated $NaHCO_3$ solution (700 ml) and twice with saturated NaCl solution (2 x 700 ml) before being dried over $MgSO_4$. The solvent was removed in vacuo and the obtained crude product was recrystallized from a mixture of ethanol and

ethyl acetate (4:1) at -28 °C to yield 1,19-nonadecane diazide as a white glittery solid in 95 % (20.2 g, 57.6 mmol) yield.

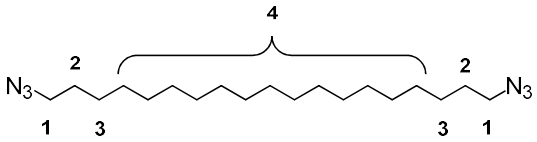

^{1}H NMR ($CDCl_3$, 25 °C, 400 MHz) δ 3.28 (t, $^{3}J_{H-H}$ = 7.0 Hz, 4H, H-1), 1.62 (quint. $^{3}J_{H-H}$ = 6.9 Hz, 4H, H-2), 1.44 – 1.22 (m, 30H, H-3 and H-4) ppm.

^{13}C NMR ($CDCl_3$, 25 °C, 101 MHz) δ 51.7 (C-1), 29.8 – 29.3 (C-4), 29.0 (C-2), 26.9 (C-3) ppm.

Synthesis of 1,23-tricosane diazide

1,23-Tricosane diazide was prepared analogous to a previously reported procedure.[21] In a two-necked round bottomed flask, a suspension of 1,23-tricosane dimesylate (22.5 g, 43,9 mmol) in 600 ml of DMF was heated to 65 °C, resulting in the formation of an orange solution, before NaN_3 (14.3 g, 219 mmol) was added. The mixture was then heated to 85 °C and stirred for 4 h before being allowed to cool down and stirred for another 12 h at room temperature. After the addition of 200 ml of distilled water, the DMF-water phase was extracted three times with 300 ml of n-pentane. The combined organic phases were then successively washed with saturated $NaHCO_3$ solution (700 ml) and twice with saturated NaCl solution (2 x 700 ml) before being dried over $MgSO_4$. The solvent was removed in vacuo and the obtained crude product was recrystallized from a mixture of ethanol and ethyl acetate (4:1) at -28 °C to yield 1,23-tricosane diazide as a glittery white solid in 89 % (15.9 g, 39.1 mmol) yield.

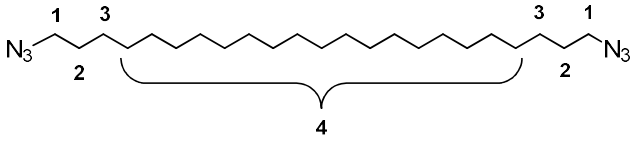

^{1}H NMR ($CDCl_3$, 25 °C, 400 MHz) δ 3.25 (t, $^{3}J_{H-H}$ = 7.0 Hz, 4H, H-1), 1.60 (quint. $^{3}J_{H-H}$ = 7.0 Hz, 4H, H-2), 1.42 – 1.18 (m, 38H, H-3 and H-4) ppm.

^{13}C NMR ($CDCl_3$, 25 °C, 101 MHz) δ 51.8 (C-1), 30.0 – 29.5 (C-4), 29.2 (C-2), 27.0 (C-3) ppm.

Synthesis of 1,19-nonadecane diamine via classic organic synthesis

In a three-necked round bottomed flask, a suspension of $LiAlH_4$ (4.0 g, 105 mmol) in 1 l of THF was cooled to 0 °C before a solution of 1,19-nonadecane diazide (12.3 g, 35.1 mmol) in 400 ml of THF was added very slowly via a dropping funnel and under rigorous stirring. After about 30 min and the addition of ca. 10 ml of the diazide-THF solution, a sudden increase in gas evolution combined with a thickening of the reaction mixture was observed. The substrate addition was stopped for 15 min until the gas evolution stopped and the viscosity of the suspension decreased again. Then, the addition of diazide was resumed at a higher rate and the remaining substrate solution added to the $LiAlH_4$ suspension over the course of 4 h. After stirring the mixture for 1 h at room temperature, it was heated to 65 °C and refluxed for another hour, followed by stirring at room temperature for an additional 12 h. The remaining excess of $LiAlH_4$ was quenched by successively slowly adding 10 ml of distilled water, 10 ml of NaOH solution (15 %, aq.), and another 40 ml of distilled water. The resulting gray suspension was filtered hot over a Buchner funnel to remove lithium salts, and the solvent of the obtained filtrate was removed in vacuo to yield a white solid as the crude product that was recrystallized from n-heptane to obtain pure 1,19-nonadecane diamine in a yield of 92 % (9.7 g, 32.5 mmol).

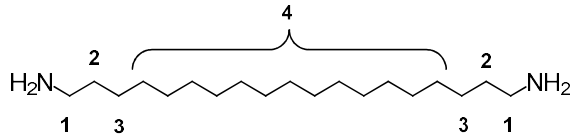

^{1}H NMR (MeOD, 25 °C, 400 MHz) δ 2.66 (t, $^3J_{H-H}$ = 7.2 Hz, 4H, H-1), 1.50 (quint, $^3J_{H-H}$ = 7.0 Hz, 4H, H-2), 1.40 - 1.26 (m, 30H, H-3 and H-4) ppm.

^{13}C NMR (MeOD, 25 °C, 101 MHz) δ 42.5 (C-1), 33.7 (C-2), 30.8 – 30.6 (C-4), 28.0 (C-3) ppm.

Synthesis of 1,23-tricosane diamine via classic organic synthesis

In a three-necked round bottomed flask, a suspension of $LiAlH_4$ (2.5 g, 64.9 mmol) in 1 l of THF was cooled to 0 °C before a solution of 1,23-tricosane diazide (8.8 g, 21.6 mmol) in 400 ml of THF was added very slowly via a dropping funnel and under rigorous stirring. After about 30 min and the addition of ca. 10 ml of the diazide-THF solution, a sudden increase in gas evolution combined with a thickening of the reaction mixture was observed. The substrate addition was stopped for 15 min until the gas evolution stopped and the viscosity of the suspension decreased again. Then, the

addition of diazide was resumed at a higher rate and the remaining substrate solution added to the $LiAlH_4$ suspension over the course of 4 h. After stirring the mixture for 1 h at room temperature, it was heated to 65 °C and refluxed for another hour, followed by stirring at room temperature for an additional 12 h. The remaining excess of $LiAlH_4$ was quenched by successively slowly adding 10 ml of distilled water, 30 ml of NaOH solution (15 %, aq.), and another 20 ml of distilled water. The resulting gray suspension was filtered hot over a Buchner funnel to remove lithium salts, and the solvent of the obtained filtrate was removed in vacuo to yield a white solid as the crude product that was recrystallized from n-heptane to obtain pure 1,23-tricosane diamine in a yield of 90 % (6.9 g, 19.5 mmol).

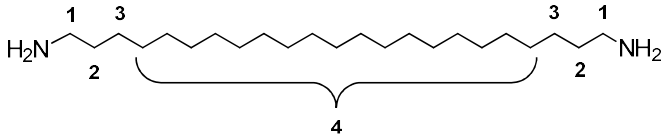

^{1}H NMR ($CDCl_3$, 25 °C, 400 MHz) δ 2.67 (t, $^3J_{H-H}$ = 7.0 Hz, 4H, H-1), 1.41 (quint, $^3J_{H-H}$ = = 6.9 Hz, 4H, H-2), 1.34 – 1.18 (m, 38H, H-3 and H-4) ppm.

^{13}C NMR ($CDCl_3$, 25 °C, 101 MHz) δ 42.3 (C-1), 34.0 (C-2), 30.3-29.5 (C-4), 26.9 (C-3) ppm.

General procedure for pressure reactor experiments regarding the synthesis of 1,19-nonadecane diamine via catalytic reduction.

Catalytic reductions of 1,19-nonadecane diazide were performed in a 20 ml stainless steel reactor equipped with glass inlet and a magnetic stirrer. The apparatus was heated with an aluminium block equipped with a thermocouple to control the temperature. Pd/C (10 wt.%) was weighed in the glass inlet, which was then inserted into the reactor before the apparatus was purged several times with nitrogen. 1,19-Nonadecane diazide (1 g, 2.85 mmol) was weighed in a Schlenk tube equipped with a magnetic stirring bar and dissolved by adding 7 ml of the chosen solvent mixture. The substrate solution was cannula-transferred into the reactor after which the apparatus was closed, pressurized with 20 bar of hydrogen, and heated to 40 °C. After 3 h of reaction time, the reactor was allowed to cool down to room temperature and vented. Catalyst residues were removed from the reaction mixture via filtration at 50 °C before the solvent was removed in vacuo to afford the crude product mixture as an off-white solid which was analyzed using ^{1}H NMR spectroscopy.

General procedure for upscaling experiments regarding the synthesis of 1,19-nonadecane diamine via catalytic reduction

All experiments were carried out in a 280 ml stainless steel pressure reactor equipped with a mechanical stirrer and a glass inlay. Heating was provided by a heating/cooling jacket controlled by a thermocouple dipping into the reaction mixture. Pd/C (10 wt.%) was weighed into the glass inlet, which was then inserted into the reactor before the apparatus was purged several times with nitrogen. 1,19-Nonadecane diazide was weighed in a Schlenk tube equipped with a magnetic stirring bar and dissolved by adding 70 ml of dry THF. The substrate solution was then cannula-transferred into the reactor, after which the apparatus was closed, pressurized with 20 bar of hydrogen, and heated to 40 °C. After 3 h of reaction time, the reactor was cooled down to room temperature and vented. Catalyst residues were removed from the reaction mixture via filtration at 50 °C before the solvent was removed in vacuo to afford the crude product mixture as an off-white solid. Recrystallization from n-heptane yielded the desired product in polycondensation grade purity.

5.4.3. Polymer Synthesis

General procedure for the synthesis of PA-19.19 oligomers

Polyamidation reactions between 1,19-nonadecane diamine and 1,19-nonadecanedioic acid were carried out in melt under inert gas atmosphere in a 100 ml Schlenk flask equipped with a magnetic stirrer. The apparatus was heated using an aluminum block equipped with a thermocouple to control the temperature. The desired amounts of crystalline 1,19-nonadecane diamine and 1,19-nonadecanedioic acid were weighed in (**Table 5.10**), the mixture was degassed and then inserted into an aluminum block preheated to 200 °C to produce of a clear melt. The melt was stirred at 200 °C under a N_2 atmosphere for 2 h before vacuum was applied to remove water formed during the course of the reaction. The reaction mixture was at 200 °C under vacuum for another 2 hours until the formation of water ceased and the reaction was complete.

Table 5.10: Experimental data for the synthesis of PA-19.19 oligoamide prepolymers.

entry	oligoamide	NH_2/COOH ratio	C_{19} diamine	C_{19} dicarboxylic acid
1	PA-19.19-1/4	1:4	3.4 mmol	13.4 mmol
2	PA-19.19-2/4	2:4	6.7 mmol	13.4 mmol
3	PA-19.19-3/4	3:4	6.7 mmol	8.9 mmol

General procedure for the synthesis of PA-23.23 oligomers

Polyamidation reactions between 1,23-tricosane diamine and 1,23-tricosanedioic acid were carried out in melt under inert gas atmosphere in a 100 ml Schlenk flask equipped with a magnetic stirrer and heated with an aluminum block equipped with a thermocouple to control the temperature. The desired amounts of crystalline 1,23-tricosane diamine and 1,23-tricosanedioic acid were weighed in (**Table 5.11**), the mixture was degassed and then heated to 130 °C to produce a clear melt. After 30 min. the temperature was increased to 200 °C. The reaction mixture was stirred under a N_2 atmosphere at 200 °C for 2 h before vacuum was applied to remove the water formed during the course of the reaction. The reaction mixture was at 200 °C under vacuum for another 2 h until the formation of water ceased and the reaction was complete.

Table 5.11: Experimental data for the synthesis of PA-23.23 oligoamide prepolymers.

entry	oligoamide	NH_2/COOH ratio	C_{23} diamine	C_{23} dicarboxylic acid
1	PA-23.23-1/4	1:4	2 mmol	8 mmol
2	PA-23.23-2/4	2:4	5.7 mmol	11.3 mmol
3	PA-23.23-3/4	3:4	5.6 mmol	7.5 mmol

Procedure for the synthesis of PA-12.12-5/7

After weighing in 5.0 g (21.7 mmol) of 1,12-dodecanedioic acid and 3.1 g (15.5 mmol) of 1,12-dodecane diamine into a 100 ml Schlenk flask equipped with a magnetic stirrer, the mixture was degassed and heated to 80 °C with the help of an aluminum block equipped with a thermo couple to control temperature. The resulting melt suspension was stirred under an N_2 atmosphere for 2 h before the temperature was raised rapidly to 200 °C. After 15 min of stirring under nitrogen, the melt was allowed to cool down to room temperature. As soon as the melt started to solidify, vacuum was applied for 15 min. to remove water formed during the course of the reaction. When all water was removed, the flask was flushed with nitrogen and reheated to 200 °C. This heating/cooling cycle was repeated for a period of 4 hours until no more additional water was formed, indicating that the reaction was complete.

General procedure for polyesterification of PA-19.19 or PA-23.23 oligoamides

Polyesterifications were carried out under inert gas atmosphere either in a 75 ml (for batch sizes < 5 g) or 100 ml (for batch sizes > 5 g) two-necked Schlenk tube equipped with a helical double ribbon or a helical full screw mechanical stirrer respectively. The apparatus was heated with an aluminium block equipped with a thermocouple to control the temperature. Stoichiometric amounts of the oligoamide prepolymer (1.0 mmol to 3.0 mmol respectively) and $PPDO_{2000}$ (1.0 mmol to 3 mmol respectively) (**Table 5.12**) as well as 0.1 wt.% of N,N'-di-2-naphthyl-1,4-phenylenediamine were weighed in, and the mixture was degassed before 0.1 mol% of a 0.02 M solution of $Ti(OBu)_4$ in toluene were added. The reaction was started by heating the mixture to 160 °C, at which point the mechanical stirrer was turned on and the stirring rate set to 160 rpm. The temperature was raised by 10 K every hour until a temperature of 200 °C was reached. After 2 h of stirring at 160 rpm under an N2 atmosphere, vacuum was applied to remove volatiles and the melt was stirred for another 12 h at 80 rpm. Finally, the stirring rate was reduced to 40 rpm, and the increasingly viscous polymer melt was stirred for another 8 h at 250 °C under vacuum to yield a poly(ester-*b*-ether-*b*-amide) copolymer.

Table 5.12: Experimental details for the polyesterification of PA-19.19 and PA-23.23 prepolymers to synthesize poly(ester-*b*-ether-*b*-amide) copolymers.

entry	oligoamide			$PPDO_{2000}$	Agitator type
	type	batch size	M_n [g mol^{-1}]		
1	PA-19.19-1/4	3.0 mmol (1.58 g)	525	3.0 mmol (6.00 g)	Helical full screw
2	PA-19.19-2/4	2.0 mmol (1.87 g)	919	2.0 mmol (4.00 g)	Helical full screw
3	PA-19.19-3/4	1.5 mmol (3.15 g)	2101	1.5 mmol (3-00 g)	Helical full screw
4	PA-23.23-1/4	3.0 mmol (1.86)	620	3.0 mmol (6.00 g)	Helical full screw
5	PA-23.23-2/4	1.0 mmol (1.09 g)	1087	1.0 mmol (2.00 g)	Helical double ribbon
6	PA-23.23-2/4	2.0 mmol (2.18 g)	1087	2.0 mmol (4.00 g)	Helical full screw
7	PA-23.23-3/4	1.5 mmol (3.74) g	2494	1.5 mmol (3.00 g)	Helical full screw

General procedure for polyesterification reactions of PA-12.12 oligoamide

Polyesterification reactions of PA-12.12-5/7 with $PPDO_{2000}$ were carried out under inert gas atmosphere in a 100 ml two-necked Schlenk tube equipped with a helical full screw mechanical stirrer. The apparatus was heated with an aluminium block equipped with a thermocouple to control the temperature. 2 mmol (2.43 g) of PA.12.12-5/7 oligoamide and 2 mmol (4.00 g) of $PPDO_{2000}$ as well as 0.1 wt.-% of N,N'-di-2-naphthyl-1,4-phenylenediamine were weighed in, and the mixture was degassed before 0.1 mol% of a 0.028 M solution of $Ti(OBu)_4$ in toluene were added. The reaction was started by heating the mixture to 190 °C, at which point the mechanical stirrer was turned on and the melt was stirred for three hours at 160 rpm. The temperature was then raised to 200 °C and the mixture was stirred under an N_2 atmosphere for another 3 h before vacuum was applied to remove volatiles and the stirring rate was lowered 40 rpm. After 12 h, the temperature was raised to 250 °C and the increasingly viscous polymer melt was stirred at 40 rpm under vacuum for another 5 h to yield an off-white poly(ester-*b*-ether-*b*-amide) copolymer.

5.4.4. Molecular weight determination by ^{1}H NMR spectroscopy

Oligoamide prepolymers

Molecular weights of oligoamide prepolymers determined from ^{1}H NMR spectra via end group analysis were calculated using the following formula:

$$M_n = DP_n \cdot M_0 = \frac{\int E_2}{\int E_1} \cdot M_0 + M_{COOH} - M_{H_2O}$$

The degree of polymerization (DP_n) was defined as the ratio of the signal intensities of the internal methylene group of the fatty acid-derived dicarboxylic acid repeat unit in alpha position to the amide group (E_2, 2.47ppm, 2H, **Figure 5.17 and 5.18**: **signal b**) and the signal of the methylene group in alpha position to the carboxylic acid end group (E_1, 2.28 ppm, 2H, **Figure 5.17 and 5.18**: **signal c**). M_0 and M_{COOH} were defined as the molecular weight of the polyamide repeat unit and the molecular weight of the aliphatic dicarboxylic acid employed as a monomer respectively.

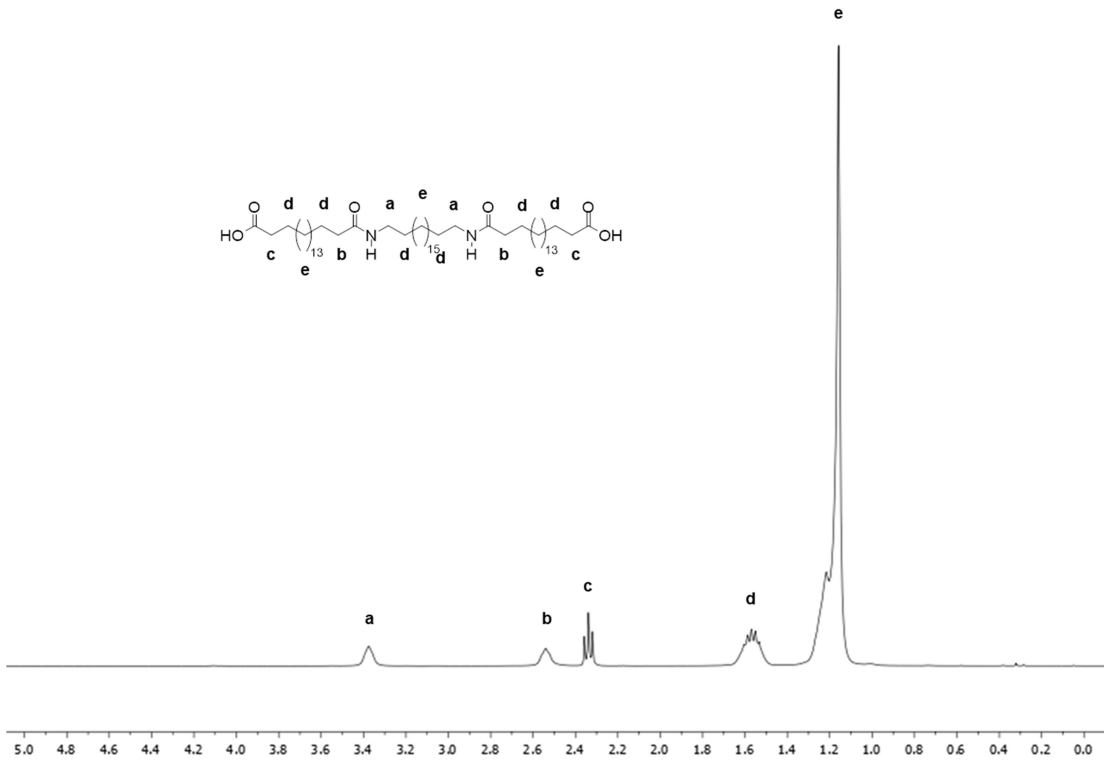

Figure 5.17: ^{1}H NMR spectrum ($CDCl_3$, 400 MHz) of PA-19.19-2/4

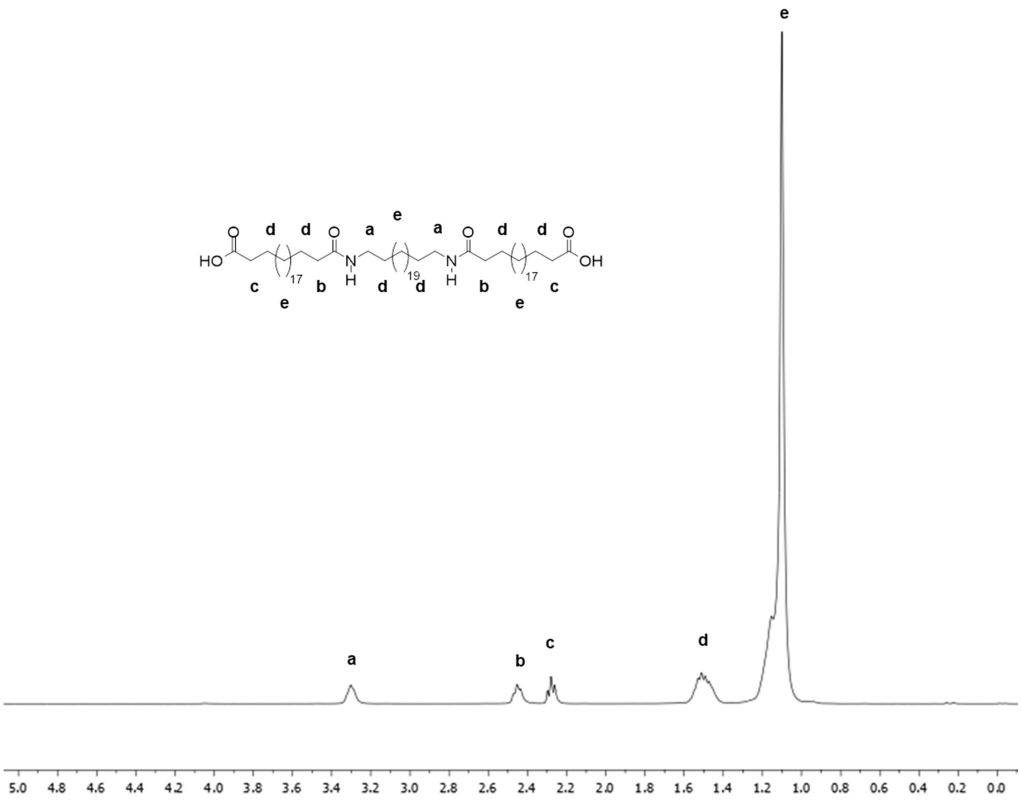

Figure 5.18: ^{1}H NMR spectrum ($CDCl_3$, 400 MHz) of PA-23.23-2/4

Poly(ester-*b*-ether-*b*-amide) copolymers

Molecular weights of poly(ester-*b*-ether-*b*-amide) copolymers determined from ^{1}H NMR spectra via end group analysis were calculated using the following formula:

$$M_n = DP_n \cdot M_0 = \frac{\int E_3}{\frac{1}{2}\int E_1 + \frac{1}{2}\int E_2} \cdot M_0$$

The degree of polymerization (DP_n) was defined as the ratio of the signal intensities of the internal methylene group of the $PPDO_{2000}$ polyether soft segment adjacent to an ester linkage (E_3, 4.06 ppm, 2H, **Figure 5.19** and **5.20**: **signal b**) and the weighted sum of the signals corresponding to possible end groups. This theoretically includes the signal of the methylene group in alpha position to a carboxylic acid end group (E_1, 2.28 ppm, 2H), though in reality the only end group observed was the methylene group adjacent to the terminal hydroxyl group of a $PPDO_{2000}$ polyether segment (E_2, 4.29 ppm, 2H, **Figure 5.19** and **5.20**: **signal a**). M_0 was defined as the molecular weight of the poly(ester-*b*-ether-*b*-amide) repeat unit.

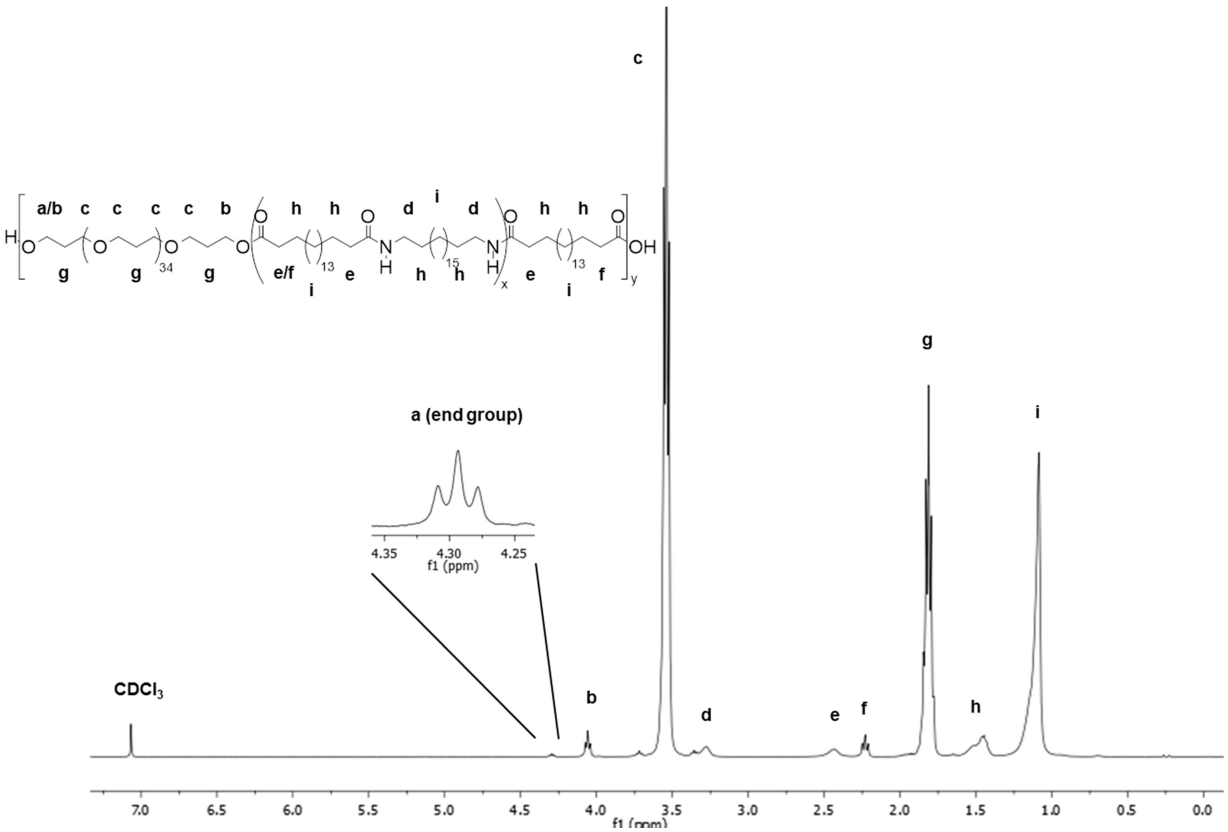

Figure 5.19: ^{1}H NMR spectrum ($CDCl_3$, 400 MHz) of TPA-$C_{19}PPDO_{2000}$-68wt%.

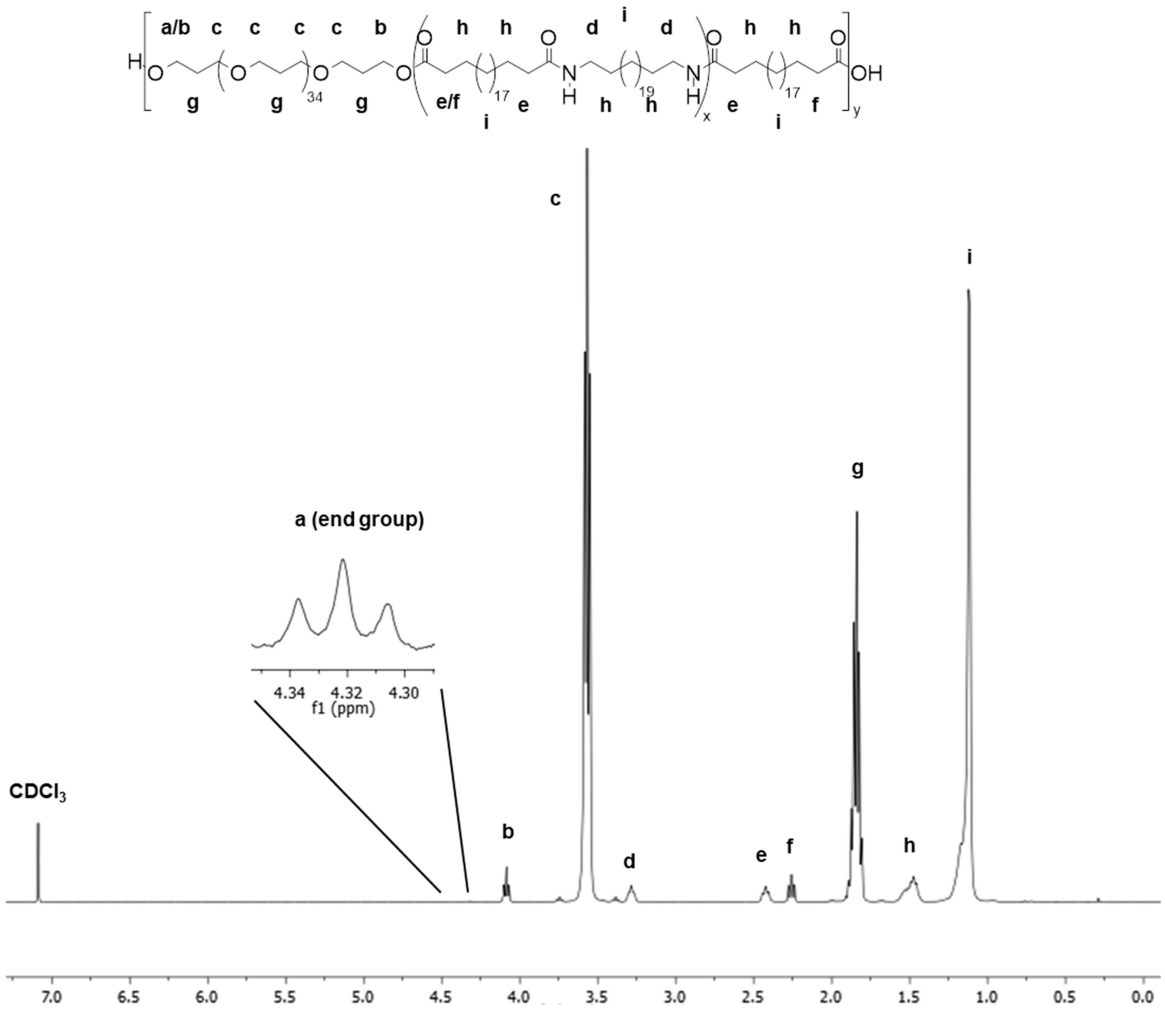

Figure 5.20: ^{1}H NMR spectrum ($CDCl_3$, 400 MHz) of TPA-C_{23}PPDO$_{2000}$-65wt%.

5.4.5. Moisture and water absorption tests

Moisture absorption

The moisture absorption from air (A_{air}) of poly(ester-*b*-ether-*b*-amide) copolymers was determined by measuring the weight loss of rectangular test specimens (length × width × thickness = 30 × 10 × 1 mm^3) cut from a larger rectangular test specimen prepared via injection molding (length × width × thickness = 90 × 10 × 1 mm^3) that were equilibrated at room temperature for 14 days and allowed to absorb moisture from air before being dried in an oven under forced-air convection at 50 °C. The dried samples were weighed in intervals of 24 hours until their weight remained stable (+/- 0.1 mg).

A_{air} was calculated using the following formula:

$$A_{air} = \frac{m_0 - m_{dry}}{m_{dry}} \cdot 100\%,$$

with m_0 being defined as the weight of the equilibrated test specimen and m_{dry} being defined as the weight of the sample after drying.

Water absorption

The water absorption (A_{H_2O}) of poly(ester-*b*-ether-*b*-amide) copolymers was measured in accordance with DIN EN ISO 62, method 1. The tests were performed on rectangular test specimens (length × width × thickness = 30 × 10 × 1 mm^3) cut from larger rectangular test specimen prepared via injection molding. The specimens were dried in an oven under forced-air convection at 50 °C and weighed at intervals of 24 hours until their weight was stable (+/- 0.1 mg). The dried samples were then immersed in distilled water (8 ml H_2O per 1 cm^2 specimen surface) at room temperature and weighed every 24 hours until their weight remained stable. The percentage increase in weight during immersion was calculated using the following formula:

$$A_{H_2O} = \frac{m_{wet} - m_{dry}}{m_{dry}} \cdot 100\%$$

with m_{wet} being defined as the weight of the test specimen after immersion in water for 24 hours and m_{dry} being defined as the weight of the dried test specimen. All cited data was obtained by averaging the results from three test specimens.

5.5. References

1. Drobny, J. G., *Handbook of Thermoplastic Elastomers*. William Andrew Publishing: Norwich, New York, **2007**.
2. a)Eustache, R.-P. Poly(Ether –b-Amide) Thermoplastic Elastomers: Structure, Properties and Applications. In *Handbook of Condensation Thermoplastic Elastomers*, Fakirov, S., (Ed.) Wiley-VCH: Weinheim, **2005**; b)Ukielski, R. Terpoly (Ester-b-Ether-b-Amide) Thermoplastic Elastomers: Synthesis, Structure, and Properties. In *Handbook of Condensation Thermoplastic Elastomers*, Fakirov, S., (Ed.) Wiley-VCH: Weinheim, Germany, **2005**, pp 117-140.
3. Malet, F. L. G. Thermoplastic Poly(Ether –b-Amide) TPE: Synthesis. In *Handbook of Condensation Thermoplastic Elastomers*, Fakirov, S., (Ed.) Wiley-VCH: Weinheim, Germany, **2005**, pp 243-257.
4. Legge, N. R.; Holden, G.; Schroeder, H., *Thermoplastic elastomers: A comprehensive review*. Carl Hansser Verlag: New York, USA, **1987**.
5. Thermoplastic polyamide elastomers: Synthesis, structures/properties, and applications. Gong, S.; Zhao, S.; Chen, X.; Liu, H.; Deng, J.; Li, S.; Feng, X.; Li, Y.; Wu, X.; Pan, K. *Macromolecular Materials and Engineering*, **2021,** *306* (12), 2100568.
6. Amide-containing segmented copolymers. Buckwalter, D. J.; Dennis, J. M.; Long, T. E. *Progress in Polymer Science*, **2015,** *45*, 1-22.
7. a)Block copolyetheramides. II. Synthesis and morphology of nylon-6 based block copolyetheramides. Chung, L. Z.; Kou, D. L.; Hu, A. T.; Tsai, H. B. *Journal of Polymer Science Part A: Polymer Chemistry*, **1992,** *30* (5), 951-953; b)Facile synthesis of polyamide 6 (PA6)-based thermoplastic elastomers with a well-defined microphase separation structure by melt polymerization. Yuan, R.; Fan, S.; Wu, D.; Wang, X.; Yu, J.; Chen, L.; Li, F. *Polymer Chemistry*, **2018,** *9* (11), 1327-1336; c)Multiblock poly (ether-ester-amide)s based on polyamide-6 and poly (ethylene glycol), 1. Effect of polyether segment length on the properties of poly (ether-ester-amide)s with various polyamide/polyether ratios. Fakirov, S.; Goranov, K.; Bosvelieva, E.; Du Chesne, A. *Die Makromolekulare Chemie: Macromolecular Chemistry and Physics*, **1992,** *193* (9), 2391-2404; d)Multiblock poly (ether-ester-amide)s based on polyamide-6 and poly (ethylene glycol), 2 Effect of composition and soft segment length on the structure of poly (ether-ester-amide s as revealed by X-ray scattering. Apostolov, A. A.; Bosvelieva, E.; Du Chesne, A.; Goranov, K.; Fakirov, S. *Die Makromolekulare Chemie: Macromolecular Chemistry and Physics*, **1993,** *194* (8), 2267-2277.

8. Synthese et caracterisation de copolycondensats sequences poly (amide-seq-ether)—II. Poly-condensation d'oligomeres polyamides-11 ω, ω'diacides ou diesters avec des oligomeres polyethers ω, ω'dihydroxy. Deleens, G.; Foy, P.; Maréchal, E. *European Polymer Journal*, **1977,** *13* (5), 343-351.
9. a)The Brill transition in polyether-b-amide segmented copolymers and composition dependence. Zhu, P.; Dong, X.; Cao, Y.; Wang, L.; Liu, X.; Wang, Z.; Wang, D. *European Polymer Journal*, **2017,** *93*, 334-346; b)High elasticity and corresponding microstructure origin of novel long chain poly (amide-block-ether) filament fibers. Wang, L.; Dong, X.; Zhu, P.; Zhang, X.; Liu, X.; Wang, D. *European Polymer Journal*, **2017,** *90*, 171-182; c)Strain-induced crystallization of segmented copolymers: Deviation from the classic deformation mechanism. Zhu, P.; Dong, X.; Wang, D. *Macromolecules*, **2017,** *50* (10), 3911-3921.
10. Ouhadi, T.; Abdou-Sabet, T.; Wussow, H.-G.; Ryan, L. M.; Plummer, L.; Baumann, F. E.; Lohmar, J.; F, V. H.; Malet, F. L. G. Thermoplastic Elastomers. In *Ullmann's Encyclopedia of Industrial Chemistry*, Gerhartz, W.; Elvers, B., (Eds.), Wiley-VCH: Weinheim, Germany, **2000**, pp 1-40.
11. a)Maréchal, E. Creation and Development of Thermoplastic Elastomers, and Their Position Among Organic Materials. In *Handbook of Condensation Thermoplastic Elastomers*, Fakirov, S., (Ed.) Wiley-VCH: Weinheim, Germany, **2005**; b)Maréchal, E. Polycondensation Reactions in Thermoplastic Elastomer Chemistry: State of the Art, Trends, and Future Developments. In *Handbook of Condensation Thermoplastic Elastomers*, Fakirov, S., (Ed.) Wiley-VCH: Weinheim, Germany, **2005**.
12. Copolyesteramide aus laurinlactam, 1, 10-decandicarbonsäure und α, ω-dihydroxy-(polytetrahydrofuran). Mumcu, S.; Burzin, K.; Felsmann, R.; Feinauer, R. *Die Angewandte Makromolekulare Chemie: Applied Macromolecular Chemistry and Physics*, **1978,** *74* (1), 49-60.
13. Gugliuzza, A. Poly(ether-block-amide) copolymers synthesis, properties and applications. In *Handbook of engineering and specialty thermoplastics*, Thomas, S.; Visakh, P. M., (Eds.), John Wiley & Sons Inc.: Hoboken, NJ, **2012**, pp 111–140.
14. A Biomechanical Double Sac (Pericardium-Pebax) for Specially Shaped Artificial Ventricles: A Computerized Study to Evaluate Its Mechanical and Volumetric Properties. Chatel, D.; Delamare, L.; Dang, P.; Lebouvier, D.; Trocherie, F. *Artificial Organs*, **1997,** *21* (10), 1098-1104.
15. a)Pebax® 2533/graphene oxide nanocomposite membranes for carbon capture. Casadei, R.; Giacinti Baschetti, M.; Yoo, M. J.; Park, H. B.; Giorgini, L. *Membranes*, **2020,** *10* (8), 188;

b)Preparation of PEBAX-1074/modified ZIF-8 nanoparticles mixed matrix membranes for CO2 removal from natural gas. Jameh, A. A.; Mohammadi, T.; Bakhtiari, O. *Separation and Purification Technology*, **2020,** *231*, 115900.

16. Development of Breathable Pebax®/PEG Films for Optimization of the Shelf-Life of Fresh Agri-Food Products. Préfol, T.; Gain, O.; Sudre, G.; Gouanvé, F.; Espuche, E. *Membranes*, **2021,** *11* (9), 692.
17. Synthesis and characterization of poly (ether-block-amide) and application as permanent antistatic agent. Wang, G.; Xue, B. *Journal of applied polymer science*, **2010,** *118* (4), 2448-2453.
18. Ehrenstein, G. W., *Polymeric Materials - Structure, Properties, Applications*. Carl Hanser Verlag: Munich, Germany, **2012**.
19. Elias, H.-G., *Macromolecules*. Vol. 3: *Physical Structures and Properties*, Wiley-VCH: Weinheim, **2005**.
20. a)Highly selective formation of unsaturated esters or cascade reactions to α, ω-diesters by the methoxycarbonylation of alkynes catalysed by palladium complexes of 1, 2-bis (ditertbutylphosphinomethyl) benzene. Núñez-Magro, A. A.; Robb, L.-M.; Pogorzelec, P. J.; Slawin, A. M.; Eastham, G. R.; Cole-Hamilton, D. J. *Chemical Science*, **2010,** *1* (6), 723-730; b)Mechanistic features of isomerizing alkoxycarbonylation of methyl oleate. Roesle, P.; Dürr, C. J.; Möller, H. M.; Cavallo, L.; Caporaso, L.; Mecking, S. *Journal of the American Chemical Society*, **2012,** *134* (42), 17696-17703; c)Dicarboxylic acid esters from the carbonylation of unsaturated esters under mild conditions. Jiménez-Rodriguez, C.; Eastham, G. R.; Cole-Hamilton, D. J. *Inorganic Chemistry Communications*, **2005,** *8* (10), 878-881; d)Highly selective formation of linear esters from terminal and internal alkenes catalysed by palladium complexes of bis-(di-tert-butylphosphinomethyl) benzene. Jiménez-Rodriguez, C.; Foster, D. F.; Eastham, G. R.; Cole-Hamilton, D. J. *Chemical communications*, **2004,** (15), 1720-1721.
21. Long-chain linear C_{19} and C_{23} monomers and polycondensates from unsaturated fatty acid esters. Stempfle, F.; Quinzler, D.; Heckler, I.; Mecking, S. *Macromolecules*, **2011,** *44* (11), 4159-4166.
22. Long-chain aliphatic polymers to bridge the gap between semicrystalline polyolefins and traditional polycondensates. Stempfle, F.; Ortmann, P.; Mecking, S. *Chemical reviews*, **2016,** *116* (7), 4597-4641.
23. a)Eller, K.; Enkes, E.; Rossbacher, R.; Höke, H. Amines, Aliphatic. In *Ullmann's Encyclopedia of Industrial Chemistry*, Gerhartz, W.; Elvers, B., (Eds.), Wiley-VCH: Weinheim, **2000**; b)Smiley, R.

A. Hexamethylenediamine. In *Ullmann's Encyclopedia of Industrial Chemistry*, Gerhartz, W.; Elvers, B., (Eds.), Wiley-VCH: Weinheim, Germany, **2000**.

24. a)Schwaderer, J. B. *Ruthenium Catalysed Amination of Bio-Based Diols - Building Blocks for Polyamides from Renewables*. Master Thesis, University of Konstanz, Konstanz, Germany, **2016**; b)Diamines for Polymer Materials via Direct Amination of Lipid- and Lignocellulose-based Alcohols with NH_3. Pingen, D.; Schwaderer, J. B.; Walter, J.; Wen, J.; Murray, G.; Vogt, D.; Mecking, S. *ChemCatChem*, **2018,** *10* (14), 3027-3033.
25. Walter, J. *Polyamides from Renewable Resources*. Master Thesis, University of Konstanz, Konstanz, Germany, **2015**.
26. Quinzler, D. *Linear Semicrystalline Polyesters and Polyamides from Plant Oil Fatty Acids via Catalytic Alkoxycarbonylation*. Ph.D. Thesis, University of Konstanz, Konstanz, Germany, **2014**.
27. a)Selective synthesis of primary amines directly from alcohols and ammonia. Gunanathan, C.; Milstein, D. *Angewandte Chemie*, **2008,** *120* (45), 8789-8792; b)Selective Synthesis of Primary Amines Directly from Alcohols and Ammonia. Gunanathan, C.; Milstein, D. *Angewandte Chemie International Edition*, **2008,** *47* (45), 8661-8664.
28. a)α, ω-Functionalized C_{19} Monomers. Walther, G.; Deutsch, J.; Martin, A.; Baumann, F. E.; Fridag, D.; Franke, R.; Köckritz, A. *ChemSusChem*, **2011,** *4* (8), 1052-1054; b)Walther, G.; Deutsch, J.; Martin, A.; Baumann, F.-E.; Fridag, D.; Köckritz, A. Poster at the 4th Workshop on *Fats and Oils as Renewable Feedstock for the Chemical Industry*, Karlsruhe, Germany, March 20-22, **2011**.
29. Selected methods for the reduction of the azido group. Amantini, D.; Fringuelli, F.; Pizza, F.; Vaccaro, L. *Organic preparations and procedures international*, **2002,** *34* (2), 109-147.
30. Kohan, M. I.; Mestemacher, S. A.; Pagilagan, R. U.; Redmond, K. Polyamides. In *Ullmann's Encyclopedia of Industrial Chemistry*, Gerhartz, W.; Elvers, B., (Eds.), Wiley-VCH: Weinheim, **2000**.
31. *Transparent Polyamide Elastomer*. Suzuki, Y.; Nakamura, M.; Aochiama, A. (Asahi), European Patent EP0221188 (A1), **1987**.
32. Elias, H.-G., *Macromolecules*. Vol. 1: *Chemical Structures and Syntheses*, Wiley-VCH: Weinheim, **2005**.
33. a)A continuum theory of rheological phenomena. Weissenberg, K. *Nature*, **1947,** *159* (4035), 310-311; b)Bird, R. B.; Armstrong, R. C.; Hassager, O., *Dynamics of polymeric liquids*. Vol. 1: Fluid mechanics, John Wiley: New York, **1987**.

34. Hydrogen bonding in micro-phase separation of poly (polyamide 12-block-polytetrahydrofuran) alternating block copolymer: Enthalpies and molecular movements. Wen, L.; Zhang, J.; Zhou, T.; Zhang, A. *Vibrational Spectroscopy*, **2016,** *86*, 160-172.
35. a)Hydrogen bonding in polymers: infrared temperature studies of an amorphous polyamide. Skrovanek, D. J.; Howe, S. E.; Painter, P. C.; Coleman, M. M. *Macromolecules*, **1985,** *18* (9), 1676-1683; b)Hydrogen bonding in polymers. 2. Infrared temperature studies of nylon 11. Skrovanek, D. J.; Painter, P. C.; Coleman, M. M. *Macromolecules*, **1986,** *19* (3), 699-705.
36. Segmental orientations and deformation mechanism of poly (ether-block-amide) films. Song, Y.; Yamamoto, H.; Nemoto, N. *Macromolecules*, **2004,** *37* (16), 6219-6226.
37. Infrared Studies of Block Copolymers. West, J. C.; Cooper, S. L. *Journal of Polymer Science: Polymer Symposia*, **1977,** *60*, 127-150.
38. a)Polyamides from lactams by centrifugal molding via anionic ring-opening polymerization. Rusu, G.; Ueda, K.; Rusu, E.; Rusu, M. *Polymer*, **2001,** *42* (13), 5669-5678; b)Morphology and properties of nylon 6-polyoxypropylene-nylon 6 block copolymers. Yeh, J.-L.; Kuo, J.-F.; Chen, C.-Y. *Materials chemistry and physics*, **1994,** *37* (2), 161-169.
39. Infrared spectra and crystal structures of polyamides. Miyake, A. *Journal of Polymer Science*, **1960,** *44* (143), 223-232.
40. Aharoni, S. M., *n-Nylons: Their Synthesis, Structure and Properties*. Wiley-VCH: Weinheim, Germany, **1997**.
41. Vieweg, R.; Müller, A., *Kunststoff-Handbuch. Band VI: Polyamide*. Carl Hanser Verlag: Munich, Germany, **1966**.
42. Studies on crystallization of high polymers by differential thermal analysis. Inoue, M. *Journal of Polymer Science Part A: General Papers*, **1963,** *1* (8), 2697-2709.
43. Chain-folded lamellar crystals of aliphatic polyamides. Investigation of nylons 4.8, 4.10, 4.12, 6.10, 6.12, 6.18 and 8.12. Jones, N.; Atkins, E.; Hill, M.; Cooper, S.; Franco, L. *Polymer*, **1997,** *38* (11), 2689-2699.
44. Crystal Transition of Nylon-12, 12 under Drawing and Annealing. Song, J.; Zhang, H.; Ren, M.; Chen, Q.; Sun, X.; Wang, S.; Zhang, H.; Mo, Z. *Macromolecular rapid communications*, **2005,** *26* (6), 487-490.
45. An investigation of the structures of polyamide series. Kinoshita, Y. *Die Makromolekulare Chemie: Macromolecular Chemistry and Physics*, **1959,** *33* (1), 1-20.

46. a)Linear semicrystalline polyesters from fatty acids by complete feedstock molecule utilization. Quinzler, D.; Mecking, S. *Angewandte Chemie International Edition*, **2010,** *49* (25), 4306-4308; b)Linear semicrystalline polyesters from fatty acids by complete feedstock molecule utilization. Quinzler, D.; Mecking, S. *Angewandte Chemie*, **2010,** *122* (25), 4402-4404.
47. Hydrogen bonding, mobility, and structural transitions in aliphatic polyamides. Murthy, N. S. *Journal of Polymer Science Part B: Polymer Physics*, **2006,** *44* (13), 1763-1782.
48. Gaymans, R. J. Polyamides. In *Synthetic Methods in Step-Growth Polymers*, Rogers, M. E.; Long, T. E., (Eds.), John Wiley and Sons: New York, USA, **2003**.
49. NMR investigations of in-situ stretched block copolymers of poly (butylene terephthalate) and poly (tetramethylene oxide). Schmidt, A.; Veeman, W. S.; Litvinov, V. M.; Gabriëlse, W. *Macromolecules*, **1998,** *31* (5), 1652-1660.
50. New polyamides with long alkane segments: nylon 6.24 and 6.34. Ehrenstein, M.; Dellsperger, S.; Kocher, C.; Stutzmann, N.; Weder, C.; Smith, P. *Polymer*, **2000,** *41* (10), 3531-3539.
51. Synthesis of copolyamides containing octadecanedioic acid: An investigation of nylon 6/6, 18 in various ratios. Bennett, C.; Zeng, J.; Kumar, S.; Mathias, L. J. *Journal of applied polymer science*, **2006,** *99* (5), 2062-2067.
52. Jia, N.; Kagan, V. A. Mechanical performance of polyamides with influence of moisture and temperature–accurate evaluation and better understanding. In *Plastics Failure - Analysis and Prevention*, Moalli, J., (Ed.) William Andrew Inc.: Norwich, USA, **2001**, pp 95-104.

6. Conclusive Summary

Synthetic polymers are an integral part of modern society, with especially engineering plastics like thermoplastic elastomers (TPEs) experiencing constant growth during the past few decades. TPEs constitute a relatively new class of polymeric material consisting of polymer blends and copolymers that combine the ductility and elastomeric properties of classic elastomers with the thermal processability of thermoplastics. This unique combination of material properties is possible because TPEs rely on physical forces like crystallization instead of the formation of irreversible covalent bonds to generate the crosslinking necessary to impart elastomeric behavior. In case of segmented copolymer TPEs, crystallizable 'hard' blocks alternate with amorphous, thermodynamically incompatible 'soft' blocks to produce microphase-separated materials in which semi-crystalline hard domains dispersed within an amorphous soft matrix serve as thermoreversible physical crosslinks.[1],[2],[3] However, as with most synthetic polymers, the production of TPEs today is still based on fossil resources. In order to make TPE production sustainable and develop materials with novel sets of properties, research is increasingly turning towards natural resources as an alternative source for novel monomers. In this context, unsaturated fatty acids from plant oils have garnered much interest in recent years because thanks to advances in catalyst research it is now possible to selectively convert unsaturated fatty acid substrates into linear long-chain α,ω-difunctionalized compounds using isomerizing alkoxycarbonylation (**Figure 6.1**).[4],[5] The thus obtained polycondensation monomers can be used to produce novel long-chain aliphatic polycondensates like polyesters[5e-g],[6] and polyamides[5f, g],[6a] with a very low functional group density that, among other material properties, can impact crystallization behavior.[5f, g],[6b],[7] For example, semi-crystalline linear long-chain polyesters exhibit a polyethylene-like orthorhombic crystal structure and unusually high melting points that approach the values recorded for linear polyethylene.[5e],[6a],[7] Because of this, plant oil-derived long-chain α,ω-difunctionalized compounds are interesting building blocks for the development of novel segmented copolymer TPEs with different types of all-aliphatic long-chain polycondensate hard blocks.

With this information in mind, linear long-chain dimethyl 1,19-nonadecanedioate (C_{19}) and diethyl 1,23-tricosanedioate (C_{23}) were prepared in polycondensation grade purity (> 99 %) either directly from readily available technical grade sunflower oil (C_{18}) or an isolated unsaturated fatty acid ester (C_{22}) respectively using a simplified isomerizing alkoxycarbonylation protocol. It could be shown that the presence of traces of water as well as upscaling to a batch size of almost 200 g have no negative

impact on the reaction. Subsequent reduction of the thus obtained α,ω-diesters with $LiAlH_4$ yielded the corresponding linear long-chain 1,19-nonadecanediol and 1,23-tricosanediol. Copolymerization of the synthesized linear long-chain α,ω-diesters with their corresponding linear long-chain α,ω-diols and a sugar-derived dihydroxy-terminated poly(1,3-propanediol) polyether soft segment ($PPDO_{1000}$ or $PPDO_{2000}$) in varying monomer ratios via melt polycondensation yielded a series of high molecular weight segmented poly(ester-*b*-ether) copolymers with long-chain PE-19.19 or PE-23.23 polyester hard segments(**Figure 6.1**) that were all-renewable and qualified as thermoplastic elastomers.

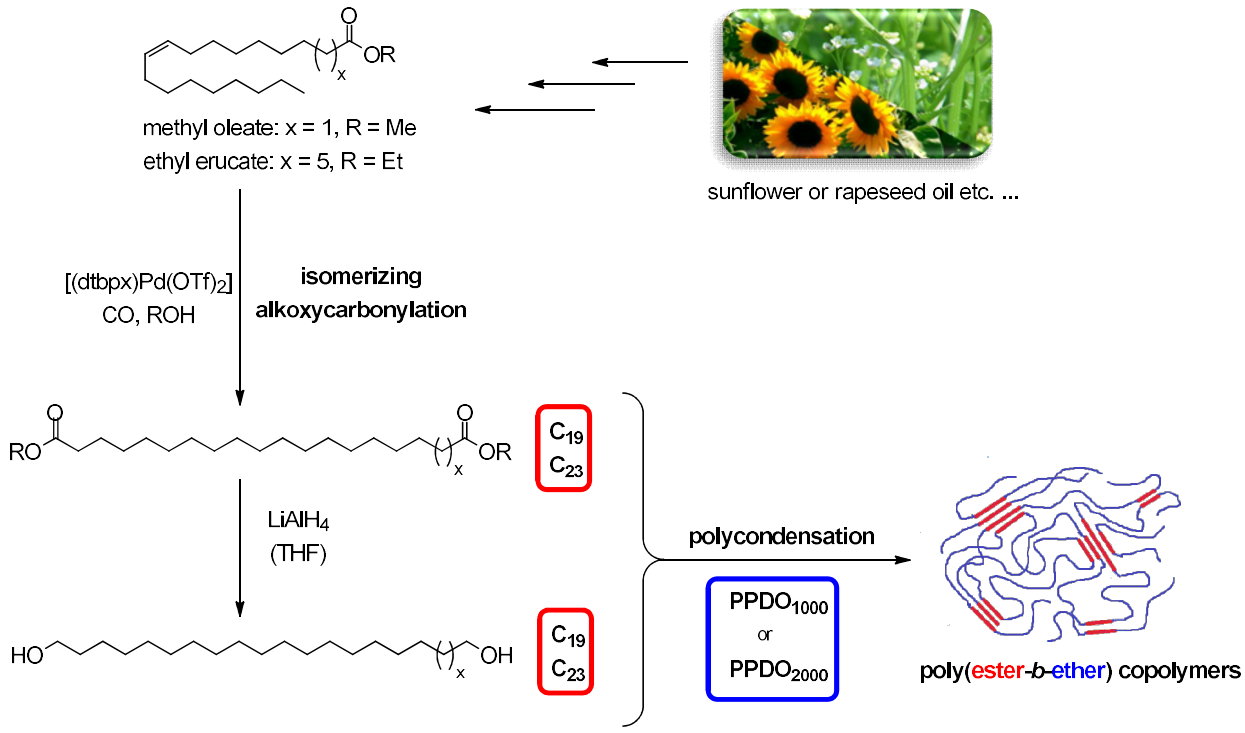

Figure 6.1: Synthesis of all-renewable segmented thermoplastic copolyester elastomers with aliphatic long-chain polyester hard segments derived from plant oils.[8]

Thanks to the long methylene sequences present in the aliphatic polyester hard segments, crystallization was driven by Van-der-Waals interactions, resulting in a polyethylene-like orthorhombic crystal structure and melting points reaching unusually high values of up to 95 °C depending on the exact copolymer composition. In order to make processing via standard thermoplastic processing techniques like injection molding possible, the addition of the respective long-chain C_{19} or C_{23}-diol to the reaction mixture as a chain extender proved necessary to ensure that the upper melt and/or crystallization points associated with the polyester hard domains exceeded

25 °C. Investigation of the mechanical properties using tensile tests and cyclic hysteresis testing performed on injection molded test specimen confirmed that even short all-aliphatic PE-19.19 and PE-23.23 polyester hard blocks are capable of functioning as physical crosslinks and impart elastomeric behavior. The synthesized materials also proved to be highly ductile, with elongations at break in some cases exceeding 1100 %. Simultaneously, the residual strain after 10 consecutive cycles of repeated elongation to 100 % remained as low as 15 %. An especially favorable combination of excellent elasticity, good ductility, and a high upper melting point of 86 °C was observed for TPC-C_{23}PPDO$_{2000}$-65wt%, a poly(ester-*b*-ether) copolymer with polyester hard segments derived from long-chain C_{23} monomers and a mol ratio of hard diol to soft PPDO$_{2000}$ macrodiol of 1:1. In comparison, a comparable all-aliphatic thermoplastic copolyester elastomer with similar block length distribution and polyester hard segments based on commercially available mid-chain dimethyl 1,12-dodecanedioate and 1,12-dodecanediol, TPC-C_{12}PPDO$_{2000}$-62wt%, exhibited similar elastomeric behavior but reduced ductility and a much lower melting point of only 66 °C due to the higher ester group density resulting in more crystal imperfections in the polyester hard domains.

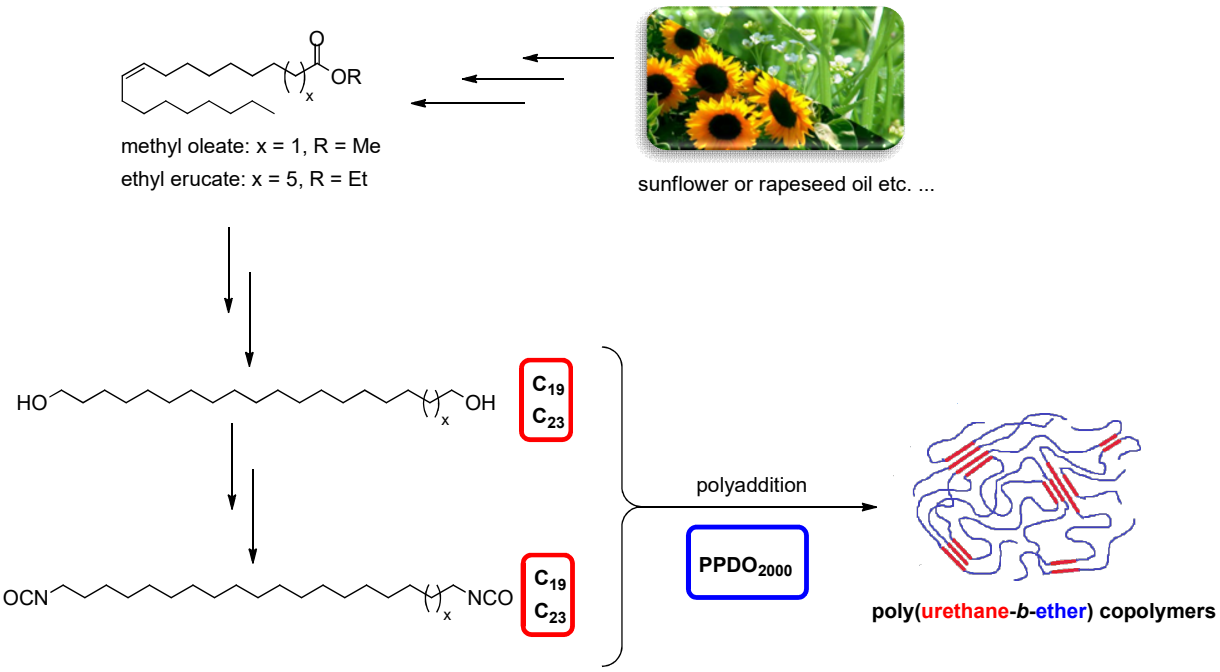

Figure 6.2: Synthesis of segmented thermoplastic polyurethane elastomers with long-chain aliphatic polyurethane hard segments derived from plant oils.[8]

Similarly, plant oil-derived unsaturated fatty acid esters were used as a starting point to prepare all-renewable segmented copolymer TPEs with long-chain aliphatic polyurethane hard segments via the diisocyanate polyaddition approach (**Figure 6.2**). Starting with the isomerizing alkoxycarbonylation of methyl oleate and ethyl erucate respectively, a multistep synthesis route was developed to ultimately yield long-chain 1,19-nonadecane diisocyanate and 1,23-tricosane diisocyanate in polycondensation grade purity (> 99 %) as the necessary polyurethane precursors. The α,ω-diesters obtained from isomerizing alkoxycarbonylation were reduced to the corresponding α,ω-diols using $LiAlH_4$, which was followed by an Appel II reaction to generate 1,19-dibromononadecane and 1,23-dibromotricosane on a 10 g scale and in yields of 88 % and 94 % respectively. In the last, decisive step the bromo substituents were replaced with isocyanate groups in a nucleophilic substitution reaction with KOCN in DMF at 120 °C (**Figure 6.3**).

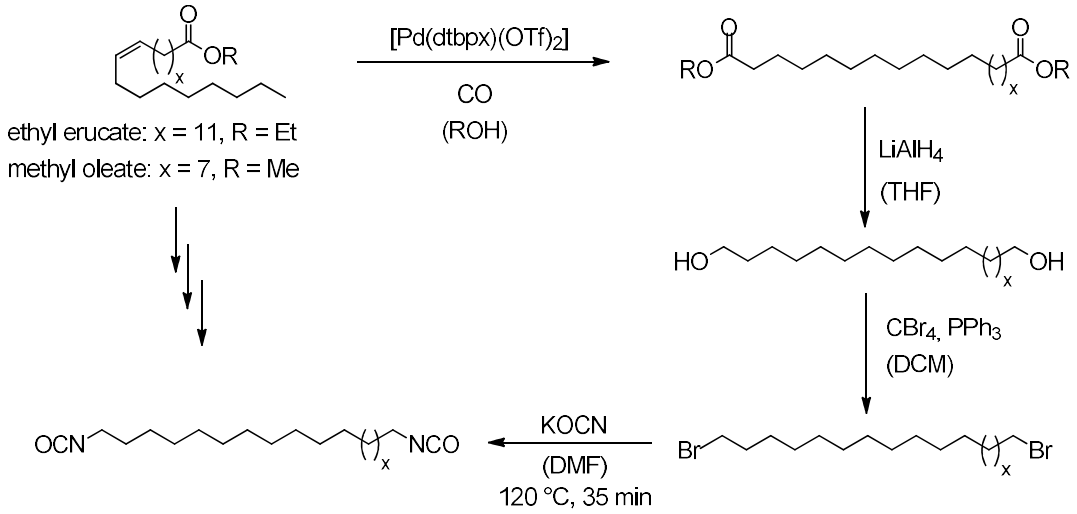

Figure 6.3: multistep synthesis for the preparation of 1,19-nonadecane diisocyanate and 1,23-tricosane diisocyanate starting from plan oil-derived unsaturated fatty acid esters.

Extensive optimization of the reaction conditions and the work-up procedure proved to be necessary in order to maximize yields and avoid side product formation, especially the generation of isocyanurate and ultimately polyisocyanurate compounds via isocyanate trimerization. This included parameters like the choice of solvent, the reaction temperature, and the reaction time relating to the batch size, in addition to choosing the right geometry for the distillation apparatus (**Figure 6.4**) to make effective distillation possible and obtain pure 1,19-nonadecane diisocyanate and 1,23-tricosane diisocyanate in yields of up to 35 % and 40 % respectively. Despite this, the scale of the reaction was

limited to less than 1 g of product due to the high reactivity of the isocyanate groups and the limited size of the cooling finger used for distillation.

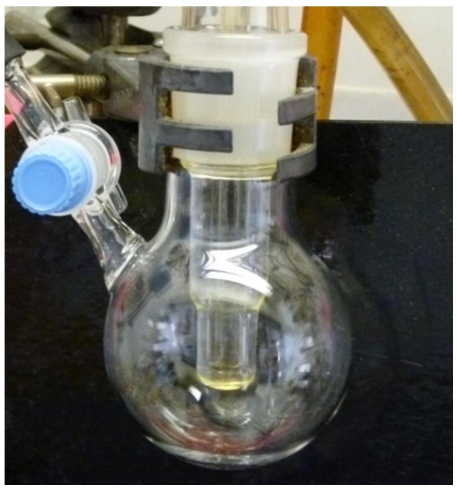

Figure 6.4: Cooling finger used for purification of long-chain aliphatic diisocyanates via distillation.

Subsequent polyaddition of 1,19-nonadecane diisocyanate and 1,23-tricosane diisocyanate respectively with varying ratios of their corresponding long-chain α,ω-diols and the amorphous $PPDO_{2000}$ polyether macrodiol in a solution polymerization procedure yielded segmented poly(urethane-*b*-ether) copolymers with a number average molecular weight of up to 5.0 x 10^4 g mol^{-1} that qualified as TPEs (**Figure 6.2**). Investigation of the polymer morphology of the synthesized thermoplastic polyurethane elastomers (TPUs) via WAXD confirmed that despite the long methylene sequences present in the aliphatic polyurethane hard segments crystallization in the hard domains is still driven by the formation of hydrogen bonds between urethane groups. Consequently, the upper melting points of these materials exceeded the melting points observed for comparable TPEs on polyester basis and, depending on the exact polymer composition, lie between 62 and 116 °C. Though, the reduced concentration of urethane groups still had an impact on the upper melting temperatures as a comparison between long-chain TPU-$C_{23}PPDO_{2000}$-63wt% and its mid-chain PU-12.12-based analogue, TPU-$C_{12}PPDO_{2000}$-59wt%, revealed. The former exhibited an upper melting point of 116 °C while the latter did not melt until a temperature of 129 °C was reached. Simultaneously, investigation of the phase structure via FTIR spectroscopy revealed that the degree of phase separation in long-chain TPUs was about 85 % independent of the exact copolymer composition, which constituted a drastic improvement when compared to mid-chain

TPU-$C_{12}PPDO_{2000}$-59wt% of only about 56 %. In addition, all synthesized long-chain TPUs exhibited acceptable or good ductility and good elastomeric behavior during tensile testing and cyclic hysteresis testing respectively. A direct correlation between increasing polyurethane hard segment content and decreasing ductility and elasticity was recorded, with the best mechanical properties being observed for copolymers whose hard segments consisted only of isolated diisocyanate units and that did not contain any long-chain diol as a chain extender. For example, TPU-$C_{19}PPDO_{2000}$-85wt% consisting only of 1,19-nonadecane diisocyanate and $PPDO_{2000}$ polyether macrodiol exhibited an elongation at break of 470 °C and a residual strain after 10 cycles of hysteresis testing of 26 °C. A direct comparison between long-chain TPU-$C_{23}PPDO_{2000}$-63wt% and mid-chain TPU-$C_{12}PPDO_{2000}$-59wt% revealed that the reduced hydrogen bond density in long-chain TPUs had a negative impact on ductility as well as elasticity.

In addition, the utilization of plant oil-derived methyl oleate and ethyl erucate as starting materials for the generation of TPEs based on linear long-chain aliphatic polyamide hard segments was investigated. Therefore, a multistep synthesis route for the transformation of the aforementioned unsaturated fatty acid esters into linear long-chain 1,19-nonadecane diamine and 1,23-tricosane diamine via reduction of the corresponding long-chain C_{19} and C_{23} α,ω-diazides was successfully developed (**Figure 6.5**). Starting with the reduction of the C_{19} and C_{23} α,ω-diesters prepared via isomerizing alkoxycarbonylation to obtain 1,19-nonadecanediol and 1,23-tricosanediol, the terminal hydroxyl groups were transformed into mesylate leaving groups using MsCl and NEt_3. Subsequent replacement of said leaving groups with azide groups via a nucleophilic substitution reaction with NaN_3 yielded 1,19-nonadecane diazide and 1,23-tricosane diazide respectively. In the last, decisive step the terminal azide groups were reduced to primary amine groups using either $LiAlH_4$ or via catalytic hydrogenation over Pd/C (10 wt.%). The first approach proved to be highly selective but also volatile in nature which limited upscaling of the reaction, while the second synthesis method was found to be highly susceptible to side reactions, specifically the generation of impossible to remove nitrile and secondary amine byproducts. Substrate concentration and catalyst load were identified as the decisive factors determining selectivity, while hydrogen pressure did not significantly affect the reaction outcome. By reducing the catalyst load to 2.5 wt.% and limiting the substrate concentration to 0.2 M both side reactions could be mostly suppressed, ultimately allowing for the synthesis of long-chain 1,19-nonadecane diamine in polycondensation grade purity (> 98 %) and in a yield of 85 % even at a batch size of 10 g.

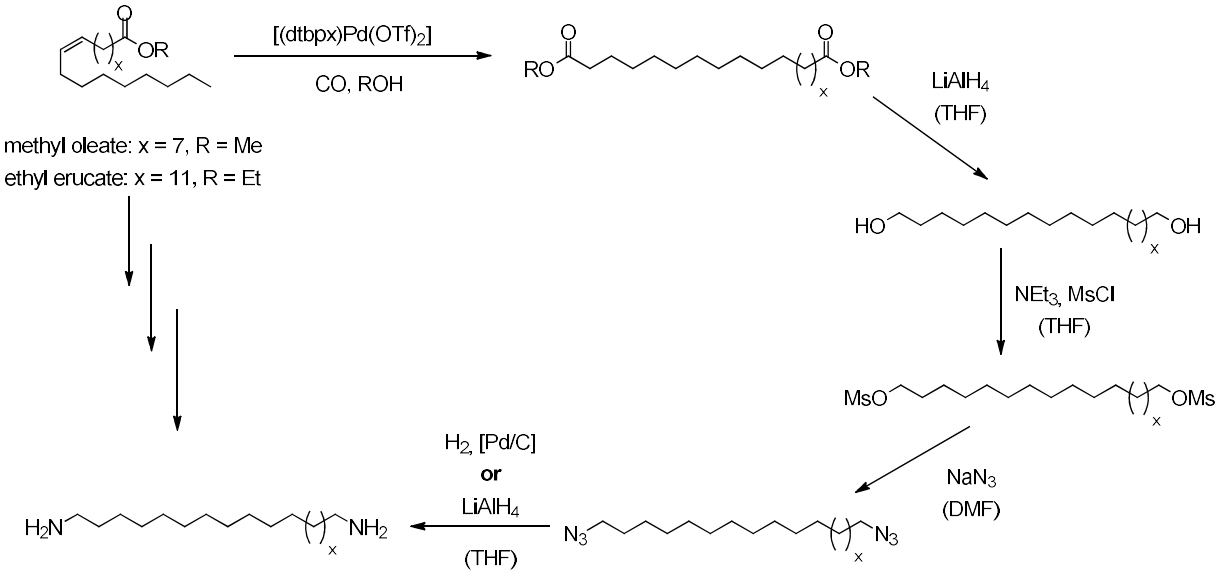

Figure 6.5: Multistep synthesis of 1,19-nonadecane diamine and 1,23-tricosane diamine starting from unsaturated fatty acid esters from plant oils.

In contrast to similar segmented long-chain TPEs on polyester or polyurethane basis, the preparation of comparable thermoplastic polyamide elastomers (TPAs) derived from hard C_{19} or C_{23} monomers and a $PPDO_{2000}$ polyether macrodiol soft segment required the development of a two-step synthesis procedure as the desired materials represent segmented poly(ester-*b*-ether-*b*-amide) multi-block copolymers containing more than one type of functional group linkage between the different blocks. This also resulted in a slightly different block length distribution in the polyamide hard segments. Melt polyamidation of 1,19-nonadecane diamine or 1,23-tricosane diamine respectively with excess of the corresponding C_{19} and C_{23} dicarboxylic acids in different ratios yielded various short, dicarboxyl-terminated PA-19.19 and PA-23.23 oligomers that, in the second melt polyesterification step, reacted with the $PPDO_{2000}$ macrodiol to produce a series of TPAs based on long-chain polyamide hard segments that reached number average molecular weights of up to $16{,}4 \times 10^4$ g mol^{-1}. As the long-chain polyamidation products produced in the first polymerization step also always contained varying small amounts of unconverted 1,19-nonadecane diacid or 1,23-tricosane diacid, the thus obtained TPAs were not segmented poly(ether-*b*-amide) copolymers but instead poly(ester-*b*-ether-*b*-amide) copolymers also containing isolated long-chain diester units (**Figure 6.6**).

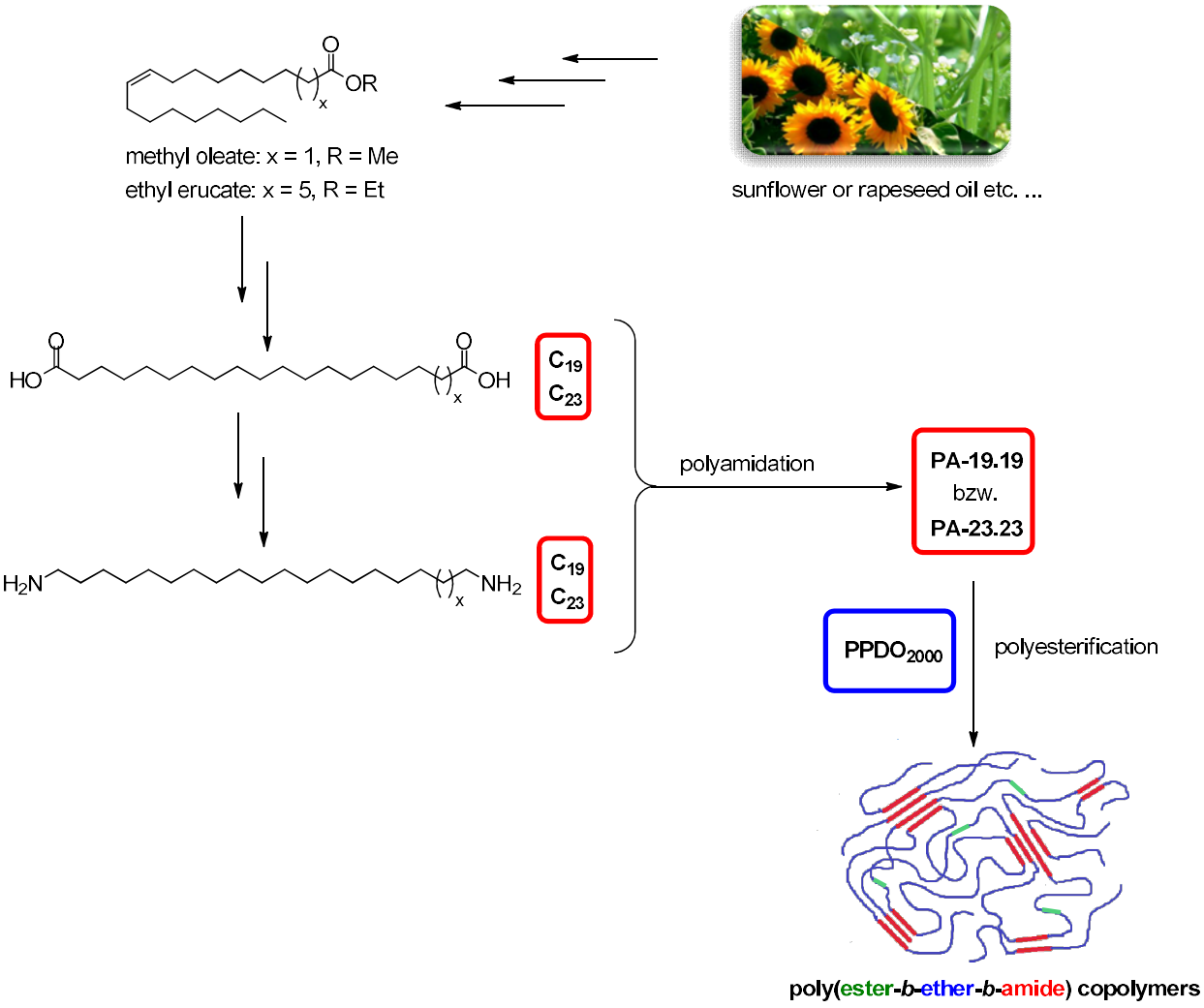

Figure 6.6: Synthesis of segmented thermoplastic polyamide elastomers based on long-chain aliphatic polyamide hard segments derived from plant oils.[8]

Investigation of the phase structure using FTIR spectroscopy confirmed the formation of strong hydrogen bonds between amide groups in a selective manner, with no participation of ester groups, which resulted in a very high degree of phase separation of the polyamide hard phase of about 95 %. Analysis of the crystal structure via WAXD revealed that crystallization of the polyamide hard blocks was driven by hydrogen bond formation, even in PEEAs based on long-chain monomers, which resulted in the formation of crystalline polyamide hard domains with a complicated polymorphic crystal structure. Isolated C_{19} and C_{23} diester blocks did not form a second type of crystalline hard phase with polyethylene-like crystallinity.

Upper melting points of the synthesized long-chain PEEAS ranged from 128 and 152 °C depending on exact polymer composition, thereby exceeding the upper melting points recorded for comparable long-chain TPCs and TPUs with similar block length distribution. The complicated polymorphic crystal structure of the synthesized long-chain PEEAS also resulted in their DSC thermograms featuring several very broad thermal transitions associated with changes in hydrogen bonds and the crystal structure. A comparison of the thermal properties of long-chain, PA-23.23-based TPA-$C_{23}PPDO_{2000}$-65wt% with its mid-chain PA-12.12-based analogue, TPA-$C_{12}PPDO_{2000}$-62wt%, of otherwise comparable overall composition revealed that the reduced hydrogen bond density in long-chain PEEAs led to a drastic decrease in the upper melting point by about 30 °C. In addition to simplifying thermoplastic processing, the lower hydrogen bond concentration also had a positive impact on moisture and water absorption. Under wet conditions, mid-chain TPA-$C_{12}PPDO_{2000}$-62wt% absorbed about 200 % more water than long-chain TPA-$C_{23}PPDO_{2000}$-65wt%. In comparison to long-chain TPCs and TPUs of similar overall composition, the synthesized long-chain PEEAs were generally less ductile while their elastomeric properties varied strongly. In general, an increasing content of $PPDO_{2000}$ polyether soft phase had a positive impact on elasticity, with copolymers containing more than 75 wt.% of $PPDO_{2000}$ exhibiting a residual strain of less than 10 % after cyclic hysteresis testing. When the mechanical properties of long-chain TPA-$C_{23}PPDO_{2000}$-65wt% were compared directly to mid-chain TPA-$C_{12}PPDO_{2000}$-62wt%, it was revealed that longer methylene sequences in the aliphatic polyamide hard blocks had a negative impact on ductility but improved elastomeric behavior.

6.1. References

1. Drobny, J. G., *Handbook of Thermoplastic Elastomers*. William Andrew Publishing: Norwich, New York, **2007**.
2. Ouhadi, T.; Abdou-Sabet, T.; Wussow, H.-G.; Ryan, L. M.; Plummer, L.; Baumann, F. E.; Lohmar, J.; F, V. H.; Malet, F. L. G. Thermoplastic Elastomers. In *Ullmann's Encyclopedia of Industrial Chemistry*, Gerhartz, W.; Elvers, B., (Eds.), Wiley-VCH: Weinheim, Germany, **2000**, pp 1-40.
3. Morphology of segmented polyester thermoplastic elastomers. Cella, R. J. *Journal of Polymer Science: Polymer Symposia*, **1973,** *42*, 727-740.
4. Catalytic isomerizing ω-functionalization of fatty acids. Goldbach, V.; Roesle, P.; Mecking, S. *ACS Catalysis*, **2015,** *5* (10), 5951-5972.
5. a)Dicarboxylic acid esters from the carbonylation of unsaturated esters under mild conditions. Jiménez-Rodriguez, C.; Eastham, G. R.; Cole-Hamilton, D. J. *Inorganic Chemistry Communications*, **2005,** *8* (10), 878-881; b)Highly selective formation of linear esters from terminal and internal alkenes catalysed by palladium complexes of bis-(di-tert-butylphosphinomethyl) benzene. Jiménez-Rodriguez, C.; Foster, D. F.; Eastham, G. R.; Cole-Hamilton, D. J. *Chemical communications*, **2004,** (15), 1720-1721; c)Highly selective formation of unsaturated esters or cascade reactions to α, ω-diesters by the methoxycarbonylation of alkynes catalysed by palladium complexes of 1, 2-bis (ditertbutylphosphinomethyl) benzene. Núñez-Magro, A. A.; Robb, L.-M.; Pogorzelec, P. J.; Slawin, A. M.; Eastham, G. R.; Cole-Hamilton, D. J. *Chemical Science*, **2010,** *1* (6), 723-730; d)Mechanistic features of isomerizing alkoxycarbonylation of methyl oleate. Roesle, P.; Dürr, C. J.; Möller, H. M.; Cavallo, L.; Caporaso, L.; Mecking, S. *Journal of the American Chemical Society*, **2012,** *134* (42), 17696-17703; e)Long-chain linear C_{19} and C_{23} monomers and polycondensates from unsaturated fatty acid esters. Stempfle, F.; Quinzler, D.; Heckler, I.; Mecking, S. *Macromolecules*, **2011,** *44* (11), 4159-4166; f)Linear semicrystalline polyesters from fatty acids by complete feedstock molecule utilization. Quinzler, D.; Mecking, S. *Angewandte Chemie International Edition*, **2010,** *49* (25), 4306-4308; g)Linear semicrystalline polyesters from fatty acids by complete feedstock molecule utilization. Quinzler, D.; Mecking, S. *Angewandte Chemie*, **2010,** *122* (25), 4402-4404.
6. a)Long-chain aliphatic polymers to bridge the gap between semicrystalline polyolefins and traditional polycondensates. Stempfle, F.; Ortmann, P.; Mecking, S. *Chemical reviews*, **2016,** *116* (7), 4597-4641; b)Long-chain aliphatic polyesters from plant oils for injection molding, film

extrusion and electrospinning. Stempfle, F.; Ritter, B. S.; Mülhaupt, R.; Mecking, S. *Green Chemistry*, **2014,** *16* (4), 2008-2014; c)Plant oil-based long-chain C_{26} monomers and their polymers. Vilela, C.; Silvestre, A. J.; Meier, M. A. *Macromolecular Chemistry and Physics*, **2012,** *213* (21), 2220-2227; d)Self-metathesis of fatty acid methyl esters: full conversion by choosing the appropriate plant oil. Mutlu, H.; Hofsäß, R.; Montenegro, R. E.; Meier, M. A. *Rsc Advances*, **2013,** *3* (15), 4927-4934.

7. Which polyesters can mimic polyethylene? Stempfle, F.; Ortmann, P.; Mecking, S. *Macromolecular rapid communications*, **2013,** *34* (1), 47-50.
8. a)Photograph of *Helianthus annuus*, "Feld mit Sonnenblumen in Sonsbeck" by Vincentz, F., **2008**, distributed under a GNU licence for free documentation. https://de.wikipedia.org/wiki/Datei:Sonsbeck_-_agri_06_ies.jpg; accessed on 20.3.2023. b) Photograph of *Crambe abyssinica*, "Crambe abyssinica" by Stüber, K., **2004**, distributed under a GNU licence for free documentation. https://de.wikipedia.org/wiki/Datei:Crambe_abyssinica0.jpg.; accessed on 20.3.2023.

7. Literature

- Abouzahr, S.; Wilkes, G. L. *Journal of applied polymer science*, **1984,** *29* (9), 2695-2711.
- Ackman, R. G.; Retson, M.; Gallay, L.; Vandenheuvel, F. *Canadian Journal of Chemistry*, **1961,** *39* (10), 1956-1963.
- Adam, N.; Avar, G.; Blankenheim, H.; Friederichs, W.; Giersig, M.; Weigand, E.; Halfmann, M.; Wittbecker, F.-W.; Larimer, D.-R.; Maier, U.; Meyer-Ahrens, S.; Noble, K.-L.; Wussow, H.-G. Polyurethanes. in *Ullmann's Encyclopedia of Industrial Chemistry*, Gerhartz, W.; Elvers, B., (Eds.), Wiley-VCH: Weinheim, **2000**.
- Aharoni, S. M., *n-Nylons: Their Synthesis, Structure and Properties*. Wiley-VCH: Weinheim, Germany, **1997**.
- Amantini, D.; Fringuelli, F.; Pizza, F.; Vaccaro, L. *Organic preparations and procedures international*, **2002,** *34* (2), 109-147.
- Antony, P.; De, S. K. *Journal of Macromolecular Science, Part C: Polymer Reviews*, **2001,** *41* (1-2), 41-77.
- Apostolov, A. A.; Bosvelieva, E.; Du Chesne, A.; Goranov, K.; Fakirov, S. *Die Makromolekulare Chemie: Macromolecular Chemistry and Physics*, **1993,** *194* (8), 2267-2277.
- Babu, R. P.; O'Connor, K.; Seeram, R. *Progress in biomaterials*, **2013,** *2* (1), 1-16.
- Barbiroli, G.; Lorenzetti, C.; Berti, C.; Fiorini, M.; Manaresi, P. *European Polymer Journal*, **2003,** *39* (4), 655-661.
- Bauch, C. G.; Wagener, K. B.; Boncella, J. M. *Die Makromolekulare Chemie, Rapid Communications*, **1991,** *12* (7), 413-417.
- Baumann, H.; Bühler, M.; Fochem, H.; Hirsinger, F.; Zoebelein, H.; Falbe, J. *Angewandte Chemie International Edition in English*, **1988,** *27* (1), 41-62.
- Bayer, O.; Müller, E.; Petersen, S.; Piepenbrink, H. F.; Windemuth, E. *Angewandte Chemie*, **1950,** *62* (3), 57-66.
- Behr, A.; Obst, D.; Westfechtel, A. *European Journal of Lipid Science and Technology*, **2005,** *107* (4), 213-219.
- Beller, M., Ed. *Catalytic Carbonylation Reactions*. 1 ed.; Topics in Organometallic Chemistry, Vol. 18, Springer: Heidelberg, **2006.**
- Bennett, C.; Kaya, E.; Sikes, A. M.; Jarrett, W. L.; Mathias, L. J. *Journal of Polymer Science Part A: Polymer Chemistry*, **2009,** *47* (17), 4409-4419.

- Bennett, C.; Mathias, L. J. *Journal of Polymer Science Part A: Polymer Chemistry*, **2005,** *43* (5), 936-945.
- Bennett, C.; Zeng, J.; Kumar, S.; Mathias, L. J. *Journal of applied polymer science*, **2006,** *99* (5), 2062-2067.
- Bessler, V. E.; Bier, G. *Die Makromolekulare Chemie: Macromolecular Chemistry and Physics*, **1969,** *122* (1), 30-37.
- Bird, R. B.; Armstrong, R. C.; Hassager, O., *Dynamics of polymeric liquids*. Vol. 1: Fluid mechanics, John Wiley: New York, **1987**.
- Borg, P.; Lê, G.; Lebrun, S.; Pées, B. *Oléagineux, Corps gras, Lipides*, **2009,** *16* (4-5-6), 211-214.
- Bouyahyi, M.; Duchateau, R. *Macromolecules*, **2014,** *47* (2), 517-524.
- Brehmer, B. Polyamides from Biomass Derived Monomers. In *Bio-Based Plastics: Materials and Applications*, Kabasci, S., (Ed.) Wiley: Chichester, U.K., **2013**, pp 275-294.
- Brooke, G. M.; Burnett, S.; Mohammed, S.; Proctor, D.; Whiting, M. C. *Journal of the Chemical Society, Perkin Transactions 1*, **1996,** (13), 1635-1645.
- Buckwalter, D. J.; Dennis, J. M.; Long, T. E. *Progress in Polymer Science*, **2015,** *45*, 1-22.
- Bunn, C. W. *Transactions of the Faraday Society*, **1939,** *35*, 482-491.
- Bunn, C. W.; Garner, E.; Bragg, W. L. *Proceedings of the Royal Society of London. Series A. Mathematical and Physical Sciences*, **1947,** *189* (1016), 39-68.
- Burns, A. B.; Register, R. A. *Macromolecules*, **2016,** *49* (24), 9521-9530.
- Carothers, W. H. *Transactions of the Faraday Society*, **1936,** *32*, 39-49.
- Casadei, R.; Giacinti Baschetti, M.; Yoo, M. J.; Park, H. B.; Giorgini, L. *Membranes*, **2020,** *10* (8), 188.
- Cella, R. J. *Journal of Polymer Science: Polymer Symposia*, **1973,** *42*, 727-740.
- Chatel, D.; Delamare, L.; Dang, P.; Lebouvier, D.; Trocherie, F. *Artificial organs*, **1997,** *21* (10), 1098-1104.
- Chatterjee, D. P.; Mandal, B. M. *Macromolecular Symposia*, **2006,** *240*, 224-231.
- Chattopadhyay, D.; Webster, D. C. *Progress in Polymer Science*, **2009,** *34* (10), 1068-1133.
- Chikkali, S.; Mecking, S. *Angewandte Chemie International Edition*, **2012,** *51* (24), 5802-5808.
- Chikkali, S.; Stempfle, F.; Mecking, S. *Macromolecular rapid communications*, **2012,** *33* (13), 1126-1129.
- Choi, K.-C.; Lee, E.-K.; Choi, S.-Y. *Journal of Industrial and Engineering Chemistry*, **2003,** *9* (5), 518-525.
- Christl, J. T.; Roesle, P.; Stempfle, F.; Wucher, P.; Göttker-Schnetmann, I.; Müller, G.; Mecking, S. *Chemistry – A European Journal*, **2013,** *19* (50), 17131-17140.

- Chuit, P. *Helvetica Chimica Acta*, **1926,** *9* (1), 264-278.
- Chung, L. Z.; Kou, D. L.; Hu, A. T.; Tsai, H. B. *Journal of Polymer Science Part A: Polymer Chemistry*, **1992,** *30* (5), 951-953.
- Clegg, W.; Elsegood, M. R.; Eastham, G. R.; Tooze, R. P.; Wang, X. L.; Whiston, K. *Chemical communications*, **1999,** (18), 1877-1878.
- Cole-Hamilton, D. J. *Angewandte Chemie International Edition*, **2010,** *49* (46), 8564-8566.
- Coleman, D. *Journal of Polymer Science*, **1954,** *14* (73), 15-28.
- Cook, F. L.; Bowers, C. W.; Liotta, C. L. *The Journal of Organic Chemistry*, **1974,** *39* (23), 3416-3418.
- Cui, X.; Li, W.; Yan, D. *Polymer international*, **2004,** *53* (11), 1729-1734.
- Cui, X.; Li, W.; Yan, D.; Yuan, C.; Di Silvestro, G. *Journal of applied polymer science*, **2005,** *98* (4), 1565-1571.
- Cywar, R. M.; Rorrer, N. A.; Hoyt, C. B.; Beckham, G. T.; Chen, E. Y.-X. *Nature Reviews Materials*, **2022,** *7* (2), 83-103.
- Dachs, K.; Kunde, J.; Metzger, H.; Wilhelm, H. (BASF), DE 1,239,473, **1962.**
- Daubeny, R. d. P.; Bunn, C. W.; Brown, C. *Proceedings of the Royal Society of London. Series A. Mathematical and Physical Sciences*, **1954**, *226* (1167), 531-542.
- De Ten Hove, C. L. F.; Penelle, J.; Ivanov, D. A.; Jonas, A. M. *Nature materials*, **2004,** *3* (1), 33-37.
- Deleens, G.; Foy, P.; Marechal, E. *European Polymer Journal*, **1977,** *13* (5), 337-342.
- Deleens, G.; Foy, P.; Maréchal, E. *European Polymer Journal*, **1977,** *13* (5), 343-351.
- Dinger, M. B.; Mol, J. C. *Advanced Synthesis & Catalysis*, **2002,** *344* (6-7), 671-677.
- Donald, S. M.; Macgregor, S. A.; Settels, V.; Cole-Hamilton, D. J.; Eastham, G. R. *Chemical communications*, **2007,** (6), 562-564.
- Drobny, J. G., *Handbook of Thermoplastic Elastomers*. William Andrew Publishing: Norwich, New York, **2007**.
- Dubois, P.; Coulembier, O.; Raquez, J.-M., Eds. *Handbook of ring-opening polymerization*. Wiley-VCH: Weinheim, **2009**.
- Dytham, R.; Weedon, B. *Tetrahedron*, **1960,** *8* (3-4), 246-260.
- Effenberger, F.; Drauz, K. *Angewandte Chemie International Edition*, **1979,** *18* (6), 474-476.
- Ehrenstein, G. W., *Polymeric Materials - Structure, Properties, Applications*. Carl Hanser Verlag: Munich, Germany, **2012**.
- Ehrenstein, M.; Dellsperger, S.; Kocher, C.; Stutzmann, N.; Weder, C.; Smith, P. *Polymer*, **2000,** *41* (10), 3531-3539.

- Ehrenstein, M.; Smith, P.; Weder, C. *Macromolecular Chemistry and Physics*, **2003,** *204* (13), 1599-1606.
- Elias, H.-G., *Macromolecules*. Vol. 1: *Chemical Structures and Syntheses*, Wiley-VCH: Weinheim, **2005**.
- Elias, H.-G., *Macromolecules*. Vol. 3: *Physical Structures and Properties*, Wiley-VCH: Weinheim, **2005**.
- Eller, K.; Enkes, E.; Rossbacher, R.; Höke, H. Amines, Aliphatic. In *Ullmann's Encyclopedia of Industrial Chemistry*, Gerhartz, W.; Elvers, B., (Eds.), Wiley-VCH: Weinheim, **2000**.
- Emptage, M.; Haynie, S. L.; Laffend, L. A.; Pucci, J. P.; Whited, G. (DuPont), U. S. Patent 6,514,733 (B1), **2003**.
- Emptage, M.; S, H.; Laffend, L.; Pucci, J. (DuPont), International Patent: WO 2001012833 (A2), **2001**.
- Engle, L.; Wagener, K. *Journal of Macromolecular Science, Part C: Polymer Reviews*, **1993,** *33* (3), 239-257.
- Eustache, R.-P. Poly(Ether –b-Amide) Thermoplastic Elastomers: Structure, Properties and Applications. In *Handbook of Condensation Thermoplastic Elastomers*, Fakirov, S., (Ed.) Wiley-VCH: Weinheim, **2005**.
- Evans, R. D.; Mighton, H. R.; Flory, P. J. *Journal of the American Chemical Society*, **1950,** *72* (5), 2018-2028.
- Fakirov, S.; Goranov, K.; Bosvelieva, E.; Du Chesne, A. *Die Makromolekulare Chemie: Macromolecular Chemistry and Physics*, **1992,** *193* (9), 2391-2404.
- Fernández, C.; Bermúdez, M.; Alla, A.; Muñoz-Guerra, S.; Tocha, E.; Vancso, G. J. *Polymer*, **2011,** *52* (7), 1515-1522.
- Fernández, C.; Bermúdez, M.; Versteegen, R.; Meijer, E.; Vancso, G. J.; Muñoz-Guerra, S. *European Polymer Journal*, **2010,** *46* (11), 2089-2098.
- Flory, P. J. *Chemical reviews*, **1946,** *39* (1), 137-197.
- Forsberg, C. W. *Applied and environmental microbiology*, **1987,** *53* (4), 639-643.
- Fradet, A.; Tessier, M. Polyesters. In *Synthetic methods in step-growth polymers*, Rogers, M. E.; Long, T. E., (Eds.), Wiley Interscience: Hoboken, New Jersey, **2003**, pp 17-134.
- Frensdorff, H. *Macromolecules*, **1971,** *4* (4), 369-375.
- Fu, C.; Zheng, Z.; Yang, Z.; Chen, Y.; Shen, L. *Progress in Organic Coatings*, **2014,** *77* (1), 53-60.
- Fuoco, T.; Meduri, A.; Lamberti, M.; Venditto, V.; Pellecchia, C.; Pappalardo, D. *Polymer Chemistry*, **2015,** *6* (10), 1727-1740.

- Furst, M. R.; Le Goff, R.; Quinzler, D.; Mecking, S.; Botting, C. H.; Cole-Hamilton, D. J. *Green Chemistry*, **2012,** *14* (2), 472-477.
- Furst, M. R.; Seidensticker, T.; Cole-Hamilton, D. J. *Green Chemistry*, **2013,** *15* (5), 1218-1225.
- Gaide, T.; Behr, A.; Arns, A.; Benski, F.; Vorholt, A. J. *Chemical Engineering and Processing: Process Intensification*, **2016,** *99*, 197-204.
- Gaide, T.; Bianga, J.; Schlipköter, K.; Behr, A.; Vorholt, A. J. *ACS Catalysis*, **2017,** *7* (6), 4163-4171.
- Gandini, A. *Macromolecules*, **2008,** *41* (24), 9491-9504.
- Gaymans, R.; Venkatraman, V.; Schuijer, J. *Journal of Polymer Science: Polymer Chemistry Edition*, **1984,** *22* (6), 1373-1382.
- Gaymans, R. J. Polyamides. In *Synthetic Methods in Step-Growth Polymers*, Rogers, M. E.; Long, T. E., (Eds.), John Wiley and Sons: New York, USA, **2003**.
- Genas, M. *Angewandte Chemie*, **1962,** *74* (15), 535-540.
- Ghebreyessus, K. Y.; Angelici, R. J. *Organometallics*, **2006,** *25* (12), 3040-3044.
- Gnanaprakasam, B.; Balaraman, E.; Gunanathan, C.; Milstein, D. *Journal of Polymer Science Part A: Polymer Chemistry*, **2012,** *50* (9), 1755-1765.
- Goebel, C. G.; Brown, A. C.; Oehlschlaeger, H. F.; Rolfes, R. P. (Emery Industries, Inc.), U.S. Patent 2,813,113 (A), **1957**.
- Goldbach, V.; Falivene, L.; Caporaso, L.; Cavallo, L.; Mecking, S. *ACS Catalysis*, **2016,** *6* (12), 8229-8238.
- Goldbach, V.; Roesle, P.; Mecking, S. *ACS Catalysis*, **2015,** *5* (10), 5951-5972.
- Gómez-Jiménez-Aberasturi, O.; Ochoa-Gómez, J. R. *Journal of Chemical Technology & Biotechnology*, **2017,** *92* (4), 705-711.
- Gong, S.; Zhao, S.; Chen, X.; Liu, H.; Deng, J.; Li, S.; Feng, X.; Li, Y.; Wu, X.; Pan, K. *Macromolecular Materials and Engineering*, **2021,** *306* (12), 2100568.
- Griehl, W.; Ruestem, D. *Industrial & Engineering Chemistry*, **1970,** *62* (3), 16-22.
- Gross, R. A.; Lu, W.; Ness, J.; Minshull, J. (Polytechnic Institute of New York University), International Patent: WO 2011008232, **2011**.
- Gugliuzza, A. Poly(ether-block-amide) copolymers synthesis, properties and applications. In *Handbook of engineering and specialty thermoplastics*, Thomas, S.; Visakh, P. M., (Eds.), John Wiley & Sons Inc.: Hoboken, NJ, **2012**, pp 111–140.
- Gunanathan, C.; Milstein, D. *Angewandte Chemie*, **2008,** *120* (45), 8789-8792.

- Gunanathan, C.; Milstein, D. *Angewandte Chemie International Edition*, **2008,** *47* (45), 8661-8664.
- Hall, A. J.; Hodge, P.; Kamau, S. D.; Ben-Haida, A. *Journal of Organometallic Chemistry*, **2006,** *691* (24-25), 5431-5437.
- Harris, B., Acrylics for the Future. In *Ingenia*, **2010**; Vol. 45, pp 18-23.
- He, Y.; Xie, D.; Zhang, X. *Journal of Materials Science*, **2014,** *49* (21), 7339-7352.
- Heintz, A. M.; McKiernan, R. L.; Gido, S. P.; Penelle, J.; Hsu, S. L.; Sasaki, S.; Takahara, A.; Kajiyama, T. *Macromolecules*, **2002,** *35* (8), 3117-3125.
- Hepburn, C., *Polyurethane Elastomers*. Springer: Heidelberg, Germany, **2012**.
- Hernandez, R.; Weksler, J.; Padsalgikar, A.; Choi, T.; Angelo, E.; Lin, J.; Xu, L.-C.; Siedlecki, C. A.; Runt, J. *Macromolecules*, **2008,** *41* (24), 9767-9776.
- Herrmann, N.; Köhnke, K.; Seidensticker, T. *ACS Sustainable Chemistry & Engineering*, **2020,** *8* (29), 10633-10638.
- Hess, S. K.; Lepetit, B.; Kroth, P. G.; Mecking, S. *European Journal of Lipid Science and Technology*, **2018,** *120* (1), 1700152.
- Hess, S. K.; Schunck, N. S.; Goldbach, V.; Ewe, D.; Kroth, P. G.; Mecking, S. *Journal of the American Chemical Society*, **2017,** *139* (38), 13487-13491.
- Hill, R.; Walker, E. *Journal of Polymer Science*, **1948,** *3* (5), 609-630.
- Hillmyer, M. A.; Tolman, W. B. *Accounts of chemical research*, **2014,** *47* (8), 2390-2396.
- Hoeschele, G. *Polymer Engineering & Science*, **1974,** *14* (12), 848-852.
- Hojabri, L.; Kong, X.; Narine, S. S. *Biomacromolecules*, **2009,** *10* (4), 884-891.
- Hojabri, L.; Kong, X.; Narine, S. S. *Journal of Polymer Science Part A: Polymer Chemistry*, **2010,** *48* (15), 3302-3310.
- Holden, G.; Bishop, E.; Legge, N. R. *Journal of Polymer Science Part C: Polymer Symposia*, **1969,** *26*, 37-57.
- Holden, G.; Kricheldorf, H. R.; Quirk, R. P., *Thermoplastic Elastomers*. Hanser: Munich, Germany, **2004**.
- Hood, M. A.; Wang, B.; Sands, J. M.; La Scala, J. J.; Beyer, F. L.; Li, C. Y. *Polymer*, **2010,** *51* (10), 2191-2198.
- Hori, Y.; Hongo, H.; Hagiwara, T. *Macromolecules*, **1999,** *32* (10), 3537-3539.
- Huang, Y.; Li, W.; Yan, D. *Polymer Bulletin*, **2002,** *49* (2), 111-118.
- Huber, T.; Firlbeck, D.; Riepl, H. M. *Journal of Organometallic Chemistry*, **2013,** *744*, 144-148.

- Huf, S.; Krügener, S.; Hirth, T.; Rupp, S.; Zibek, S. *European Journal of Lipid Science and Technology*, **2011,** *113* (5), 548-561.
- Inoue, M. *Journal of Polymer Science Part A: General Papers*, **1963,** *1* (8), 2697-2709.
- Ishioka, R.; Kitakuni, E.; Y., I. Aliphatic Polyesters: "Bionolle". In *Biopolymers*, Steinbüchel, A.; Doi, Y., (Eds.), Vol. 4, Wiley-VCH: Weinheim, **2002**, pp 275-297.
- Iwakura, Y.; Uno, K. *Nippon Kagaku Zasshi*, **1957,** *78* (10), 1507-1510.
- Iwakura, Y.; Uno, K. *Nippon Kagaku Zasshi*, **1957,** *78* (10), 1511-1516.
- Jameel, F.; Kohls, E.; Stein, M. *ChemCatChem*, **2019,** *11* (19), 4894-4906.
- Jameh, A. A.; Mohammadi, T.; Bakhtiari, O. *Separation and Purification Technology*, **2020,** *231*, 115900.
- Jedliński, Z.; Juzwa, M.; Adamus, G.; Kowalczuk, M.; Montaudo, M. *Macromolecular Chemistry and Physics*, **1996,** *197* (9), 2923-2929.
- Jia, N.; Kagan, V. A. Mechanical performance of polyamides with influence of moisture and temperature–accurate evaluation and better understanding. In *Plastics Failure - Analysis and Prevention*, Moalli, J., (Ed.) William Andrew Inc.: Norwich, USA, **2001**, pp 95-104.
- Jiménez-Rodriguez, C.; Eastham, G. R.; Cole-Hamilton, D. J. *Inorganic Chemistry Communications*, **2005,** *8* (10), 878-881.
- Jones, N.; Atkins, E.; Hill, M.; Cooper, S.; Franco, L. *Polymer*, **1997,** *38* (11), 2689-2699.
- Kennedy, J. P.; Castner, K. F. *Journal of Polymer Science: Polymer Chemistry Edition*, **1979,** *17* (7), 2055-2070.
- Kerenkan, A. E.; Béland, F.; Do, T.-O. *Catalysis Science & Technology*, **2016,** *6* (4), 971-987.
- Kinoshita, Y. *Die Makromolekulare Chemie: Macromolecular Chemistry and Physics*, **1959,** *33* (1), 1-20.
- Kinoshita, Y. *Die Makromolekulare Chemie: Macromolecular Chemistry and Physics*, **1959,** *33* (1), 21-31.
- Köckritz, A.; Martin, A. *European Journal of Lipid Science and Technology*, **2011,** *113* (1), 83-91.
- Kohan, M. I.; Mestemacher, S. A.; Pagilagan, R. U.; Redmond, K. Polyamides. In *Ullmann's Encyclopedia of Industrial Chemistry*, Gerhartz, W.; Elvers, B., (Eds.), Wiley-VCH: Weinheim, **2000**.
- Köpnick, H.; Schmidt, M.; Brügging, W.; Rüter, J.; Kaminsky, W. Polyesters. In *Ullmann's Encyclopedia of Industrial Chemistry*, Gerhartz, W. E., B., (Ed.) Wiley-VCH: Weinheim, **2000**.
- Korshak, V. V.; Vinogradova, S. V., *Polyesters*. Pergamon Press: Oxford, U.K., **1965**.
- Kraus, G. A. *CLEAN–Soil, Air, Water*, **2008,** *36* (8), 648-651.
- Kreye, O.; Mutlu, H.; Meier, M. A. *Green Chemistry*, **2013,** *15* (6), 1431-1455.
- Kreye, O.; Wald, S.; Meier, M. A. *Advanced Synthesis & Catalysis*, **2013,** *355* (1), 81-86.

- Kricheldorf, H., *Polycondensation: History and New Results*. Springer: Heidelberg, Germany, **2013**.
- Król, P. *Progress in materials science*, **2007,** *52* (6), 915-1015.
- Kwiatkowska, M.; Kowalczyk, I.; Kwiatkowski, K.; Zubkiewicz, A. *Polymers*, **2020,** *12* (2), 271.
- Labet, M.; Thielemans, W. *Chemical Society Reviews*, **2009,** *38* (12), 3484-3504.
- Lasprilla, A. J.; Martinez, G. A.; Lunelli, B. H.; Jardini, A. L.; Maciel Filho, R. *Biotechnology advances*, **2012,** *30* (1), 321-328.
- Lebarbé, T.; More, A. S.; Sane, P. S.; Grau, E.; Alfos, C.; Cramail, H. *Macromolecular rapid communications*, **2014,** *35* (4), 479-483.
- Lee, H. N.; Rosen, B. M.; Fenyvesi, G.; Sunkara, H. B. *Journal of Polymer Science Part A: Polymer Chemistry*, **2012,** *50* (20), 4311-4315.
- Legge, N. R.; Holden, G.; Schroeder, H., *Thermoplastic elastomers: A comprehensive review*. Carl Hansser Verlag: New York, USA, **1987**.
- Li, W.; Yan, D. *Journal of applied polymer science*, **2003,** *88* (10), 2462-2467.
- Lligadas, G.; Ronda, J.; Galia, M.; Biermann, U.; Metzger, J. *Journal of Polymer Science Part A: Polymer Chemistry*, **2006,** *44* (1), 634-645.
- Lligadas, G.; Ronda, J. C.; Galia, M.; Cádiz, V. *Biomacromolecules*, **2010,** *11* (11), 2825-2835.
- Lu, W.; Ness, J. E.; Xie, W.; Zhang, X.; Minshull, J.; Gross, R. A. *Journal of the American Chemical Society*, **2010,** *132* (43), 15451–15455.
- Maass, H.-J.; Wiegleb, K.; Michalke, K.; Eberhardt, P.; Techritz, K. *Plaste und Kautschuk*, **1987,** *34* (7), 251-254.
- Maisonneuve, L.; Lamarzelle, O.; Rix, E.; Grau, E.; Cramail, H. *Chemical reviews*, **2015,** *115* (22), 12407-12439.
- Maisonneuve, L.; Lebarbé, T.; Grau, E.; Cramail, H. *Polymer Chemistry*, **2013,** *4* (22), 5472-5517.
- Malet, F. L. G. Thermoplastic Poly(Ether–*b*-Amide) TPE: Synthesis. In *Handbook of Condensation Thermoplastic Elastomers*, Fakirov, S., (Ed.) Wiley-VCH: Weinheim, Germany, **2005**, pp 243-257.
- Mandelkern, L.; Alamo, R. G. Thermodynamic Quantities Governing Melting In *Physical Properties of Polymers Handbook*, Mark, J. E., (Ed.) Springer: Heidelberg, Germany, **2007**, pp 165-186.
- Maréchal, E. Creation and Development of Thermoplastic Elastomers, and Their Position Among Organic Materials. In *Handbook of Condensation Thermoplastic Elastomers*, Fakirov, S., (Ed.) Wiley-VCH: Weinheim, Germany, **2005**.

- Maréchal, E. Polycondensation Reactions in Thermoplastic Elastomer Chemistry: State of the Art, Trends, and Future Developments. In *Handbook of Condensation Thermoplastic Elastomers*, Fakirov, S., (Ed.) Wiley-VCH: Weinheim, Germany, **2005**.
- Martello, M. T.; Hillmyer, M. A. *Macromolecules*, **2011,** *44* (21), 8537-8545.
- McKiernan, R. L.; Gido, S. P.; Penelle, J. *Polymer*, **2002,** *43* (10), 3007-3017.
- McKiernan, R. L.; Heintz, A. M.; Hsu, S. L.; Atkins, E. D.; Penelle, J.; Gido, S. P. *Macromolecules*, **2002,** *35* (18), 6970-6974.
- McKiernan, R. L.; Sikorski, P.; Atkins, E. D.; Gido, S. P.; Penelle, J. *Macromolecules*, **2002,** *35* (22), 8433-8439.
- Meier, M. A. *Macromolecular rapid communications*, **2019,** *40* (1), 1800524.
- Meier, M. A.; Metzger, J. O.; Schubert, U. S. *Chemical Society Reviews*, **2007,** *36* (11), 1788-1802.
- Metzger, J. O.; Bornscheuer, U. *Applied microbiology and biotechnology*, **2006,** *71* (1), 13-22.
- Miller, J. A.; Lin, S. B.; Hwang, K. K.; Wu, K.; Gibson, P.; Cooper, S. L. *Macromolecules*, **1985,** *18* (1), 32-44.
- Miyake, A. *Journal of Polymer Science*, **1960**, *44* (143), 223-232.
- Mock, J. A. *Plastics Engineering*, **1983,** *39* (2), 13-19.
- More, A. S.; Lebarbé, T.; Maisonneuve, L.; Gadenne, B.; Alfos, C.; Cramail, H. *European Polymer Journal*, **2013,** *49* (4), 823-833.
- Morton, M.; McGrath, J. E.; Juliano, P. C. *Journal of Polymer Science Part C: Polymer Symposia*, **1969,** *26*, 99-115.
- Mosnáček, J.; Yoon, J. A.; Juhari, A.; Koynov, K.; Matyjaszewski, K. *Polymer*, **2009,** *50* (9), 2087-2094.
- Mueller, P. A.; Murphy, E. R.; Rajagopalan, B.; Congalidis, J. P.; Minter, A. R. *Macromolecular Symposia*, **2011,** *302* (1), 56-68.
- Mukai, K.; Sema, Y.; Tomita, K. *Biotechnology letters*, **1993,** *15* (6), 601-604.
- Mumcu, S.; Burzin, K.; Felsmann, R.; Feinauer, R. *Angewandte Makromolekulare Chemie*, **1978,** *74*, 49-60.
- Murthy, N. S. *Journal of Polymer Science Part B: Polymer Physics*, **2006,** *44* (13), 1763-1782.
- Mutlu, H.; Hofsäß, R.; Montenegro, R. E.; Meier, M. A. *Rsc Advances*, **2013,** *3* (15), 4927-4934.
- Mutlu, H.; Meier, M. A. *European Journal of Lipid Science and Technology*, **2010,** *112* (1), 10-30.
- Narisetty, V.; Okibe, M. C.; Amulya, K.; Jokodola, E. O.; Coulon, F.; Tyagi, V. K.; Lens, P. N.; Parameswaran, B.; Kumar, V. *Bioresource Technology*, **2022**, 127513.

- Naughton, F. C. *Journal of the American Oil Chemists' Society*, **1974,** *51* (3), 65-71.
- Neffgen, S.; Kušan, J.; Fey, T.; Keul, H.; Höcker, H. *Macromolecular Chemistry and Physics*, **2000,** *201* (16), 2108-2114.
- Ngo, H. L.; Jones, K.; Foglia, T. A. *Journal of the American Oil Chemists' Society*, **2006,** *83* (7), 629-634.
- Nguyen, P. H.; Spoljaric, S.; Seppälä, J. *European Polymer Journal*, **2018,** *109*, 16-25.
- Niaounakis, M., *Biopolymers: applications and trends*. William Andrew Publishing: Norwich, New York, **2015**.
- Nivinskiene, O.; Butkiene, R.; Mockutë, D. *Chemija (Vilnius)*, **2003,** *14* (1), 52-56.
- Nomura, R.; Ueno, A.; Endo, T. *Macromolecules*, **1994,** *27* (2), 620-621.
- Núñez-Magro, A. A.; Robb, L.-M.; Pogorzelec, P. J.; Slawin, A. M.; Eastham, G. R.; Cole-Hamilton, D. J. *Chemical Science*, **2010,** *1* (6), 723-730.
- Nuyken, O.; Pask, S. D. *Polymers*, **2013,** *5* (2), 361-403.
- O'Gara, J. E.; Wagener, K. B.; Hahn, S. F. *Die Makromolekulare Chemie, Rapid Communications*, **1993,** *14* (10), 657-662.
- Ortmann, P.; Heckler, I.; Mecking, S. *Green Chemistry*, **2014,** *16* (4), 1816-1827.
- Ortmann, P.; Lemke, T. A.; Mecking, S. *Macromolecules*, **2015,** *48* (5), 1463-1472.
- Ortmann, P.; Mecking, S. *Macromolecules*, **2013,** *46* (18), 7213-7218.
- Ouhadi, T.; Abdou-Sabet, T.; Wussow, H.-G.; Ryan, L. M.; Plummer, L.; Baumann, F. E.; Lohmar, J.; F, V. H.; Malet, F. L. G. Thermoplastic Elastomers. In *Ullmann's Encyclopedia of Industrial Chemistry*, Gerhartz, W.; Elvers, B., (Eds.), Wiley-VCH: Weinheim, Germany, **2000**, pp 1-40.
- Pang, J.; Zheng, M.; Sun, R.; Song, L.; Wang, A.; Wang, X.; Zhang, T. *Bioresource Technology*, **2015,** *175*, 424-429.
- Pang, J.; Zheng, M.; Sun, R.; Wang, A.; Wang, X.; Zhang, T. *Green Chemistry*, **2016,** *18* (2), 342-359.
- Papageorgiou, G. Z.; Papageorgiou, D. G.; Terzopoulou, Z.; Bikiaris, D. N. *European Polymer Journal*, **2016,** *83*, 202-229.
- Pavone, A. IHS Chemical: Process Economics Program Review 2013-03 IHS Markit: **2013**.
- Peacock, A. J., *Handbook of Polyethylene - Structures, Properties and Applications*. CRC Press: Boca Raton, Florida, USA, **2000**.
- Pepels, M.; Bouyahyi, M.; Heise, A.; Duchateau, R. *Macromolecules*, **2013,** *46* (11), 4324-4334.

- Pepels, M. P.; Hansen, M. R.; Goossens, H.; Duchateau, R. *Macromolecules*, **2013,** *46* (19), 7668-7677.
- Pepels, M. P.; Koeken, R. A.; van der Linden, S. J.; Heise, A.; Duchateau, R. *Macromolecules*, **2015,** *48* (14), 4779-4792.
- Pepels, M. P. F. *Exploring the Potential of Polymacrolactones as Polyethylene-Mimicks*. Ph.D. Thesis, Eindhoven Unversity of Technology, Eindhoven, Netherlands, **2015**.
- Perkins, W. G.; Porter, R. S. *Journal of Materials Science*, **1977,** *12* (12), 2355-2388.
- Perry, E.; Savory, J. *Journal of applied polymer science*, **1967,** *11* (12), 2473-2483.
- Petrović, Z. S.; Ferguson, J. *Progress in Polymer Science*, **1991,** *16* (5), 695-836.
- Pfister, D. P.; Xia, Y.; Larock, R. C. *ChemSusChem*, **2011,** *4* (6), 703-717.
- Pingen, D.; Schwaderer, J. B.; Walter, J.; Wen, J.; Murray, G.; Vogt, D.; Mecking, S. *ChemCatChem*, **2018,** *10* (14), 3027-3033.
- Préfol, T.; Gain, O.; Sudre, G.; Gouanvé, F.; Espuche, E. *Membranes*, **2021,** *11* (9), 692.
- Press release by BASF of March 5, 2015
- Press release by Clariant of February 2, 2022
- Pugh, R. I.; Drent, E.; Pringle, P. G. *Chemical communications*, **2001,** (16), 1476-1477.
- Quinzler, D. *Linear Semicrystalline Polyesters and Polyamides from Plant Oil Fatty Acids via Catalytic Alkoxycarbonylation*. Ph.D. Thesis, University of Konstanz, Konstanz, Germany, **2014**.
- Quinzler, D.; Mecking, S. *Angewandte Chemie International Edition*, **2010,** *49* (25), 4306-4308.
- Quinzler, D.; Mecking, S. *Angewandte Chemie*, **2010,** *122* (25), 4402-4404.
- Randall, D.; Lee, S., *The Polyurethanes Book*. Wiley VCH: Weinheim, Germany, **2003**.
- Rani, G. U.; Sharma, S., Biopolymers, Bioplastics and Biodegradables: An Introduction. In *Encyclopedia of Materials: Plastics and Polymers*, 1 ed.; Hashmi, M. S. J., Ed. Elsevier Science: Amsterdam, Netherlands, **2022**; Vol. 2, pp 474-486.
- Report on the future of petrochemicals by IEA/OECD of **2018**.
- Rodriguez, C. J.; Foster, D. F.; Eastham, G. R.; Cole-Hamilton, D. J. *Chemical communications*, **2004,** (15), 1720-1721.
- Roesle, P.; Caporaso, L.; Schnitte, M.; Goldbach, V.; Cavallo, L.; Mecking, S. *Journal of the American Chemical Society*, **2014,** *136* (48), 16871-16881.
- Roesle, P.; Dürr, C. J.; Möller, H. M.; Cavallo, L.; Caporaso, L.; Mecking, S. *Journal of the American Chemical Society*, **2012,** *134* (42), 17696-17703.

- Roesle, P.; Stempfle, F.; Hess, S. K.; Zimmerer, J.; Río Bártulos, C.; Lepetit, B.; Eckert, A.; Kroth, P. G.; Mecking, S. *Angewandte Chemie International Edition*, **2014,** *53* (26), 6800-6804.
- Roslaniec, Z. Polyester Thermoplastic Elastomers: Synthesis, Properties, and Some Applications. In *Handbook of Condensation Thermoplastic Elastomers*, Fakirov, S., (Ed.) Wiley-VCH: Weinheim, Germany, **2005**.
- Rusu, G.; Ueda, K.; Rusu, E.; Rusu, M. *Polymer*, **2001,** *42* (13), 5669-5678.
- Saghian, N.; Gertner, D. *Journal of the American Oil Chemists Society*, **1974,** *51* (8), 363-367.
- Saito, Y.; Hara, K.; Kinoshita, S. *Polymer Journal*, **1982,** *14* (1), 19-31.
- Saito, Y.; Nansai, S.; Kinoshita, S. *Polymer Journal*, **1972,** *3* (2), 113-121.
- Saotome, K.; Komoto, H. *Journal of Polymer Science Part A-1: Polymer Chemistry*, **1966,** *4* (6), 1463-1473.
- Saotome, K.; Komoto, H. *Journal of Polymer Science Part A1: Polymer Chemistry*, **1967,** *5* (1), 119-126.
- Saudan, L. A.; Saudan, C. M.; Debieux, C.; Wyss, P. *Angewandte Chemie*, **2007,** *119* (39), 7617-7620.
- Schaeffer, W. D. (Union Oil Company of California), U. S. Patent 3,017,420, **1962**.
- Schaffer, S.; Haas, T. *Organic Process Research & Development*, **2014,** *18* (6), 752-766.
- Schmidt, A.; Veeman, W. S.; Litvinov, V. M.; Gabriëlse, W. *Macromolecules*, **1998,** *31* (5), 1652-1660.
- Schörken, U.; Kempers, P. *European Journal of Lipid Science and Technology*, **2009,** *111* (7), 627-645.
- Schrock, A. K.; Hamilton, H. S.; Johnson, N. D.; del Rosario, C.; Thompson, B.; Ulrich, K.; Coggio, W. D. *Polymer*, **2016,** *101*, 233-240.
- Schroeder, L.; Cooper, S. L. *Journal of Applied Physics*, **1976,** *47* (10), 4310-4317.
- Schwaderer, J. B. *Ruthenium Catalysed Amination of Bio-Based Diols - Building Blocks for Polyamides from Renewables*. Master Thesis, University of Konstanz, Konstanz, Germany, **2016**.
- Shein, T. I.; Vlasova, L. N. *Polymer Science U.S.S.R.*, **1964,** *5* (4), 564-569.
- Sheldon, R. A. *Green Chemistry*, **2014,** *16* (3), 950-963.
- Shen, L.; Worrell, E.; Patel, M. *Biofuels, Bioproducts and Biorefining: Innovation for a sustainable economy*, **2010,** *4* (1), 25-40.
- Sheth, J. P.; Xu, J.; Wilkes, G. L. *Polymer*, **2003,** *44* (3), 743-756.
- Shim, J. S.; Asthana, S.; Omura, N.; Kennedy, J. P. *Journal of Polymer Science Part A: Polymer Chemistry*, **1998,** *36* (17), 2997-3012.
- Shin, J.; Lee, Y.; Tolman, W. B.; Hillmyer, M. A. *Biomacromolecules*, **2012,** *13* (11), 3833-3840.

- Skrovanek, D. J.; Howe, S. E.; Painter, P. C.; Coleman, M. M. *Macromolecules*, **1985,** *18* (9), 1676-1683.
- Skrovanek, D. J.; Painter, P. C.; Coleman, M. M. *Macromolecules*, **1986,** *19* (3), 699-705.
- Smiley, R. A. Hexamethylenediamine. In *Ullmann's Encyclopedia of Industrial Chemistry*, Gerhartz, W.; Elvers, B., (Eds.), Wiley-VCH: Weinheim, Germany, **2000**.
- Smith, M. B.; March, J., *March's Advanced Organic Chemistry: Reactions, Mechanisms, and Structure*. 6 ed.; Wiley VCH: Hoboken, New Jersey, USA, **2007**.
- Snyder, M. D. (DuPont), U.S. Patent 2,623,031 (A), **1952**.
- Song, Y.; Yamamoto, H.; Nemoto, N. *Macromolecules*, **2004,** *37* (16), 6219-6226.
- Song, J.; Zhang, H.; Ren, M.; Chen, Q.; Sun, X.; Wang, S.; Zhang, H.; Mo, Z. *Macromolecular rapid communications*, **2005**, *26* (6), 487-490.
- Soutelo-Maria, A.; Dubois, J.-L.; Couturier, J.-L.; Cravotto, G. *Catalysts*, **2018,** *8* (10), 464.
- Stempfle, F. *Aliphatic Polyester Materials from Polycondensation of Seed- and Algae Oil-Based Long-Chain Monomers*. Ph.D. Thesis, University of Konstanz, Konstanz, Germany, **2015**.
- Stempfle, F.; Ortmann, P.; Mecking, S. *Macromolecular rapid communications*, **2013,** *34* (1), 47-50.
- Stempfle, F.; Ortmann, P.; Mecking, S. *Chemical reviews*, **2016,** *116* (7), 4597-4641.
- Stempfle, F.; Quinzler, D.; Heckler, I.; Mecking, S. *Macromolecules*, **2011,** *44* (11), 4159-4166.
- Stempfle, F.; Ritter, B. S.; Mülhaupt, R.; Mecking, S. *Green Chemistry*, **2014,** *16* (4), 2008-2014.
- Stempfle, F.; Roesle, P.; Mecking, S. Long-Chain Polyesters via Chemical Catalytic Conversions of Fatty Acid Ester. In *Biobased Monomers, Polymers, and Materials*, Gross, R. A.; Smith, P. B., (Eds.), ACS Symposium Series, Vol. 1105, ACS Publishing: Washington, D.C., **2012**, pp 151-164.
- Stempfle, F.; Schemmer, B.; Oechsle, A.-L.; Mecking, S. *Polymer Chemistry*, **2015,** *6* (40), 7133-7137.
- Sunkara, H. B.; Miller, R. W. *"DuPont™ Cerenol™ - A New Family of High Performance Polyether glycols"*, Fifth Annual World Congress on Industrial Biotechnology & Bioprocessing, Chicago, April 27–30, **2008**.
- Suzuki, Y.; Nakamura, M.; Aochiama, A. (Asahi), European Patent EP0221188 (A1), **1987**.
- Tanikella, M. S. S. R. (DuPont), U.S. Patent 4,404,411 (A), **1983**.
- Tant, M. R.; Mauritz, K. A.; Wilkes, G. L., Eds. *Ionomers: Synthesis, Structure, Properties and Applications*. Chapman & Hall: London, U.K., **1997**.
- Teong, S. P.; Li, X.; Zhang, Y. *Green Chemistry*, **2019,** *21* (21), 5753-5780.
- Thakker, C.; Martínez, I.; San, K. Y.; Bennett, G. N. *Biotechnology journal*, **2012,** *7* (2), 213-224.

- TPE Global Market Forecast to 2026 by MarketsAndMarkets Inc. of **2021**.
- Trifan, D. S.; Terenzi, J. F. *Journal of Polymer Science*, **1958,** *28* (117), 443-445.
- Trzaskowski, J.; Quinzler, D.; Bährle, C.; Mecking, S. *Macromolecular rapid communications*, **2011,** *32* (17), 1352-1356.
- Tsuji, H. Poly(Lactic Acid). In *Bio-Based Plastics: Materials and Applications*, Kabasci, S., (Ed.) Wiley: Chichester, U.K., **2013**, pp 171-239.
- Twitchett, H. *Chemical Society Reviews*, **1974,** *3* (2), 209-230.
- Ukielski, R. Terpoly (Ester-b-Ether-b-Amide) Thermoplastic Elastomers: Synthesis, Structure, and Properties. In *Handbook of Condensation Thermoplastic Elastomers*, Fakirov, S., (Ed.) Wiley-VCH: Weinheim, Germany, **2005**, pp 117-140.
- Unverferth, M.; Kreye, O.; Prohammer, A.; Meier, M. A. *Macromolecular rapid communications*, **2013,** *34* (19), 1569-1574.
- Van Der Meulen, I.; Gubbels, E.; Huijser, S.; Sablong, R.; Koning, C. E.; Heise, A.; Duchateau, R. *Macromolecules*, **2011,** *44* (11), 4301-4305.
- Van der Meulen, I.; Huijser, S.; Gubbels, E.; Heise, A.; Duchateau, R.; Koning, C. E. (Saudi Basic Industries Corporation), U.S. Patent 8,933,190 (B2), **2015**.
- Van der Ploeg, F. *Journal of Economic Literature*, **2011,** *49* (2), 366-420.
- Van Leeuwen, P. W. N. M.; Chadwick, J. C., *Carbonylation Reactions. Homogeneous Catalysts: Activity − Stability − Deactivation*. Wiley-VCH: Weinheim, Germany, **2011**.
- Van Putten, R.-J.; Van Der Waal, J. C.; De Jong, E.; Rasrendra, C. B.; Heeres, H. J.; de Vries, J. G. *Chemical reviews*, **2013,** *113* (3), 1499-1597.
- Verhé, R. G. Industrial Products from Lipids and Proteins. In *Renewable Bioresources: Scope and Modification for Non-Food Applications*, Stevens, C. V.; Verhé, R. G., (Eds.), Wiley: Chichester, U.K., **2004**, p 208−250.
- Vieweg, R.; Müller, A., *Kunststoff-Handbuch. Band VI: Polyamide*. Carl Hanser Verlag: Munich, Germany, **1966**.
- Vilela, C.; Silvestre, A. J.; Meier, M. A. *Macromolecular Chemistry and Physics*, **2012,** *213* (21), 2220-2227.
- Vollenweider, S.; Lacroix, C. *Applied microbiology and biotechnology*, **2004,** *64* (1), 16-27.
- von Gizycki, U. *Angewandte Chemie*, **1971,** *83* (11), 406-407.
- Vrouenraets, C. M. F.; Sikkema, D. J. (AKZO), U.S. Patent 4,493,870 (A), **1983**.

- Walter, J. *Polyamides from Renewable Resources*. Master Thesis, University of Konstanz, Konstanz, Germany, **2015**.
- Walther, G.; Deutsch, J.; Martin, A.; Baumann, F. E.; Fridag, D.; Franke, R.; Köckritz, A. *ChemSusChem*, **2011,** *4* (8), 1052-1054.
- Walther, G.; Deutsch, J.; Martin, A.; Baumann, F.-E.; Fridag, D.; Köckritz, A. Poster at the 4th Workshop on *Fats and Oils as Renewable Feedstock for the Chemical Industry*, Karlsruhe, Germany, March 20-22, **2011**.
- Walther, G.; Knöpke, L. R.; Rabeah, J.; Chęciński, M. P.; Jiao, H.; Bentrup, U.; Brückner, A.; Martin, A.; Köckritz, A. *Journal of catalysis*, **2013,** *297*, 44-55.
- Wanamaker, C. L.; O'Leary, L. E.; Lynd, N. A.; Hillmyer, M. A.; Tolman, W. B. *Biomacromolecules*, **2007,** *8* (11), 3634-3640.
- Wang, G.; Xue, B. *Journal of applied polymer science*, **2010,** *118* (4), 2448-2453.
- Wang, L.; Dong, X.; Zhu, P.; Zhang, X.; Liu, X.; Wang, D. *European Polymer Journal*, **2017,** *90*, 171-182.
- Wang, S.; Vajjala Kesava, S.; Gomez, E. D.; Robertson, M. L. *Macromolecules*, **2013,** *46* (18), 7202-7212.
- Wang, Z.; Yuan, L.; Tang, C. *Accounts of chemical research*, **2017,** *50* (7), 1762-1773.
- Weissenberg, K. *Nature*, **1947,** *159* (4035), 310-311.
- Wen, L.; Zhang, J.; Zhou, T.; Zhang, A. *Vibrational Spectroscopy*, **2016,** *86*, 160-172.
- West, J. C.; Cooper, S. L. *Journal of Polymer Science: Polymer Symposia*, **1977,** *60*, 127-150.
- Whiteley, K. S. Polyolefins. In *Ullmann's Encyclopedia of Industrial Chemistry*, Gerhartz, W. E., B., (Ed.) Wiley-VCH: Weinheim, Germany, **2000**.
- Witsiepe, W. Segmented Polyester Thermoplastic Elastomers. In *ACS Advances in Chemistry*, Platzer, N. A. J., (Ed.) ACS Advances in Chemistry, Vol. 129: *Polymerization Reactions and New Polymers*, ACS Publications: **1973**, pp 39-66.
- Witt, T.; Häußler, M.; Kulpa, S.; Mecking, S. *Angewandte Chemie*, **2017,** *129* (26), 7697-7702.
- Witt, T.; Häußler, M.; Kulpa, S.; Mecking, S. *Angewandte Chemie International Edition*, **2017,** *56* (26), 7589-7594.
- Witt, T.; Mecking, S. *Green Chemistry*, **2013,** *15* (9), 2361-2364.
- Woo, E.; Barlow, J.; Paul, D. *Polymer*, **1985,** *26* (5), 763-773.
- Xu, Y.; Petrovic, Z.; Das, S.; Wilkes, G. L. *Polymer*, **2008,** *49* (19), 4248-4258.
- Yeh, J.-L.; Kuo, J.-F.; Chen, C.-Y. *Materials chemistry and physics*, **1994,** *37* (2), 161-169.

- Yilgor, I.; Yilgor, E.; Guler, I. G.; Ward, T. C.; Wilkes, G. L. *Polymer*, **2006,** *47* (11), 4105-4114.
- Yilgör, I.; Yilgör, E.; Wilkes, G. L. *Polymer*, **2015,** *58*, A1-A36.
- Yim, H.; Haselbeck, R.; Niu, W.; Pujol-Baxley, C.; Burgard, A.; Boldt, J.; Khandurina, J.; Trawick, J. D.; Osterhout, R. E.; Stephen, R. *Nature chemical biology*, **2011,** *7* (7), 445-452.
- Yoda, R. *Journal of Biomaterials Science, Polymer Edition*, **1998,** *9* (6), 561-626.
- Yuan, R.; Fan, S.; Wu, D.; Wang, X.; Yu, J.; Chen, L.; Li, F. *Polymer Chemistry*, **2018,** *9* (11), 1327-1336.
- Zeng, H.; Guan, Z. *Journal of the American Chemical Society*, **2011,** *133* (5), 1159-1161.
- Zhang, C. Biodegradable Polyesters: Synthesis, Properties, Applications. In *Biodegradable Polyesters*, Fakirov, S., (Ed.) Wiley-VCH: Weinheim, Germany, **2015**.
- Zhong, Z.; Dijkstra, P. J.; Feijen, J. *Macromolecular Chemistry and Physics*, **2000,** *201* (12), 1329-1333.
- Zhou, W.; Zhang, Y.; Xu, Y.; Wang, P.; Gao, L.; Zhang, W.; Ji, J. *Polymer degradation and stability*, **2014,** *109*, 21-26.
- Zhu, P.; Dong, X.; Cao, Y.; Wang, L.; Liu, X.; Wang, Z.; Wang, D. *European Polymer Journal*, **2017,** *93*, 334-346.
- Zhu, P.; Dong, X.; Wang, D. *Macromolecules*, **2017,** *50* (10), 3911-3921.
- Zhu, Y.; Jang, S. H. A.; Tham, Y. H.; Algin, O. B.; Maguire, J. A.; Hosmane, N. S. *Organometallics*, **2012,** *31* (7), 2589-2596.
- Zhu, Y.; Romain, C.; Williams, C. K. *Nature*, **2016,** *540* (7633), 354-362.
- Zibek, S.; Wagner, W.; Hirth, T.; Rupp, S.; Huf, S. *Chemie Ingenieur Technik*, **2009,** *81* (11), 1797-1808.